APPENDIX C-1

ION BALANCE SUMMARY--PHASE II KINETIC TESTING

Parameter Measured	Ionic Species	Week 10		Week 15		Week 20		Week 25	
		mg/L	meq/L	mg/L	meq/L	mg/L	meq/L	mg/L	meq/L
Column No. II-04									
anion									
Alkalinity	HCO3-	2.5	0.0499	3	0.0599	1.5	0.0300	0.5	0.0100
Arsenic	As(OH)4-	0.00288	0.0000	0.00132	0.0000	0.002	0.0000	0.00129	0.0000
Chloride	Cl-	0.61	0.0172						
Fluoride	F-	0.163	0.0086	0.154	0.0081	0.207	0.0109	0.376	0.0198
Nitrite/Nitrate	NO3-							0.011	0.0008
Phosphorous	H2PO4-								
Selenium	SeO4 2-			0.001	0.0000	0.002	0.0001	0.0072	0.0002
Sulphate	SO4 2-	86	1.7906	86	1.7906	89	1.8531	73	1.5199
Sum of anions (meq/L)			**1.866**		**1.859**		**1.894**		**1.551**
cation									
Aluminum	Al 3+	0.0028	0.0003	0.0193	0.0021	0.166	0.0185	0.626	0.0696
Ammonia	NH4+	0.029	0.0021						
Barium	Ba 2+	0.00574	0.0001	0.0105	0.0002	0.027	0.0004	0.0459	0.0007
Beryllium	Be 2+							0.00122	0.0003
Cadmium	Cd 2+	0.000979	0.0000	0.00554	0.0001	0.013	0.0002	0.011	0.0002
Calcium	Ca 2+	12.6	0.6287	11.9	0.5938	11.85	0.5913	6.15	0.3069
Cobalt	Co 2+	0.0434	0.0015	0.149	0.0051	0.268	0.0091	0.186	0.0063
Copper	Cu 2+	0.0288	0.0009	0.539	0.0170	2.835	0.0892	4.78	0.1504
Iron	Fe 2+					0.398	0.0143	3.84	0.1375
Lead	Pb 2+	0.000263	0.0000	0.00106	0.0000	0.006	0.0001	0.026	0.0003
Lithium	Li +	0.0208	0.0030	0.0193	0.0028	0.018	0.0026	0.0143	0.0021
Magnesium	Mg 2+	8.5	0.6994	8.77	0.7217	9.42	0.7751	5.76	0.4740
Manganese	Mn 2+	0.215	0.0078	0.414	0.0151	0.548	0.0199	0.288	0.0105
Nickel	Ni 2+	0.169	0.0058	0.654	0.0223	1.465	0.0499	1.43	0.0487
Potassium	K+	7.7	0.1969	7.3	0.1867	8.55	0.2187	5.6	0.1432
Silver	Ag +	0.000083	0.0000					0.000019	0.0000
Sodium	Na +	6	0.2610	3	0.1305	2.7	0.1174		
Strontium	Sr 2+	0.31	0.0071	0.337	0.0077	0.352	0.0080	0.163	0.0037
Uranium	UO2+	0.000011	0.0000	0.000032	0.0000	0.00027	0.0000	0.00257	0.0000
Zinc	Zn 2+	0.0583	0.0018	0.452	0.0138	1.035	0.0317	0.821	0.0251
Sum of cations (meq/L)			**1.816**		**1.719**		**1.946**		**1.379**

APPENDIX C-1

ION BALANCE SUMMARY--PHASE II KINETIC TESTING

Parameter Measured	Ionic Species	Week 0		Week 1		Week 3		Week 5	
		mg/L	meq/L	mg/L	meq/L	mg/L	meq/L	mg/L	meq/L
Column No. H-05									
anion									
Alkalinity	HCO3-	73.5	1.4684	71.5	1.4284	45	0.8990	40.5	0.8091
Arsenic	As(OH)4-	0.00295	0.0000	0.00178	0.0000	0.00063	0.0000	0.00056	0.0000
Chloride	Cl-	3.48	0.0982	2.43	0.0685	0.55	0.0155		
Fluoride	F-	0.062	0.0033	0.053	0.0028				
Nitrite/Nitrate	NO3-	0.107	0.0076	0.054	0.0039				
Phosphorous	H2PO4-								
Selenium	SeO4 2-	0.0023	0.0001	0.0013	0.0000				
Sulphate	SO4 2-	178	3.7061	53	1.1035	27	0.5622	23	0.4789
Sum of anions (meq/L)			**5.284**		**2.607**		**1.477**		**1.288**
cation									
Aluminum	Al 3+	0.0049	0.0005	0.0056	0.0006	0.0045	0.0005	0.005	0.0006
Ammonia	NH4+	0.218	0.0156	0.036	0.0026	0.041	0.0029		
Barium	Ba 2+	0.00264	0.0000	0.00146	0.0000	0.00159	0.0000	0.00202	0.0000
Beryllium	Be 2+								
Cadmium	Cd 2+								
Calcium	Ca 2+	8.46	0.4222	4.03	0.2011	5.4	0.2695	6.13	0.3059
Cobalt	Co 2+	0.0003	0.0000						
Copper	Cu 2+	0.00592	0.0002	0.00698	0.0002	0.00152	0.0000	0.00425	0.0001
Iron	Fe 2+								
Lead	Pb 2+	0.000162	0.0000						
Lithium	Li +								
Magnesium	Mg 2+	13.2	1.0862	5.72	0.4707	6.27	0.5159	6.85	0.5637
Manganese	Mn 2+	0.00126	0.0000	0.000669	0.0000	0.000816	0.0000	0.0011	0.0000
Nickel	Ni 2+	0.00613	0.0002	0.0022	0.0001	0.002	0.0001	0.00254	0.0001
Potassium	K+	9	0.2302	9.1	0.2327	6.5	0.1662	6	0.1535
Silver	Ag +	0.00011	0.0000	0.000029	0.0000	0.000016	0.0000		
Sodium	Na +	76.3	3.3189	42.8	1.8617	15.7	0.6829	9.6	0.4176
Strontium	Sr 2+	0.169	0.0039	0.0794	0.0018	0.0901	0.0021	0.124	0.0028
Uranium	UO2+	0.000011	0.0000						
Zinc	Zn 2+	0.0018	0.0001	0.0017	0.0001				
Sum of cations (meq/L)			**5.078**		**2.772**		**1.640**		**1.444**

APPENDIX C-1

ION BALANCE SUMMARY--PHASE II KINETIC TESTING

Parameter Measured	Ionic Species	Week 10		Week 15		Week 20		Week 25	
		mg/L	meq/L	mg/L	meq/L	mg/L	meq/L	mg/L	meq/L
Column No. II-05									
anion									
Alkalinity	HCO3-	28	0.5594	19	0.3796	17	0.3396	13	0.2597
Arsenic	As(OH)4-	0.00048	0.0000	0.00017	0.0000	0.00017	0.0000	0.00019	0.0000
Chloride	Cl-								
Fluoride	F-								
Nitrite/Nitrate	NO3-			0.0342	0.0024				
Phosphorous	H2PO4-								
Selenium	SeO4 2-								
Sulphate	SO4 2-	34	0.7079	36	0.7496	49	1.0202	46	0.9578
Sum of anions (meq/L)			**1.267**		**1.132**		**1.360**		**1.217**
cation									
Aluminum	Al 3+	0.0046	0.0005	0.0343	0.0038	0.0098	0.0011	0.0057	0.0006
Ammonia	NH4+	0.022	0.0016						
Barium	Ba 2+	0.00241	0.0000	0.00256	0.0000	0.00462	0.0001	0.00271	0.0000
Beryllium	Be 2+								
Cadmium	Cd 2+								
Calcium	Ca 2+	7.01	0.3498	7.34	0.3663	10.3	0.5140	8.35	0.4167
Cobalt	Co 2+			0.00011	0.0000	0.00013	0.0000	0.00018	0.0000
Copper	Cu 2+	0.00192	0.0001	0.00448	0.0001	0.00551	0.0002	0.00376	0.0001
Iron	Fe 2+								
Lead	Pb 2+					0.000115	0.0000		
Lithium	Li +								
Magnesium	Mg 2+	6.43	0.5291	6.12	0.5036	8.25	0.6789	5.32	0.4378
Manganese	Mn 2+	0.00154	0.0001	0.00192	0.0001	0.00254	0.0001	0.00251	0.0001
Nickel	Ni 2+	0.00452	0.0002	0.00431	0.0001	0.00472	0.0002	0.00843	0.0003
Potassium	K+	4.9	0.1253	3.9	0.0997	5.1	0.1304	3.4	0.0870
Silver	Ag +	0.000114	0.0000						
Sodium	Na +	3.8	0.1653	3.3	0.1435	3.9	0.1696	2.3	0.1000
Strontium	Sr 2+	0.097	0.0022	0.0881	0.0020	0.11	0.0025	0.069	0.0016
Uranium	UO2+								
Zinc	Zn 2+			0.0011	0.0000	0.0056	0.0002	0.0013	0.0000
Sum of cations (meq/L)			**1.174**		**1.119**		**1.497**		**1.044**

APPENDIX C-1

ION BALANCE SUMMARY--PHASE II KINETIC TESTING

Parameter Measured	Ionic Species	Week 0		Week 1		Week 3		Week 5	
		mg/L	meq/L	mg/L	meq/L	mg/L	meq/L	mg/L	meq/L
Column No. II-06									
anion									
Alkalinity	HCO3-	26.5	0.5294	70	1.3985	45	0.8990	38	0.7592
Arsenic	As(OH)4-	0.00069	0.0000	0.00046	0.0000	0.00026	0.0000	0.00023	0.0000
Chloride	Cl-	9.91	0.2795	11.3	0.3187	5.58	0.1574	3.02	0.0852
Fluoride	F-			0.033	0.0017				
Nitrite/Nitrate	NO3-			0.069	0.0049				
Phosphorous	H2PO4-								
Selenium	SeO4 2-	0.0012	0.0000	0.0021	0.0001	0.0018	0.0000	0.0012	0.0000
Sulphate	SO4 2-	36	0.7496	86	1.7906	83	1.7281	56	1.1660
Sum of anions (meq/L)			**1.559**		**3.515**		**2.785**		**2.010**
cation									
Aluminum	Al 3+	0.0046	0.0005	0.0112	0.0012	0.0073	0.0008	0.0029	0.0003
Ammonia	NH4+	0.059	0.0042	0.063	0.0045	0.065	0.0046		
Barium	Ba 2+	0.0011	0.0000	0.00215	0.0000	0.00233	0.0000	0.00234	0.0000
Beryllium	Be 2+								
Cadmium	Cd 2+								
Calcium	Ca 2+	3.35	0.1672	7.12	0.3553	7.09	0.3538	6.57	0.3278
Cobalt	Co 2+								
Copper	Cu 2+	0.00412	0.0001	0.0101	0.0003	0.0117	0.0004	0.0124	0.0004
Iron	Fe 2+								
Lead	Pb 2+	0.000053	0.0000			0.00113	0.0000	0.000055	0.0000
Lithium	Li +								
Magnesium	Mg 2+	7.73	0.6361	20.7	1.7034	19.7	1.6211	16.4	1.3495
Manganese	Mn 2+	0.00215	0.0001	0.00359	0.0001	0.00389	0.0001	0.00393	0.0001
Nickel	Ni 2+	0.00347	0.0001	0.00673	0.0002	0.00546	0.0002	0.00492	0.0002
Potassium	K+	5.8	0.1483	13.5	0.3453	11.9	0.3044	8.4	0.2148
Silver	Ag +	0.00022	0.0000	0.000097	0.0000	0.000264	0.0000	0.000212	0.0000
Sodium	Na +	16.7	0.7264	31.7	1.3789	15.8	0.6873	9.1	0.3958
Strontium	Sr 2+	0.0283	0.0006	0.059	0.0013	0.0499	0.0011	0.0464	0.0011
Uranium	UO2+								
Zinc	Zn 2+	0.001	0.0000	0.0013	0.0000	0.0018	0.0001	0.0015	0.0000
Sum of cations (meq/L)			**1.684**		**3.791**		**2.974**		**2.290**

APPENDIX C-1

ION BALANCE SUMMARY--PHASE II KINETIC TESTING

Parameter Measured	Ionic Species	Week 10		Week 15		Week 20		Week 25	
		mg/L	meq/L	mg/L	meq/L	mg/L	meq/L	mg/L	meq/L
Column No. II-06									
anion									
Alkalinity	HCO3-	16	0.3196	18	0.3596	14	0.2797	7.5	0.1498
Arsenic	As(OH)4-	0.00041	0.0000						
Chloride	Cl-	2.96	0.0835	1.24	0.0350	0.65	0.0183	0.53	0.0149
Fluoride	F-								
Nitrite/Nitrate	NO3-			0.0312	0.0022	0.0165	0.0012		
Phosphorous	H2PO4-								
Selenium	SeO4 2-	0.0016	0.0000			0.0017	0.0000	0.0025	0.0001
Sulphate	SO4 2-	143	2.9774	201	4.1850	159	3.3105	178	3.7061
Sum of anions (meq/L)			**3.381**		**4.582**		**3.610**		**3.871**
cation									
Aluminum	Al 3+	0.0016	0.0002	0.0028	0.0003	0.003	0.0003		
Ammonia	NH4+					0.021	0.0015		
Barium	Ba 2+	0.00478	0.0001	0.00631	0.0001	0.0062	0.0001	0.00623	0.0001
Beryllium	Be 2+								
Cadmium	Cd 2+								
Calcium	Ca 2+	13.1	0.6537	20.6	1.0279	15.5	0.7735	14.2	0.7086
Cobalt	Co 2+	0.00013	0.0000	0.00067	0.0000	0.0008	0.0000	0.00062	0.0000
Copper	Cu 2+	0.0194	0.0006	0.0069	0.0002	0.00837	0.0003	0.00301	0.0001
Iron	Fe 2+								
Lead	Pb 2+								
Lithium	Li +					0.0059	0.0009		
Magnesium	Mg 2+	25	2.0572	35.5	2.9212	29.9	2.4604	29.8	2.4522
Manganese	Mn 2+	0.00823	0.0003	0.044	0.0016	0.0591	0.0022	0.0505	0.0018
Nickel	Ni 2+	0.00804	0.0003	0.131	0.0045	0.162	0.0055	0.135	0.0046
Potassium	K+	6.9	0.1765	8.4	0.2148	9.6	0.2455	6.9	0.1765
Silver	Ag +	0.000308	0.0000			0.000079	0.0000	0.000017	0.0000
Sodium	Na +	5.3	0.2305	4.2	0.1827	2.6	0.1131		
Strontium	Sr 2+	0.0755	0.0017	0.0919	0.0021	0.0683	0.0016	0.0489	0.0011
Uranium	UO2+								
Zinc	Zn 2+					0.0021	0.0001	0.0015	0.0000
Sum of cations (meq/L)			**3.121**		**4.355**		**3.605**		**3.345**

APPENDIX C-1

ION BALANCE SUMMARY--PHASE II KINETIC TESTING

Parameter Measured	Ionic Species	Week 0		Week 1		Week 3		Week 5	
		mg/L	meq/L	mg/L	meq/L	mg/L	meq/L	mg/L	meq/L
Column No. II-07									
anion									
Alkalinity	HCO3-	73	1.4584	59.5	1.1887	42	0.8391	55	1.0988
Arsenic	As(OH)4-	0.0174	0.0002	0.0241	0.0003	0.0263	0.0004	0.0247	0.0003
Chloride	Cl-	11	0.3103	4.65	0.1312	1.46	0.0412	0.68	0.0192
Fluoride	F-	0.664	0.0350	0.429	0.0226	0.168	0.0088	0.05	0.0026
Nitrite/Nitrate	NO3-	0.28	0.0200	0.106	0.0076				
Phosphorous	H2PO4-								
Selenium	SeO4 2-	0.0028	0.0001	0.0026	0.0001	0.002	0.0001		
Sulphate	SO4 2-	43	0.8953	17	0.3540	7	0.1457	4	0.0833
Sum of anions (meq/L)			**2.719**		**1.704**		**1.035**		**1.204**
cation									
Aluminum	Al 3+	0.075	0.0083	0.109	0.0121	0.148	0.0165	0.0883	0.0098
Ammonia	NH4+	0.516	0.0368	0.19	0.0136	0.053	0.0038		
Barium	Ba 2+	0.00143	0.0000	0.000711	0.0000	0.000826	0.0000	0.00142	0.0000
Beryllium	Be 2+								
Cadmium	Cd 2+	0.00005	0.0000						
Calcium	Ca 2+	3.94	0.1966	5.04	0.2515	8.76	0.4371	14.9	0.7435
Cobalt	Co 2+	0.0009	0.0000	0.00014	0.0000	0.00014	0.0000	0.00042	0.0000
Copper	Cu 2+	0.00611	0.0002	0.00405	0.0001	0.00082	0.0000	0.00345	0.0001
Iron	Fe 2+								
Lead	Pb 2+	0.000205	0.0000	0.00008	0.0000			0.000083	0.0000
Lithium	Li +								
Magnesium	Mg 2+	0.65	0.0535	0.89	0.0732	1.55	0.1275	2.05	0.1687
Manganese	Mn 2+	0.0049	0.0002	0.00164	0.0001	0.00252	0.0001	0.0102	0.0004
Nickel	Ni 2+	0.0016	0.0001					0.00069	0.0000
Potassium	K+	11.8	0.3018	8.8	0.2251	5.8	0.1483	3.8	0.0972
Silver	Ag +	0.000022	0.0000						
Sodium	Na +	47.8	2.0792	23	1.0004	7.5	0.3262	3.8	0.1653
Strontium	Sr 2+	0.0674	0.0015	0.0849	0.0019	0.136	0.0031	0.251	0.0057
Uranium	UO2+	0.000422	0.0000	0.000258	0.0000	0.000313	0.0000	0.000408	0.0000
Zinc	Zn 2+	0.0033	0.0001	0.0029	0.0001	0.0011	0.0000	0.0034	0.0001
Sum of cations (meq/L)			**2.678**		**1.578**		**1.063**		**1.191**

APPENDIX C-1

ION BALANCE SUMMARY--PHASE II KINETIC TESTING

Parameter Measured	Ionic Species	Week 10		Week 15		Week 20		Week 25	
		mg/L	meq/L	mg/L	meq/L	mg/L	meq/L	mg/L	meq/L
Column No. II-07									
anion									
Alkalinity	HCO3-	40	0.7991	40.5	0.8091	38.5	0.7692	34	0.6793
Arsenic	As(OH)4-	0.0332	0.0004	0.0336	0.0004	0.0417	0.0006	0.0571	0.0008
Chloride	Cl-								
Fluoride	F-	0.04	0.0021						
Nitrite/Nitrate	NO3-			0.0529	0.0038				
Phosphorous	H2PO4-								
Selenium	SeO4 2-	0.001	0.0000						
Sulphate	SO4 2-	5	0.1041	4	0.0833	13	0.2707	5	0.1041
Sum of anions (meq/L)			**0.906**		**0.897**		**1.040**		**0.784**
cation									
Aluminum	Al 3+	0.142	0.0158	0.138	0.0153	0.215	0.0239	0.224	0.0249
Ammonia	NH4+	0.023	0.0016						
Barium	Ba 2+	0.000657	0.0000	0.000657	0.0000	0.000914	0.0000	0.000503	0.0000
Beryllium	Be 2+								
Cadmium	Cd 2+								
Calcium	Ca 2+	11.6	0.5788	14.9	0.7435	16.8	0.8383	13.7	0.6836
Cobalt	Co 2+	0.00012	0.0000	0.00016	0.0000	0.00021	0.0000	0.00021	0.0000
Copper	Cu 2+	0.00049	0.0000	0.00331	0.0001	0.00147	0.0000	0.00044	0.0000
Iron	Fe 2+								
Lead	Pb 2+								
Lithium	Li +								
Magnesium	Mg 2+	1.22	0.1004	1.09	0.0897	1.29	0.1062	0.92	0.0757
Manganese	Mn 2+	0.00386	0.0001	0.0051	0.0002	0.00495	0.0002	0.00512	0.0002
Nickel	Ni 2+					0.00066	0.0000		
Potassium	K+								
Silver	Ag +								
Sodium	Na +								
Strontium	Sr 2+	0.167	0.0038	0.167	0.0038	0.195	0.0045	0.127	0.0029
Uranium	UO2+	0.000499	0.0000	0.000467	0.0000	0.00104	0.0000	0.000654	0.0000
Zinc	Zn 2+			0.0015	0.0000			0.001	0.0000
Sum of cations (meq/L)			**0.701**		**0.853**		**0.973**		**0.787**

APPENDIX C-1

ION BALANCE SUMMARY--PHASE II KINETIC TESTING

Parameter Measured	Ionic Species	Week 0		Week 1		Week 3		Week 5	
		mg/L	meq/L	mg/L	meq/L	mg/L	meq/L	mg/L	meq/L
Column No. II-08									
anion									
Alkalinity	HCO3-	14	0.2797	10.5	0.2098	5.5	0.1099	6	0.1199
Arsenic	As(OH)4-	0.00623	0.0001	0.00884	0.0001	0.0108	0.0001	0.00995	0.0001
Chloride	Cl-	1.6	0.0451						
Fluoride	F-	0.224	0.0118	0.22	0.0116	0.087	0.0046	0.029	0.0015
Nitrite/Nitrate	NO3-	0.138	0.0098	0.052	0.0037			0.086	0.0061
Phosphorous	H2PO4-								
Selenium	SeO4 2-	0.0023	0.0001	0.0012	0.0000				
Sulphate	SO4 2-	137	2.8525	56	1.1660	29	0.6038	9	0.1874
Sum of anions (meq/L)			**3.199**		**1.391**		**0.718**		**0.315**
cation									
Aluminum	Al 3+	0.168	0.0187	0.65	0.0723	0.573	0.0637	0.652	0.0725
Ammonia	NH4+	0.028	0.0020						
Barium	Ba 2+	0.00309	0.0000	0.00443	0.0001	0.00389	0.0001	0.00369	0.0001
Beryllium	Be 2+								
Cadmium	Cd 2+								
Calcium	Ca 2+	7.41	0.3698	0.821	0.0410	0.387	0.0193	0.178	0.0089
Cobalt	Co 2+	0.0014	0.0000	0.00059	0.0000	0.00057	0.0000	0.00052	0.0000
Copper	Cu 2+	0.0107	0.0003	0.0126	0.0004	0.00489	0.0002	0.00596	0.0002
Iron	Fe 2+	0.034	0.0012	0.153	0.0055	0.166	0.0059	0.149	0.0053
Lead	Pb 2+	0.000261	0.0000	0.000692	0.0000	0.00065	0.0000	0.000642	0.0000
Lithium	Li +	0.0172	0.0025	0.0094	0.0014	0.0075	0.0011	0.0058	0.0008
Magnesium	Mg 2+	3.54	0.2913	0.54	0.0444	0.31	0.0255	0.21	0.0173
Manganese	Mn 2+	0.00919	0.0003	0.00255	0.0001	0.00202	0.0001	0.00161	0.0001
Nickel	Ni 2+	0.0159	0.0005	0.00413	0.0001	0.00357	0.0001	0.00306	0.0001
Potassium	K+	6	0.1535	2.4	0.0614	2.2	0.0563		
Silver	Ag +	0.000096	0.0000	0.000013	0.0000				
Sodium	Na +	50.1	2.1792	24.7	1.0744	14.2	0.6177	7.2	0.3132
Strontium	Sr 2+	0.222	0.0051	0.0286	0.0007	0.0143	0.0003	0.00681	0.0002
Uranium	UO2+	0.000086	0.0000	0.000083	0.0000	0.000065	0.0000	0.000064	0.0000
Zinc	Zn 2+	0.0143	0.0004	0.003	0.0001	0.0019	0.0001	0.0014	0.0000
Sum of cations (meq/L)			**3.025**		**1.302**		**0.790**		**0.419**

APPENDIX C-1

ION BALANCE SUMMARY--PHASE II KINETIC TESTING

Parameter Measured	Ionic Species	Week 10		Week 15		Week 20		Week 25	
		mg/L	meq/L	mg/L	meq/L	mg/L	meq/L	mg/L	meq/L
Column No. II-08									
anion									
Alkalinity	HCO3-	3.5	0.0699	3.5	0.0699	1.5	0.0300	1.5	0.0300
Arsenic	As(OH)4-	0.0106	0.0001	0.00724	0.0001	0.00349	0.0000	0.0021	0.0000
Chloride	Cl-								
Fluoride	F-	0.022	0.0012						
Nitrite/Nitrate	NO3-			0.0693	0.0049				
Phosphorous	H2PO4-								
Selenium	SeO4 2-								
Sulphate	SO4 2-	16	0.3331	14	0.2915	44	0.9161	40	0.8328
Sum of anions (meq/L)			**0.404**		**0.366**		**0.946**		**0.863**
cation									
Aluminum	Al 3+	0.0892	0.0099	0.0088	0.0010	0.0034	0.0004	0.0097	0.0011
Ammonia	NH4+								
Barium	Ba 2+	0.00101	0.0000	0.000572	0.0000	0.00202	0.0000	0.00192	0.0000
Beryllium	Be 2+								
Cadmium	Cd 2+					0.000064	0.0000	0.000055	0.0000
Calcium	Ca 2+	0.893	0.0446	1.53	0.0763	5.86	0.2924	4.78	0.2385
Cobalt	Co 2+	0.00155	0.0001	0.00383	0.0001	0.0231	0.0008	0.0292	0.0010
Copper	Cu 2+	0.00395	0.0001	0.00653	0.0002	0.007	0.0002	0.0203	0.0006
Iron	Fe 2+							0.109	0.0039
Lead	Pb 2+	0.000182	0.0000	0.000089	0.0000	0.000283	0.0000	0.000633	0.0000
Lithium	Li +	0.0076	0.0011	0.0063	0.0009	0.0099	0.0014	0.0092	0.0013
Magnesium	Mg 2+	0.7	0.0576	1.28	0.1053	5.34	0.4394	4.99	0.4106
Manganese	Mn 2+	0.00315	0.0001	0.00608	0.0002	0.0379	0.0014	0.0495	0.0018
Nickel	Ni 2+	0.00882	0.0003	0.0177	0.0006	0.12	0.0041	0.136	0.0046
Potassium	K+	2.9	0.0742	3	0.0767	3.5	0.0895	3.5	0.0895
Silver	Ag +	0.00005	0.0000						
Sodium	Na +	4.7	0.2044	2.9	0.1261	3.4	0.1479		
Strontium	Sr 2+	0.0324	0.0007	0.0485	0.0011	0.184	0.0042	0.147	0.0034
Uranium	UO2+	0.000021	0.0000	0.000026	0.0000	0.000049	0.0000	0.000213	0.0000
Zinc	Zn 2+	0.0022	0.0001	0.0025	0.0001	0.0076	0.0002	0.0172	0.0005
Sum of cations (meq/L)			**0.393**		**0.389**		**0.982**		**0.757**

APPENDIX C-1

ION BALANCE SUMMARY--PHASE II KINETIC TESTING

Parameter Measured	Ionic Species	Week 0		Week 1		Week 3		Week 5	
		mg/L	meq/L	mg/L	meq/L	mg/L	meq/L	mg/L	meq/L
Column No. II-09									
anion									
Alkalinity	HCO3-	75	1.4984	39	0.7791	69	1.3785	63	1.2586
Arsenic	As(OH)4-	0.00201	0.0000	0.00083	0.0000	0.00187	0.0000	0.00105	0.0000
Chloride	Cl-	2.23	0.0629	0.6	0.0169				
Fluoride	F-	0.223	0.0117	0.112	0.0059	0.15	0.0079	0.08	0.0042
Nitrite/Nitrate	NO3-	0.14	0.0100	0.05	0.0036				
Phosphorous	H2PO4-								
Selenium	SeO4 2-	0.0038	0.0001	0.0019	0.0000	0.0055	0.0001	0.005	0.0001
Sulphate	SO4 2-	52	1.0827	19	0.3956	15	0.3123	3	0.0625
Sum of anions (meq/L)			**2.666**		**1.201**		**1.699**		**1.325**
cation									
Aluminum	Al 3+	0.225	0.0250	0.356	0.0396	0.532	0.0592	0.486	0.0540
Ammonia	NH4+					0.039	0.0028		
Barium	Ba 2+	0.000599	0.0000	0.000803	0.0000	0.000812	0.0000	0.000559	0.0000
Beryllium	Be 2+								
Cadmium	Cd 2+								
Calcium	Ca 2+	1.93	0.0963	1.77	0.0883	1.47	0.0734	1.8	0.0898
Cobalt	Co 2+	0.00018	0.0000	0.00028	0.0000	0.00044	0.0000	0.00029	0.0000
Copper	Cu 2+	0.0116	0.0004	0.0163	0.0005	0.0292	0.0009	0.0233	0.0007
Iron	Fe 2+	0.777	0.0278	1.31	0.0469	2.01	0.0720	1.47	0.0526
Lead	Pb 2+	0.000543	0.0000	0.00069	0.0000	0.00124	0.0000	0.000911	0.0000
Lithium	Li +								
Magnesium	Mg 2+	1.26	0.1037	1.44	0.1185	2.1	0.1728	1.77	0.1456
Manganese	Mn 2+	0.00403	0.0001	0.00728	0.0003	0.0106	0.0004	0.00706	0.0003
Nickel	Ni 2+	0.00221	0.0001	0.00299	0.0001	0.00754	0.0003	0.00354	0.0001
Potassium	K+					2.9	0.0742		
Silver	Ag +	0.000025	0.0000	0.00005	0.0000	0.00056	0.0000	0.000027	0.0000
Sodium	Na +	53.5	2.3271	21.3	0.9265	37.9	1.6486	28.9	1.2571
Strontium	Sr 2+	0.0281	0.0006	0.0181	0.0004	0.0171	0.0004	0.0234	0.0005
Uranium	UO2+	0.000026	0.0000			0.000023	0.0000	0.000016	0.0000
Zinc	Zn 2+	0.0039	0.0001	0.0038	0.0001	0.0061	0.0002	0.0042	0.0001
Sum of cations (meq/L)			**2.581**		**1.221**		**2.105**		**1.601**

APPENDIX C-1

ION BALANCE SUMMARY--PHASE II KINETIC TESTING

Parameter Measured	Ionic Species	Week 10		Week 15		Week 20		Week 25	
		mg/L	meq/L	mg/L	meq/L	mg/L	meq/L	mg/L	meq/L
Column No. II-09									
anion									
Alkalinity	HCO3-	49	0.9789	42	0.8391	39	0.7791	45	0.8990
Arsenic	As(OH)4-	0.00094	0.0000	0.0004	0.0000	0.00041	0.0000	0.0005	0.0000
Chloride	Cl-								
Fluoride	F-	0.054	0.0028	0.028	0.0015				
Nitrite/Nitrate	NO3-			0.0603	0.0043	0.0123	0.0009	0.0086	0.0006
Phosphorous	H2PO4-								
Selenium	SeO4 2-	0.0034	0.0001	0.0018	0.0000	0.0018	0.0000	0.0017	0.0000
Sulphate	SO4 2-	15	0.3123	11	0.2290	25	0.5205	10	0.2082
Sum of anions (meq/L)			**1.294**		**1.074**		**1.301**		**1.108**
cation									
Aluminum	Al 3+	0.057	0.0063	0.22	0.0245	0.0534	0.0059	0.0759	0.0084
Ammonia	NH4+	0.021	0.0015			0.024	0.0017		
Barium	Ba 2+	0.0007	0.0000	0.000788	0.0000	0.00124	0.0000	0.0012	0.0000
Beryllium	Be 2+								
Cadmium	Cd 2+								
Calcium	Ca 2+	2.41	0.1203	4.29	0.2141	7.12	0.3553	7.74	0.3862
Cobalt	Co 2+			0.00028	0.0000			0.0001	0.0000
Copper	Cu 2+	0.00457	0.0001	0.0215	0.0007	0.00503	0.0002	0.0091	0.0003
Iron	Fe 2+	0.086	0.0031	0.877	0.0314	0.096	0.0034	0.214	0.0077
Lead	Pb 2+	0.00012	0.0000	0.000682	0.0000	0.000169	0.0000	0.000311	0.0000
Lithium	Li +								
Magnesium	Mg 2+	0.59	0.0485	1.9	0.1563	2.61	0.2148	2.68	0.2205
Manganese	Mn 2+	0.00202	0.0001	0.0064	0.0002	0.00428	0.0002	0.00468	0.0002
Nickel	Ni 2+	0.00062	0.0000	0.00376	0.0001	0.00133	0.0000	0.00147	0.0001
Potassium	K+	2.7	0.0691	3.8	0.0972	5.2	0.1330	5.05	0.1292
Silver	Ag +	0.000123	0.0000	0.000022	0.0000			0.000013	0.0000
Sodium	Na +	23.6	1.0265	16.3	0.7090	15.2	0.6612	9.05	0.3937
Strontium	Sr 2+	0.0343	0.0008	0.0597	0.0014	0.117	0.0027	0.1013	0.0023
Uranium	UO2+	0.000013	0.0000			0.000016	0.0000	0.000012	0.0000
Zinc	Zn 2+			0.003	0.0001	0.0013	0.0000	0.0014	0.0000
Sum of cations (meq/L)			**1.276**		**1.235**		**1.378**		**1.149**

APPENDIX C-1

ION BALANCE SUMMARY--PHASE II KINETIC TESTING

Parameter Measured	Ionic Species	Week 0		Week 1		Week 3		Week 5	
		mg/L	meq/L	mg/L	meq/L	mg/L	meq/L	mg/L	meq/L
Column No. II-10									
anion									
Alkalinity	HCO3-	64.5	1.2886	54	1.0788	23.5	0.4695	23	0.4595
Arsenic	As(OH)4-	0.00149	0.0000	0.00175	0.0000	0.00041	0.0000	0.00042	0.0000
Chloride	Cl-	2.21	0.0623	0.51	0.0144				
Fluoride	F-	0.204	0.0107	0.182	0.0096	0.056	0.0029	0.026	0.0014
Nitrite/Nitrate	NO3-	0.167	0.0119	0.051	0.0036				
Phosphorous	H2PO4-								
Selenium	SeO4 2-	0.001	0.0000						
Sulphate	SO4 2-	25	0.5205	9	0.1874	6	0.1249	4	0.0833
Sum of anions (meq/L)			**1.894**		**1.294**		**0.597**		**0.544**
cation									
Aluminum	Al 3+	0.197	0.0219	0.362	0.0402	0.132	0.0147	0.197	0.0219
Ammonia	NH4+								
Barium	Ba 2+	0.000582	0.0000	0.00109	0.0000	0.000349	0.0000	0.0005	0.0000
Beryllium	Be 2+								
Cadmium	Cd 2+								
Calcium	Ca 2+	0.743	0.0371	0.409	0.0204	0.184	0.0092	0.183	0.0091
Cobalt	Co 2+	0.00023	0.0000	0.00054	0.0000	0.00017	0.0000	0.00026	0.0000
Copper	Cu 2+	0.0104	0.0003	0.025	0.0008	0.00925	0.0003	0.0136	0.0004
Iron	Fe 2+	0.324	0.0116	0.697	0.0250	0.26	0.0093	0.37	0.0133
Lead	Pb 2+	0.000864	0.0000	0.00113	0.0000	0.000454	0.0000	0.000606	0.0000
Lithium	Li +								
Magnesium	Mg 2+	0.71	0.0584	0.89	0.0732	0.37	0.0304	0.47	0.0387
Manganese	Mn 2+	0.00281	0.0001	0.00654	0.0002	0.00224	0.0001	0.00342	0.0001
Nickel	Ni 2+	0.00273	0.0001	0.00563	0.0002	0.00194	0.0001	0.00326	0.0001
Potassium	K+	3.5	0.0895						
Silver	Ag +	0.000011	0.0000	0.000064	0.0000	0.00001	0.0000	0.000019	0.0000
Sodium	Na +	41.2	1.7921	26.6	1.1570	12.8	0.5568	11.8	0.5133
Strontium	Sr 2+	0.0156	0.0004	0.00806	0.0002	0.00393	0.0001	0.00393	0.0001
Uranium	UO2+	0.000011	0.0000	0.000015	0.0000				
Zinc	Zn 2+	0.0043	0.0001	0.0039	0.0001	0.0018	0.0001	0.0023	0.0001
Sum of cations (meq/L)			**2.012**		**1.317**		**0.621**		**0.597**

APPENDIX C-1

ION BALANCE SUMMARY--PHASE II KINETIC TESTING

Parameter Measured	Ionic Species	Week 10		Week 15		Week 20		Week 25	
		mg/L	meq/L	mg/L	meq/L	mg/L	meq/L	mg/L	meq/L
Column No. II-10									
anion									
Alkalinity	HCO3-	13.5	0.2697	10.5	0.2098	15	0.2997	9.5	0.1898
Arsenic	As(OH)4-	0.00039	0.0000	0.00017	0.0000	0.00032	0.0000	0.00031	0.0000
Chloride	Cl-								
Fluoride	F-	0.026	0.0014						
Nitrite/Nitrate	NO3-			0.0886	0.0063	0.0128	0.0009		
Phosphorous	H2PO4-								
Selenium	SeO4 2-								
Sulphate	SO4 2-	9	0.1874	5	0.1041	22	0.4581	7	0.1457
Sum of anions (meq/L)			**0.458**		**0.320**		**0.759**		**0.336**
cation									
Aluminum	Al 3+	0.0756	0.0084	0.134	0.0149	0.0335	0.0037	0.126	0.0140
Ammonia	NH4+								
Barium	Ba 2+	0.000321	0.0000	0.000364	0.0000	0.000386	0.0000	0.000367	0.0000
Beryllium	Be 2+								
Cadmium	Cd 2+								
Calcium	Ca 2+	0.177	0.0088	0.171	0.0085	0.87	0.0434	0.338	0.0169
Cobalt	Co 2+	0.0001	0.0000	0.00021	0.0000			0.00016	0.0000
Copper	Cu 2+	0.00491	0.0002	0.00931	0.0003	0.00374	0.0001	0.00825	0.0003
Iron	Fe 2+	0.14	0.0050	0.327	0.0117	0.061	0.0022	0.238	0.0085
Lead	Pb 2+	0.000212	0.0000	0.000366	0.0000	0.000086	0.0000	0.000284	0.0000
Lithium	Li +								
Magnesium	Mg 2+	0.24	0.0197	0.36	0.0296	0.67	0.0551	0.44	0.0362
Manganese	Mn 2+	0.00129	0.0000	0.00251	0.0001	0.000762	0.0000	0.00207	0.0001
Nickel	Ni 2+	0.00126	0.0000	0.00245	0.0001	0.00088	0.0000	0.00201	0.0001
Potassium	K+					3.1	0.0793		
Silver	Ag +	0.000077	0.0000						
Sodium	Na +	8.6	0.3741	6.8	0.2958	15.1	0.6568	6.3	0.2740
Strontium	Sr 2+	0.0043	0.0001	0.00359	0.0001	0.0227	0.0005	0.00865	0.0002
Uranium	UO2+								
Zinc	Zn 2+	0.001	0.0000	0.0017	0.0001			0.0013	0.0000
Sum of cations (meq/L)			**0.416**		**0.361**		**0.841**		**0.350**

APPENDIX C-1

ION BALANCE SUMMARY--PHASE II KINETIC TESTING

Parameter Measured	Ionic Species	Week 0		Week 1		Week 3		Week 5	
		mg/L	meq/L	mg/L	meq/L	mg/L	meq/L	mg/L	meq/L

Notes:

1. Concentrations listed in mg/L are laboratory-measured values for the parameters listed. Concentrations listed in meq/L are calculated values for the ionic species listed. Refer to the Form Factor Report for the basis of the conversion.

APPENDIX C-2
QUALITY CONTROL REPORT

TOTAL DISSOLVED SOLIDS EVALUATION
FOR
PHASE I AND II KINETIC TESTING

APPENDIX C-2

CALCULATED TOTAL DISSOLVED SOLIDS--PHASE I KINETIC TESTING

Column No.	Parameter	Ion	Week 0 mg/L	Week 1 mg/L	Week 3 mg/L	Week 5 mg/L	Week 10 mg/L	Week 15 mg/L
Column No. I-01								
	Alkalinity	HCO3-	67.0450	76.7970	31.6940	25.5990	22.5515	21.9420
	Aluminum	Al 3+	0.9780	0.3030	0.1620	0.0873	0.0572	0.0390
	Ammonia	NH4+	0.3349	0.1236	0.1043	0.0425		0.0283
	Arsenic	As(OH)4-	0.0928	0.0453	0.0491	0.0445	0.0325	0.0231
	Barium	Ba 2+	0.0016	0.0014	0.0006	0.0007	0.0007	0.0007
	Beryllium	Be 2+						
	Boron	B(OH)3	2.3967	1.2698	0.6864	0.5663	0.3432	0.2688
	Cadmium	Cd 2+	0.0001					
	Calcium	Ca 2+	0.5280	1.1900	2.7500	4.6200	5.7800	6.8700
	Chloride	Cl-	12.2000	0.8400				0.5700
	Cobalt	Co 2+	0.0002		0.0001	0.0002	0.0004	0.0007
	Copper	Cu 2+	0.0081	0.0023	0.0015	0.0008	0.0021	0.0010
	Fluoride	F-	0.5200	0.2540	0.0940	0.0530	0.0730	0.0300
	Iron	Fe 2+	0.2100	0.0620				
	Lead	Pb 2+	0.0007	0.0003	0.0003	0.0001		
	Lithium	Li +			0.0095	0.0086	0.0054	
	Magnesium	Mg 2+	0.5200	0.7200	1.6200	2.8900	3.7300	4.4300
	Manganese	Mn 2+	0.0025	0.0026	0.0038	0.0075	0.0143	0.0245
	Nickel	Ni 2+	0.0010			0.0006	0.0009	0.0016
	Nitrite/Nitrate	NO3-	0.6505	0.1721	0.1022	0.0575	0.0509	0.1195
	Phosphorous	H2PO4-						
	Potassium	K+	5.5000	8.3000	6.9000	4.4000	2.5000	2.3000
	Selenium	SeO4 2-	0.0038					
	Silicon	SiO2	6.6768	5.1146	4.9434	4.6224	4.5796	4.4940
	Silver	Ag +	0.0006	0.0001	0.0001	0.0000	0.0002	
	Sodium	Na +	40.6000	29.5000	10.7000	8.2000	4.5000	2.8000
	Strontium	Sr 2+	0.0092	0.0227	0.0530	0.0878	0.0855	0.0941
	Sulphate	SO4 2-	29.0000	14.0000	15.0000	25.0000	21.0000	28.0000
	Uranium	UO2+	0.0002	0.0002	0.0001	0.0001	0.0001	0.0001
	Zinc	Zn 2+	0.0040			0.0015		0.0011
	Calculated TDS (mg/L)		**167.28**	**138.72**	**74.87**	**76.29**	**65.31**	**72.04**

APPENDIX C-2
CALCULATED TOTAL DISSOLVED SOLIDS--PHASE I KINETIC TESTING

Column No.	Parameter	Ion	Week 0 mg/L	Week 1 mg/L	Week 3 mg/L	Week 5 mg/L	Week 10 mg/L	Week 15 mg/L
Column No. I-02								
	Alkalinity	HCO3-	4.2665	0.0000	0.0000	0.0000	0.0000	0.0000
	Aluminum	Al 3+		0.1210	0.1200	0.3000		
	Ammonia	NH4+	0.6260	0.5049	0.1159	0.0541		
	Arsenic	As(OH)4-					0.0050	
	Barium	Ba 2+	0.0582	0.0431	0.0214	0.0147	0.0079	0.0074
	Beryllium	Be 2+						
	Boron	B(OH)3	2.9744					
	Cadmium	Cd 2+		0.0773	0.0612	0.0254	0.0073	0.0028
	Calcium	Ca 2+	19.0000	21.3000	4.0800	2.0800	1.6500	1.2100
	Chloride	Cl-	124.0000	29.6000	3.8200	12.3000	10.7000	12.4000
	Cobalt	Co 2+	0.4640	4.8100	8.2100	6.7800	2.2700	0.9390
	Copper	Cu 2+	0.0539	0.0752	0.8180	0.6340	0.0039	0.0200
	Fluoride	F-	0.0240		2.6000	0.0250	0.0420	
	Iron	Fe 2+	97.6000	176.0000	290.0000	232.0000	165.0000	128.0000
	Lead	Pb 2+	0.0032	0.0140	0.0525	0.0490	0.0061	0.0038
	Lithium	Li +						
	Magnesium	Mg 2+	16.9000	22.3000	9.4200	6.5300	6.0100	4.1400
	Manganese	Mn 2+	10.2000	9.8100	9.2000	7.8200	5.2900	3.2800
	Nickel	Ni 2+	148.0000	276.0000	405.0000	338.0000	141.0000	83.9000
	Nitrite/Nitrate	NO3-	1.7169	0.3602	0.2611	0.3544	2.5842	0.1505
	Phosphorous	H2PO4-						
	Potassium	K+	5.2000					
	Selenium	SeO4 2-					0.0615	
	Silicon	SiO2	3.7878	5.4784	4.1730	4.2800	4.7936	4.3656
	Silver	Ag +						
	Sodium	Na +	33.2000	18.1000				
	Strontium	Sr 2+	0.3780	0.3010	0.0290	0.0150	0.0179	0.0156
	Sulphate	SO4 2-	542.0000	837.0000	1220.0000	991.0000	629.0000	374.0000
	Uranium	UO2+						
	Zinc	Zn 2+	0.5370	2.4800	0.8900	0.3200	0.0510	0.0300
	Calculated TDS (mg/L)		**1010.99**	**1404.38**	**1958.87**	**1602.58**	**968.50**	**612.46**

APPENDIX C-2
CALCULATED TOTAL DISSOLVED SOLIDS--PHASE I KINETIC TESTING

Column No.	Parameter	Ion	Week 0 mg/L	Week 1 mg/L	Week 3 mg/L	Week 5 mg/L	Week 10 mg/L	Week 15 mg/L
Column No. I-03								
	Alkalinity	HCO3-	35.9605	149.3275	81.6730	74.3590	71.3115	67.6545
	Aluminum	Al 3+	0.0035	0.0066	0.0031	0.0026	0.0067	0.0036
	Ammonia	NH4+	0.1984	0.0386	0.0283			
	Arsenic	As(OH)4-		0.0026	0.0062	0.0009	0.0013	0.0014
	Barium	Ba 2+	0.0674	0.0537	0.0360	0.0336	0.0386	0.0412
	Beryllium	Be 2+						
	Boron	B(OH)3	0.0744	0.1430	0.0686	0.0572		
	Cadmium	Cd 2+						
	Calcium	Ca 2+	20.2000	14.1000	9.8700	10.3000	11.0000	10.8000
	Chloride	Cl-	203.0000	198.0000	54.9000	38.4000	23.5000	18.8000
	Cobalt	Co 2+	0.0003	0.0004	0.0001			
	Copper	Cu 2+	0.0021	0.0058	0.0010	0.0009	0.0023	0.0009
	Fluoride	F-	0.0250	0.0220		0.0500	0.0370	
	Iron	Fe 2+						
	Lead	Pb 2+	0.0001	0.0002	0.0002	0.0001	0.0002	
	Lithium	Li +						
	Magnesium	Mg 2+	38.9000	58.7000	19.2000	14.4000	10.2000	8.5400
	Manganese	Mn 2+	0.0046	0.0085	0.0034	0.0028	0.0031	0.0034
	Nickel	Ni 2+	0.0093	0.0169	0.0040	0.0021	0.0034	0.0021
	Nitrite/Nitrate	NO3-	0.3044			0.0239	0.0637	0.0974
	Phosphorous	H2PO4-						
	Potassium	K+	25.5000	34.7000	18.7000	15.3000	10.7000	8.7000
	Selenium	SeO4 2-						
	Silicon	SiO2	7.8324	10.0580	8.7098	7.9180	8.2818	8.0036
	Silver	Ag +				0.0002	0.0000	
	Sodium	Na +	26.4000	29.6000	10.7000	7.9000	5.0000	3.5000
	Strontium	Sr 2+	0.1600	0.0921	0.0518	0.0469	0.0433	0.0397
	Sulphate	SO4 2-		6.0000	7.0000	4.0000	4.0000	5.0000
	Uranium	UO2+					0.0000	0.0001
	Zinc	Zn 2+	0.0017	0.0025		0.0011		
	Calculated TDS (mg/L)		**358.64**	**500.88**	**210.96**	**172.80**	**144.19**	**131.19**

APPENDIX C-2
CALCULATED TOTAL DISSOLVED SOLIDS--PHASE I KINETIC TESTING

Column No.	Parameter	Ion	Week 0 mg/L	Week 1 mg/L	Week 3 mg/L	Week 5 mg/L	Week 10 mg/L	Week 15 mg/L
Column No. 1-04								
	Alkalinity	HCO3-	74.3590	193.8210	70.7020	56.0740	31.6940	15.2375
	Aluminum	Al 3+				0.0022	0.0012	
	Ammonia	NH4+	0.1340	0.0657				
	Arsenic	As(OH)4-	0.0014	0.0021		0.0010	0.0007	0.0009
	Barium	Ba 2+	0.0074	0.0182	0.0196	0.0186	0.0237	0.0355
	Beryllium	Be 2+						
	Boron	B(OH)3	6.6352	14.3000	10.1244	8.1224	4.9135	5.1022
	Cadmium	Cd 2+					0.0001	0.0001
	Calcium	Ca 2+	5.5800	11.8000	20.3000	22.9000	21.5000	18.0000
	Chloride	Cl-	96.8000	34.0000	7.0700	130.0000	85.7000	54.7000
	Cobalt	Co 2+		0.0018	0.0023	0.0018	0.0026	0.0060
	Copper	Cu 2+	0.0051	0.0594	0.0128	0.0118	0.0185	0.0045
	Fluoride	F-	0.0260	0.0220		0.0250	0.0320	
	Iron	Fe 2+						
	Lead	Pb 2+			0.0005			
	Lithium	Li +						
	Magnesium	Mg 2+	15.5000	68.8000	47.1000	40.2000	34.4000	40.4000
	Manganese	Mn 2+	0.0012	0.0105	0.0121	0.0149	0.0285	0.0847
	Nickel	Ni 2+	0.0224	0.1210	0.1010	0.0703	0.0877	0.3410
	Nitrite/Nitrate	NO3-	0.3713			0.0336	0.0739	0.1151
	Phosphorous	H2PO4-						
	Potassium	K+	12.5000	43.2000	32.3000	27.4000	18.4000	17.8000
	Selenium	SeO4 2-				0.0045	0.0043	0.0069
	Silicon	SiO2	7.3616	8.2176	5.4998	4.9862	5.0504	5.5426
	Silver	Ag +		0.0009	0.0004	0.0004	0.0003	0.0001
	Sodium	Na +	42.2000	79.4000	29.8000	20.0000	9.6000	6.8000
	Strontium	Sr 2+	0.0721	0.1620	0.1600	0.1130	0.0647	0.0761
	Sulphate	SO4 2-	40.0000	112.0000	106.0000	119.0000	122.0000	187.0000
	Uranium	UO2+						
	Zinc	Zn 2+				0.0035	0.0029	0.0076
	Calculated TDS (mg/L)		**301.58**	**566.00**	**329.20**	**428.98**	**333.60**	**351.26**

APPENDIX C-2
CALCULATED TOTAL DISSOLVED SOLIDS--PHASE I KINETIC TESTING

Column No.	Parameter	Ion	Week 0 mg/L	Week 1 mg/L	Week 3 mg/L	Week 5 mg/L	Week 10 mg/L	Week 15 mg/L
Column No. I-05								
	Alkalinity	HCO3-	90.2060	119.4620	49.3695	42.0555	34.7415	28.6465
	Aluminum	Al 3+	1.2000	0.1960	0.2960	0.1550	0.1520	0.1220
	Ammonia	NH4+	0.5345	0.1984	0.0773			
	Arsenic	As(OH)4-	0.0458	0.0252	0.0483	0.0382	0.0208	0.0137
	Barium	Ba 2+	0.0016	0.0023	0.0012	0.0018	0.0014	0.0017
	Beryllium	Be 2+						
	Boron	B(OH)3	2.3852	1.4758	0.9724	0.7608	0.4633	0.3546
	Cadmium	Cd 2+						
	Calcium	Ca 2+	0.9930	4.3800	4.3300	6.5800	9.7200	9.9900
	Chloride	Cl-	12.4000	1.8200	0.8900	1.5500	1.2700	0.9000
	Cobalt	Co 2+	0.0001					
	Copper	Cu 2+	0.0051	0.0015	0.0016	0.0012	0.0031	0.0018
	Fluoride	F-	0.7450	0.2480	0.1910	0.0670	0.0750	0.0340
	Iron	Fe 2+	0.0950					
	Lead	Pb 2+	0.0006	0.0002	0.0002	0.0001		
	Lithium	Li +		0.0129	0.0090	0.0092	0.0068	
	Magnesium	Mg 2+	0.3400	1.9200	1.6100	2.1000	2.4000	1.9100
	Manganese	Mn 2+	0.0008	0.0034	0.0015	0.0024	0.0049	0.0063
	Nickel	Ni 2+	0.0006	0.0006			0.0014	
	Nitrite/Nitrate	NO3-	0.5222	0.1788	0.1589	0.0770	0.0690	0.1239
	Phosphorous	H2PO4-						
	Potassium	K+	7.5000	14.7000	8.5000	6.7000	2.9000	2.3000
	Selenium	SeO4 2-	0.0040	0.0018	0.0025			
	Silicon	SiO2	6.5056	5.4356	5.4356	5.0504	5.3714	5.2430
	Silver	Ag +	0.0000	0.0000	0.0001		0.0000	
	Sodium	Na +	39.1000	33.0000	13.1000	8.7000	4.9000	2.5000
	Strontium	Sr 2+	0.0121	0.0647	0.0540	0.0665	0.0685	0.0671
	Sulphate	SO4 2-	11.0000	6.0000	10.0000	15.0000	20.0000	20.0000
	Uranium	UO2+	0.0002	0.0003	0.0002	0.0002	0.0002	0.0002
	Zinc	Zn 2+	0.0016			0.0012	0.0011	
	Calculated TDS (mg/L)		**173.60**	**189.13**	**95.05**	**88.92**	**82.17**	**72.21**

APPENDIX C-2
CALCULATED TOTAL DISSOLVED SOLIDS--PHASE I KINETIC TESTING

Column No.	Parameter	Ion	Week 20 mg/L	Week 25 mg/L	Week 30 mg/L	Week 40 mg/L	Week 50 mg/L
Column No. I-01							
	Alkalinity	HCO3-	19.5040	17.6755	21.3325	10.9710	7.3140
	Aluminum	Al 3+	0.0312	0.0309	0.0309	0.0089	0.0087
	Ammonia	NH4+	0.0489	0.0386		0.0068	
	Arsenic	As(OH)4-	0.0156	0.0117	0.0075	0.0026	0.0009
	Barium	Ba 2+	0.0012	0.0019	0.0013	0.0009	0.0012
	Beryllium	Be 2+					
	Boron	B(OH)3	0.2460	0.2631	0.3432	0.1945	0.1144
	Cadmium	Cd 2+				0.0002	0.0004
	Calcium	Ca 2+	7.7100	9.8800	13.6000	9.0300	9.8900
	Chloride	Cl-		0.5700			
	Cobalt	Co 2+	0.0015	0.0021	0.0019	0.0061	0.0265
	Copper	Cu 2+	0.0090	0.0004	0.0006	0.0003	0.0009
	Fluoride	F-	0.0270	0.0610	0.0380	0.0380	0.0480
	Iron	Fe 2+					
	Lead	Pb 2+		0.0001	0.0001		0.0001
	Lithium	Li +				0.0053	
	Magnesium	Mg 2+	5.1800	6.6700	10.0000	6.8200	7.9900
	Manganese	Mn 2+	0.0419	0.0642	0.1010	0.1830	0.3530
	Nickel	Ni 2+	0.0025	0.0034	0.0031	0.0111	0.0484
	Nitrite/Nitrate	NO3-	0.0841	0.0752	0.0797		
	Phosphorous	H2PO4-					
	Potassium	K+			2.2000		
	Selenium	SeO4 2-					
	Silicon	SiO2	4.2800	3.9590	3.7022	2.5252	2.6108
	Silver	Ag +					
	Sodium	Na +	2.2000	2.1000			
	Strontium	Sr 2+	0.0948	0.1180	0.1460	0.0982	0.0710
	Sulphate	SO4 2-	35.0000	46.0000	66.0000	47.0000	61.0000
	Uranium	UO2+	0.0001	0.0001	0.0001	0.0000	0.0000
	Zinc	Zn 2+	0.0042	0.0033	0.0027	0.0120	0.0296
	Calculated TDS (mg/L)		**74.48**	**87.53**	**117.59**	**76.91**	**89.51**

APPENDIX C-2
CALCULATED TOTAL DISSOLVED SOLIDS--PHASE I KINETIC TESTING

Column No.	Parameter	Ion	Week 20 mg/L	Week 25 mg/L	Week 30 mg/L	Week 40 mg/L	Week 50 mg/L
Column No. I-02							
	Alkalinity	HCO3-	0.0000	0.0000	0.0000	0.0000	0.0000
	Aluminum	Al 3+				0.0052	
	Ammonia	NH4+	0.0515			0.0296	
	Arsenic	As(OH)4-				0.0002	
	Barium	Ba 2+	0.0067			0.0023	
	Beryllium	Be 2+					
	Boron	B(OH)3				0.0686	
	Cadmium	Cd 2+	0.0024			0.0008	
	Calcium	Ca 2+	1.1300			0.4300	
	Chloride	Cl-	1.8200				
	Cobalt	Co 2+	0.6740			0.3630	
	Copper	Cu 2+	0.0124			0.0048	
	Fluoride	F-					
	Iron	Fe 2+	138.0000			89.5000	
	Lead	Pb 2+	0.0066			0.0024	
	Lithium	Li +					
	Magnesium	Mg 2+	3.8500			1.5600	
	Manganese	Mn 2+	2.7200			1.5900	
	Nickel	Ni 2+	67.7000			39.9000	
	Nitrite/Nitrate	NO3-	0.0974				
	Phosphorous	H2PO4-					
	Potassium	K+					
	Selenium	SeO4 2-				0.0081	
	Silicon	SiO2	4.1302			1.4274	
	Silver	Ag +				0.0000	
	Sodium	Na +					
	Strontium	Sr 2+	0.0161			0.0049	
	Sulphate	SO4 2-	383.0000				
	Uranium	UO2+				0.0000	
	Zinc	Zn 2+	0.0310			0.0127	
	Calculated TDS (mg/L)		**603.25**	**0.00**	**0.00**	**134.91**	**0.00**

APPENDIX C-2
CALCULATED TOTAL DISSOLVED SOLIDS--PHASE I KINETIC TESTING

Column No.	Parameter	Ion	Week 20 mg/L	Week 25 mg/L	Week 30 mg/L	Week 40 mg/L	Week 50 mg/L
Column No. I-03							
	Alkalinity	HCO3-	62.1690	48.1505	49.3695	32.9130	49.3695
	Aluminum	Al 3+	0.0035	0.0035	0.0031	0.0033	0.0067
	Ammonia	NH4+	0.0451				
	Arsenic	As(OH)4-	0.0006	0.0005	0.0007	0.0003	
	Barium	Ba 2+	0.0445	0.0361	0.0421	0.0232	0.0308
	Beryllium	Be 2+					
	Boron	B(OH)3					
	Cadmium	Cd 2+					
	Calcium	Ca 2+	11.0000	9.2600	12.7000	7.0700	7.6300
	Chloride	Cl-	18.4000	17.1000	28.8000	11.3000	8.3600
	Cobalt	Co 2+		0.0002			
	Copper	Cu 2+	0.0076	0.0007	0.0003	0.0025	0.0006
	Fluoride	F-					
	Iron	Fe 2+					
	Lead	Pb 2+	0.0001				
	Lithium	Li +					
	Magnesium	Mg 2+	7.9000	5.9900	8.3200	4.7100	5.7700
	Manganese	Mn 2+	0.0037	0.0040	0.0027	0.0027	0.0038
	Nickel	Ni 2+	0.0024	0.0131	0.0018	0.0031	0.0014
	Nitrite/Nitrate	NO3-	0.0531		0.0487		
	Phosphorous	H2PO4-					
	Potassium	K+	7.3000	6.1000	7.9000	3.6000	4.0000
	Selenium	SeO4 2-					
	Silicon	SiO2	8.0464	7.2332	7.5756	5.1360	5.4998
	Silver	Ag +					
	Sodium	Na +	3.4000	2.9000	3.8000		
	Strontium	Sr 2+	0.0373	0.0312	0.0394	0.0216	0.0223
	Sulphate	SO4 2-		3.0000	6.0000	4.0000	
	Uranium	UO2+					
	Zinc	Zn 2+	0.0016	0.0035			0.0014
	Calculated TDS (mg/L)		**118.41**	**99.83**	**124.60**	**68.79**	**80.70**

APPENDIX C-2
CALCULATED TOTAL DISSOLVED SOLIDS--PHASE I KINETIC TESTING

Column No.	Parameter	Ion	Week 20 mg/L	Week 25 mg/L	Week 30 mg/L	Week 40 mg/L	Week 50 mg/L
Column No. I-04							
	Alkalinity	HCO3-	8.5330	6.0950	4.8760	1.2190	1.2190
	Aluminum	Al 3+					0.0270
	Ammonia	NH4+	0.0438				0.0068
	Arsenic	As(OH)4-	0.0006	0.0008	0.0011		
	Barium	Ba 2+	0.0458	0.0390	0.0309	0.0314	0.0287
	Beryllium	Be 2+					
	Boron	B(OH)3	4.8448	4.8277	3.8496	3.7180	3.8324
	Cadmium	Cd 2+	0.0002	0.0003	0.0005	0.0012	0.0048
	Calcium	Ca 2+	16.4000	12.4000	11.0000	9.5100	8.3400
	Chloride	Cl-	2.3300	43.1000	2.9300	2.1800	
	Cobalt	Co 2+	0.0142	0.0293	0.0463	0.4920	0.9500
	Copper	Cu 2+	0.0318	0.0029	0.0036	0.0133	0.0207
	Fluoride	F-					
	Iron	Fe 2+				0.0660	0.6500
	Lead	Pb 2+					
	Lithium	Li +					
	Magnesium	Mg 2+	59.0000	65.6000	75.0000	76.2000	87.8000
	Manganese	Mn 2+	0.1790	0.3650	0.5490	0.8500	1.5600
	Nickel	Ni 2+	1.2100	4.1600	9.9800	54.7000	81.7000
	Nitrite/Nitrate	NO3-	0.0708	0.0575	0.1106		
	Phosphorous	H2PO4-					
	Potassium	K+	16.5000	16.2000	16.2000	12.0000	12.2000
	Selenium	SeO4 2-	0.0134	0.0194	0.0215	0.0217	
	Silicon	SiO2	6.6554	7.1690	7.1476	5.9064	10.1222
	Silver	Ag +	0.0002	0.0000	0.0000		
	Sodium	Na +	6.3000	5.4000	5.1000	3.5000	3.1000
	Strontium	Sr 2+	0.0738	0.0779	0.0626	0.0612	0.0592
	Sulphate	SO4 2-	288.0000	332.0000	332.0000	341.0000	460.0000
	Uranium	UO2+					
	Zinc	Zn 2+	0.0181	0.0231	0.0270	0.0400	0.0800
	Calculated TDS (mg/L)		**410.26**	**497.57**	**468.94**	**511.51**	**671.70**

APPENDIX C-2
CALCULATED TOTAL DISSOLVED SOLIDS--PHASE I KINETIC TESTING

Column No.	Parameter	Ion	Week 20 mg/L	Week 25 mg/L	Week 30 mg/L	Week 40 mg/L	Week 50 mg/L
Column No. I-05							
	Alkalinity	HCO3-	22.5515	20.1135	20.7230	13.4090	10.9710
	Aluminum	Al 3+	0.0980	0.0743	0.0666	0.0337	0.0159
	Ammonia	NH4+	0.0399				
	Arsenic	As(OH)4-	0.0098	0.0068	0.0049	0.0029	0.0020
	Barium	Ba 2+	0.0014	0.0017	0.0017	0.0009	0.0009
	Beryllium	Be 2+					
	Boron	B(OH)3	0.3718	0.3146	0.3432	0.1602	0.1430
	Cadmium	Cd 2+					
	Calcium	Ca 2+	11.1000	11.2000	15.4000	8.9600	7.7700
	Chloride	Cl-		0.9900			
	Cobalt	Co 2+		0.0001		0.0001	0.0002
	Copper	Cu 2+	0.0067	0.0004	0.0006	0.0049	0.0008
	Fluoride	F-	0.0510	0.0480	0.0350	0.0400	0.0470
	Iron	Fe 2+					
	Lead	Pb 2+					
	Lithium	Li +					
	Magnesium	Mg 2+	2.3100	2.2600	3.1800	2.1200	2.3600
	Manganese	Mn 2+	0.0087	0.0125	0.0164	0.0230	0.0455
	Nickel	Ni 2+	0.0028	0.0089	0.0023	0.0032	0.0011
	Nitrite/Nitrate	NO3-	0.0443	0.0664	0.0575		
	Phosphorous	H2PO4-					
	Potassium	K+	3.6000				
	Selenium	SeO4 2-					
	Silicon	SiO2	5.8422	5.5426	5.0076	4.1302	3.6380
	Silver	Ag +					
	Sodium	Na +					
	Strontium	Sr 2+	0.0677	0.0811	0.1010	0.0660	0.0529
	Sulphate	SO4 2-	31.0000	30.0000	46.0000	23.0000	19.0000
	Uranium	UO2+	0.0001	0.0001	0.0002	0.0000	0.0000
	Zinc	Zn 2+	0.0014	0.0018	0.0029	0.0017	0.0025
	Calculated TDS (mg/L)		**77.11**	**70.72**	**90.94**	**51.96**	**44.05**

APPENDIX C-2

CALCULATED TOTAL DISSOLVED SOLIDS--PHASE I KINETIC TESTING

Column No.	Parameter	Ion	Week 20 mg/L	Week 25 mg/L	Week 30 mg/L	Week 40 mg/L	Week 50 mg/L

Notes:

1. Alkalinity as CaCO3 reported by laboratory. HCO3- estimated by dividing by 0.8202.
2. Ammonia as N reported by lab. NH4+ estimated by multiplying by 1.288.
3. Dissolved Arsenic converted to As(OH)4- by multiplying by 1.91.
4. Boron converted to B(OH)3 by multiplying by 5.72
5. Nitrite/Nitrate as N reported by lab. Assumed nitrate was primary species; multiplied reported value by 4.4.
6. Phosporous reported by lab. HPO42- estimated by multiplying by 3.10.
7. Dissolved Se converted to SeO42- by multiplying by 1.81.
8. Dissolved silicon converted to SiO2 by multiplying by 2.14.
9. Dissolved uranium converted to UO2+ by multiplying by 1.134.

APPENDIX C-2

CALCULATED TOTAL DISSOLVED SOLIDS--PHASE II KINETIC TESTING

Column No.	Parameter	Ion	Week 0 mg/L	Week 1 mg/L	Week 3 mg/L	Week 5 mg/L	Week 10 mg/L
II-01							
	Alkalinity	HCO3-	75.5780	57.9025	26.2085	21.9420	14.0185
	Aluminum	Al 3+	0.0523	0.0481	0.1100	0.1210	0.0664
	Ammonia	NH4+	0.5358	0.0708			0.0309
	Arsenic	As(OH)4-	0.0420	0.0626	0.0932	0.1350	0.1157
	Barium	Ba 2+	0.0046	0.0029	0.0017	0.0010	0.0009
	Beryllium	Be 2+					
	Boron	B(OH)3	1.7675	1.5902	0.5949	0.3546	0.1716
	Cadmium	Cd 2+		0.0001			
	Calcium	Ca 2+	9.7400	12.7000	9.9100	9.0400	7.1600
	Chloride	Cl-	4.2000	1.4200		0.5000	
	Cobalt	Co 2+	0.0005	0.0005	0.0005	0.0006	0.0009
	Copper	Cu 2+	0.0043	0.0045	0.0008	0.0023	0.0013
	Fluoride	F-	0.4240	0.2220	0.1000	0.0380	0.0280
	Iron	Fe 2+					
	Lead	Pb 2+	0.0001	0.0001	0.0001	0.0001	0.0001
	Lithium	Li +	0.0117	0.0132	0.0084	0.0060	
	Magnesium	Mg 2+	4.5300	4.9800	3.4100	2.9900	2.2800
	Manganese	Mn 2+	0.0101	0.0126	0.0100	0.0108	0.0142
	Nickel	Ni 2+	0.0075	0.0027	0.0016	0.0013	0.0018
	Nitrite/Nitrate	NO3-	0.2655	0.2390			
	Phosphorous	H2PO4-					
	Potassium	K+	20.0000	11.4000	4.0000	2.1000	
	Selenium	SeO4 2-	0.0051	0.0033	0.0020		
	Silicon	SiO2	8.3460	6.8694	4.9648	4.7080	3.4240
	Silver	Ag +		0.0001			0.0000
	Sodium	Na +	48.5000	16.9000	3.1000		
	Strontium	Sr 2+	0.1960	0.1960	0.1200	0.1180	0.0688
	Sulphate	SO4 2-	111.0000	57.0000	30.0000	22.0000	18.0000
	Uranium	UO2+	0.0007	0.0012	0.0012	0.0012	0.0004
	Zinc	Zn 2+	0.0014	0.0058	0.0027	0.0023	0.0017
	Calculated TDS (mg/L)		**285.22**	**171.65**	**82.64**	**64.07**	**45.39**

APPENDIX C-2

CALCULATED TOTAL DISSOLVED SOLIDS--PHASE II KINETIC TESTING

Column No.	Parameter	Ion	Week 0 mg/L	Week 1 mg/L	Week 3 mg/L	Week 5 mg/L	Week 10 mg/L
II-02							
	Alkalinity	HCO3-	99.3485	75.5780	49.3695	43.8840	36.5700
	Aluminum	Al 3+	0.1580	0.1720	0.1120	0.1360	0.1370
	Ammonia	NH4+	0.6865	0.2808	0.1095	0.0270	
	Arsenic	As(OH)4-	0.0114	0.0118	0.0057	0.0052	0.0040
	Barium	Ba 2+	0.0013	0.0009	0.0011	0.0011	0.0010
	Beryllium	Be 2+					
	Boron	B(OH)3	4.0440	3.6837	1.7846	1.3213	0.9209
	Cadmium	Cd 2+					
	Calcium	Ca 2+	2.4000	2.9700	7.0300	9.1800	10.3000
	Chloride	Cl-	4.5200	2.7500	0.8800		0.5300
	Cobalt	Co 2+					
	Copper	Cu 2+	0.0017	0.0031	0.0004	0.0008	0.0009
	Fluoride	F-	0.5630	0.3700	0.1160	0.0440	0.0380
	Iron	Fe 2+					
	Lead	Pb 2+	0.0002	0.0001		0.0001	0.0001
	Lithium	Li +		0.0055	0.0081	0.0081	0.0062
	Magnesium	Mg 2+	1.2500	1.4600	2.9500	3.7400	3.6400
	Manganese	Mn 2+	0.0040	0.0012	0.0026	0.0042	0.0053
	Nickel	Ni 2+	0.0006		0.0006	0.0009	0.0006
	Nitrite/Nitrate	NO3-	0.3496	0.2478			
	Phosphorous	H2PO4-					
	Potassium	K+	17.0000	13.8000	10.1000	6.1000	3.2000
	Selenium	SeO4 2-	0.0076	0.0078	0.0040	0.0027	
	Silicon	SiO2	5.5212	5.1146	4.0018	3.9376	2.9318
	Silver	Ag +	0.0000	0.0000			0.0001
	Sodium	Na +	60.0000	31.8000	7.8000	4.0000	
	Strontium	Sr 2+	0.0442	0.0553	0.1030	0.1490	0.1180
	Sulphate	SO4 2-	73.0000	38.0000	17.0000	17.0000	17.0000
	Uranium	UO2+	0.0016	0.0008	0.0005	0.0005	0.0004
	Zinc	Zn 2+	0.0096	0.0014	0.0011		
	Calculated TDS (mg/L)		**268.92**	**176.31**	**101.38**	**89.54**	**75.40**

APPENDIX C-2
CALCULATED TOTAL DISSOLVED SOLIDS--PHASE II KINETIC TESTING

Column No.	Parameter	Ion	Week 0 mg/L	Week 1 mg/L	Week 3 mg/L	Week 5 mg/L	Week 10 mg/L
II-03							
	Alkalinity	HCO3-	95.0820	97.5200	99.9580	78.0160	58.5120
	Aluminum	Al 3+	0.0114	0.0110	0.0078	0.0072	0.0098
	Ammonia	NH4+	0.3787				
	Arsenic	As(OH)4-	0.0051	0.0036	0.0016	0.0011	0.0017
	Barium	Ba 2+	0.0025	0.0020	0.0049	0.0046	0.0049
	Beryllium	Be 2+					
	Boron	B(OH)3	6.6924	4.6561	2.3223	1.4414	0.9610
	Cadmium	Cd 2+					
	Calcium	Ca 2+	2.3000	2.4800	3.5800	4.1500	4.0700
	Chloride	Cl-	43.5000	16.8000	3.4600	2.0000	2.2100
	Cobalt	Co 2+					0.0001
	Copper	Cu 2+	0.0030	0.0023	0.0009	0.0013	0.0017
	Fluoride	F-		0.0240			
	Iron	Fe 2+					
	Lead	Pb 2+	0.0001	0.0001			0.0001
	Lithium	Li +					
	Magnesium	Mg 2+	6.6800	6.1900	7.6400	6.3800	4.7000
	Manganese	Mn 2+	0.0008	0.0005	0.0006	0.0005	0.0019
	Nickel	Ni 2+	0.0018	0.0009	0.0009	0.0009	0.0006
	Nitrite/Nitrate	NO3-	0.8142			0.2921	
	Phosphorous	H2PO4-					
	Potassium	K+	19.7000	19.5000	21.7000	15.3000	11.3000
	Selenium	SeO4 2-					
	Silicon	SiO2	8.7954	8.2818	9.9938	8.2390	5.4356
	Silver	Ag +	0.0001	0.0000			0.0002
	Sodium	Na +	51.7000	30.2000	10.2000	6.1000	3.4000
	Strontium	Sr 2+	0.0118	0.0112	0.0162	0.0175	0.0139
	Sulphate	SO4 2-	26.0000	15.0000			
	Uranium	UO2+					0.0000
	Zinc	Zn 2+	0.0019	0.0031	0.0019		
	Calculated TDS (mg/L)		**261.68**	**200.69**	**158.89**	**121.95**	**90.62**

APPENDIX C-2
CALCULATED TOTAL DISSOLVED SOLIDS--PHASE II KINETIC TESTING

Column No.	Parameter	Ion	Week 0 mg/L	Week 1 mg/L	Week 3 mg/L	Week 5 mg/L	Week 10 mg/L
II-04							
	Alkalinity	HCO3-	38.3985	37.7890	14.0185	7.3140	3.0475
	Aluminum	Al 3+	0.0379	0.2170	0.0194	0.0115	0.0028
	Ammonia	NH4+	0.7883	0.1906	0.1906	0.0889	0.0374
	Arsenic	As(OH)4-	0.0110	0.0258	0.0126	0.0114	0.0055
	Barium	Ba 2+	0.0114	0.0041	0.0046	0.0036	0.0057
	Beryllium	Be 2+					
	Boron	B(OH)3	4.1699	4.4101	2.6484	1.5902	1.2584
	Cadmium	Cd 2+	0.0002	0.0001	0.0001	0.0001	0.0010
	Calcium	Ca 2+	28.5000	8.1600	15.5000	11.0000	12.6000
	Chloride	Cl-	2.6100	3.4400	0.6300		0.6100
	Cobalt	Co 2+	0.0020	0.0003	0.0023	0.0044	0.0434
	Copper	Cu 2+	0.0127	0.0078	0.0027	0.0103	0.0288
	Fluoride	F-	0.5200	0.6130	0.2310	0.1090	0.1630
	Iron	Fe 2+		0.0350			
	Lead	Pb 2+	0.0001	0.0002	0.0001	0.0001	0.0003
	Lithium	Li +	0.0467	0.0165	0.0419	0.0327	0.0208
	Magnesium	Mg 2+	13.6000	4.3800	9.0200	6.6600	8.5000
	Manganese	Mn 2+	0.0557	0.0084	0.0486	0.0594	0.2150
	Nickel	Ni 2+	0.0497	0.0031	0.0171	0.0247	0.1690
	Nitrite/Nitrate	NO3-	0.7655	0.3806			
	Phosphorous	H2PO4-					
	Potassium	K+	32.6000	12.3000	15.3000	11.6000	7.7000
	Selenium	SeO4 2-	0.0052	0.0040	0.0029	0.0018	
	Silicon	SiO2	4.0660	5.2644	6.7624	7.5756	7.8110
	Silver	Ag +	0.0000	0.0000			0.0001
	Sodium	Na +	126.0000	76.6000	33.5000	15.2000	6.0000
	Strontium	Sr 2+	0.6830	0.2070	0.3300	0.2990	0.3100
	Sulphate	SO4 2-	415.0000	198.0000	168.0000	95.0000	86.0000
	Uranium	UO2+	0.0003	0.0004	0.0001	0.0000	0.0000
	Zinc	Zn 2+	0.0068	0.0030	0.0031	0.0048	0.0583
	Calculated TDS (mg/L)		**667.94**	**352.06**	**266.29**	**156.60**	**134.59**

APPENDIX C-2
CALCULATED TOTAL DISSOLVED SOLIDS--PHASE II KINETIC TESTING

Column No.	Parameter	Ion	Week 0 mg/L	Week 1 mg/L	Week 3 mg/L	Week 5 mg/L	Week 10 mg/L
II-05							
	Alkalinity	HCO3-	89.5965	87.1585	54.8550	49.3695	34.1320
	Aluminum	Al 3+	0.0049	0.0056	0.0045	0.0050	0.0046
	Ammonia	NH4+	0.2808	0.0464	0.0528		0.0283
	Arsenic	As(OH)4-	0.0056	0.0034	0.0012	0.0011	0.0009
	Barium	Ba 2+	0.0026	0.0015	0.0016	0.0020	0.0024
	Beryllium	Be 2+					
	Boron	B(OH)3	6.6352	4.7362	2.1278	1.4414	0.8065
	Cadmium	Cd 2+					
	Calcium	Ca 2+	8.4600	4.0300	5.4000	6.1300	7.0100
	Chloride	Cl-	3.4800	2.4300	0.5500		
	Cobalt	Co 2+	0.0003				
	Copper	Cu 2+	0.0059	0.0070	0.0015	0.0043	0.0019
	Fluoride	F-	0.0620	0.0530			
	Iron	Fe 2+					
	Lead	Pb 2+	0.0002				
	Lithium	Li +					
	Magnesium	Mg 2+	13.2000	5.7200	6.2700	6.8500	6.4300
	Manganese	Mn 2+	0.0013	0.0007	0.0008	0.0011	0.0015
	Nickel	Ni 2+	0.0061	0.0022	0.0020	0.0025	0.0045
	Nitrite/Nitrate	NO3-	0.4735	0.2390			
	Phosphorous	H2PO4-					
	Potassium	K+	9.0000	9.1000	6.5000	6.0000	4.9000
	Selenium	SeO4 2-	0.0042	0.0024			
	Silicon	SiO2	14.3808	13.3108	7.4472	7.2118	4.6866
	Silver	Ag +	0.0001	0.0000	0.0000		0.0001
	Sodium	Na +	76.3000	42.8000	15.7000	9.6000	3.8000
	Strontium	Sr 2+	0.1690	0.0794	0.0901	0.1240	0.0970
	Sulphate	SO4 2-	178.0000	53.0000	27.0000	23.0000	34.0000
	Uranium	UO2+	0.0000				
	Zinc	Zn 2+	0.0018	0.0017			
	Calculated TDS (mg/L)		**400.07**	**222.73**	**126.00**	**109.74**	**95.91**

APPENDIX C-2
CALCULATED TOTAL DISSOLVED SOLIDS--PHASE II KINETIC TESTING

Column No.	Parameter	Ion	Week 0 mg/L	Week 1 mg/L	Week 3 mg/L	Week 5 mg/L	Week 10 mg/L
II-06							
	Alkalinity	HCO3-	32.3035	85.3300	54.8550	46.3220	19.5040
	Aluminum	Al 3+	0.0046	0.0112	0.0073	0.0029	0.0016
	Ammonia	NH4+	0.0760	0.0811	0.0837		
	Arsenic	As(OH)4-	0.0013	0.0009	0.0005	0.0004	0.0008
	Barium	Ba 2+	0.0011	0.0022	0.0023	0.0023	0.0048
	Beryllium	Be 2+					
	Boron	B(OH)3	3.3920	8.5228	5.7200	3.5979	2.3566
	Cadmium	Cd 2+					
	Calcium	Ca 2+	3.3500	7.1200	7.0900	6.5700	13.1000
	Chloride	Cl-	9.9100	11.3000	5.5800	3.0200	2.9600
	Cobalt	Co 2+					0.0001
	Copper	Cu 2+	0.0041	0.0101	0.0117	0.0124	0.0194
	Fluoride	F-		0.0330			
	Iron	Fe 2+					
	Lead	Pb 2+	0.0001		0.0011	0.0001	
	Lithium	Li +					
	Magnesium	Mg 2+	7.7300	20.7000	19.7000	16.4000	25.0000
	Manganese	Mn 2+	0.0022	0.0036	0.0039	0.0039	0.0082
	Nickel	Ni 2+	0.0035	0.0067	0.0055	0.0049	0.0080
	Nitrite/Nitrate	NO3-		0.3053			
	Phosphorous	H2PO4-					
	Potassium	K+	5.8000	13.5000	11.9000	8.4000	6.9000
	Selenium	SeO4 2-	0.0022	0.0038	0.0033	0.0022	0.0029
	Silicon	SiO2	4.7508	13.2466	9.0522	7.8110	4.3656
	Silver	Ag +	0.0002	0.0001	0.0003	0.0002	0.0003
	Sodium	Na +	16.7000	31.7000	15.8000	9.1000	5.3000
	Strontium	Sr 2+	0.0283	0.0590	0.0499	0.0464	0.0755
	Sulphate	SO4 2-	36.0000	86.0000	83.0000	56.0000	143.0000
	Uranium	UO2+					
	Zinc	Zn 2+	0.0010	0.0013	0.0018	0.0015	
	Calculated TDS (mg/L)		**120.06**	**277.94**	**212.87**	**157.30**	**222.61**

APPENDIX C-2
CALCULATED TOTAL DISSOLVED SOLIDS--PHASE II KINETIC TESTING

Column No.	Parameter	Ion	Week 0 mg/L	Week 1 mg/L	Week 3 mg/L	Week 5 mg/L	Week 10 mg/L
II-07							
	Alkalinity	HCO3-	88.9870	72.5305	51.1980	67.0450	48.7600
	Aluminum	Al 3+	0.0750	0.1090	0.1480	0.0883	0.1420
	Ammonia	NH4+	0.6646	0.2447	0.0683		0.0296
	Arsenic	As(OH)4-	0.0332	0.0460	0.0502	0.0472	0.0634
	Barium	Ba 2+	0.0014	0.0007	0.0008	0.0014	0.0007
	Beryllium	Be 2+					
	Boron	B(OH)3	2.3624	1.9734	1.1154	0.6006	0.3260
	Cadmium	Cd 2+	0.0001				
	Calcium	Ca 2+	3.9400	5.0400	8.7600	14.9000	11.6000
	Chloride	Cl-	11.0000	4.6500	1.4600	0.6800	
	Cobalt	Co 2+	0.0009	0.0001	0.0001	0.0004	0.0001
	Copper	Cu 2+	0.0061	0.0041	0.0008	0.0035	0.0005
	Fluoride	F-	0.6640	0.4290	0.1680	0.0500	0.0400
	Iron	Fe 2+					
	Lead	Pb 2+	0.0002	0.0001		0.0001	
	Lithium	Li +					
	Magnesium	Mg 2+	0.6500	0.8900	1.5500	2.0500	1.2200
	Manganese	Mn 2+	0.0049	0.0016	0.0025	0.0102	0.0039
	Nickel	Ni 2+	0.0016			0.0007	
	Nitrite/Nitrate	NO3-	1.2390	0.4691			
	Phosphorous	H2PO4-					
	Potassium	K+	11.8000	8.8000	5.8000	3.8000	
	Selenium	SeO4 2-	0.0051	0.0047	0.0036		0.0018
	Silicon	SiO2	8.4958	5.8422	4.8792	3.8734	3.0388
	Silver	Ag +	0.0000				
	Sodium	Na +	47.8000	23.0000	7.5000	3.8000	
	Strontium	Sr 2+	0.0674	0.0849	0.1360	0.2510	0.1670
	Sulphate	SO4 2-	43.0000	17.0000	7.0000	4.0000	5.0000
	Uranium	UO2+	0.0005	0.0003	0.0004	0.0005	0.0006
	Zinc	Zn 2+	0.0033	0.0029	0.0011	0.0034	
	Calculated TDS (mg/L)		**220.80**	**141.12**	**89.84**	**101.21**	**70.39**

APPENDIX C-2
CALCULATED TOTAL DISSOLVED SOLIDS--PHASE II KINETIC TESTING

Column No.	Parameter	Ion	Week 0 mg/L	Week 1 mg/L	Week 3 mg/L	Week 5 mg/L	Week 10 mg/L
II-08							
	Alkalinity	HCO3-	17.0660	12.7995	6.7045	7.3140	4.2665
	Aluminum	Al 3+	0.1680	0.6500	0.5730	0.6520	0.0892
	Ammonia	NH4+	0.0361				
	Arsenic	As(OH)4-	0.0119	0.0169	0.0206	0.0190	0.0202
	Barium	Ba 2+	0.0031	0.0044	0.0039	0.0037	0.0010
	Beryllium	Be 2+					
	Boron	B(OH)3	2.3795	1.7732	0.9953	0.4919	0.3661
	Cadmium	Cd 2+					
	Calcium	Ca 2+	7.4100	0.8210	0.3870	0.1780	0.8930
	Chloride	Cl-	1.6000				
	Cobalt	Co 2+	0.0014	0.0006	0.0006	0.0005	0.0016
	Copper	Cu 2+	0.0107	0.0126	0.0049	0.0060	0.0040
	Fluoride	F-	0.2240	0.2200	0.0870	0.0290	0.0220
	Iron	Fe 2+	0.0340	0.1530	0.1660	0.1490	
	Lead	Pb 2+	0.0003	0.0007	0.0007	0.0006	0.0002
	Lithium	Li +	0.0172	0.0094	0.0075	0.0058	0.0076
	Magnesium	Mg 2+	3.5400	0.5400	0.3100	0.2100	0.7000
	Manganese	Mn 2+	0.0092	0.0026	0.0020	0.0016	0.0032
	Nickel	Ni 2+	0.0159	0.0041	0.0036	0.0031	0.0088
	Nitrite/Nitrate	NO3-	0.6107	0.2301		0.3806	
	Phosphorous	H2PO4-					
	Potassium	K+	6.0000	2.4000	2.2000		2.9000
	Selenium	SeO4 2-	0.0042	0.0022			
	Silicon	SiO2	4.8364	6.8908	6.4414	6.0134	3.6380
	Silver	Ag +	0.0001	0.0000			0.0001
	Sodium	Na +	50.1000	24.7000	14.2000	7.2000	4.7000
	Strontium	Sr 2+	0.2220	0.0286	0.0143	0.0068	0.0324
	Sulphate	SO4 2-	137.0000	56.0000	29.0000	9.0000	16.0000
	Uranium	UO2+	0.0001	0.0001	0.0001	0.0001	0.0000
	Zinc	Zn 2+	0.0143	0.0030	0.0019	0.0014	0.0022
	Calculated TDS (mg/L)		**231.31**	**107.26**	**61.12**	**31.67**	**33.66**

APPENDIX C-2
CALCULATED TOTAL DISSOLVED SOLIDS--PHASE II KINETIC TESTING

Column No.	Parameter	Ion	Week 0 mg/L	Week 1 mg/L	Week 3 mg/L	Week 5 mg/L	Week 10 mg/L
II-09							
	Alkalinity	HCO3-	91.4250	47.5410	84.1110	76.7970	59.7310
	Aluminum	Al 3+	0.2250	0.3560	0.5320	0.4860	0.0570
	Ammonia	NH4+			0.0502		0.0270
	Arsenic	As(OH)4-	0.0038	0.0016	0.0036	0.0020	0.0018
	Barium	Ba 2+	0.0006	0.0008	0.0008	0.0006	0.0007
	Beryllium	Be 2+					
	Boron	B(OH)3	2.5740	1.2584	1.5272	0.9266	0.4404
	Cadmium	Cd 2+					
	Calcium	Ca 2+	1.9300	1.7700	1.4700	1.8000	2.4100
	Chloride	Cl-	2.2300	0.6000			
	Cobalt	Co 2+	0.0002	0.0003	0.0004	0.0003	
	Copper	Cu 2+	0.0116	0.0163	0.0292	0.0233	0.0046
	Fluoride	F-	0.2230	0.1120	0.1500	0.0800	0.0540
	Iron	Fe 2+	0.7770	1.3100	2.0100	1.4700	0.0860
	Lead	Pb 2+	0.0005	0.0007	0.0012	0.0009	0.0001
	Lithium	Li +					
	Magnesium	Mg 2+	1.2600	1.4400	2.1000	1.7700	0.5900
	Manganese	Mn 2+	0.0040	0.0073	0.0106	0.0071	0.0020
	Nickel	Ni 2+	0.0022	0.0030	0.0075	0.0035	0.0006
	Nitrite/Nitrate	NO3-	0.6195	0.2213			
	Phosphorous	H2PO4-					
	Potassium	K+			2.9000		2.7000
	Selenium	SeO4 2-	0.0069	0.0034	0.0100	0.0091	0.0062
	Silicon	SiO2	8.1320	6.3772	10.6358	7.7254	5.0290
	Silver	Ag +	0.0000	0.0001	0.0006	0.0000	0.0001
	Sodium	Na +	53.5000	21.3000	37.9000	28.9000	23.6000
	Strontium	Sr 2+	0.0281	0.0181	0.0171	0.0234	0.0343
	Sulphate	SO4 2-	52.0000	19.0000	15.0000	3.0000	15.0000
	Uranium	UO2+	0.0000		0.0000	0.0000	0.0000
	Zinc	Zn 2+	0.0039	0.0038	0.0061	0.0042	
	Calculated TDS (mg/L)		**214.96**	**101.34**	**158.47**	**123.03**	**109.77**

APPENDIX C-2
CALCULATED TOTAL DISSOLVED SOLIDS--PHASE II KINETIC TESTING

Column No.	Parameter	Ion	Week 0 mg/L	Week 1 mg/L	Week 3 mg/L	Week 5 mg/L	Week 10 mg/L
II-10							
	Alkalinity	HCO3-	78.6255	65.8260	28.6465	28.0370	16.4565
	Aluminum	Al 3+	0.1970	0.3620	0.1320	0.1970	0.0756
	Ammonia	NH4+					
	Arsenic	As(OH)4-	0.0028	0.0033	0.0008	0.0008	0.0007
	Barium	Ba 2+	0.0006	0.0011	0.0003	0.0005	0.0003
	Beryllium	Be 2+					
	Boron	B(OH)3	3.6722	2.3967	0.9724	0.6235	0.4118
	Cadmium	Cd 2+					
	Calcium	Ca 2+	0.7430	0.4090	0.1840	0.1830	0.1770
	Chloride	Cl-	2.2100	0.5100			
	Cobalt	Co 2+	0.0002	0.0005	0.0002	0.0003	0.0001
	Copper	Cu 2+	0.0104	0.0250	0.0093	0.0136	0.0049
	Fluoride	F-	0.2040	0.1820	0.0560	0.0260	0.0260
	Iron	Fe 2+	0.3240	0.6970	0.2600	0.3700	0.1400
	Lead	Pb 2+	0.0009	0.0011	0.0005	0.0006	0.0002
	Lithium	Li +					
	Magnesium	Mg 2+	0.7100	0.8900	0.3700	0.4700	0.2400
	Manganese	Mn 2+	0.0028	0.0065	0.0022	0.0034	0.0013
	Nickel	Ni 2+	0.0027	0.0056	0.0019	0.0033	0.0013
	Nitrite/Nitrate	NO3-	0.7390	0.2257			
	Phosphorous	H2PO4-					
	Potassium	K+	3.5000				
	Selenium	SeO4 2-	0.0018				
	Silicon	SiO2	12.2836	10.2078	3.8734	4.1302	2.7606
	Silver	Ag +	0.0000	0.0001	0.0000	0.0000	0.0001
	Sodium	Na +	41.2000	26.6000	12.8000	11.8000	8.6000
	Strontium	Sr 2+	0.0156	0.0081	0.0039	0.0039	0.0043
	Sulphate	SO4 2-	25.0000	9.0000	6.0000	4.0000	9.0000
	Uranium	UO2+	0.0000	0.0000			
	Zinc	Zn 2+	0.0043	0.0039	0.0018	0.0023	0.0010
	Calculated TDS (mg/L)		**169.45**	**117.36**	**53.32**	**49.87**	**37.90**

APPENDIX C-2

CALCULATED TOTAL DISSOLVED SOLIDS--PHASE II KINETIC TESTING

Column No.	Parameter	Ion	Week 0 mg/L	Week 1 mg/L	Week 3 mg/L	Week 5 mg/L	Week 10 mg/L

Notes:

1. Alkalinity as CaCO3 reported by laboratory. HCO3- estimated by dividing by 0.8202.
2. Ammonia as N reported by lab. NH4+ estimated by multiplying by 1.288.
3. Dissolved Arsenic converted to As(OH)4- by multiplying by 1.91.
4. Boron converted to B(OH)3 by multiplying by 5.72
5. Nitrite/Nitrate as N reported by lab. Assumed nitrate was primary species; multiplied reported value by 4.4.
6. Phosporous reported by lab. HPO42- estimated by multiplying by 3.10.
7. Dissolved Se converted to SeO42- by multiplying by 1.81.
8. Dissolved silicon converted to SiO2 by multiplying by 2.14.
9. Dissolved uranium converted to UO2+ by multiplying by 1.134.

ENVIRONMENTAL MINERALOGY OF SAMPLES FROM THE EAGLE DEPOSIT, MICHIGAN – PART 1

Prepared for: **Geochimica, Inc.**
Ojai, California

April, 2004



J.L. Jambor
Leslie Investments Ltd
Research and Consulting
316 Rosehill Wynd
Tsawwassen, B.C. V4M 3L9
Ph: (604)948-1368
Fax: (604)948-1369
E-mail: JLJambor@aol.com

EXECUTIVE SUMMARY

Five samples from the Eagle Ni-Cu deposit in Michigan, which are the first-received of 15 to be examined, were investigated by optical microscopy and other methods to determine the environmentally relevant mineralogy. The examined samples consist of footwall and hanging-wall siltstones, massive and semi-massive sulfides, and unmineralized peridotite. Except for the peridotite, all of the samples were indicated in previous acid–base accounting to be potentially acid-producing, and the principal acid-generating source in the two sulfide-rich samples would be the oxidation of their abundant pyrrhotite. The sample of peridotite, which is the rock type that hosts the potential ore, is low in sulfides and contains a small amount of calcite; however, the rock contains a major amount of olivine + serpentine, and these two minerals would account for the bulk of the high neutralization potential indicated by the acid–base tests. The hanging-wall and footwall siltstones contain an appreciable amount of sulfides (~1%), almost all of which occurs as disseminated pyrrhotite. The siltstones consist mainly of quartz, muscovite, albite, and chlorite, an assemblage that inadequately explains the measured amounts of neutralization potential, which are 11–14 kg $CaCO_3$ equivalent per tonne of material. However, the hanging-wall siltstone contains dolomite within spotted alteration that is probably a thermal metamorphic effect related to peridotite intrusion, and the additional presence of liberated dolomite grains suggests that fracture-controlled dolomite was likely incorporated within the core interval that was utilized for the static-test bulk sample. Such fracture control is evident in the core of the footwall siltstone, whose mineralogical reference sample contains fracture-fill calcite, but both dolomite and calcite were observed in the microscopy section. The presence of carbonates provides an explanation for the higher-than-expected values of neutralization potential for both siltstones. Energy-dispersion analyses indicate that the Fe contents of the calcite, and of the dolomite from both siltstones, are low, and both minerals are near their end-members in composition.

INTRODUCTION

Five samples from the Eagle Ni–Cu project in Michigan were received by LRC on February 18, 2004. The Eagle deposit is a potential orebody whose resource has been reported to be five million tonnes grading 3.6% Ni and 3% Cu, with accompanying credits in Pt and Au (*The Northern Miner*, April 2–8, 2004). The deposit is currently under examination by Kennecott Canada Exploration, and the work undertaken for this report is part of broader studies being conducted by Geochimica Inc., with the latter the reporting authority for the work performed by LRC. The five samples are the initial batch of a group of 15 that is to be examined mineralogically, with the focus on the potential waste rocks and on environmental aspects rather than petrography. Nonetheless, the textures and textural relationships are readily evident in the various photomicrographs embodied in this report; moreover, an extensive petrographic description by B. Jago of Lakefield Research (2002) is available for 16 drill-core samples from the deposit.

The five samples received by LRC, each about 150 g, had been crushed, and the material consisted both of fragments (chips) and fines. The largest chips were up to 2 × 2 cm wide and about 2 mm thick. As well, for each sample a corresponding piece of core, typically about 6 cm long, was provided. The core had been sawn along its length in two cuts at right angles to one another, but with both parallel to the elongation. Each of the resulting two flat faces was therefore about 6 cm long and 3 to 3½ cm wide, and the sample represented a quarter section of the original core. Viewed on end, therefore, the two right-angle cut faces and the arcuate exterior of the core have the geometry of the surface of a quarter of a pie. The sample numbers and lithology are summarized in Table 1.

Table 1. Sample numbers and related data*

Number	Lithology	S, wt%	NP
VR71100A	siltstone, hanging wall	1.06	14
VR71120A	massive sulfide	36.1	–4
VR71213A	peridotite	0.2	42
VR71325A	net-texture sulfides in peridotite	12.85	41
VR71499A	siltstone, footwall	1.23	11

*Data provided by Kennecott Canada Exploration; NP = neutralization potential

METHODS

The cores were retained intact for reference purposes; the crushed samples are portions of the material used in the static and kinetic tests, and these portions were therefore deemed to be the more appropriate for the mineralogical study. To obtain samples for the X-ray diffraction and optical studies, the complete contents of each of the submitted crushed samples were individually emptied onto a clean sheet of paper, and the resulting cone was vertically quartered. Minor modifications of this procedure for specific samples are given in the descriptions in the next section.

To obtain good representation in the sections for optical microscopy, the selected split was further crushed with a hammer to reduce the size of the largest chips, thereby minimizing the risk of have a few large chips dominating the representation in a section. This crushed material was then split, with the two halves bagged separately, one for X-ray diffractometry and the other for the optical section. After completion of this 'coarse crush', one of the bags of each sample was randomly chosen to be the X-ray material. That material was further crushed with a hammer, and the pulp was immersed in acetone and ground by hand using a mortar and pestle. Although such a grind yields a fineness suitable for standard X-ray diffractometry, for Rietveld refinements a final mechanical grind is used to reduce the particle size to <10 μm. Details of the procedures related to the Rietveld refinements, which were done by M. Raudsepp and E. Pani of the University of British Columbia, are given in Appendix 1.

The polished thin sections were prepared by Vancouver Petrographics Ltd as standard 26 × 46 mm glass slides. Water was used as the lubricant in the preparation procedure. The sections were received by LRC on March 4, 2004.

Although the Sampling and Analysis Plan for the Eagle project indicates that all 15 of the mineralogy samples are to be examined by X-ray diffractometry (XRD) and Rietveld refinements, some flexibility is also indicated in the plan. Thus, for the initial five samples it was decided, following the preliminary optical examination, that X-ray data would not be obtained for the massive sulfide sample and that, in its place, reconnaissance scanning electron microscopy (SEM) and qualitative energy-dispersion analyses (EDS) would be used to identify some of the carbonate-mineral grains that had been observed by optical microscopy. The SEM–EDS examinations were done with a Philips XL-30 instrument housed in the Department of

Earth and Ocean Sciences at the University of British Columbia.

SAMPLE DESCRIPTIONS AND RESULTS

In standard petrographic descriptions, the alteration products of the initially crystallized minerals are commonly referred to as 'secondary' minerals. A typical example is the serpentinization of olivine, wherein olivine is the primary magmatic mineral and is subsequently altered to (replaced by) 'secondary' serpentine during a more hydrous event that may be part of the crystallization continuum or related to a later episode. Confusion may arise because it is also common to refer to minerals formed by weathering, including supergene products, as 'secondary' minerals even though the alteration conditions and processes may be quite different from those of the first example, serpentinization. In the present study, no minerals attributable to weathering processes have been observed; all of the minerals, including serpentine, are therefore regarded as being part of the primary assemblage. In environmental mineralogy, 'secondary' minerals are those that form by weathering, most commonly oxidation, after the rock has been anthropogenically exposed or displaced from its geological setting.

Sample VR71100A

The sample is of hangingwall siltstone. The core shows that good bedding is present, with the downside half of the core dark, slightly greenish gray and massive and in sharp but undisturbed contact with the black upper half. Sub-millimetric sulfides are disseminated throughout the core but are much more abundant in the greenish gray lower half. Megascopic aggregation of the sulfides is absent; only two loosely clustered concentrations, each <2 mm across, are present, and no fracture-controlled sulfides are evident.

The as-received sample for the mineralogical studies is coarsely crushed, with some chips up to the aforementioned maximum size. The material is dark gray, fine-grained, and many of the chips have a conchoidal fracture. In addition to barely visible disseminated sulfides, a minute amount of sulfides was visible along 'fractures', up to ~1 mm in width and 15 mm in length; however, bedding is not clearly evident in the chips, and it was not certain whether the sulfides were fracture-controlled or were concentrations along sedimentary planes whose exposure merely simulated the appearance of fracture fill. The assumption was that a good indication of

overall sulfide content would be obtainable from the bulk-sample chemical analysis of wt% S, coupled with the sulfide mineralogy; therefore, to decrease the risk that the sulfide 'veinlets' might not be included in the polished thin section, 12 of the relevant chips were hand-picked and added to the otherwise random split that was subsequently gently, coarsely crushed to provide material for the optical and XRD studies.

The polished thin section contains about 25 chips, with the largest ones ranging from 5 × 7 mm to 1 × 2 mm. The megascopic color of the chips varies from brownish gray to black, and in many of them disseminated 'pin-point' sulfides are visible. One of the intermediate-size chips consists largely of sulfides.

Optical microscopy with reflected light showed that some chips, including the largest one in the section, are devoid of sulfide minerals even though at least a few disseminated grains are present in most chips. The megascopic sulfide-rich chip is shown in Figure 1, and a smaller but equally sulfide-rich chip is shown in Figure 2. These, which are the only two of their type in the section, consist of extremely fine-grained pyrite, locally accompanied by minute amounts of intimately associated marcasite. Otherwise, however, the remainder of the sulfides, i.e., the disseminated grains in all other chips, consist largely of pyrrhotite; chalcopyrite is erratically distributed and sparse, and in one chip the principal sulfide is sphalerite (Fig. 2). Relative to the microscopy observations, the chemical value of 1.06 wt% S (Table 1) seems to be high but of an appropriate order of magnitude. Much of the pyrrhotite occurs as extremely fine-grained blebs that are not readily observable at the optical magnifications typically used to estimate sulfide abundances. Even taking into account the erratic presence of the pyritiferous chips, however, the quantity of pyrite determined by the Rietveld analysis is too high (Table 2).

The fine-grained character of the siltstone is apparent in transmitted light, but quartz, muscovite, and chlorite are identifiable, and the Rietveld analysis indicates that plagioclase (albite) is abundant and that a small amount of kaolinite is present (Table 2). The siltstone could be characterized as texturally uniform except that "spotted alteration" is abundant in some chips and absent in others (Fig. 3). The spotted alteration is interpreted to be a thermal metamorphic effect and is of interest because the spots have been the loci of deposition of some of the sparse carbonates that were observed in the siltstone. The spots consist predominantly of concentrations of chlorite, but some spots consist largely of quartz (Fig. 1) and others largely of K-feldspar. A

Table 2. Quantitative mineralogy of siltstone VR71100A*

wt. %				
	quartz	28.0	kaolinite	2.2
	plagioclase	12.6	pyrite	3.9
	muscovite	37.8	pyrrhotite	3.0
	chlorite	12.5		

*Quantitative values for all samples are values normalized to 100 wt%

peculiarity of the chloritic spots is that they are not apparent in plain transmitted light but are observable with the polarizers crossed because of their low birefringence, and are most evident in reflected light (Fig. 3). A feature that attracts the eye to the spots in reflected light is that many are surrounded by a narrow rim of rutile, which has a high reflectance and a pronounced internal reflection (Fig. 4).

The NP of the siltstone sample was determined to be 14 (all NP values referred to herein are in kg $CaCO_3$ equivalent per tonne of material), which is too high for the mineral assemblage reported in Table 2. However, the presence of a small amount of dolomite in the siltstone accounts for the higher-than-expected NP value. One chip in the section contains an elongate particle of dolomite, about 150 × 500 μm, that may be fracture-controlled but whose irregular margins suggest otherwise (Fig. 5). Several much small liberated grains were also observed, and several minute grains of dolomite are associated with the spotted alteration, particularly but not exclusively those in which the chief mineral within the spots is K-feldspar or quartz (Figs. l, 4, 5). EDS spectra of the dolomite, including the elongate particle in Figure 5 and the porphyroblast-type particles in Figure 6, are consistent in their similarity; Fe and Mn are barely detectable and vary only slightly from grain to grain. A representative spectrum is shown in Figure 7. No calcite was detected, and neither the core nor a sample of pulverized material was observed to effervesce upon the addition of a calcite-reactive weak HCl solution.

Following the completion of the preceding study, the as-received sample was searched specifically for fracture-controlled carbonates. The seven selected chips were treated with alizarin solution and then with 15% HNO_3. No calcite was detected, but all reacted appropriately for the presence of dolomite. A sulfide mineral, thought to be pyrite, also occurs sparingly in fractures.

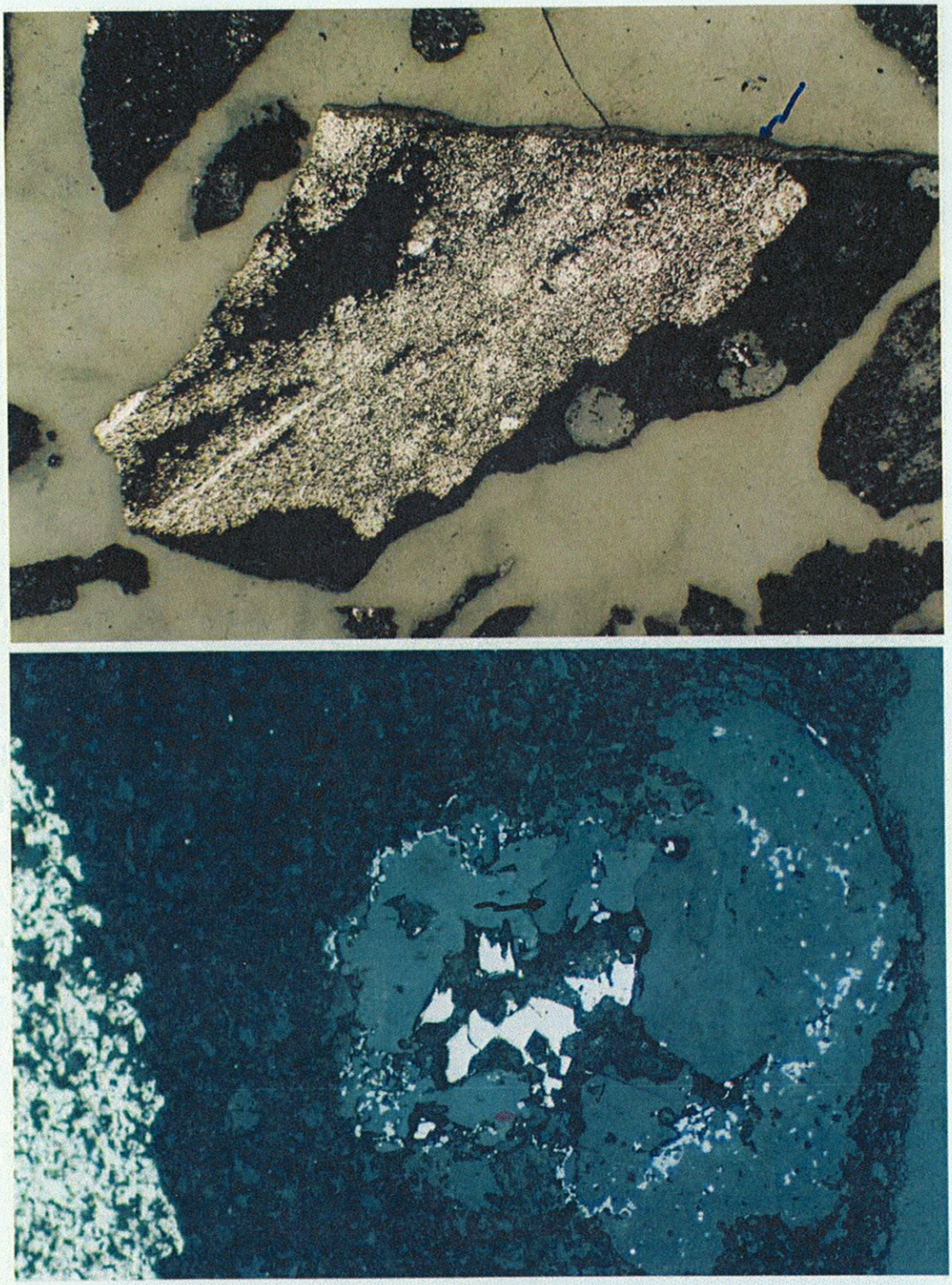


Figure 1. Siltstone VR71100A in plain reflected light. The upper photo (width of field 5.6 mm) shows the most sulfide-rich chip in the polished thin section. The sulfide is fine-grained pyrite (as is evident along the left margin of the lower photo). Below and right of center are two circular bodies ('spots') consisting mainly of quartz, and along the top of the chip is an almost horizontal, crosscutting veinlet of chlorite (arrow). The lower photo, width of field 0.625 mm, is of the 'spot' on the right in the upper photo. The slightly pinkish white mineral at the core is pyrrhotite; most of the outer mass consists of quartz with blebs of rutile, but a few grains of dolomite are present (e.g., at arrow).

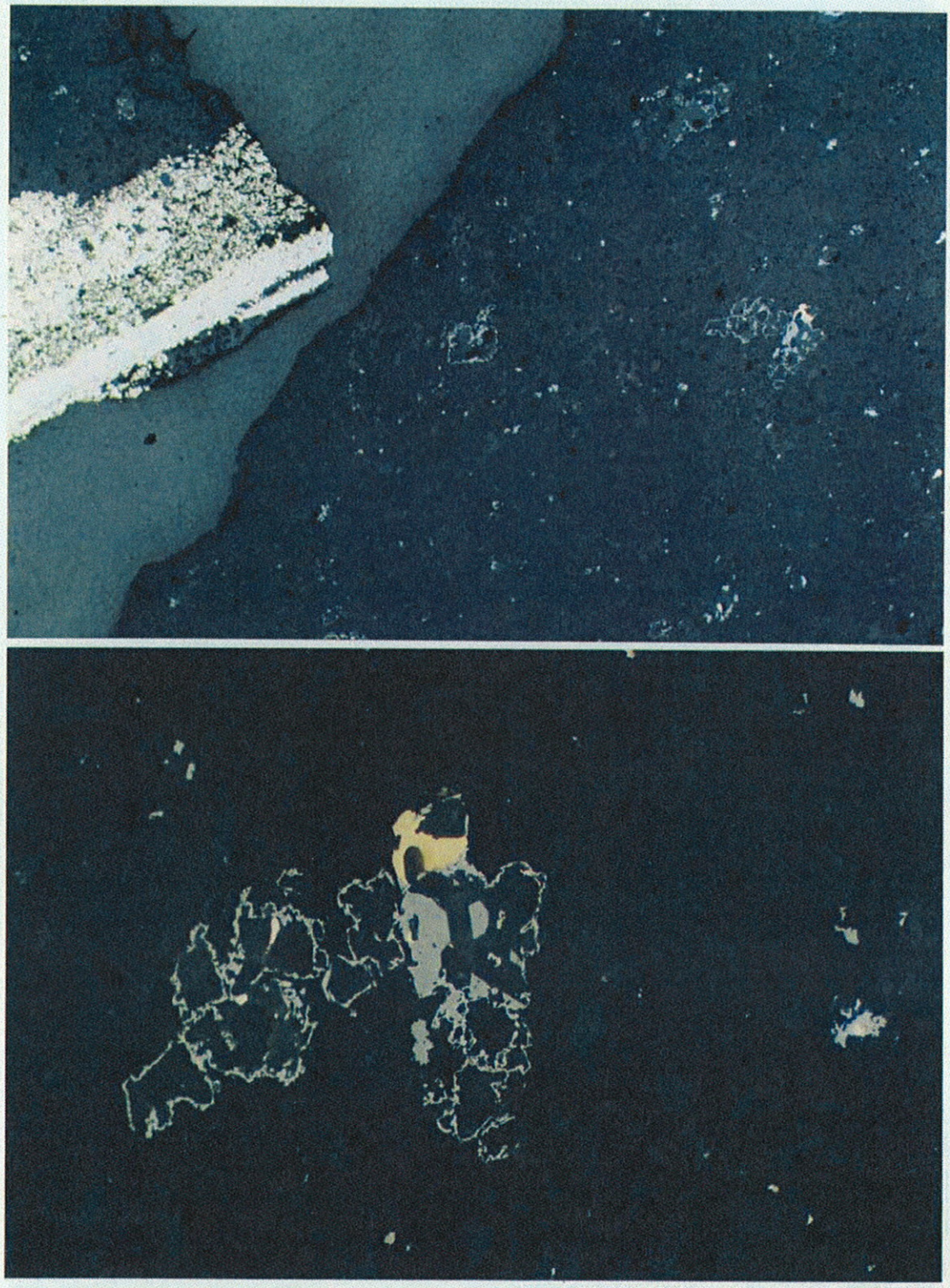


Figure 2. Siltstone VR71100A in plain reflected light, width of field 2.6 mm, showing on the left the only other pyritiferous chip in the section. In the much larger chip to the right of the pyrite, chloritic spots are outlined by a gray mineral, which typically is rutile but in this chip is sphalerite. The lower photo is an enlargement (width of field 0.625 mm) of the area at mid-height on the far right of the upper photo, showing yellow chalcopyrite and grayish rims of sphalerite. EDS spectra indicate that the sphalerite contains a minor amount of Fe.

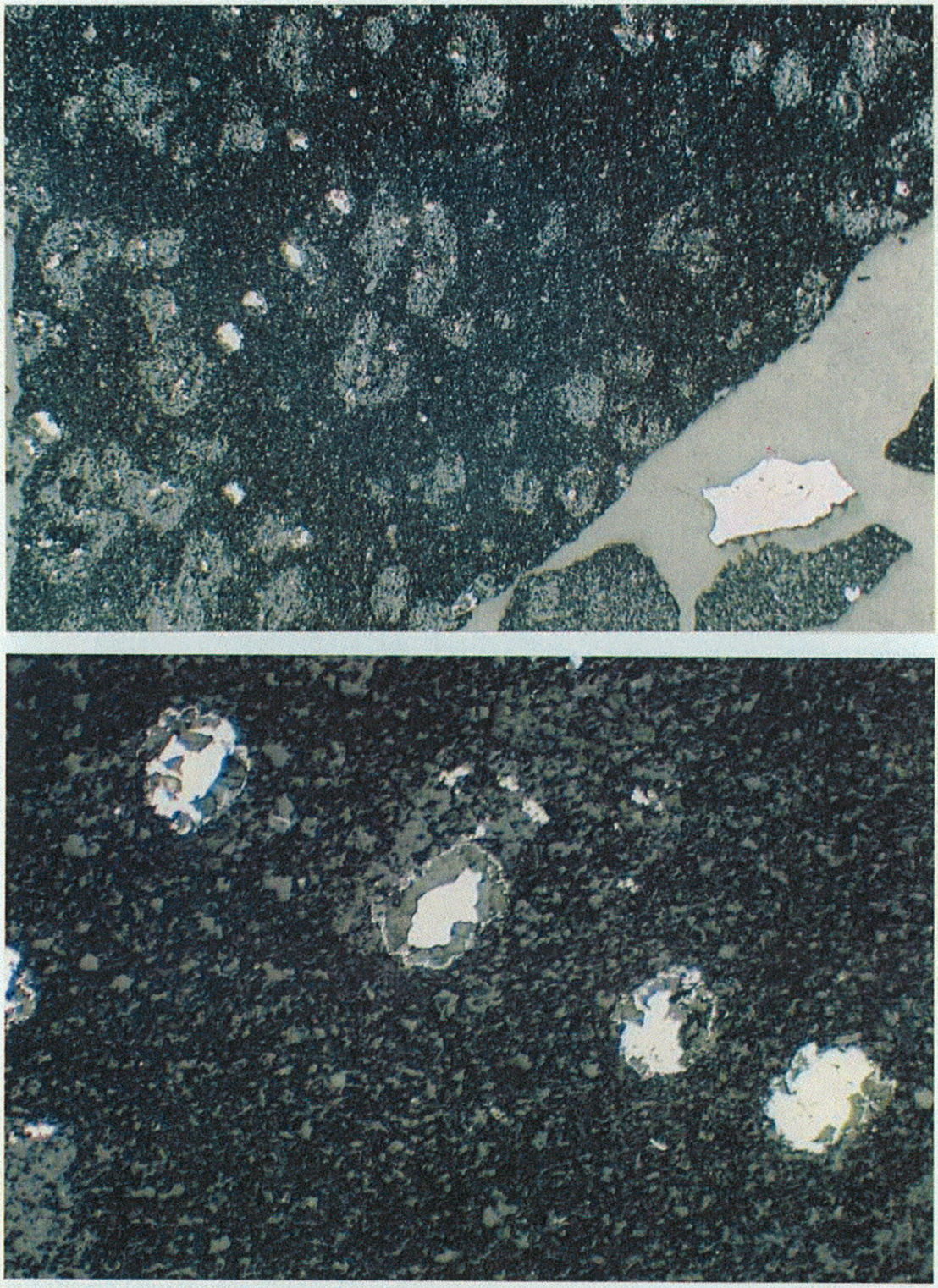


Figure 3. Siltstone VR71100A in plain reflected light. Upper photo, width of field 2.6 mm, shows the extensive spotted alteration, here mainly chloritic, that is present in some chips. The whitish grain at the bottom right is pyrrhotite whose large size is not in conformity with the siltstone assemblage. The lower photo is an enlargement (width of field 0.625 mm) of the train of pyrrhotite grains to the left of center and trending northeasterly in the upper photo. Pyrrhotite (white) at the cores of spots is surrounded by chlorite (dark) which in turn has a narrow rim of rutile (grayish white).

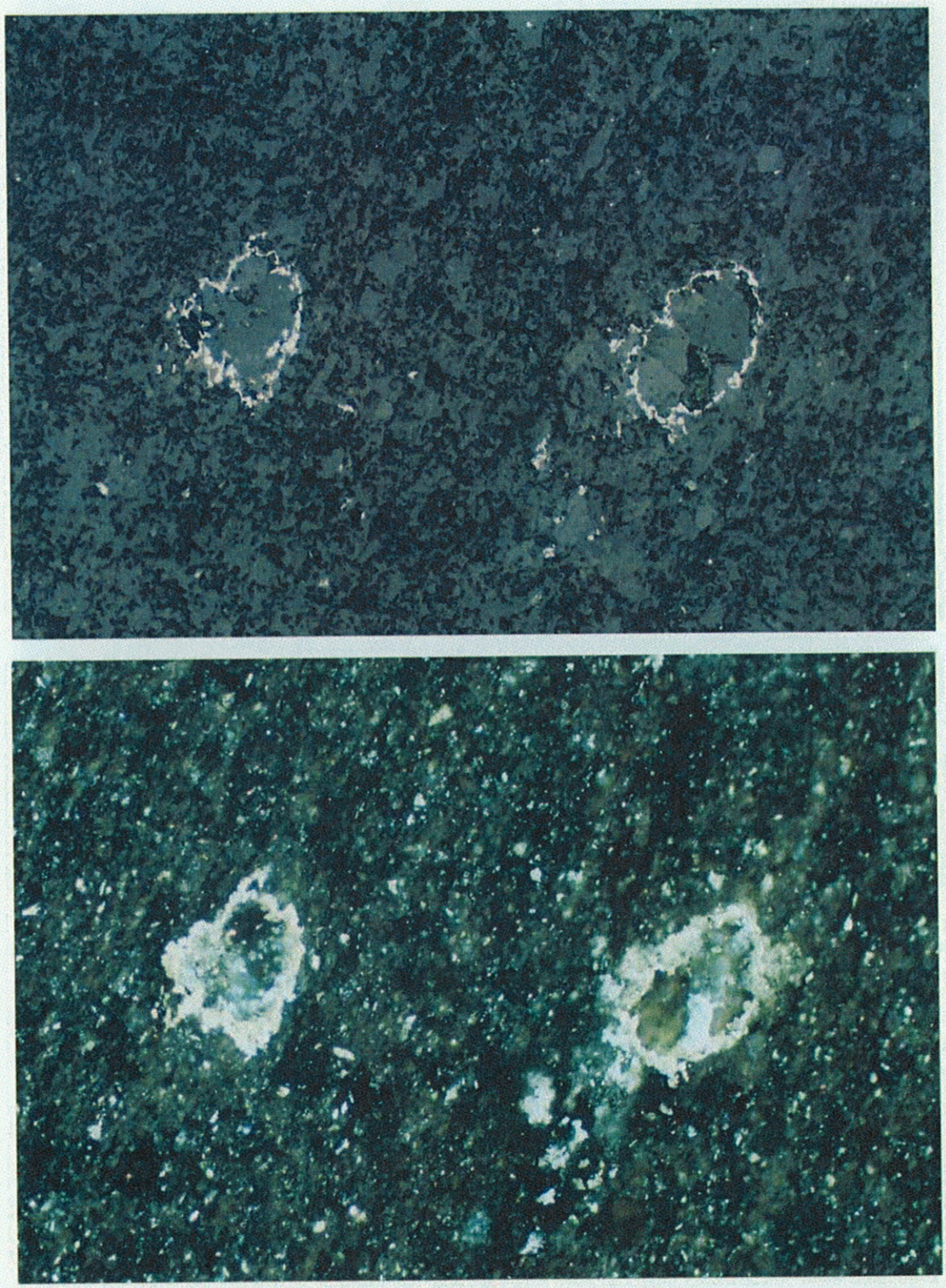


Figure 4. Siltstone VR71100A in plain reflected light (top) and the same field with polarizers almost crossed and internal reflection (width of field 0.625 mm). The core mineral in this case is K-feldspar, accompanied by minor chlorite, and the bright outer rim of rutile has distinct internal reflection.

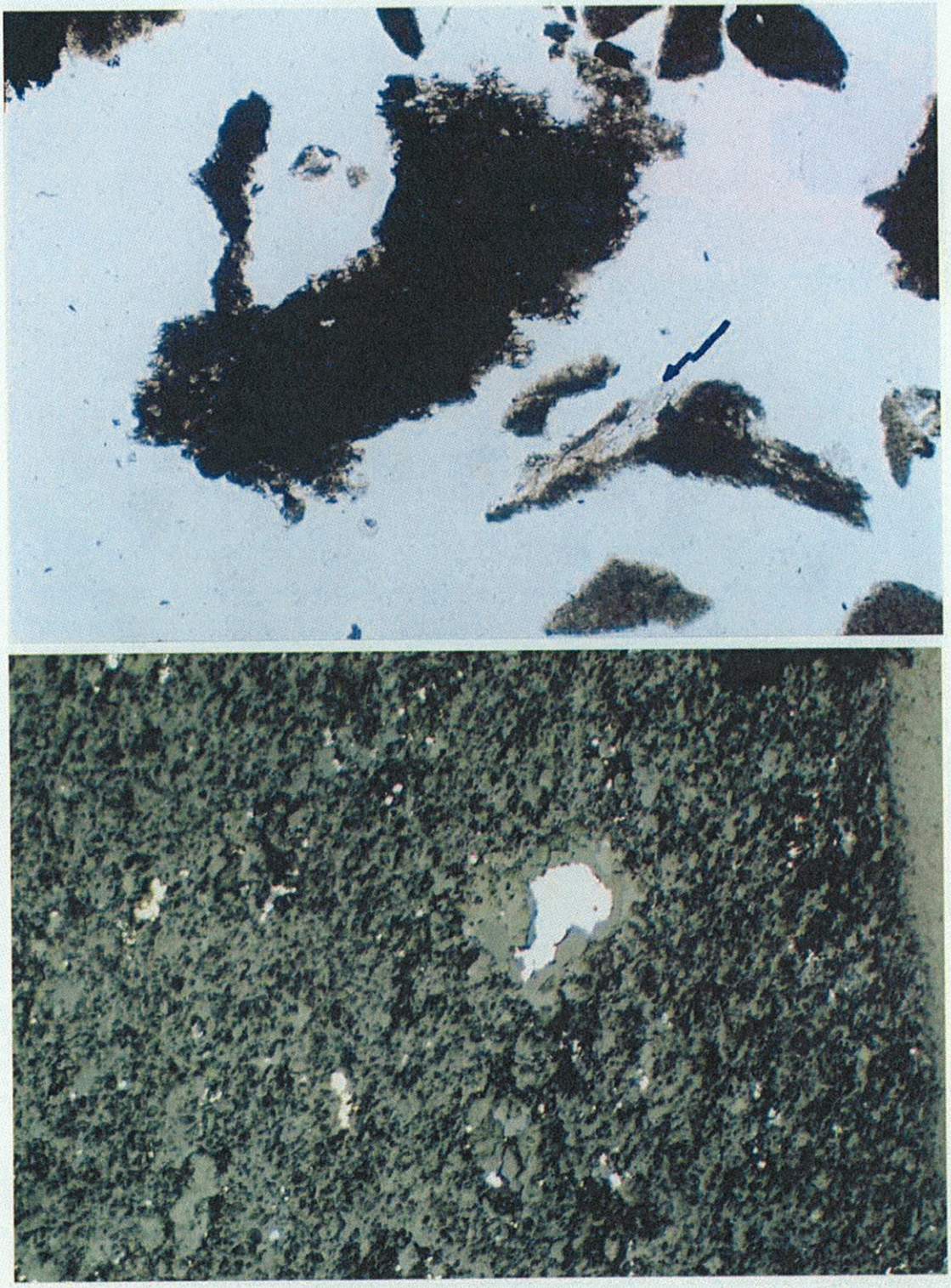


Figure 5. Dolomite occurrences in siltstone VR71100A. The upper photo in plain transmitted light, width of field 2.6 mm, shows an elongate clot or possible veinlet of dolomite (colorless feature at arrow). The lower photo, in plain reflected light, width of field 1.3 mm, shows a 'spot' in which the pyrrhotite core (white) is in direct contact with a dolomite rim, which in turn is partly surrounded by chlorite.

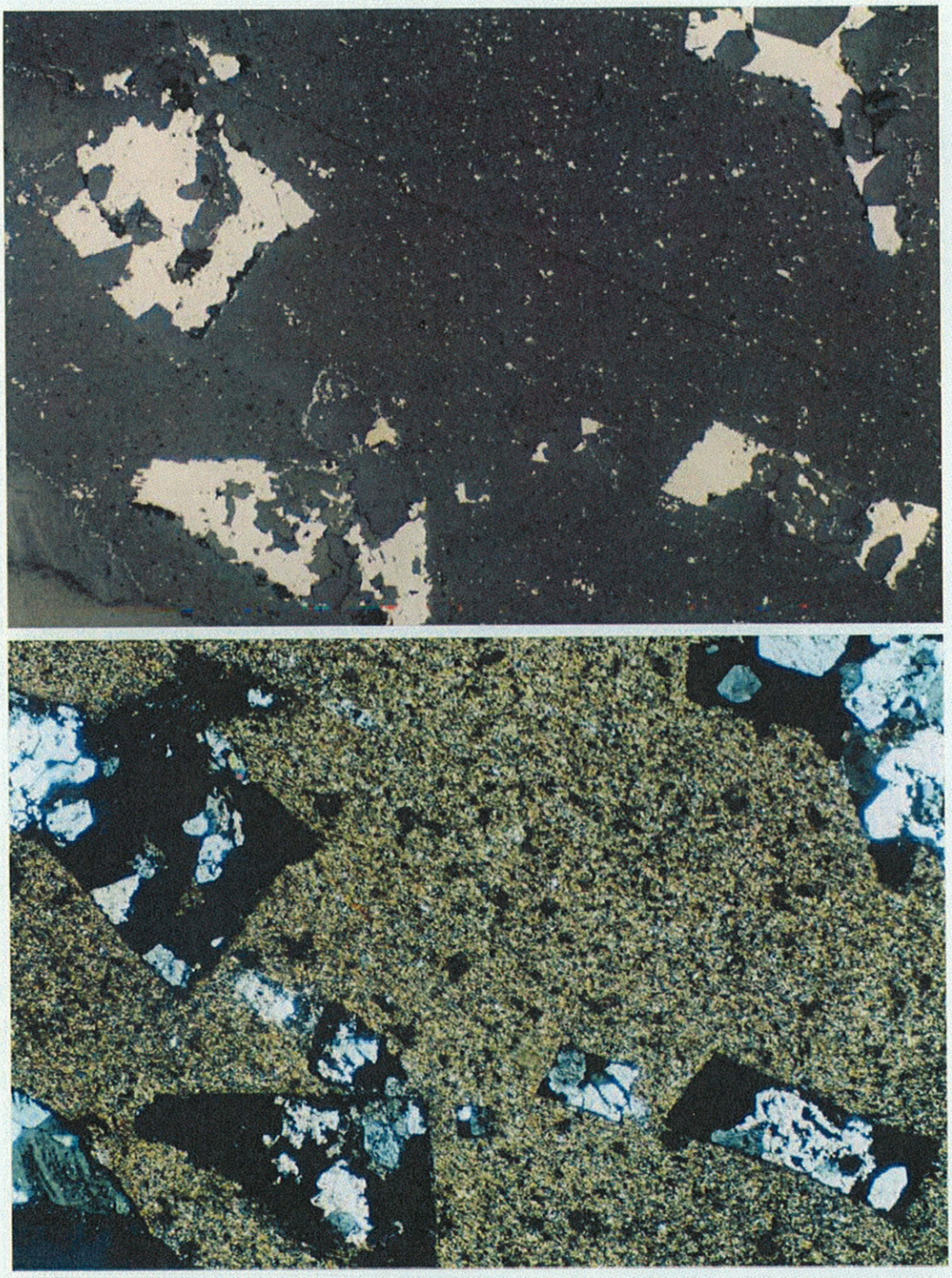


Figure 6. Porphyroblast-type development in siltstone VR71100A, width of field 2.6 mm. The upper photo in plain reflected light shows abundant pinkish white pyrrhotite accompanied by smaller, yellow grains of chalcopyrite. The lower photo is of the same field in transmitted light with crossed polarizers. The well-formed, coarse-grained, pseudomorphs of porphyroblasts consist of pyrrhotite (opaque), quartz, K-feldspar, and dolomite. The irregular, whitish mineral making up the bulk of the non-opaque portion of the rectangular porphyroblast pseudomorph at the bottom right corner is dolomite.

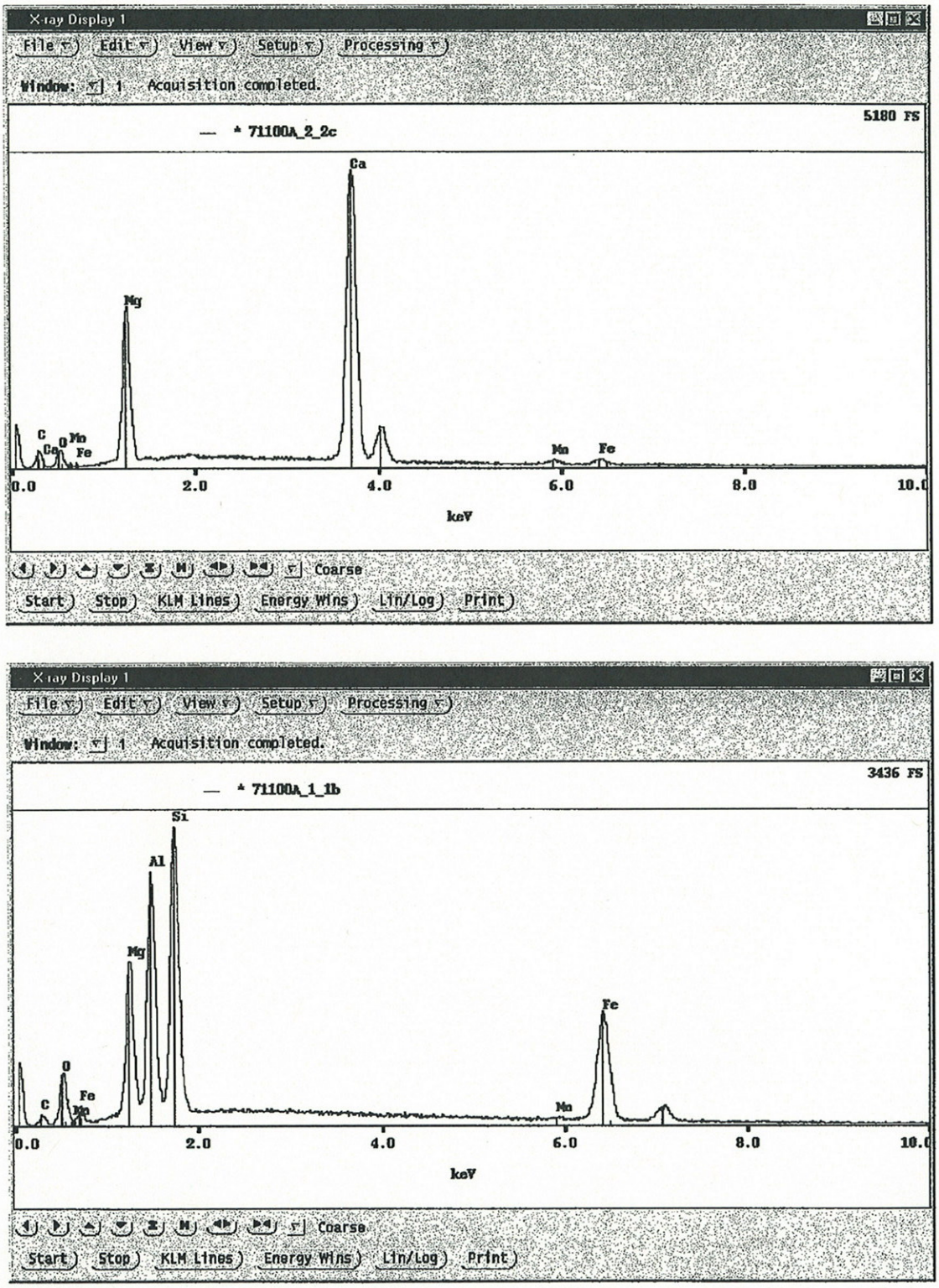


Figure 7. EDS spectra, siltstone VR71100A. The upper spectrum is typical for dolomite in the sample. The lower spectrum shows the typically Fe-rich character of the chlorite.

Sample VR71120A

Sample VR71120 consists of massive sulfides. The core is pyrrhotite-rich, strongly magnetic, and the exterior shows abundant chalcopyrite, including a largely monomineralic patch about 2 cm across. The cut faces also show abundant, large irregular concentrations of chalcopyrite, and on the cut faces the chalcopyrite is elongate to sinuous, with a poorly developed elongation along the core length. The segregation of the chalcopyrite into relatively large patches, in contrast to dissemination, seems to be a characteristic feature.

A random split of the crushed sample, including the fines, was taken for the mineralogical study. The largest chip in the polished thin section is about 20 × 5 × 5 mm, but most of the larger ones are approximately 4 to 5 mm in diameter. Microscopic examination revealed the assemblage to consist of massive sulfides wherein pyrrhotite, pentlandite, and chalcopyrite are accompanied by a much smaller amount (~5%) of magnetite, and the four minerals make up at least 99% of the mineral assemblage. The striking feature is the high sulfide-mineral content, which is at least as great as that of some sulfide concentrates. The bulk of the sulfides occurs as large anhedral grains with uncomplicated contacts (Fig. 8). A volumetrically minute proportion of the pentlandite is present as flame-like intergrowths in pyrrhotite, but not in chalcopyrite, and a small amount of chalcopyrite is present as oriented, rod or lath-like intergrowths with pyrrhotite (Fig. 8). Most of the magnetite is present as anhedral, rarely subhedral, grains that are included within chalcopyrite or at its grain boundaries, but the association is not exclusive and is only less common in pentlandite and pyrrhotite. Magnetite also occurs as narrow veinlets that cut all three sulfides.

The relative abundances in the section are pyrrhotite > chalcopyrite > pentlandite > magnetite, with pyrrhotite making up about half the total sulfide content. Minute amounts of cubanite and violarite were detected by Jago (2002) in some of the Eagle sulfide-rich samples, but the minerals were not observed in the VR71120A section. Extensive microprobe analyses of pyrrhotite in three head samples (Lane 2002) gave means of (wt%) 0.66 Ni and 0.01 Co (n = 100), 0.36 Ni and 0.00 Co (n = 100), and 0.58 Ni and 0.01 Co (n = 99).

From the perspective of reconnaissance environmental mineralogy, little can be added to the brief description given above. The content of potential NP contributors is negligible, and the application of HCl to a portion of the powdered sample did not yield any effervescence.

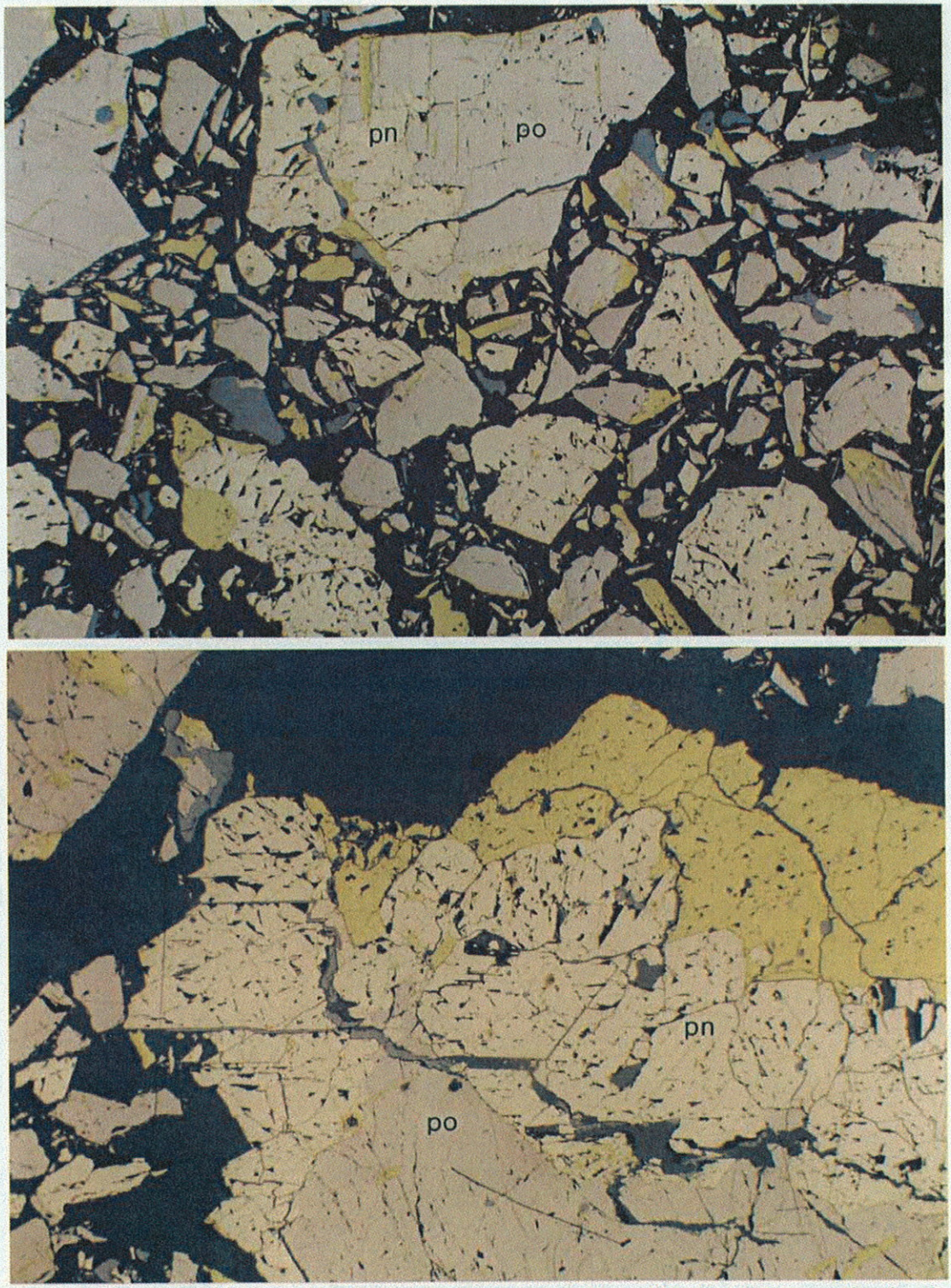


Figure 8. Massive sulfide sample VR71120A in plain reflected light, width of field 5.1 mm, showing the sulfide-rich character of the sample. The yellow mineral is chalcopyrite, the smooth, slightly pinkish mineral is pyrrhotite (**po**), which in the largest particle in the upper photo contains vertically aligned laths of chalcopyrite, and the whitest, characteristically pitted mineral is pentlandite (**pn**). The gray mineral is magnetite, which occurs as anhedral grains and veinlets.

Sample VR71213A

The sample is of peridotite, which in the core is massive and uniformly coarse-grained. The as-received crushed sample contained only a small proportion, estimated to be <10%, of fines. The sample was split in half, and because the size of the larger chips was such that only two or three could be accommodated in a polished thin section, one of the halves was further crushed and the resulting minus 5 mm fraction was used for the mineralogy study.

Megascopic examination of the polished thin section did not indicate the presence of sulfides; although numerous high-reflectance disseminated opaque grains of up to half a millimeter across were observed, these were of a steel-grey color and subsequently were determined to be magnetite and ilmenite. Sulfide grains observed microscopically proved to be mainly of pyrrhotite, the largest about 100 μm across. Pentlandite occurs as isolated anhedral grains, but most are attached to pyrrhotite or intergrown with it; flames of pentlandite within pyrrhotite were observed but are rare. Chalcopyrite is present in only trace amounts, hence pyrrhotite >> pentlandite >> chalcopyrite. The sulfide content was estimated to be ~0.1%, with pyrrhotite accounting for >90% of the total.

Transmitted-light microscopy revealed that olivine and clinopyroxene are the principal silicate minerals. Even though much of the olivine has been altered to serpentine, the residual olivine still optically exceeds the abundance of clinopyroxene. Accessory orthopyroxene is present, but the amount is insufficient to be quantified in the Rietveld mineralogy (Table 3). Comparison of the qualitative optical impressions and the quantitative Rietveld data gave some unexpected differences, most notably in the high proportion of magnetite and chlorite detected by the X-ray data. Almost all, if not all, of the large opaque grains in the section are ilmenite rather than magnetite; much smaller grains of primary magnetite are common but would account for no more than about 2% magnetite. However, alteration of olivine has released solid-solution Fe that formed abundant blebs and veinlet-like trains of magnetite in serpentine (Figs. 9, 10), which is the predominant form of magnetite in the section.

Table 3. Quantitative mineralogy of peridotite VR7123A

wt%				
	olivine	18.4	amphibole	4.0
	clinopyroxene	13.9	talc	10.8
	magnetite	8.4	lizardite	9.2
	plagioclase	10.6	chlorite	20.6
	biotite	4.0		

Chlorite occurs abundantly as an alteration of biotite, but also replaced olivine and, to a much lesser extent, pyroxene (Figs. 10, 11). Talc occurs typically at the periphery of mesh-texture, serpentinized olivine. The serpentine was identified by XRD as lizardite, all of which is extremely fine-grained, polycrystalline, and non-fibrous. The serpentine species that has the well-known commercially utilized fibrous habit is clinochrysotile rather than lizardite, but no fibrous veinlets, even on a microscopic scale, were observed.

The measured NP of VR71213 is 42, which even in the presence of olivine and serpentine, is too high unless carbonates are present. In a HCl test of the powdered bulk sample, several pinpoint areas gave the strong and instantaneous effervescence characteristic of calcite. Several calcite-bearing areas were identified optically, the most notable a large homogeneous grain about 100 × 250 to 300 μm, which may have been even larger prior to crushing of the sample (Fig. 12). More typical, however, are minute, polycrystalline aggregates of the type shown in Figure 13. Tests with alizarin solution indicated that all of the carbonate occurrences are calcite, and EDS spectra indicate that the mineral is near the end-member in composition.

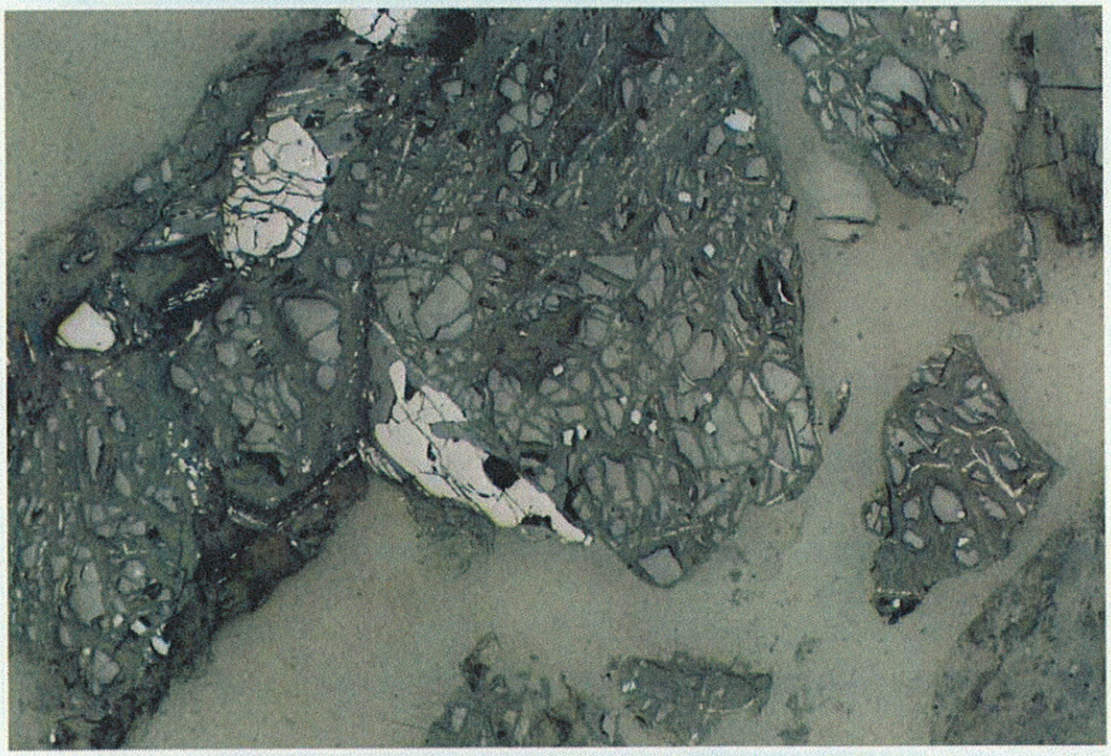


Figure 9. Peridotite VR71213A in plain reflected light, width of field 2.6 mm, showing the typical texture of residual 'islands' of largely replaced olivine. The large, pale gray, high-reflectance grains are ilmenite, and between the olivine islands are thread-like trains of magnetite that formed by alteration of the olivine. Immediately to the right of the large ilmenite grain below center is a group of similarly whitish, small anhedral grains of primary, non-alteration magnetite.

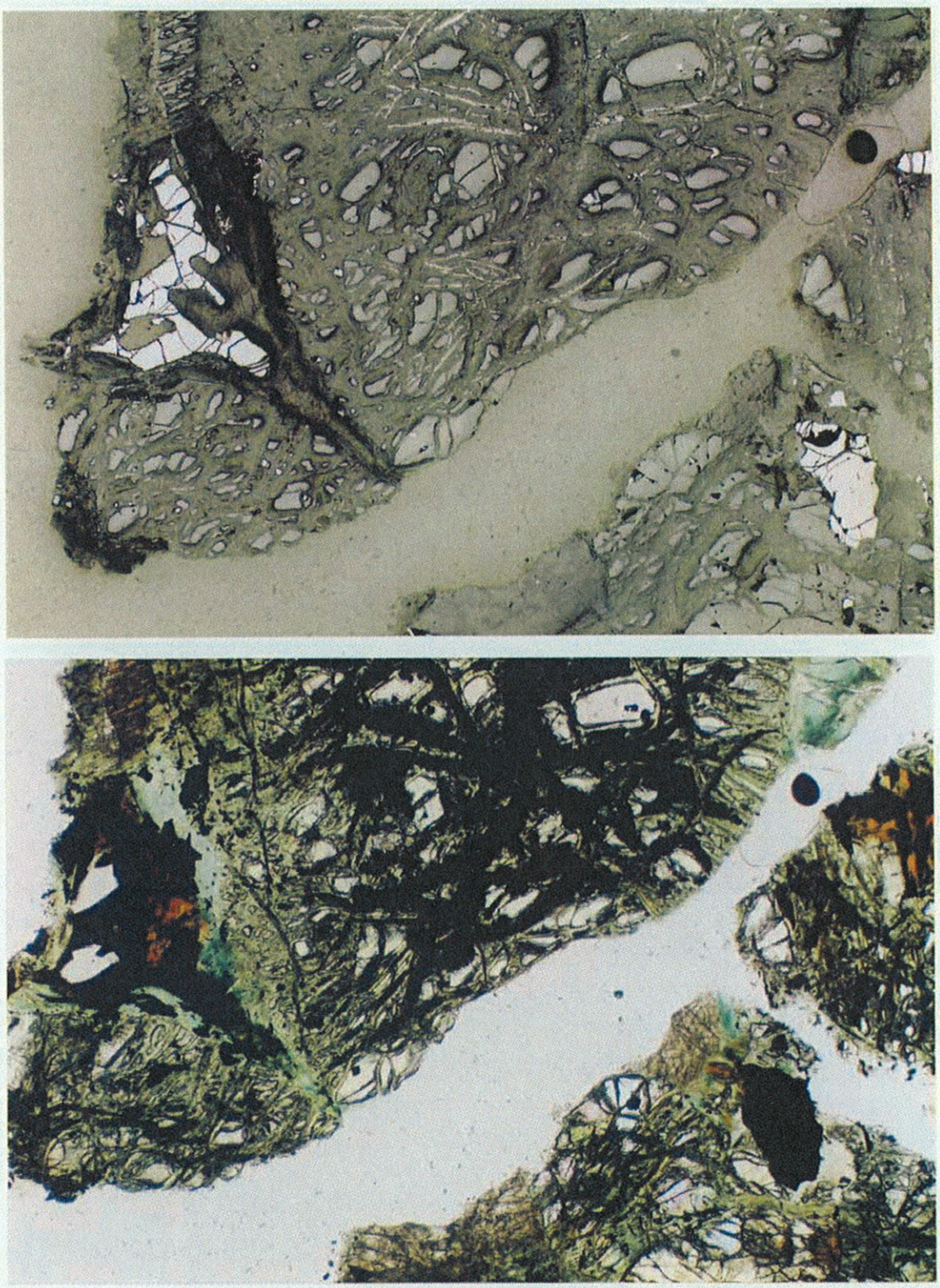


Figure 10. Peridotite VR71213A in plain reflected light (top) and the corresponding field in plain transmitted light (bottom), width of field 2.6 mm. The large, high-reflectance grains are ilmenite, and amidst the residual islands of olivine is thread-like magnetite. In the lower photo, the residual olivine is colorless, the brown mineral is biotite, and the green mineral is chlorite.

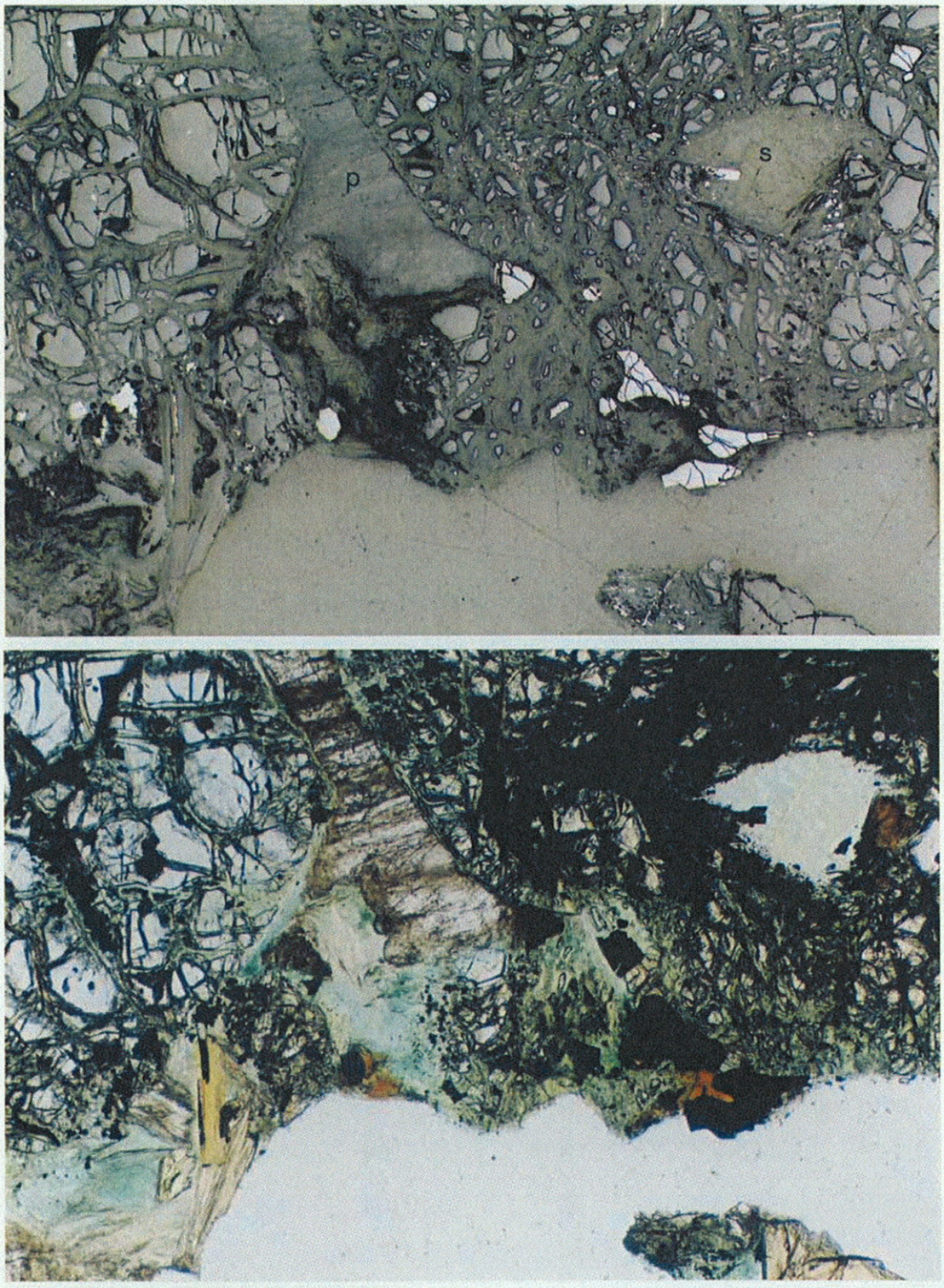


Figure 11. Peridotite VR71213A in plain reflected light (top) and the corresponding field in plain transmitted light (bottom) and with polarizers crossed (next page), width of field 2.6 mm. The high-reflectance grains are ilmenite, and between the residual islands of olivine is plagioclase (**p**). Within the pocket of serpentine (**s**) is a small, white, tabular grain that consists of pyrrhotite rimmed by pentlandite. In the lower photo, biotite is brown, chlorite is green, and the serpentine is colorless.

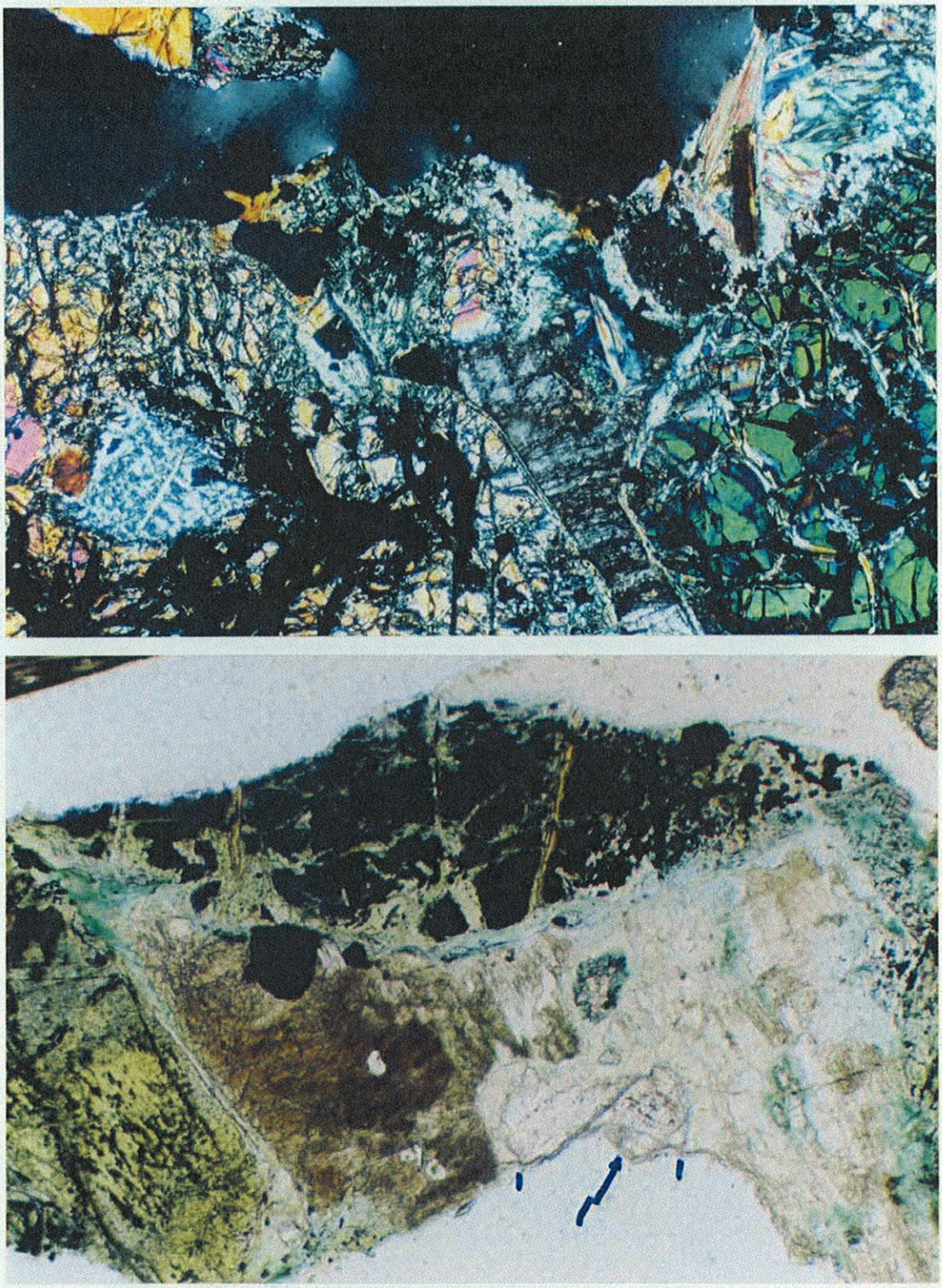


Figure 12. Peridotite VR71213A. Upper photo is the continuation of Figure 11, but with polarizers crossed. The lower photo, in plain transmitted light, width of field 1.25 mm, shows a large grain of calcite, 250 to 300 μm long (at arrow, with margins indicated), within chlorite and serpentine.

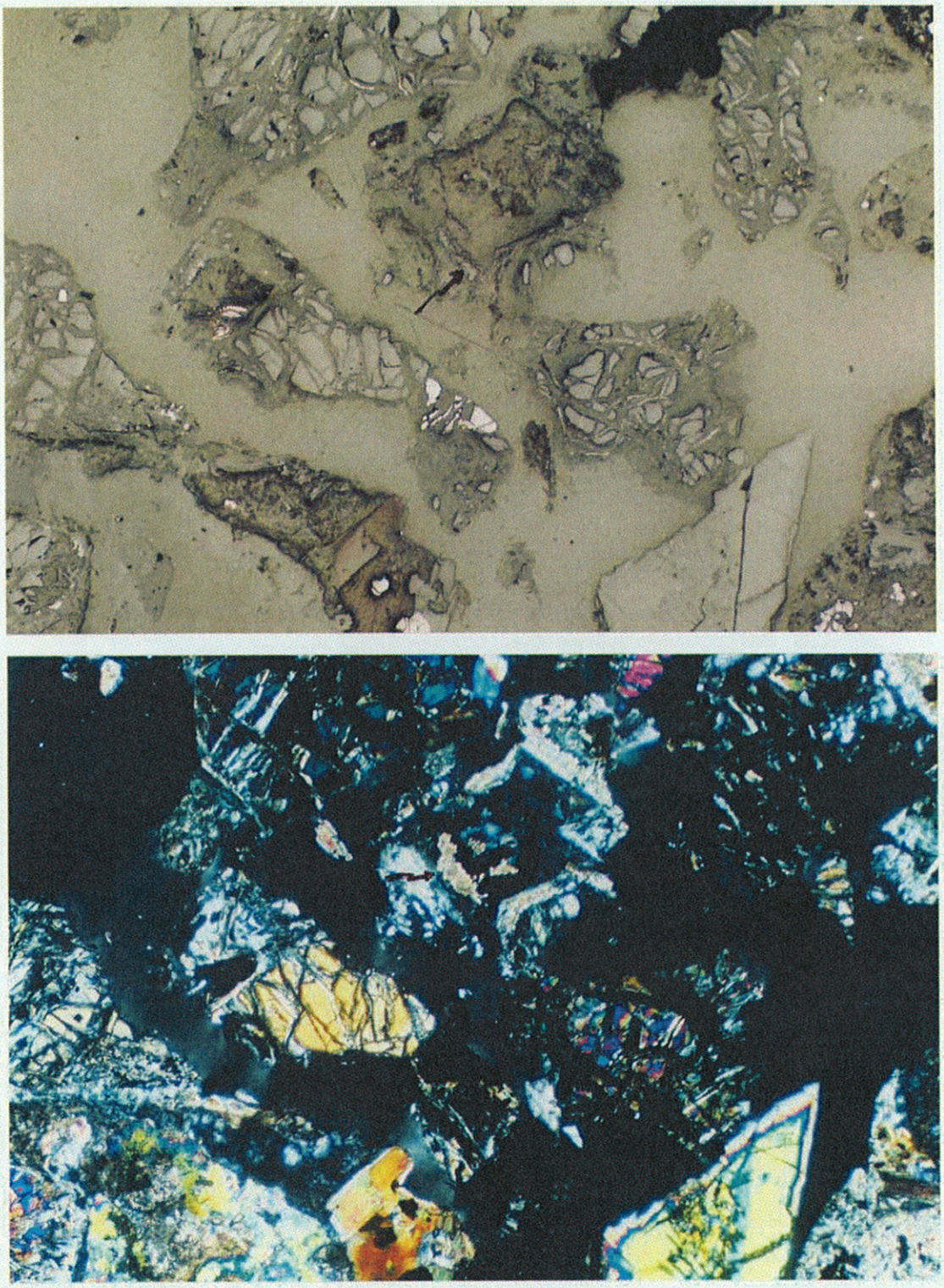


Figure 13. Peridotite VR71213A in plain reflected light (top), and the same area in transmitted light with polarizers crossed, width of field 2.6 mm. The arrow near the center in both photos points to the typical habit of occurrences of calcite, which is as fine-grained, irregular aggregates within serpentine (here, mainly black and enclosed within a narrow rim of talc).

Sample VR71325A

The sample is reported to be of net-texture sulfides in peridotite (Table 1). The core is similar in appearance to that of peridotite VR71213A except that a major amount of pyrrhotite-rich sulfides is evenly distributed throughout the network sample. The sulfides are of millimetric size, of irregular outline, and commonly form rims or partial rims on the original coarse-grained mafic minerals, thus resulting in the network arrangement. For the mineralogical study, the original crushed sample was split in half, and one of the halves was gently crushed only to reduce the size of the largest chips. This re-crushed fraction was then split, and one of the halves, including the fines, was used for the mineralogical study.

Transmitted-light microscopy revealed some significant differences from the peridotite, most notably in the decrease in residual 'island' or mesh-type olivine, and in the commensurate large increase in the amount of serpentine (Figs. 14, 15). Other minerals, such as plagioclase, biotite that has been partly altered to chlorite, and brownish amphibole replacement of clinopyroxene, are present in accessory amounts but are of insufficient abundance to have been detected in the Rietveld analysis. The result is a much simpler and 'cleaner' mineralogy that, in transmitted light, lacks the optically complex intergrowths and turbidity observed in the peridotite. In that regard, a notable difference is the absence of quantifiable chlorite and talc (Table 4), which are major minerals in the examined sample of peridotite.

The sulfide mineralogy is like that of the massive sulfides insofar as pyrrhotite, pentlandite, and chalcopyrite are the represented species. The pyrrhotite differs in that, in contrast to its characteristically smooth, uniform appearance in the massive sulfides, in the network sample almost all of the grains are fractured; nonetheless, the fractures are relatively widely spaced and broad, and the distinction from the denser and more complex pattern in pentlandite is still readily apparent. That the fractures in the pyrrhotite are not polishing or handling artifacts is confirmed by the presence of serpentine as the infill. The pyrrhotite lacks the rod-shaped intergrowths with chalcopyrite (as in Fig. 8), and whereas flame-like intergrowths of pentlandite in pyrrhotite have been observed, especially at the grain boundaries of pyrrhotite, such intergrowths are uncommon. Unlike the massive peridotite? sulfide sample, wherein the large, megascopically visible oxide mineral is ilmenite, in the network-texture sample the oxide mineral is magnetite. The major part of the very high magnetite content (12 wt%, Table 4) is attributable to the thread-like occurrences of serpentine that has been derived by the alteration

Table 4. Quantitative mineralogy of network-sulfide sample VR71213A

wt%	olivine	6.2	pyrrhotite	37.4
	lizardite	27.0	pentlandite	8.8
	clinopyroxene	5.2	chalcopyrite	3.4
	magnetite	12.0		

of olivine.

The measured NP of the network-sulfide sample is 41 (Table 1), which is regarded here as to high because, in the absence of carbonate minerals, nearly all of the NP would have to be derivable from olivine and lizardite; thus, because of the high proportion of sulfides and magnetite in the sample (assuming them for NP purposes to be inert), the magnitude of the NP values assignable to each of olivine and lizardite would have to be at least 100. A test with HCl on a portion of the powdered sample did not yield visible effervescence, and other than an uncertain trace of carbonate alteration within a grain of plagioclase, carbonates were not observed microscopically. It is important to note that the statement that the measured NP value is 'too high' does not imply that the sample was incorrectly processed or erroneously measured; several explanations can be offered as to how such values can be achieved while adhering to the Sobek test protocol. However, the topic is probably immaterial because the rock is most likely to be processed as ore.

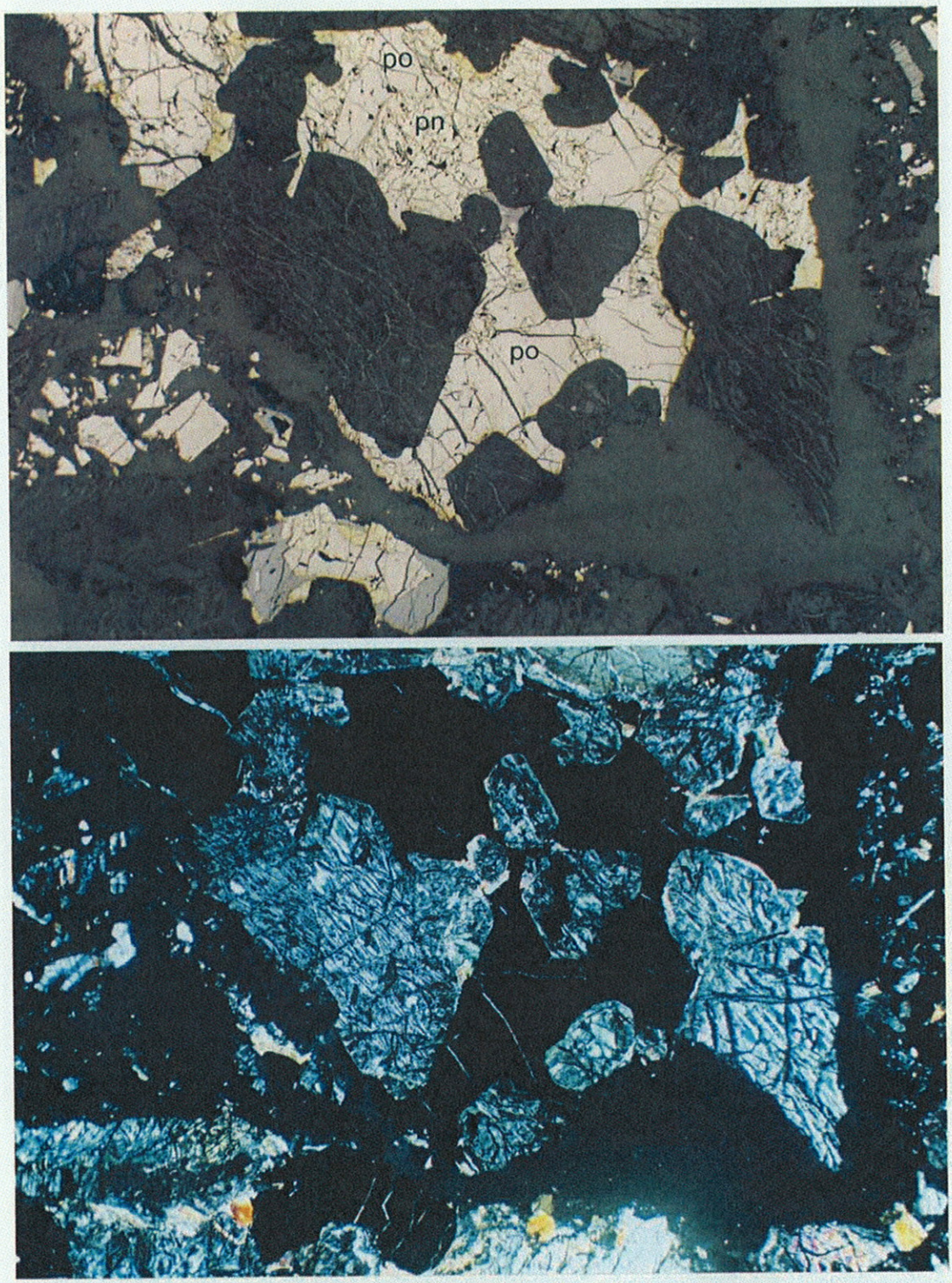


Figure 14. Sample VR7325A (network-texture sulfides) in plain reflected light (top) and the same field in transmitted light with polarizers crossed (bottom), width of field 5.1 mm. The upper photo shows the well-defined crystal outlines of former olivine grains, now consisting of serpentine with abundant threads of magnetite, and the inter-crystal occurrence of the sulfides: chalcopyrite (yellow), coarsely fractured pyrrhotite (smooth surface, **po**), and the more densely fractured pentlandite (**pn**). The gray mineral at the bottom is magnetite. The lower photo shows the pseudomorphism of olivine by the almost monomineralic serpentine.

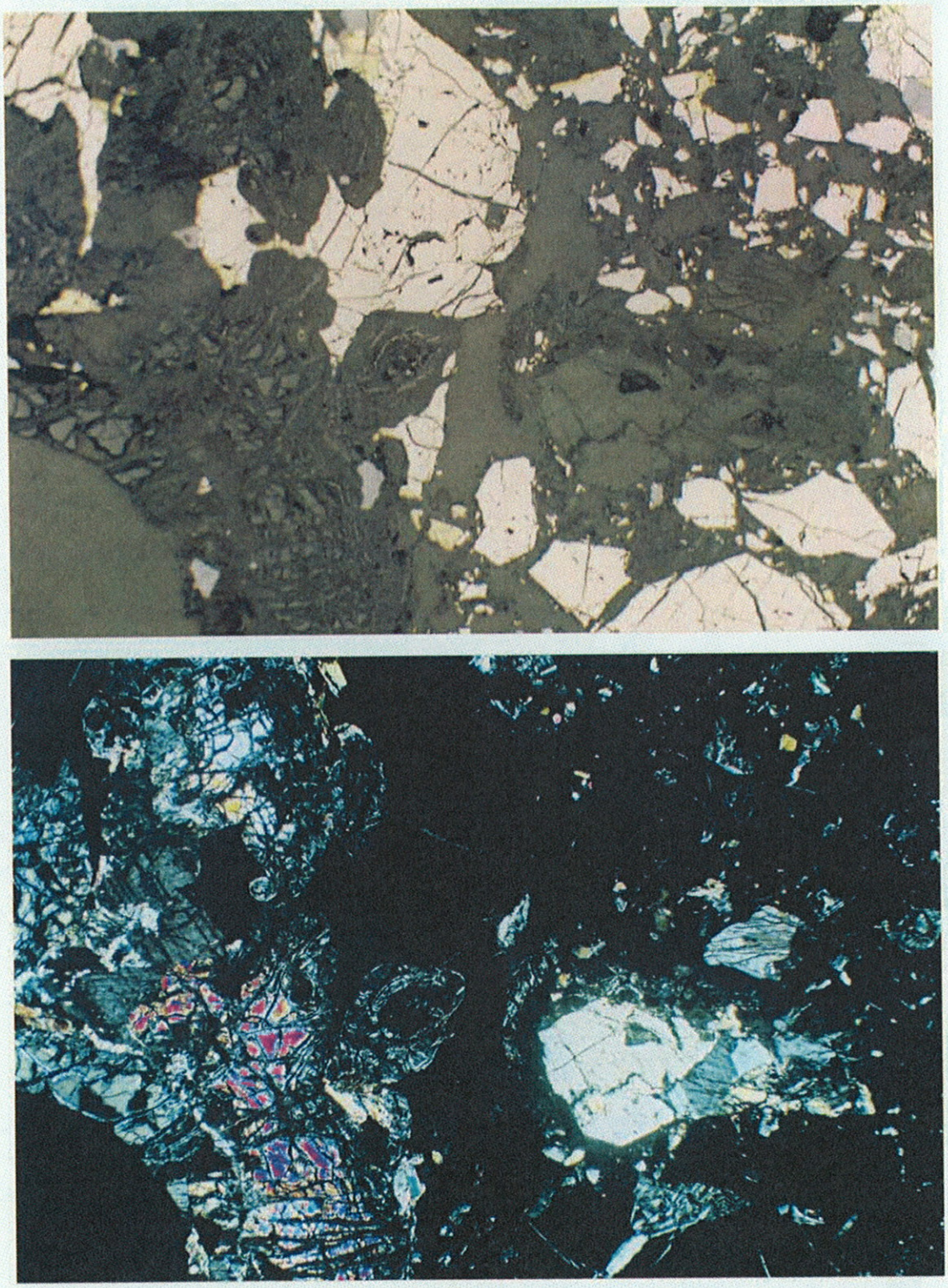


Figure 15. Sample VR7325A (network-texture sulfides) in plain reflected light (top) and the same field in transmitted light with polarizers crossed (bottom), width of field 5.1 mm. The main sulfides are pyrrhotite and chalcopyrite. The lower photo shows residual islands of olivine (violet) on the left, and clinopyroxene on the right.

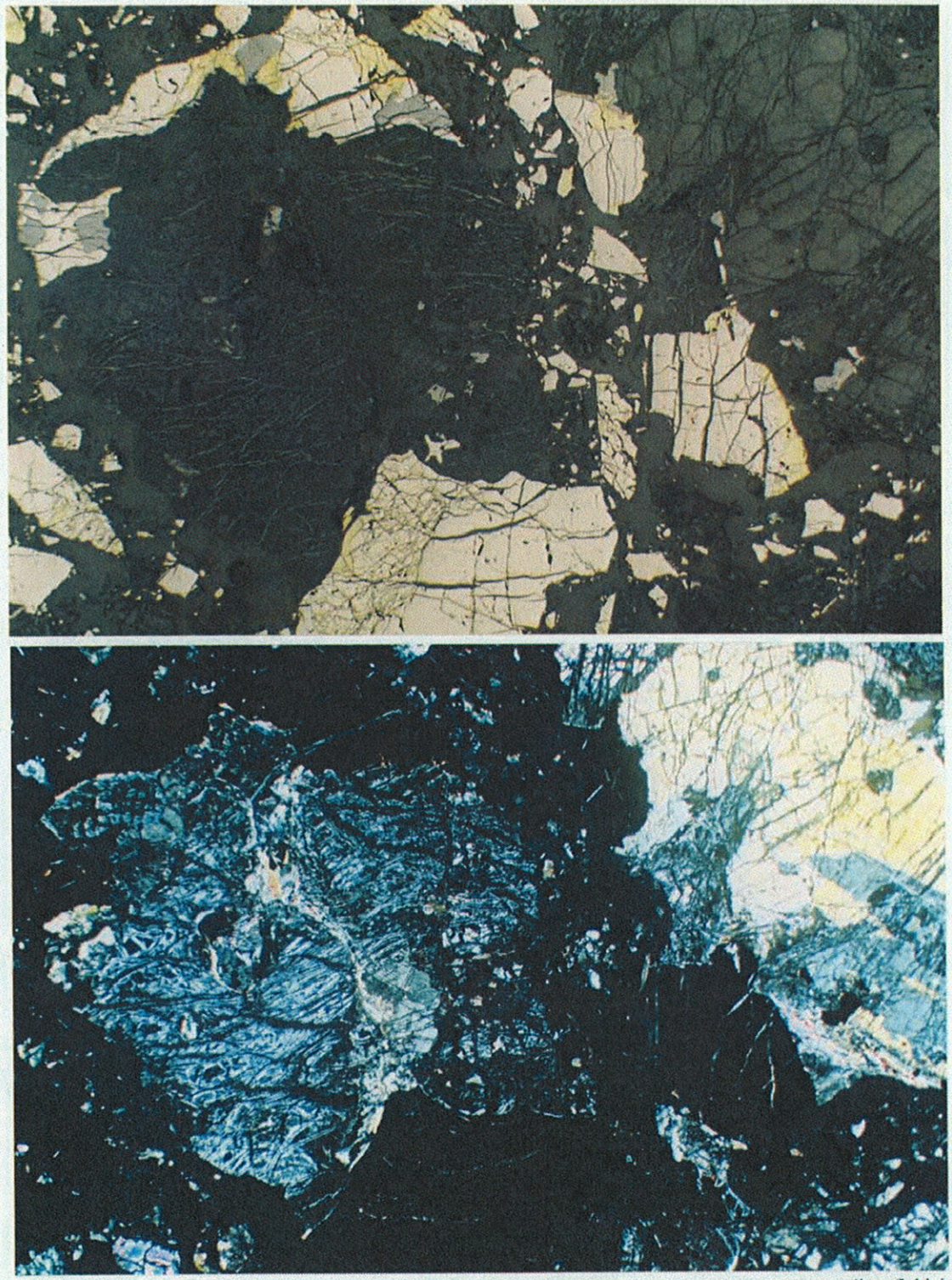


Figure 16. Sample VR7325A (net-texture sulfides) in plain reflected light (top), and the corresponding field in transmitted light and polarizers crossed, width of field 5.1 mm. At the top left (upper photo) are pyrrhotite, chalcopyrite, and magnetite; at the bottom is a large particle of pyrrhotite with attached (on its left) pentlandite (and chalcopyrite). The fracture fill in the pyrrhotite is serpentine. In the lower photo, the area on the left is serpentine, within which (below and left of the photo center) is an aggregate of grayish, twinned plagioclase. At the upper right, the large yellowish particle is clinopyroxene.

Sample VR71499A

The sample is designated as footwall siltstone (Table 1). The core is black and massive, with evenly disseminated sub-millimetric sulfides (~1%). Only two spots of aggregation of the sulfides are evident, and in those the sulfides are loosely clustered in areas of about 2 mm in diameter rather than compactly aggregated. One end of the core has a broken, sharply irregular surface, but the other end is a smoothly planar fracture surface at a low angle to the core length. Residual fracture-fill material, <1 mm in thickness, partly coats the surface. The material effervesces strongly in HCl, and a test with alizarin solution confirmed that calcite is the principal mineral.

For the mineralogical study, the crushed sample was split in half, and one of the halves was gently crushed to reduce the size of the largest chips. Half of the resulting product, including the fines, was used for the mineralogy. Prior to the optical examination, a HCl test of a small portion of the sample gave a vigorous effervescence at one spot and a slow effervescence at two others, thus indicating that calcite is present, that the carbonates are unevenly distributed, and that possibly more than one type of carbonate mineral is present.

Most of the chips in the polished thin section are gray, but a few are black, and the minute grains of disseminated sulfides visible in the core are also megascopically visible in the chips. The optical microscopy revealed that the rock is fine-grained and similar to the hanging-wall siltstone, including the presence of chloritic spotted alteration (Figs. 17, 18). Rutile rims are present but are less conspicuous than in the hanging-wall siltstone. The Rietveld-determined quantitative mineralogy of the two siltstones (Table 5) shows a remarkable similarity in the abundances of the non-sulfide minerals. A few anomalously coarse-grained non-siltstone particles, among which are olivine, pyroxene, and peridotite, are present but quantitatively are no more than a trace amount of the total assemblage.

Table 5. Comparison of the quantitative mineralogy of the hanging-wall (VR71100A) and footwall (VR71499A) siltstones

		VR71100A	VR71499A		VR71100A	VR71499A
wt%	quartz	28.0	26.9	kaolinite	2.2	2.4
	plagioclase	12.6	12.3	pyrite	3.9	–
	muscovite	37.8	41.4	pyrrhotite	3.0	3.6
	chlorite	12.5	13.3			

Reflected-light microscopy showed that nearly all of the sulfide consists of pyrrhotite, which is present as minute disseminated grains and as concentrations at the rims and within the cores of the chloritic spots. One chip, however, consists of fine-grained pyrite with associated calcite, and is likely a fragment of fracture fill (Fig. 19). The chemically determined content of 1.2 wt% S (Table 1) is in accord with the optical estimate of sulfide abundance.

The NP of the sample is 11 (Table 1), the bulk of which would have been derived from chlorite and carbonates. A rough, order-of-magnitude approximation of the carbonate-mineral content in the optical section is 0.3–0.4 vol.%. The suspicion, although highly tenuous, that two carbonate minerals might be present proved to be correct; both calcite and dolomite are present. EDS spectra of the calcite indicate that it is close to the end-member in composition, and spectra of the dolomite are almost identical to the spectrum shown in Figure 7, i.e., also close to end-member in composition.

Although veinlet calcite is thought to be recognizable (Figs. 17, 19), nearly all of the carbonate grains are liberated. One dolomite grain is 350 × 500 μm; the relatively coarse size and liberation suggest that both dolomite and calcite occur as veinlets in the footwall siltstone.

REFERENCES

Jago, B.C. (2002) Petrographic description and X-ray diffraction characterization of serpentine minerals in 16 drill core samples. Unpublished private report by Lakefield Research for Kennecott Exploration.

Lane, G. (2002) Mineralogical determination of pentlandite and chalcopyrite distribution in three head samples and a bulk rougher tail. Unpublished private report by Lakefield Research for Kennecott Inc.

Mandarino, J.A. and Back, M.E. (2004) Fleischer's Glossary of Mineral Species 2004. Mineralogical Record, Tucson, Arizona.

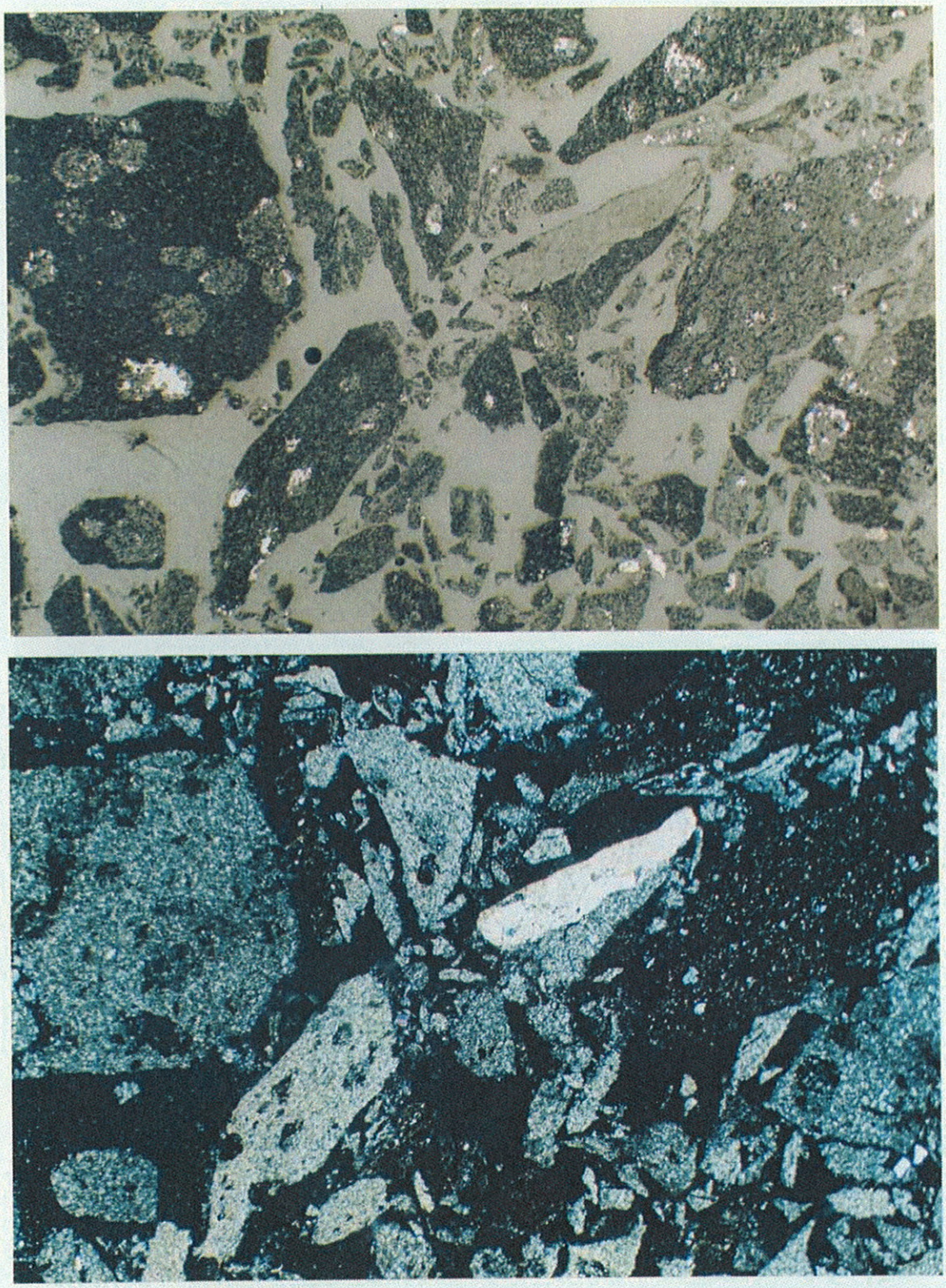


Figure 17. Footwall siltstone VR71499A in plain reflected light (top), and the same area in transmitted light with polarizers crossed (bottom), width of field 5.1 mm, showing the spotted character and fine grain size. White grains in the upper photo are pyrrhotite, and to the right of center is a calcite veinlet that is conspicuous in the lower photo as the whitish, elongate particle pointing to the top right corner.

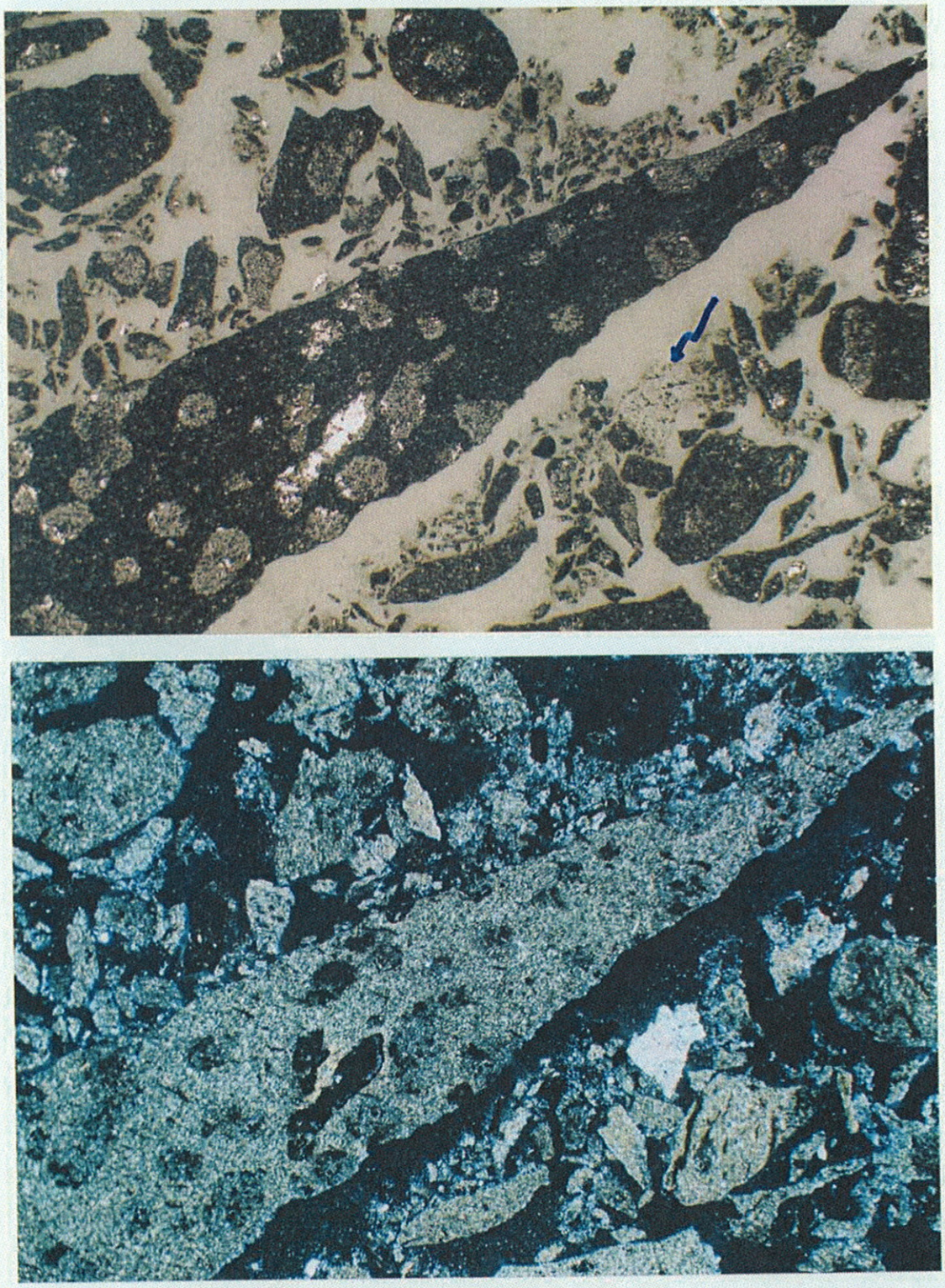


Figure 18. Footwall siltstone VR71499A in plain reflected light (top) and in transmitted light with crossed polarizers (bottom), width of field 5.1 mm. The features are as in Figure 17, but the arrow points to a large particle that is dolomite rather than calcite.

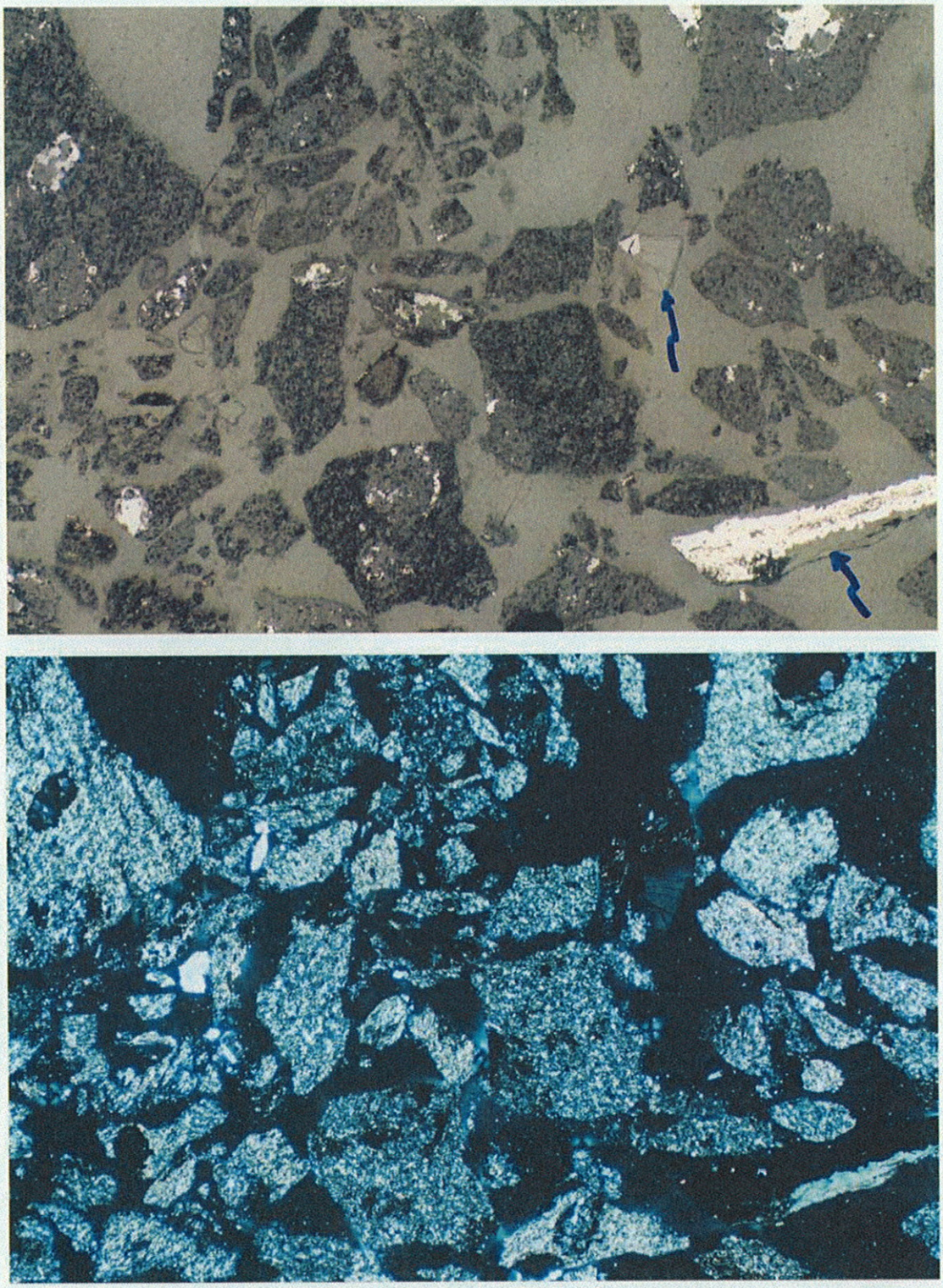


Figure 19. Footwall siltstone VR71499A in plain reflected light (top) and in transmitted light with polarizers crossed (bottom), width of field 2.6 mm. The white mineral is pyrrhotite, except that the elongate particle at the bottom right corner is pyrite with associated calcite (at arrow). The other arrow points to a grain of olivine.

APPENDIX 1

QUANTITATIVE PHASE ANALYSIS OF FOUR POWDER SAMPLES USING THE RIETVELD METHOD AND X-RAY POWDER DIFFRACTION DATA.

J.L. Jambor, Ph.D.
Leslie Research and Consulting
316Rosehill Wynd
Tsawwassen, B.C. V4M 3L9

Mati Raudsepp, Ph.D.
Elisabetta Pani, Ph.D.
Dept. of Earth & Ocean Sciences
6339 Stores Road
The University of British Columbia
Vancouver, BC V6T 1Z4

March 31, 2004

EXPERIMENTAL METHOD

The four samples "VR71325A", "VR71100A", "VR71499A" and "VR71213" were ground into fine powder to the optimum grain-size range for X-ray analysis (<10μm) by grinding under ethanol in a vibratory McCrone Micronising Mill for 7 minutes. Step-scan X-ray powder-diffraction data were collected over a range 3-70°2θ with CuKα radiation on a standard Siemens (Bruker) D5000 Bragg-Brentano diffractometer equipped with a diffracted-beam graphite monochromator crystal, 2 mm (1°) divergence and antiscatter slits, 0.6 mm receiving slit and incident-beam Soller slit. The long fine-focus Cu X-ray tube was operated at 40 kV and 40 mA, using a take-off angle of 6°.

RESULTS AND DISCUSSION

The X-ray diffractograms were analyzed using the International Centre for Diffraction Database PDF-4 using Search-Match software by Siemens (Bruker). X-ray powder-diffraction data were refined with Rietveld Topas 2.1 (Bruker AXS). The results of quantitative phase analysis by Rietveld refinement are given in Table 1. These amounts represent the relative amounts of crystalline phases normalized to 100%. Rietveld refinement plots for the samples are shown in Figures 1 - 4.

Table 1. Results of quantitative phase analysis (wt.%)					
	Ideal Formula	VR71100A	VR71213	VR71325A	VR71499A
Quartz	SiO_2	28.0			26.9
Plagioclase	$NaAlSi_3O_8 - CaAl_2Si_2O_8$	12.6	10.6		12.3
Muscovite	$KAl_2AlSi_3O_{10}(OH)_2$	37.8			41.4
Biotite	$K(Mg,Fe^{2+})_3AlSi_3O_{10}(OH)_2$		4.0		
Chlorite	$(Mg,Fe^{2+})_5Al(Si_3Al)O_{10}(OH)_8$	12.5	20.6		13.3
Talc	$Mg_3Si_4O_{10}(OH)_2$		10.8		
Tremolite	$\square Ca_2Mg_5Si_8O_{22}(OH)_2$		4.0		
Kaolinite	$Al_2Si_2O_5(OH)_4$	2.2			2.4
Lizardite	$Mg_3Si_2O_5(OH)_4$		9.2	27.0	
Augite	$(Ca,Na)(Mg,Fe,Al,Ti)(Si,Al)_2O_6$		13.9	5.2	
Pyrite	FeS_2	3.9			
Chalcopyrite	$CuFeS_2$			3.4	
Pyrrhotite	$Fe_{1-x}S$	3.0		37.4	3.6
Magnetite	$Fe^{2+}Fe_2^{3+}O4$		8.4	12.0	
Forsterite	Mg_2SiO_4		18.4	6.2	
Pentlandite	$(Fe,Ni)_9S_8$			8.8	
Total		100.0	100.0	100.0	100.0

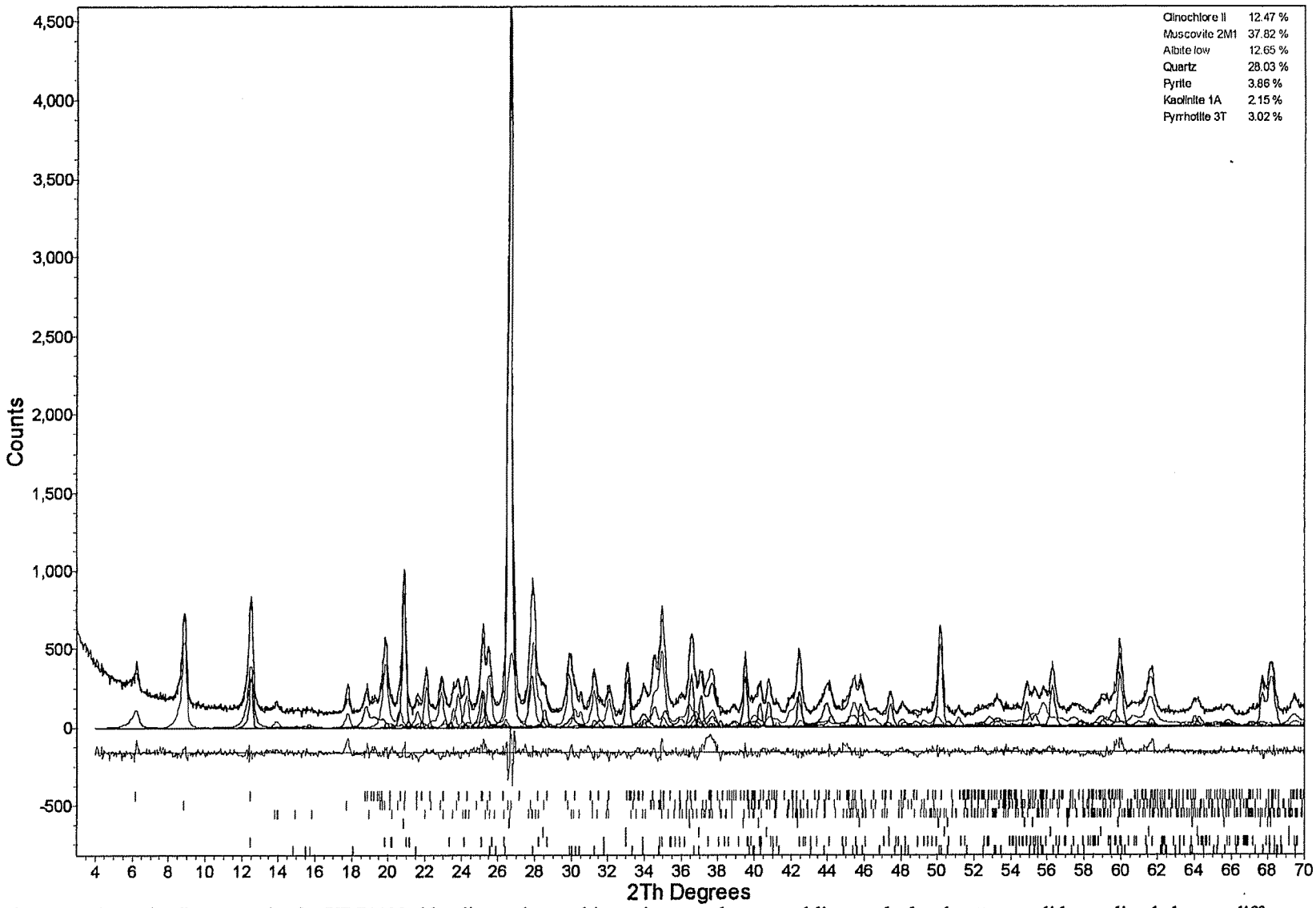


Figure 1. Rietveld refinement plot for **VR71100** (blue line - observed intensity at each step; red line - calculated pattern; solid grey line below – difference between observed and calculated intensities; vertical bars, positions of all Bragg reflections). Coloured lines are individual diffraction patterns of all phases.

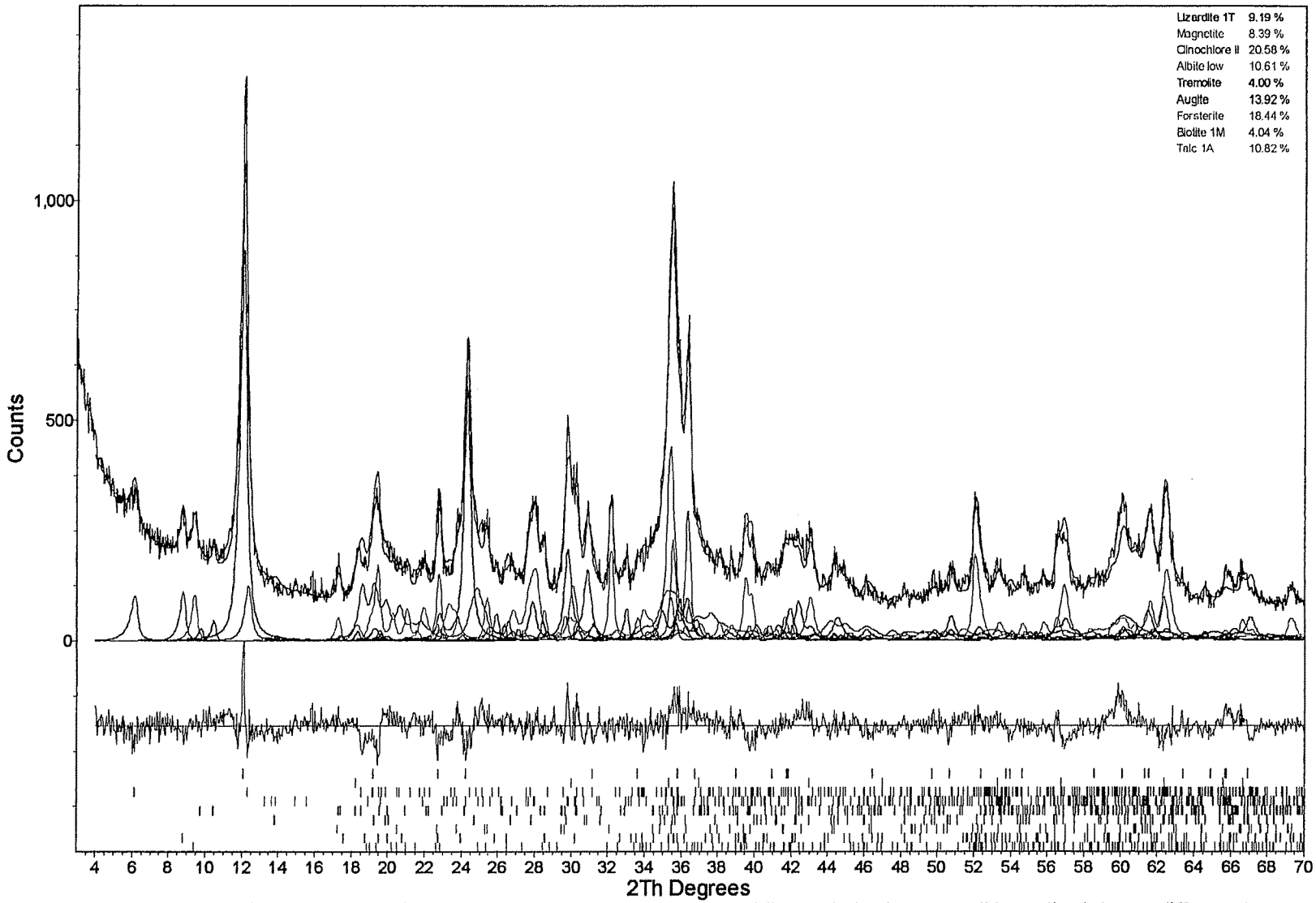


Figure 2. Rietveld refinement plot for **VR71213** (blue line - observed intensity at each step; red line - calculated pattern; solid grey line below – difference between observed and calculated intensities; vertical bars, positions of all Bragg reflections). Coloured lines are individual diffraction patterns of all phases.

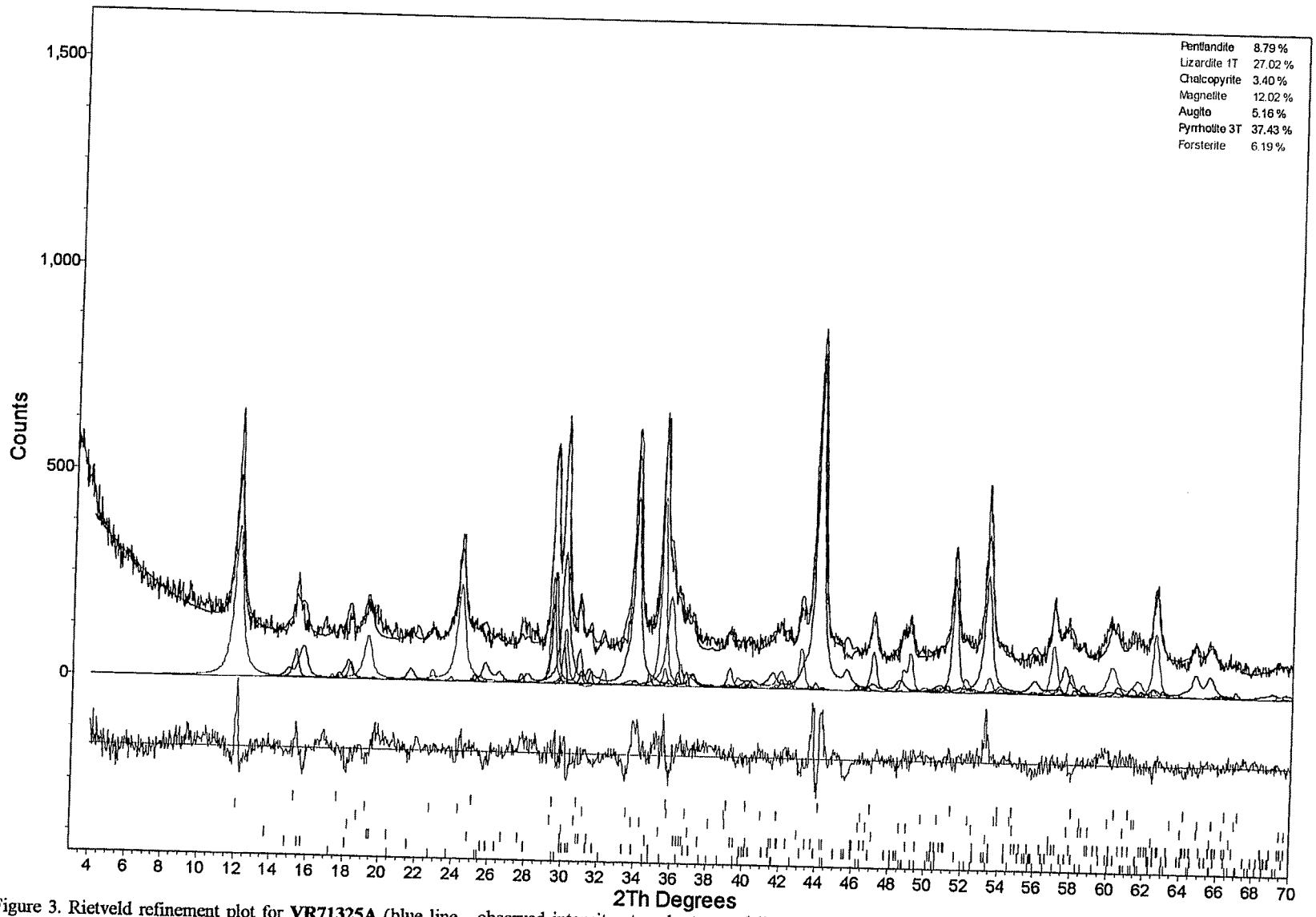


Figure 3. Rietveld refinement plot for **VR71325A** (blue line - observed intensity at each step; red line - calculated pattern; solid grey line below – difference between observed and calculated intensities; vertical bars, positions of all Bragg reflections). Coloured lines are individual diffraction patterns of all phases.

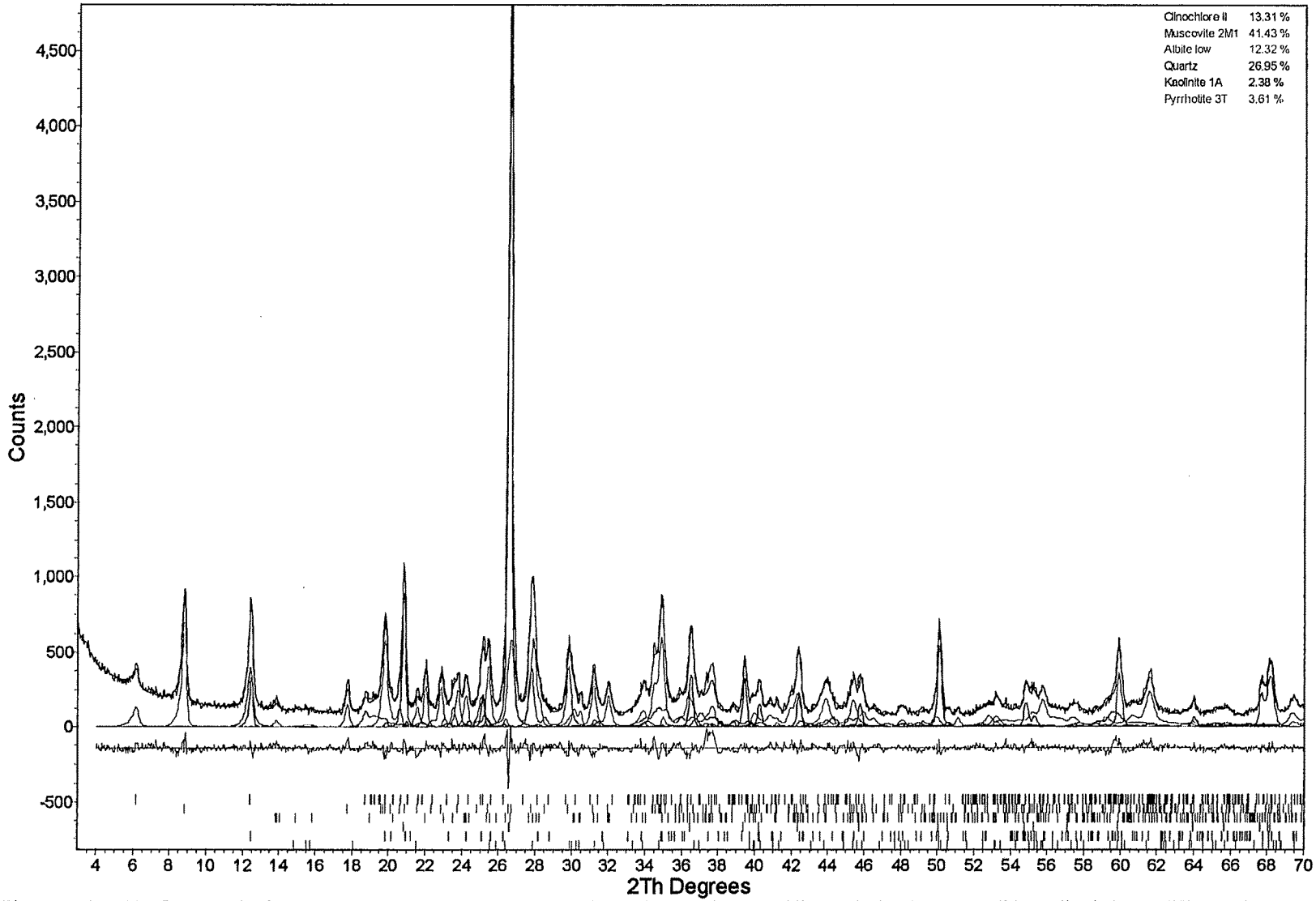


Figure 4. Rietveld refinement plot for sample **VR71499A** (blue line - observed intensity at each step; red line - calculated pattern; solid grey line below – difference between observed and calculated intensities; vertical bars, positions of all Bragg reflections). Coloured lines are individual diffraction patterns of all phases.

APPENDIX 2

Nomenclature and ideal formulas* of minerals referred to in the text and Appendix 1

albite	$NaAlSi_3O_8$; sodic plagioclase; forms a series with anorthite $CaAl_2Si_2O_8$, within which the division is at formula Na:Ca = 1:1
amphibole	group name; $AB_2C_5T_8O_{22}X_2$ wherein *A* is K or Ca, *B* is typically Ca, Mg, Fe^{2+}, Mn, *C* is generally Al, *T* is Si, and *X* is OH, Cl, F
augite	clinopyroxene group, $(Ca,Na)(Mg,Fe,Al,Ti)(Si,Al)_2O_6$
biotite	general name for dark mica; most commonly phlogopite $K(Mg,Fe)_3AlSi_3O_{10}(OH)_2$
calcite	$CaCO_3$
chalcopyrite	$CuFeS_2$
chlorite	group name; most commonly clinochlore $(Mg,Fe^{2+})_5Al(Si_3Al)O_{10}(OH)_8$
clinopyroxene	general term for monoclinic pyroxenes; most commonly augite $(Ca,Na)(Mg,Fe,Al,Ti)(Si,Al)_2O_6$ or diopside
cubanite	$CuFe_2S_3$
diopside	pyroxene group; monoclinic, $CaMgSi_2O_6$
dolomite	$CaMg(CO_3)_2$
feldspar	general term that includes the albite–anorthite series and K-dominant members
forsterite	olivine group; Mg_2SiO_4
ilmenite	$Fe^{2+}TiO_3$
kaolinite	clay mineral, $Al_2Si_2O_5(OH)_4$
K-feldspar	$KAlSi_3O_8$, feldspar group; generally the species microcline, less commonly orthoclase
lizardite	serpentine group, $Mg_3Si_2O_5(OH)_4$

magnetite	$Fe^{2+}Fe^{3+}{}_2O_4$
marcasite	FeS_2, the orthorhombic polymorph of pyrite
mica	group name that includes muscovite, phlogopite, and biotite
muscovite	mica group; $KAl_2AlSi_3O_{10}(OH)_2$
olivine	group name, most commonly the Mg member forsterite
orthopyroxene	orthorhombic members of the pyroxene group, as distinct from the clinopyroxenes; typically enstatite $Mg_2Si_2O_6$
pentlandite	$(Fe,Ni)_9S_8$
plagioclase	group name for the feldspar series $NaAlSi_3O_8$ (albite) – $CaAl_2Si_2O_8$ (anorthite)
pyrite	FeS_2
pyroxene	group name; includes clinopyroxenes and orthopyroxenes
pyrrhotite	$Fe_{1-x}S$
quartz	SiO_2
rutile	TiO_2
serpentine	group name; most commonly lizardite or clinochrysotile, both $Mg_3Si_2O_5(OH)_4$
sphalerite	ZnS, most commonly (Zn,Fe)S
talc	$Mg_3Si_4O_{10}(OH)_2$
tremolite	$Ca_2Mg_5Si_8O_{22}(OH)_2$; amphibole group; forms a series with actinolite $Ca_2(Mg,Fe)_5Si_8O_{22}(OH)_2$
violarite	$FeNi_2S_4$, cubic

*Ideal formulas from Mandarino and Back (2004)

ENVIRONMENTAL MINERALOGY OF SAMPLES FROM THE EAGLE DEPOSIT, MICHIGAN – PART 2

Prepared for: **Geochimica, Inc.**
Ojai, California

May, 2004

J.L. Jambor
Leslie Investments Ltd
Research and Consulting
316 Rosehill Wynd
Tsawwassen, B.C. V4M 3L9
Ph: (604)948-1368
Fax: (604)948-1369
E-mail: JLJambor@aol.com

EXECUTIVE SUMMARY

The environmental mineralogy of ten samples from the Eagle Ni–Cu deposit in Michigan was examined as a follow-up to the investigation of five sample for which the results were reported in Part 1. The rocks examined vary from massive sulfides to peridotite and pyroxenite, hornfels, and hanging-wall and footwall siltstone. The most significant change from the Part 1 study is the recognition that fracture-controlled carbonates, both calcite and dolomite, are appreciable local contributors of NP to the bulk-sample values of the siltstone and hornfels. The peridotite and pyroxenite also contain small amounts of carbonate minerals, but most of the measured NP in peridotite is attributable to the presence of olivine and serpentine. Non-opaque minerals are almost absent in the two samples of massive sulfides that have been examined; the only non-opaque mineral identified is siderite, the presence of which was not detected in any of the other samples. Energy-dispersion spectra indicate that calcite in the Eagle samples is close to the end-member in composition, and that the dolomite typically contains only small amounts of Fe and Mn. Quantitative electron-microprobe analyses, keyed to peak heights in the energy-dispersion spectra, indicate that the maximum MnO and FeO contents of veinlet dolomite are about 2.1 and 4.5 wt%, respectively, and the maxima for calcite are <3 wt% MnO and <1% FeO.

INTRODUCTION

In Part 1 of this study the environmental mineralogy of the first five of 15 samples from the Eagle Ni–Cu deposit in Michigan was described (LRC 2004). The remaining ten samples, received on April 13, 2004, are described in this report. As in the initial study, both crushed material and intact, sawn reference cores were submitted to LRC, and the crushed material was used for the optical part of the mineralogical investigation. The only difference in procedures was that the initial equal split of the crushed material was done by Canadian Environmental & Metallurgical Inc., which thereupon ground to minus 200 mesh one of the halves of each sample. Nine of the ten as-received ground samples were submitted directly by LRC to M. Raudsepp of the University of British Columbia for Rietveld analysis; the tenth sample was withheld because it consisted of massive sulfides for which bulk-sample X-ray examination and quantitative mineralogy were deemed to be of limited benefit. The sample numbers and related data are given in Table 1.

Table 1. Samples received and related data

Sample	Lithology	wt% S	NP	wt% C_{total}
VR90425A	hanging-wall siltstone	0.77	8.8	<0.05
VR91625A	footwall siltstone	1.39	12.3	0.11
VR91620A	hanging-wall sandstone	0.31	5.6	<0.05
VR71109A	hornfels	0.7	25.3	0.25
VR91306A	hornfels, mineralized	2.72	20.6	0.11
VR71275A	pyroxenite	0.99	24.6	<0.05
VR91267A	peridotite	0.89	22.2	0.05
VR71373A	mineralized peridotite	2.44	34.4	0.06
VR90181A	massive sulfide	32.4	0.9	<0.05
VR90125A	semi-massive sulfide	8.13	23.9	0.05

DESCRIPTIONS AND RESULTS

Sample VR90425A

The core, like those described in Part 1, had been twice cut along the length such that the sawn surfaces are at right angles and the sample therefore represents a quarter of the original core. The rock, which is hanging-wall siltstone, is black, massive, and lacks recognizable

bedding. The two ends are planar and at a low angle to the core length, but the planes are not at the same angles and are only sub-parallel. One of the ends is smooth and has a sandy color when viewed under a binocular microscope, but no surficial deposits are evident. The other end of the core is rougher, and tests with acid and alizarin solution showed that a small area on the rough surface is calcite-bearing, but carbonates were not detected elsewhere on the core.

At mid height along the core length one of the cut surfaces has a 1-mm pyritic veinlet that parallels the planar ends, but the veinlet seems to have ramified and does not continue to the second cut surface. Part of the second surface instead has several barely visible, sub-millimetric sulfide veinlets that are highly irregular and, although chaotic, seem to be predominantly both in the direction of core elongation and at a steep angle to it.

The polished thin section consists of as-received crushed material that was split and crushed further to obtain a good representation in the section. The section contains at least 50 millimetric chips, the largest ~2 × 4 mm, and abundant sub-millimetric fines. All chips in the section are pale brownish. Disseminated sulfides are megascopically visible, but all are sub-millimetric; the sulfide content was estimated to be about 0.5%

The section as viewed in transmitted light has a uniform 'pelletal' or 'globular' texture (Fig. 1). Locally coarser grained areas within the section reveal the presence of quartz, chlorite, muscovite, and albite; the assemblage and combination of fine grain size are similar to those of the siltstone described in Part 1. The overall particle sizes are 25 μm or less, and the minerals within the globules are slightly coarser grained and less turbid than the surrounding material, thus suggesting that the textural feature is related to weak recrystallization; the lack of planar or oriented development, in turn, suggests a relationship to thermal rather than to dynamic metamorphism.

Two of the chips in the section contain narrow chlorite veinlets in which lath elongation is perpendicular to the wallrock. The wider veinlet is only about 75 μm in width, and neither of the veinlets has associated carbonate minerals. A few pockets of monomineralic chlorite in which lath lengths are up to 50 μm were also observed, and these appear to be uncomplicated segregations with the host rock. Only one carbonate grain, 30 μm across and liberated, was observed. Although calcite was detected on the fractured surface of the core, alizarin staining of the mineral in the optical section indicated that grain to be of dolomite rather than calcite.

Reflected-light examination revealed that, aside from the pervasive globular texture

evident in transmitted light, a spotted texture is also present. As was described in Part 1 for the siltstone, the spots are conspicuous in reflected light because many have a narrow rim of high-reflectance rutile. In the VR90425A siltstone, the spots are less abundant than observed previously, and their distribution seems to be random and spatially independent of the globular texture. Other than a trace of chalcopyrite, all of the sulfide in the section consists of pyrite, the largest particle of which is a polycrystalline aggregate almost 300 μm across (Fig. 2). More typical than such aggregates are disseminated fine grains, but many of the chips are sulfide-barren or contain no more than a bleb or two of pyrite (Fig. 2). The coarsest grains in the section are compact, homogeneous, and liberated; there does not seem to be a gradation in size between the liberated and the much smaller within-host disseminated grains, and the inference is that the liberated grains are from fracture fill. No veinlets of the relatively coarse pyrite were observed in the optical section, but pyrite of appropriate size occurs on fracture surfaces of the core, and a few veinlets in which the pyrite is only a few micrometers wide but forms a braided veinlet pattern were observed in the microscopy section.

The quantitative mineralogy, as determined by Rietveld refinement of the X-ray data for the sample, is given in Table 2. The sulfide content was estimated optically to be about 0.5%, which on the usual pyrite:wt% S correlation of 1:1 suggests a sulfur content of 0.5 wt%. The bulk-sample chemically determined value is 0.77 wt% S, but the difference is not considered to be disputatious. The measured NP is low (8.8), a portion of which is thought to be attributable to fracture-fill carbonates.

Table 2. Quantitative mineralogy of hanging-wall siltstone VR90425A

wt%	quartz	27.9	albite	8.8
	muscovite	43.0	chlorite	9.9
	K-feldspar	8.5	pyrite	1.9

Mineral quantities are normalized to 100 wt% here and in all subsequent tables.

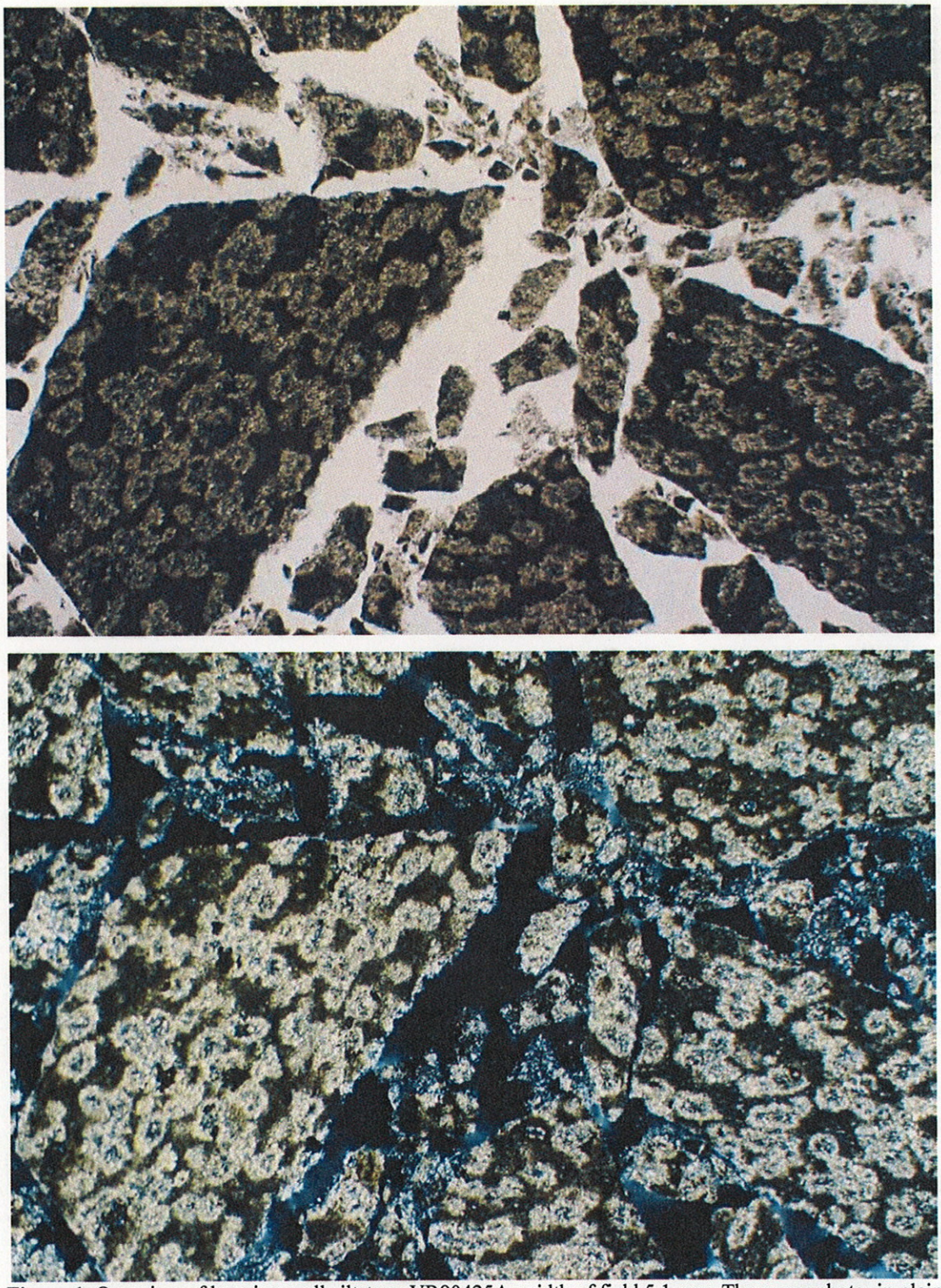


Figure 1. Overview of hanging-wall siltstone VR90425A, width of field 5.1 mm. The upper photo, in plain transmitted light, shows the characteristic pelletal or globular texture and the almost opaque nature of the inter-globule rock. The lower photo of the same area, taken with polarizers almost crossed, shows the typical fine-grained character of the siltstone, and the slightly coarser grain size of the globules (the bluish color is from mounting medium. See also Figure 2 of the same area.

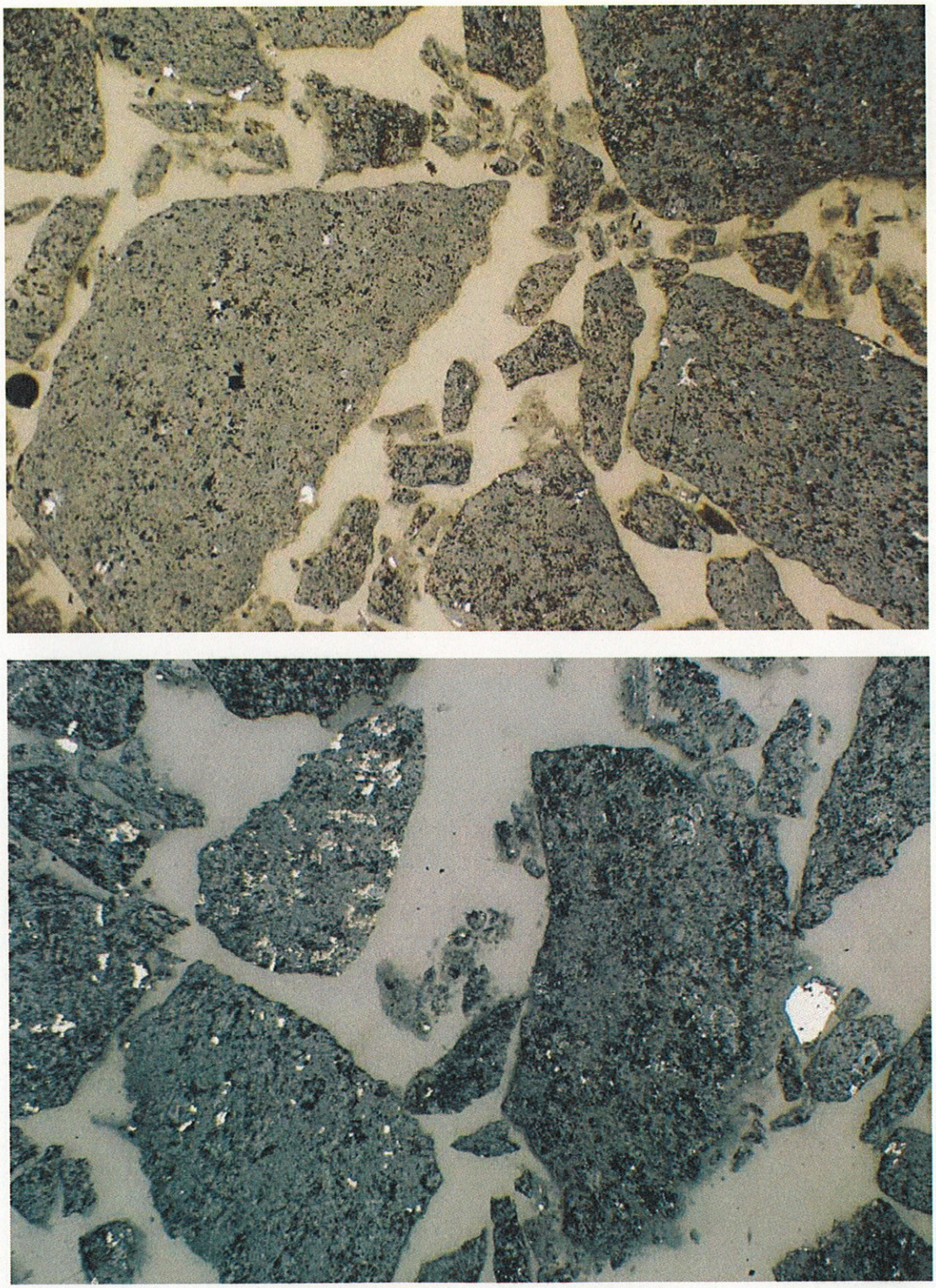


Figure 2. The upper photo is of the same field as Figure 1, but here in plain reflected light. The disseminated white grains in the various chips are illustrative of the typical fine-grained character and distribution of pyrite in the section, as is also evident in the lower photo of another area, at the same magnification. The largest grain of pyrite in the section is at the far right (white).

Sample VR91625A

The sample is of footwall siltstone that is dark grey, massive, and lacks visible bedding. As in the preceding siltstone core, the broken ends of the quartered core are planar and sub-parallel at a low angle to the core length. The planar surfaces are clean breaks that exposed fresh, undisturbed rock. Throughout the core is evenly disseminated pyrite or pyrrhotite, the grains of which are neither aggregated nor aligned. The sulfides are sub-millimetric but the grains are numerous; a value of ~1% sulfides was chosen as an indication of the magnitude of their abundance.

In the crushed sample the pronounced conchoidal fracture that is characteristic of the hanging-wall (VR90425A) siltstone is less evident, and fragments (chips) are commonly tabular rather than equant. No fracture-fill surfaces were observed in the as-received sample, which was split and further crushed to obtain the material for the polished thin section.

The optical section contains >50 chips, with almost all <2 mm across. Two distinct populations of chips are megascopically evident: about 10 15% of the chips are black and opaque, and the remainder of the chips is translucent and brownish gray. Sub-millimetric sulfide grains are disseminated throughout the section in roughly triple the abundance of that in the preceding sample of hanging-wall siltstone.

Microscopic examination revealed that the black, opaque chips have a high carbonaceous content but are otherwise similar to the non-opaque majority (Fig. 3). The results from the quantitative determination of mineralogy indicate that the major-mineral assemblages in the examined samples of siltstones, be they from the hanging wall or footwall, do not vary appreciably with regard to environmental mineralogy (Tables 2 and 3, and Part 1), although in terms of metamorphic systematics there is an indication that K-feldspar may have crystallized at the expense of muscovite within the thermal aureole.

In one of the chips in the optical section, grain sizes of many of the clasts are 30 50 μm across, which is a size coarser than that of the typical siltstone. The coarser grained chip contains carbonate-mineral clasts, but not a carbonate cement, and such clasts make up 5 10% of the chip. A second chip, only a bit coarser in grain size, is similarly but slightly less calcareous. Aside from the two calcareous chips, carbonate minerals with other habits are present. Several relatively coarse liberated grains, up to 100 μm across but of a polycrystalline character that is distinct from the optically uniform or coarser liberated grains, occur within the siltstone host

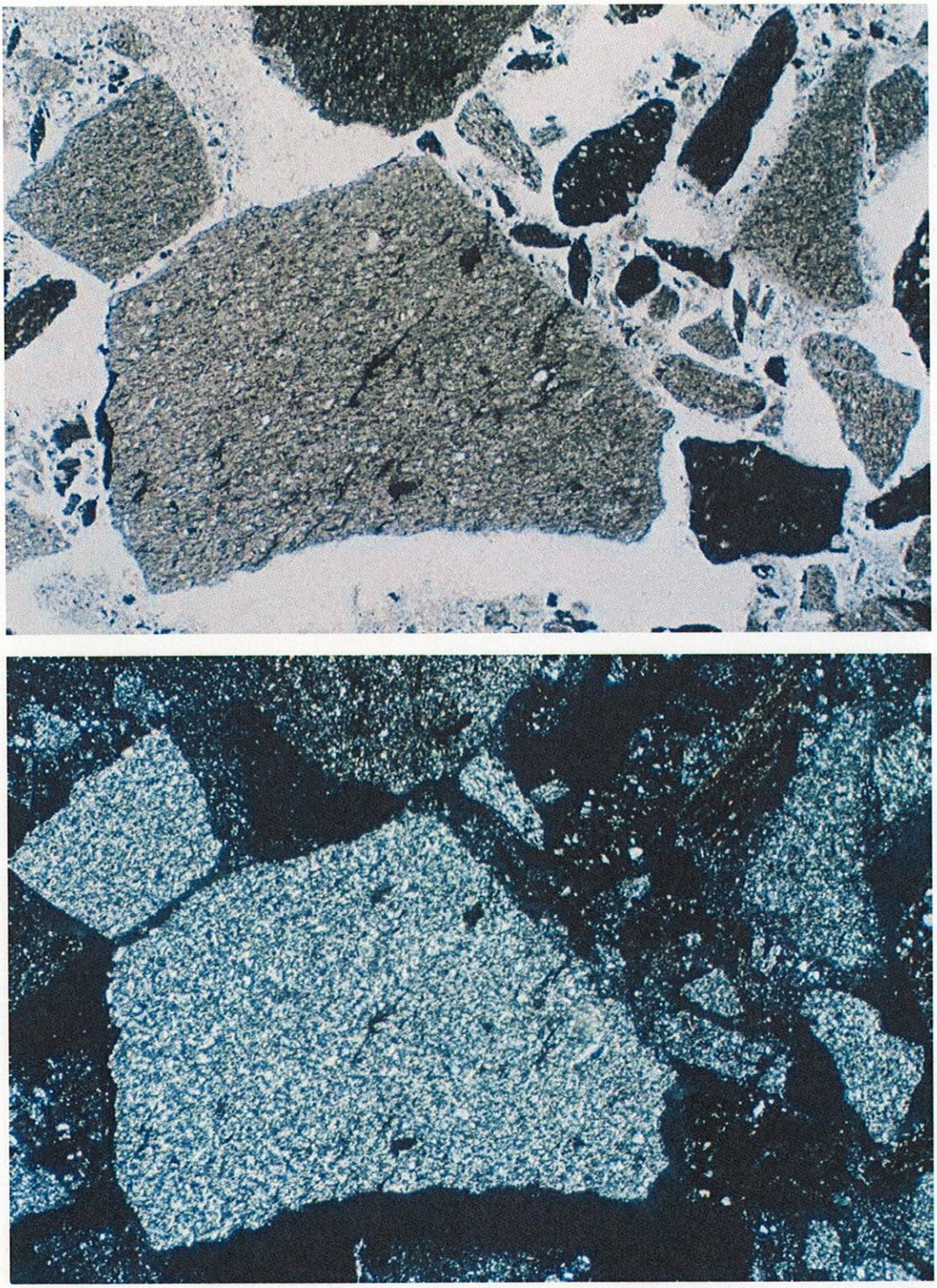


Figure 3. Footwall siltstone VR91625A in plain transmitted light (top), and the same field with polarizers crossed (bottom), width of field 5.1 mm. The upper photo shows the fine-grained character and the two distinct populations of chips (opaque and translucent). Figure 4 is the same area in reflected light.

Table 3. Quantitative mineralogy of footwall siltstone VR91625A

wt%	quartz	29.4	chlorite	13.4
	muscovite	37.5	calcite	0.6
	albite	15.4	pyrrhotite	3.1
			rutile	0.6

(Fig. 4). As well, disseminated carbonate grains of a size like those of siltstone quartz were observed; although difficult to identify because of their small size, the carbonate grains of this type seem to be sparse.

In contrast to the fine-grained pyrite in hanging-wall siltstone VR90425A (Fig. 2), the sulfides in the sample of footwall siltstone are predominantly of pyrrhotite in relatively coarse grains, typically 100 to 300 μm across. Some chips also contain disseminated fine grains, most of which are ≤15 μm. Many of the large pyrrhotite grains have narrow, peripheral concentrations of rutile that are too discontinuous to be called rims (Fig. 5). Traces of pentlandite occur as flames within pyrrhotite, which also contains trace amounts of pyrite and chalcopyrite as inclusions. Extremely fine-grained, polycrystalline, inclusion-riddled marcasite, some with associated pyrite and some with pyrrhotite, has also been observed but is quantitatively insignificant. Sulfide abundances in the more strongly carbonaceous chips do not seem to differ from those of the other chips.

The overall sulfide content of the optical section was estimated to be between 1 and 2%, and probably closer to the higher value. The carbonate-mineral content, even with the presence of the two calcareous chips (Fig. 6), was estimated to be <1 %, and most likely ~0.5%. Areas tested with alizarin solution indicate that the liberated grains of carbonate and the aggregates within the siltstone are calcite; the calcareous chips are also calcite-bearing, but it is uncertain whether all of the carbonate grains are calcite. The higher carbonate-mineral content relative to that in hanging-wall siltstone VR90425A (the preceding sample) accounts for the higher NP value (12.8 versus 8.8).

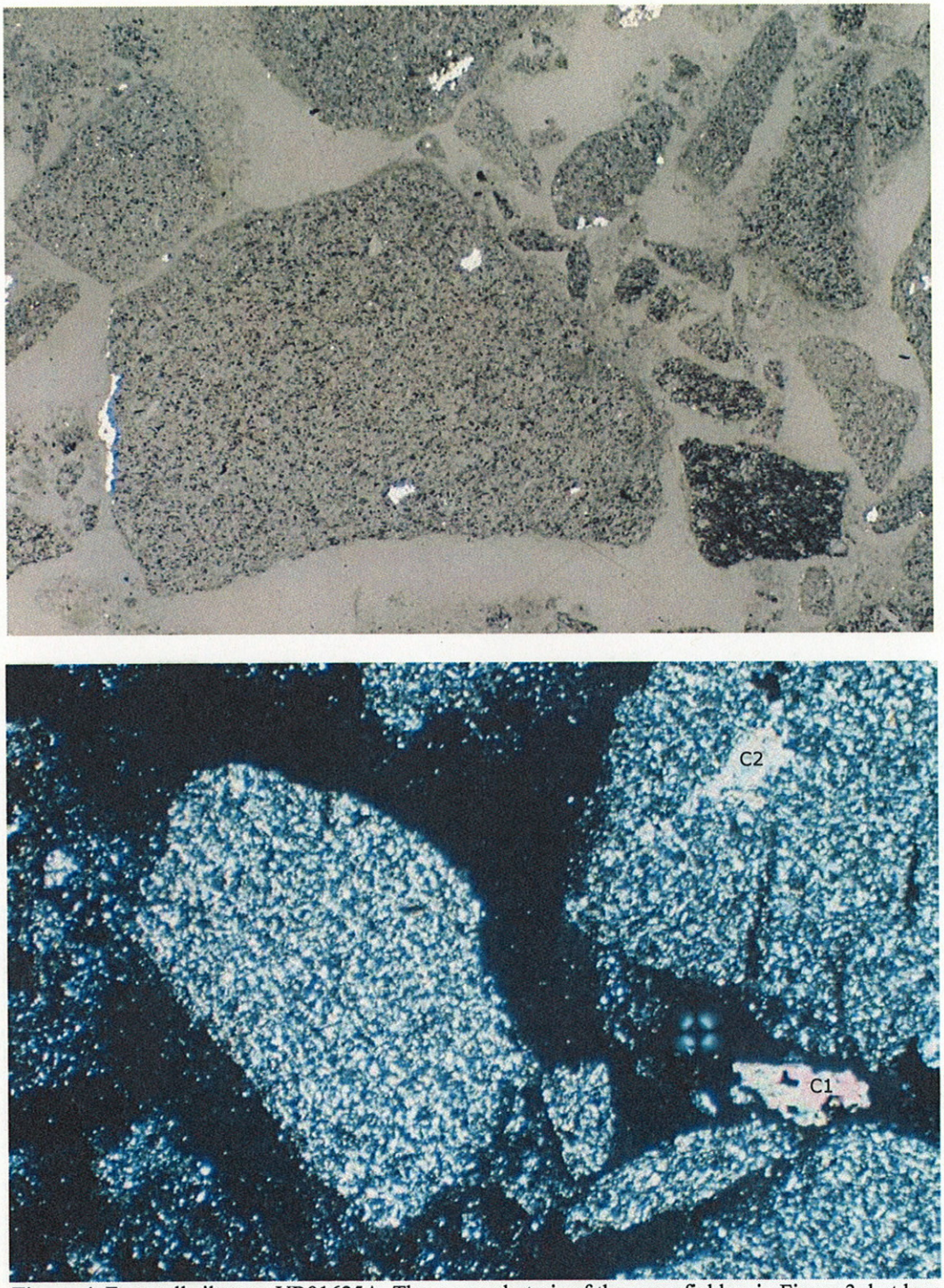


Figure 4. Footwall siltstone VR91625A. The upper photo is of the same field as in Figure 3, but here in reflected light. The white grains are pyrrhotite, and on the far left is a pyrrhotite-bearing veinlet whose continuation at the upper end is marked by grains of chalcopyrite rather than of pyrrhotite. The lower photo, in transmitted light with polarizers crossed, width of field 5.1 mm, shows the different carbonate types: **C1** at the lower right is the liberated type, **C2** consists of within-matrix, irregular aggregates, and **C3** consists of sparse fine-grained, disseminated grains (not distinguishable in the photo) within the siltstone.

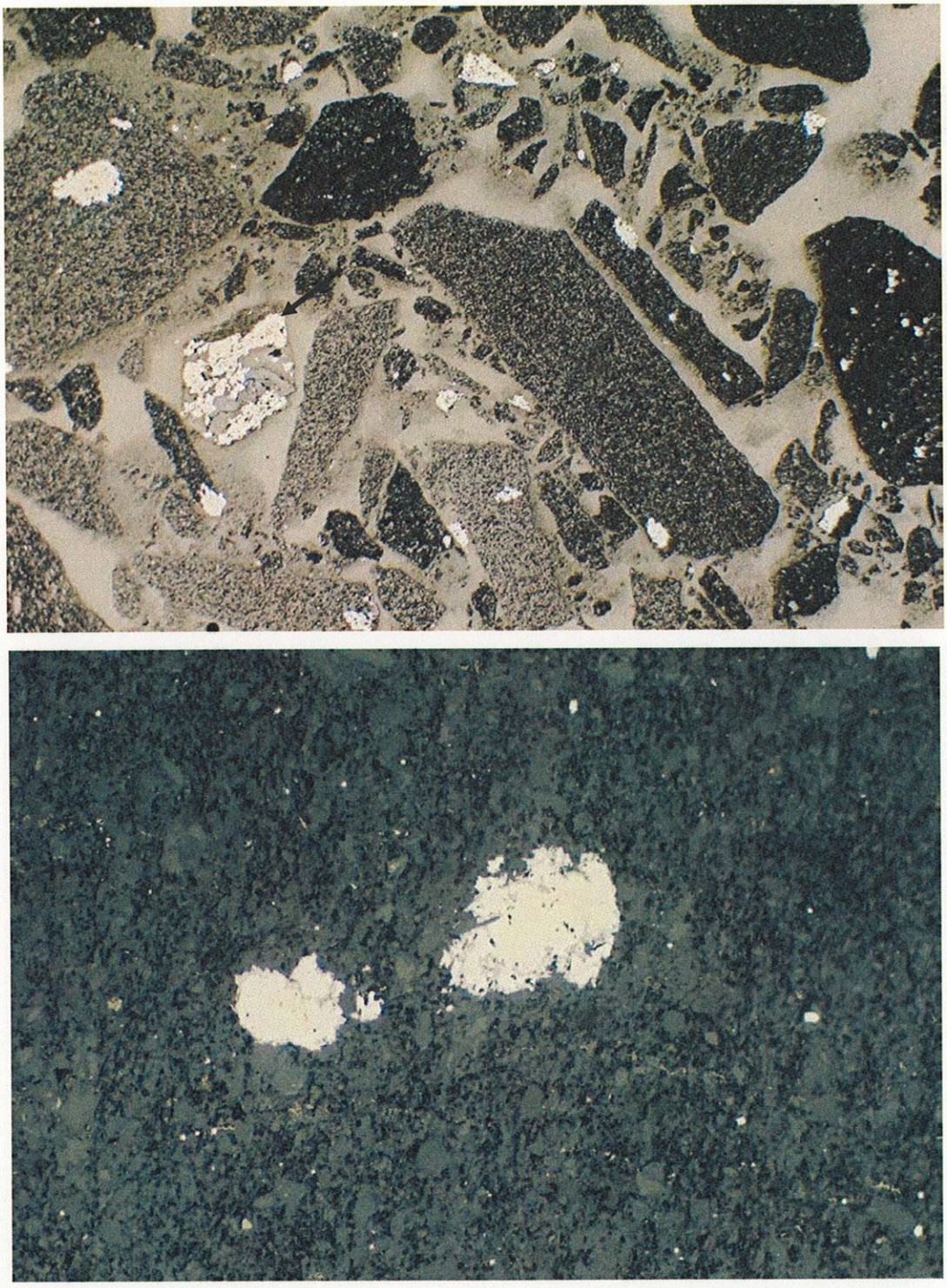


Figure 5. Siltstone VR91625A in plain reflected light. The upper photo (width of field 5.1 mm) shows the general nature of the siltstone (black chips are more carbonaceous) and the distribution of pyrrhotite (white). The arrow points to a chip that is part of a veinlet. At the arrow head is a zone of pyrrhotite, and the remainder of the white is marcasite; the associated light gray minerals are calcite and quartz. The lower photo (width of field 0.625 mm) shows pyrrhotite with peripheral rutile.

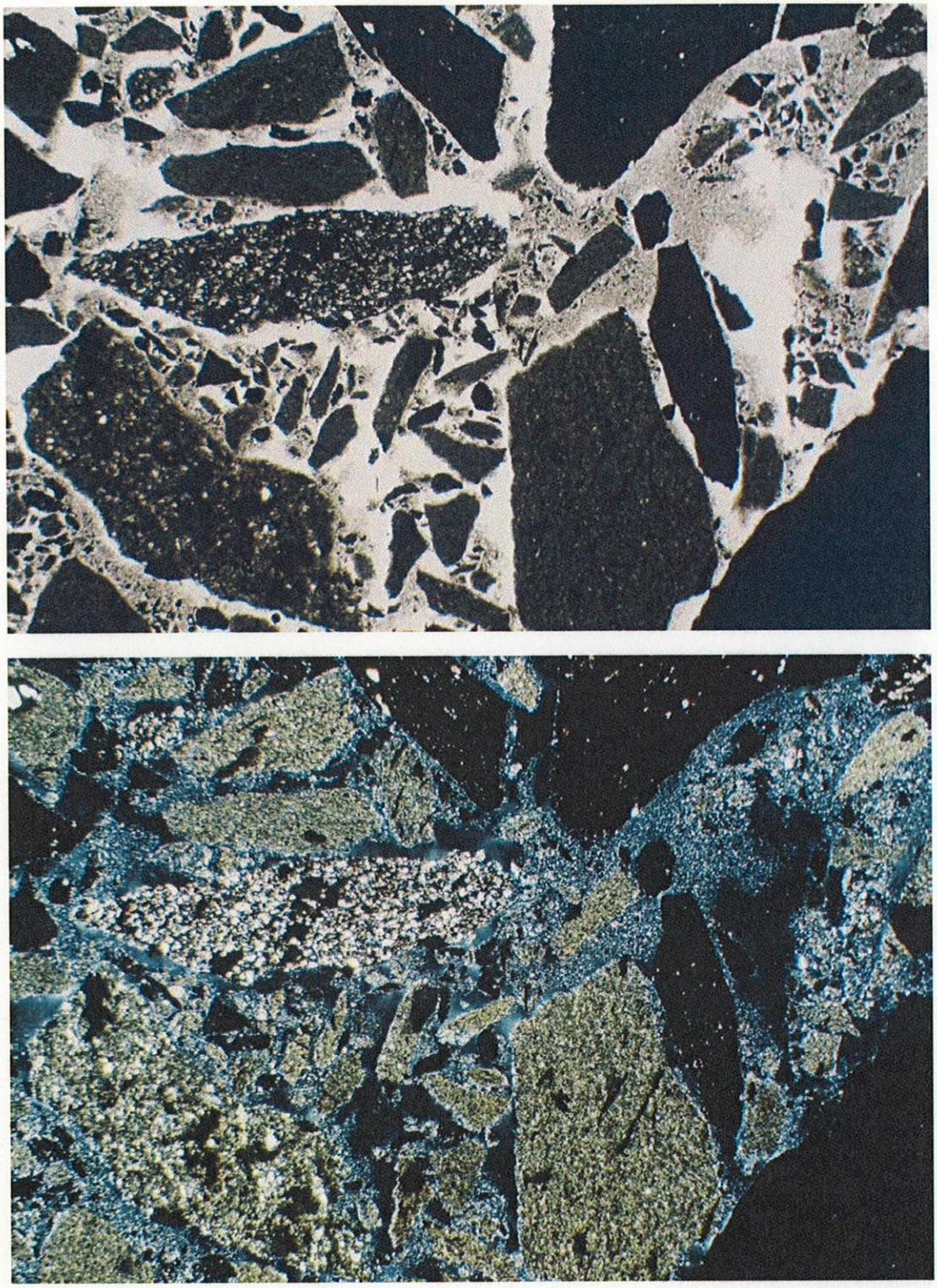


Figure 6. Siltstone VR91625A in plain transmitted light (top) and the same field with crossed polarizers (bottom), width of field 5.1 mm. The elongate chip at mid-height, left, is one of the coarser grained, calcareous chips.

Sample VR91620A

The sample is of dark gray hanging-wall sandstone. The core ends are planar at about 45 60° to the core length and are sub-parallel; one end is greenish white and is sulfide- and probably muscovite-rich, whereas the other end is rougher and not mineralogically distinct. No carbonates were detected with alizarin solution or acid. Disseminated, sub-millimetric sulfides are sparingly visible on the sawn surfaces. In the sample of crushed material, no fracture-fill pieces were observed. The sample was split and further crushed for the polished thin section.

The optical section contains numerous chips, with about 20 of the largest ones in the 2 to 3 mm range. No carbonaceous chips are present; all are grayish and translucent. Megascopic sub-millimetric sulfides are sparse, with the abundance estimated to be <0.5%.

Microscopic examination showed that a few siltstone chips are present, but the others are coarser grained, less turbid, and have quartz grain sizes of 50 100 μm (Fig. 7). Albite is common, and muscovite and chlorite occur as shreds within the phyllosilicate-dominant matrix. The quantitative mineralogy is given in Table 4. Carbonate minerals are present only in trace amounts. Five grains, ranging from about 25 to 60 μm across, were observed in the sandstone, wherein they occur as clasts. Four liberated grains, the largest ~70 × 250 μm and the smallest ~30 μm across, were observed. Tests with alizarin solution indicated that both calcite and dolomite are present.

Pervasive, finely disseminated sulfides are absent; the bulk occurs as polycrystalline particles of pyrite, most commonly 40 to 200 μm across. A few of the particles are marcasite rather than pyrite, and most of the pyrite has associated with it a subordinate amount of polycrystalline marcasite that is concentrated at the periphery or is adjacent to non-sulfide inclusions within the aggregates. A few, minute, isolated grains of chalcopyrite are present. The sulfide content of the section was estimated to be 0.1%, with pyrite > marcasite >> chalcopyrite. The low NP value (5.6; Table 1) is in accord with the expectations from the mineralogy.

Table 4. Quantitative mineralogy, VR91620A

wt%	quartz	47.0	chlorite	9.6
	muscovite	15.0	pyrite	0.5
	albite	27.5	rutile	0.5

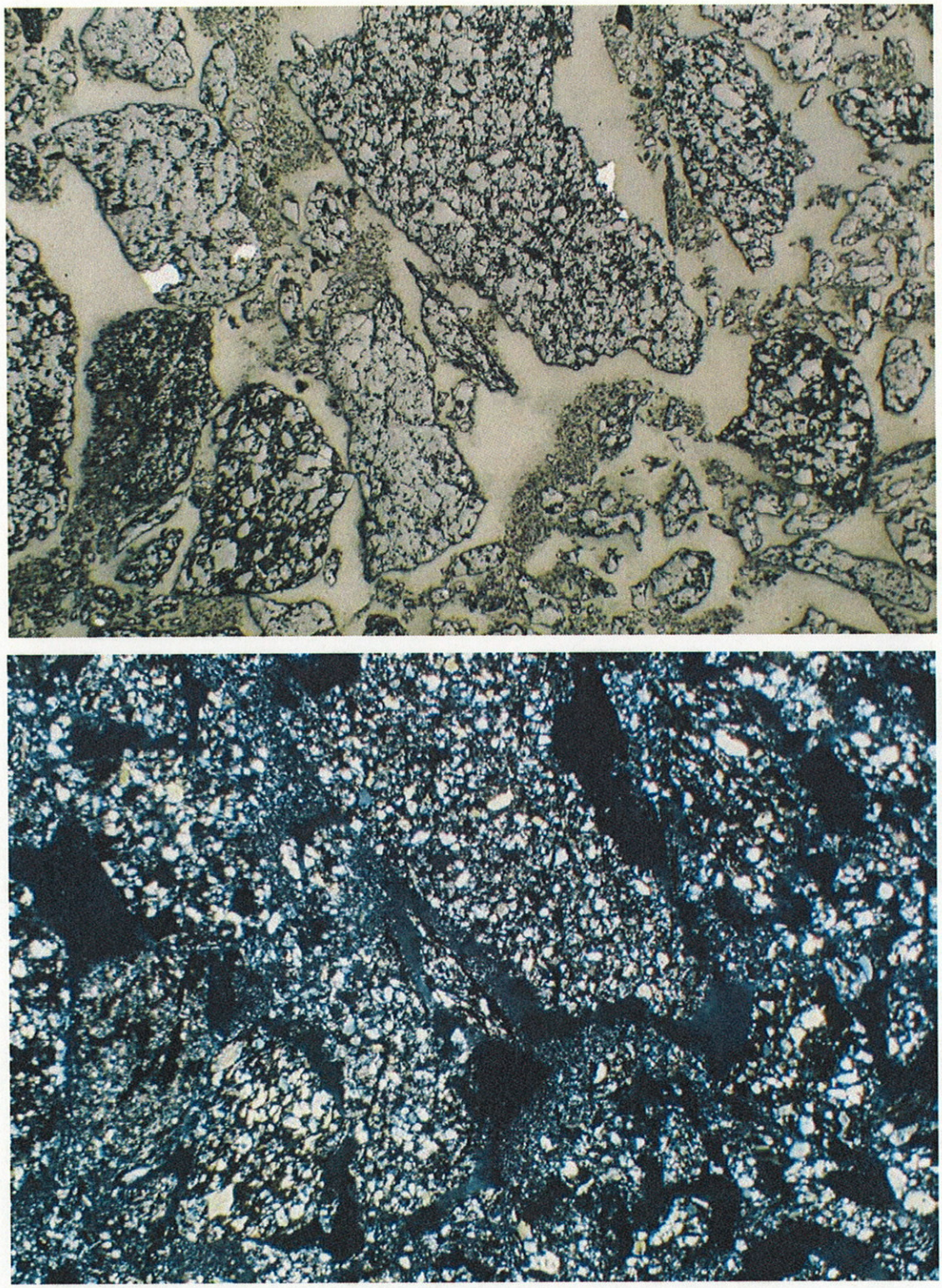


Figure 7. Sandstone VR91620A in plain reflected light (top), and the same area in transmitted light with crossed polarizers (bottom), width of field 5.1 mm, showing the typical sparingly distributed pyrite (white). The lower photo illustrates the coarser grain size relative to that of siltstone; the absence of bright colors is a reflection of the low mica content relative to that of siltstone.

Sample VR71109A

Hornfels sample VR71109A is dark gray, slightly greenish, massive and homogeneous except for a slightly lighter, elongate 'clot' about 6 mm wide and 4 cm long. No sulfides are visible. One of the core ends is planar, has a greenish sandy appearance, and is almost normal (~10°) to the core length. The other end is rougher, yellowish sandy, and is at a steep angle to the core length. No reaction with alizarin or acid was obtained from the core.

The crushed material consists of roughly equant chips with an irregular to conchoidal fracture. One chip ~5 mm in diameter is white; about half its volume was added to the material for the optical section, and the remainder was retained for separate examination. Another chip seemed to have a whitish veinlet, about 2 mm wide; only a small portion was added to the material for optical study. Subsequent examination of the two chips indicated that both the white chip and the veinlet consist of carbonates whose behavior with the test solutions suggested that each chip is a mixture of calcite and dolomite.

The section contains more than a hundred chips, of which about 3% are black and opaque and the others are slightly greenish. The largest chips are about 2 mm across and are numerous. One of the larger chips consists of pyrite, and several smaller sulfide-bearing chips are megascopically observable. The sulfide content was estimated to be of the order of 1%.

The rock, which is classified as hornfels (Table 1) is of the fine-grained siltstone type and has a mottled texture (Figs. 8, 9) that is similar to the globular texture of the siltstone illustrated in Figure 1. The black opaque chips are not texturally different and are distinguishable only because of their high carbonaceous content. Rutilated, ring-type spots are common but are not a predominant feature. One quartz–chlorite veinlet, ~30 μm wide and 1.2 mm long, occurs at the margin of a chip, and a shorter chloritic veinlet at a right angle to the long veinlet cuts the chip. Neither veinlet is carbonate-bearing.

The quantitative mineralogy is given in Table 5. The most outstanding feature in the optical section is the high content of carbonate minerals, which occur as cleavage fragments up to 1 mm across, and as fine- and coarse-grained aggregates, with the latter commonly showing well-defined zoning (Fig. 10). Carbonates either as grains or as veinlets within the hornfels were not observed; thus, the carbonates presumably represent liberated fracture-fill material, among which are likely to be some of the particles that are mentioned in the second paragraph above. Tests with alizarin solution indicated that calcite and dolomite commonly coexist on a

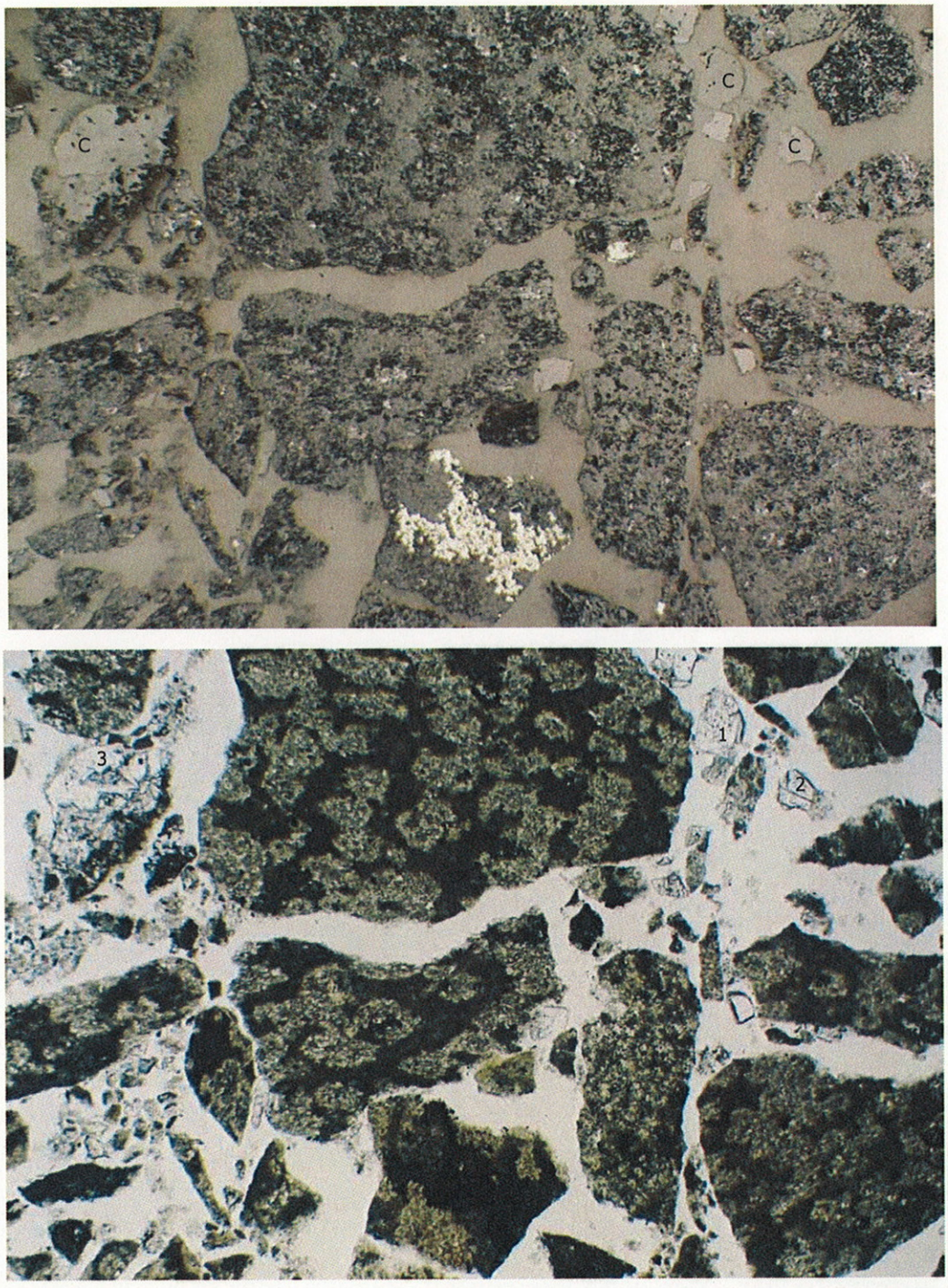


Figure 8. Hornfels VR71109A in plain reflected light (top) and in plain transmitted light (bottom), width of field 5.1 mm, showing the typical texture (see also Fig. 9). Numerous carbonate grains are present (e.g., **C** at the left and right in the upper photo), and these appear as the coarser, colorless grains (**1**, **2**, **3**) in the lower photo. The typical occurrence of fine-grained aggregations of pyrite is evident in the chip at the bottom of the upper photo. EDS spectra for the labelled grains are given in Appendix 2.

Table 5. Quantitative mineralogy of VR71109A

wt%	quartz	29.7	chlorite	10.1
	muscovite	39.6	pyrite	1.4
	K-feldspar	11.6	pyrrhotite	1.1
	albite	6.6		

microscopic scale. Age relations are variable, but dolomite more commonly is the younger mineral. The aggregates that show zoning are of dolomite; zoning was not detected in coarse grains of calcite. EDS spectra of the various labelled grains in Figures 8 and 10 are given in Appendix 2. Both the calcite and the dolomite have low Fe and Mn contents.

The sulfides are present in two dissimilar forms: (a) as fine-grained aggregates, typified by the pyrite-rich chip shown in Figure 8, and (b) as large, liberated grains of pyrite and pyrrhotite (Fig. 10). As well, several grains of chalcopyrite occur within the hornfels. Both pyrite and pyrrhotite are represented by the large, liberated grains, but the two occur independently. Pyrite is predominant. Only one minute grain of marcasite, within pyrite, was observed. The within-hornfels sulfide content was estimated to be ~0.2%, but the large size and homogeneity of the liberated grains probably doubles the sulfide content to about 0.4%. The bulk-sample value is 0.7 wt% S (Table 1). Almost all of the high NP (25.3) is attributable to calcite and dolomite.

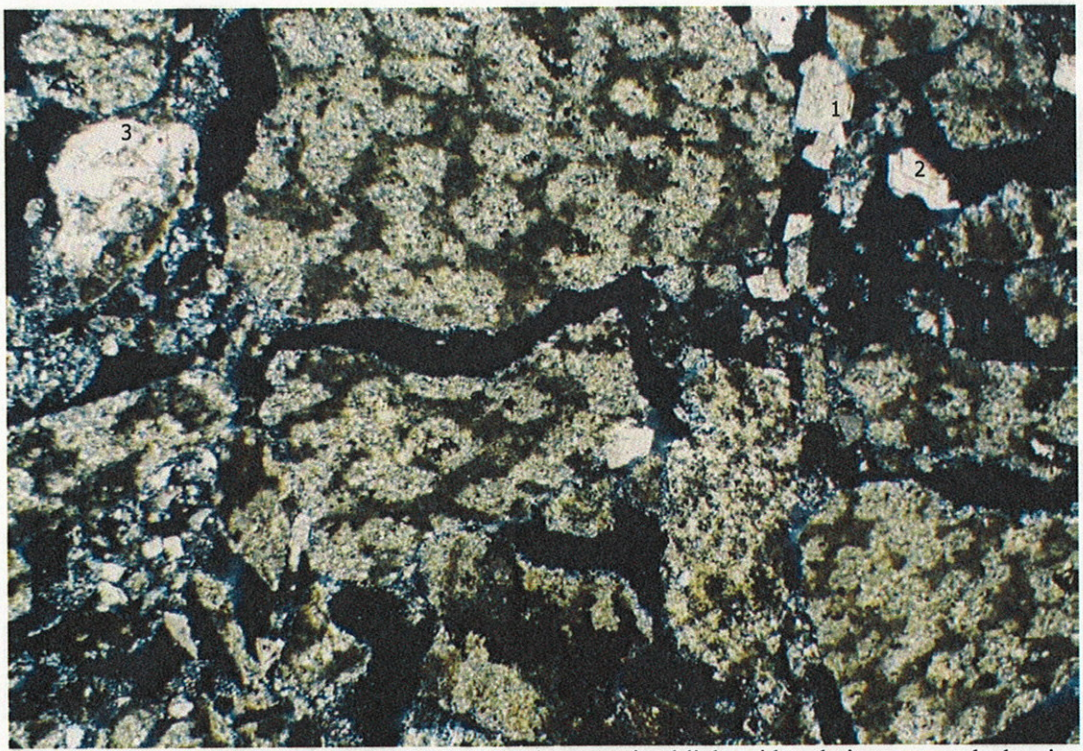


Figure 9. The same field as in Figure 8, but here in transmitted light with polarizers crossed, showing the fine-grained character of the hornfels and the much coarser grain size of the carbonate minerals.

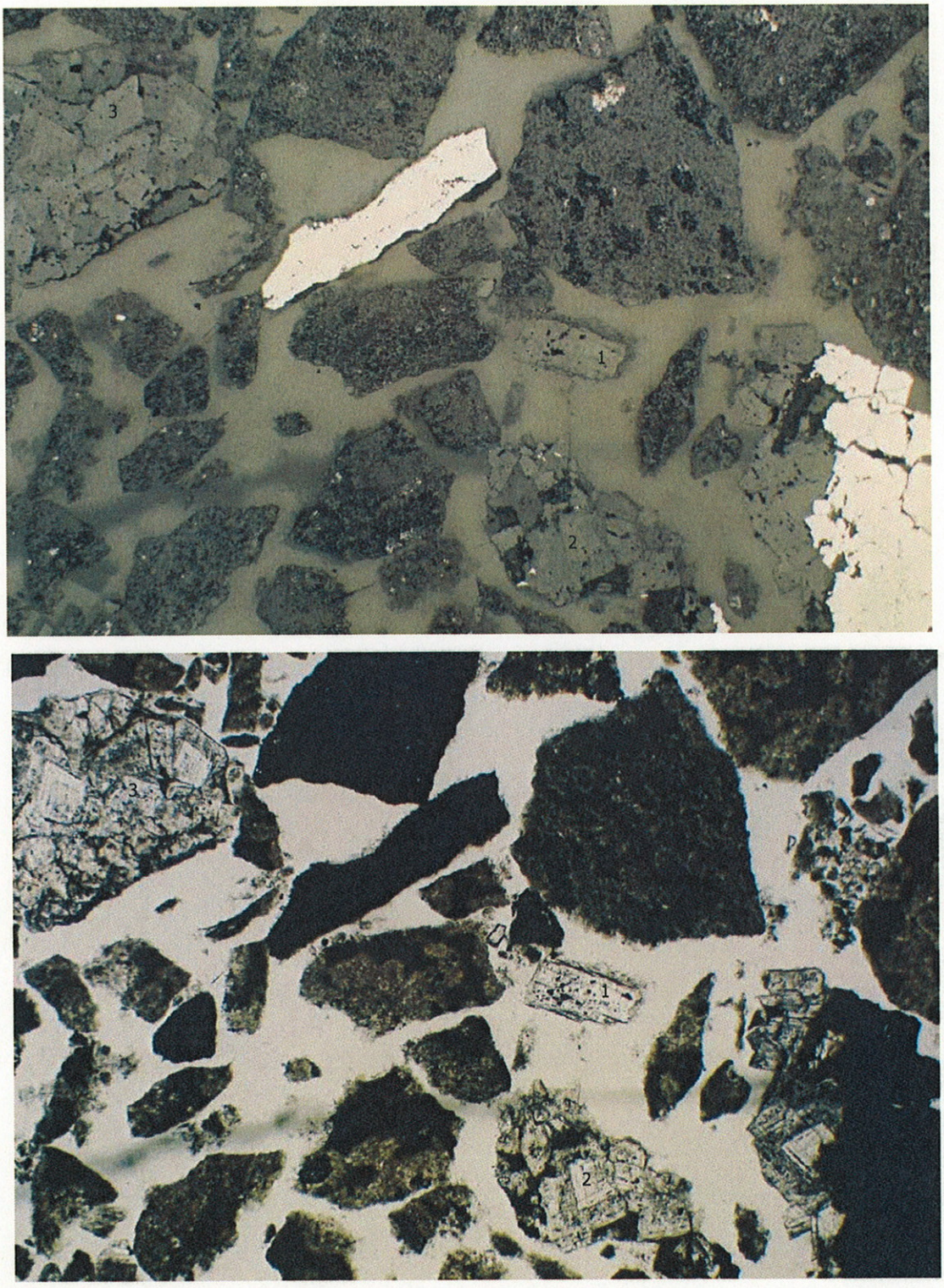


Figure 10. Hornfels VR71109A in plain reflected light (top), and the same field in plain transmitted light (bottom), width of field 5.1 mm. The upper photo shows two large particles of liberated-type pyrite, and the lower photo shows aggregates of zoned dolomite. EDS spectra for the labelled grains are given in Appendix 2.

Sample VR91306A

Sample VR91306A is of weakly mineralized hornfels. Two pieces of core were received. One is the 'standard' quartered core, about 10 cm long, which contains only traces of sub-millimetric disseminated sulfides and is similar in appearance to hornfels VR71109A. One end of the core has a rough, steeply dipping fracture surface, which appears to be chloritic and which has a small amount of associated dolomite. Within the core and about 1 cm from the fractured surface is a chloritic veinlet, about 1 mm wide, that did not give a reaction for carbonate. The opposite end of the core apparently has two intersecting fracture planes; the main one is smoothly planar and has a chloritic surface, whereas the other is rough and uncoated. Carbonates were not detected on either surface.

The hornfels is apparently irregularly mineralized, and a smaller piece of core, about 5 cm long, was provided as an example of the mineralized material. The core is highly fractured along rough, irregular surfaces, to the extent that the as-received example was no longer intact. The sample contains about 10% chalcopyrite that occurs predominantly as irregular aggregates, up to about 5 mm wide, that have an uneven distribution. Tests with alizarin solution and acid indicate that dolomite is locally present on the irregularly fractured surfaces.

The as-received crushed sample was noted to be chalcopyrite-rich, but no veinlets or obvious fractured surfaces were observed within the chips. The material selected for the optical section was therefore a random split. The resulting optical section contains >50 chips, the largest about 2 × 3 mm. Most are megascopically gray or slightly brownish, and a few consist solely of pyrite. Chalcopyrite is visible in several of the smaller chips. The overall sulfide content of the section is high and was estimated, prior to the optical examination, to be ~7%.

Transmitted-light microscopy revealed that the grain size of the rock is like that of the sandstone rather than the siltstone; grain diameters are commonly to 100 μm, many are to 150 μm, and a few are to 200 μm. Many of the grains are slightly pinkish and turbid, presumably as a result of permeation by sub-microscopic hematite. Quartz and chlorite are predominant, and the mineral affected by hematite staining is K-feldspar. Shreds of muscovite are abundant in some chips and are absent in others. A few grains of amphibole were observed, but the mineral has been extensively chloritized. Chlorite occurs predominantly as a matrix for the quartz and feldspar, but one chip of about 0.3 × 0.9 mm consists of an aggregate of radial sheaves, each ~100 μm in diameter. Several fine-grained, polycrystalline, monomineralic aggregates of chlorite

Table 6. Quantitative mineralogy of VR91306A

wt%	quartz	32.5	chlorite	18.0
	muscovite	13.4	chalcopyrite	4.1
	K-feldspar	9.4	pyrite	2.0
	albite	18.9	pyrrhotite	0.8

are present, as are several predominantly monomineralic chlorite veinlets; both have also been observed to locally contain inclusions of dolomite.

The section is carbonate-rich, with the largest grain a cleavage fragment that is ½ mm along an edge. Several others of only slightly smaller size are present (Figs. 11-13). One chip has a coarse-grained carbonate veinlet, or part of a veinlet, along one side, but otherwise all of the large carbonate grains are liberated, and no aggregates, clasts, or cementation within the quartzose portions of the hornfels were observed. There is, however, a pronounced association between chlorite and carbonates, and some of that material may have been derived from chlorite-rich aggregates within the hornfels rather than from veinlets. Despite the conspicuousness of the large carbonate grains, the overall content of carbonate minerals was estimated to be no more than 1% of the optical section. Tests with alizarin solution indicated the mineral to be dolomite, and no calcite was detected. EDS analyses of four carbonate grains confirmed that all are dolomite; spectra for the dolomite and for chlorite are given in Appendix 2. No carbonates were detectable in the quantitative mineralogical analysis (Table 6).

The sulfide content of the section is in percentage amounts and consists almost wholly of pyrite and chalcopyrite. The pyrite occurs as fine-grained aggregates within the hornfels (exemplified by the pyritiferous chip at the lower right of Fig. 13), and as coarse, homogeneous grains that are either liberated or intergrown with dolomite (Figs. 12, 13). The chalcopyrite occurs within the hornfels (Fig. 12) and as liberated grains. Although a few exceptions were noted, >99% of the chalcopyrite does not coexist as intergrowths with pyrite. Trace amounts of ilmenite, marcasite, a grain of metallic iron, and traces of sphalerite are present, with the sphalerite occurring at the periphery of chalcopyrite or as occluded blebs within the chalcopyrite. Although a small amount of pyrrhotite is reported in the quantitative analysis (Table 6), none was identified as present in the optical section; however, a few grains of pentlandite, either isolated or in contact with chalcopyrite of similar size, were observed in the section.

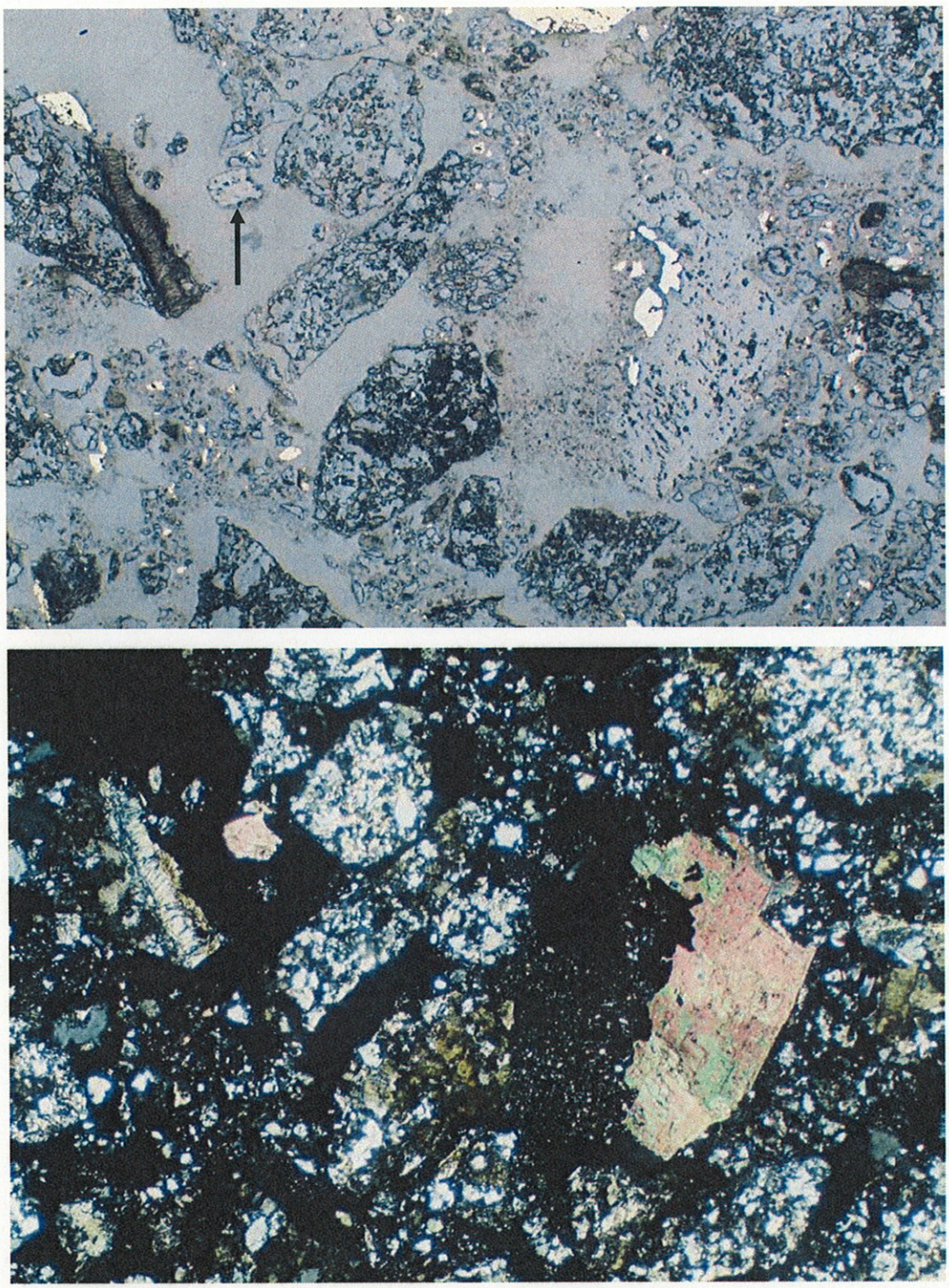


Figure 11. Hornfels VR91306A in plain reflected light (top) and in transmitted light with crossed polarizers (bottom), width of field 2.6 mm. In the upper photo, whitish grains in the left half are chalcopyrite; the arrow points to a grain of liberated dolomite, and immediately to its left is a blackish veinlet of chlorite. The large white grains to the right of center are pyrite attached to a coarse grain of dolomite whose large size is evident in the lower photo. EDS spectra for the dolomite and chlorite are given in Appendix 2.

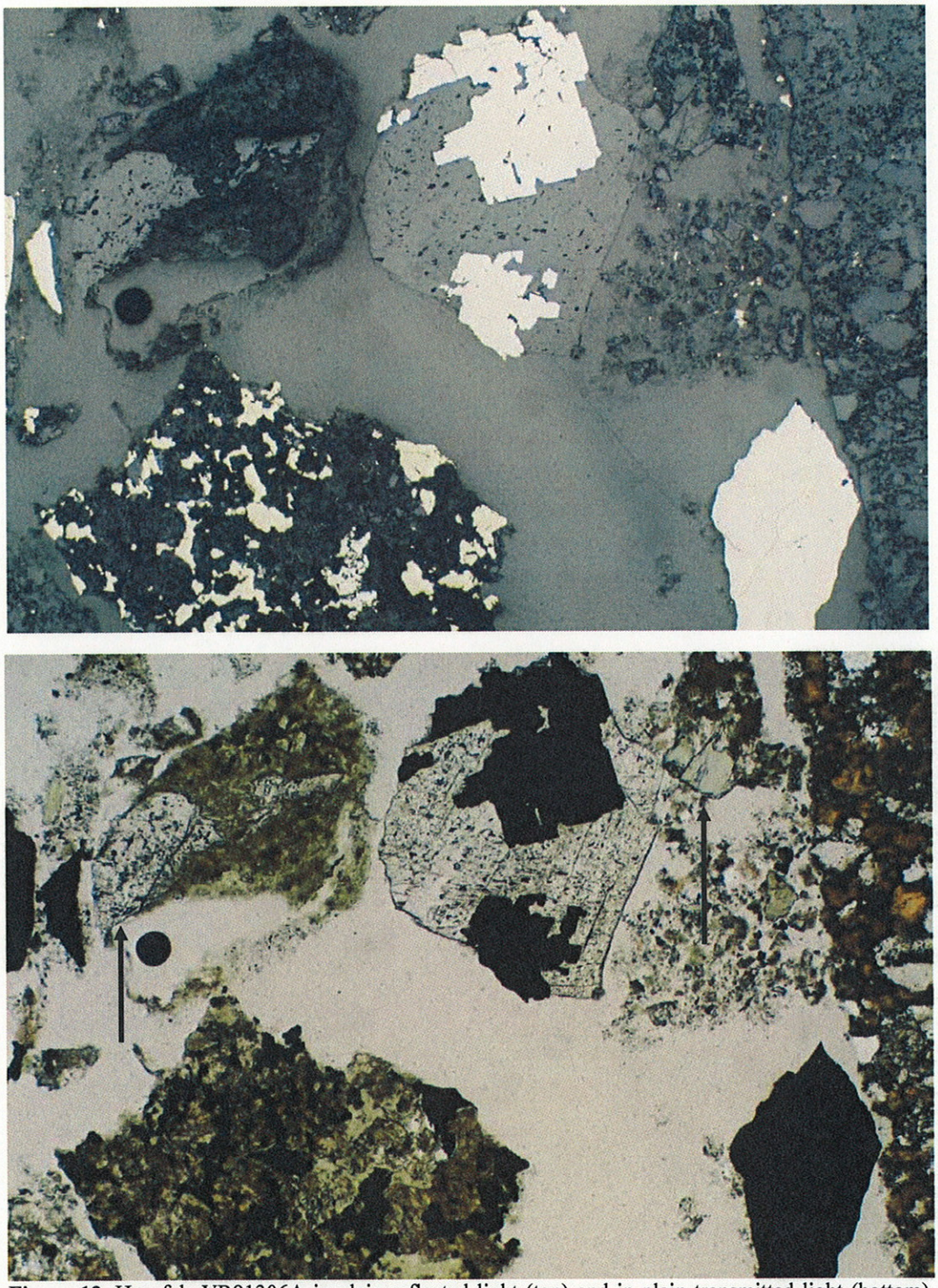


Figure 12. Hornfels VR91306A in plain reflected light (top) and in plain transmitted light (bottom), width of field 5.1 mm; the same field is shown in the upper photo of Figure 13. The sulfide in the chip at the bottom left is chalcopyrite, and the large white grains are pyrite. The pyrite above center is in dolomite; the arrow on the left points to dolomite with associated fine-grained chlorite (see Fig. 13), and the arrow on the right points to coarse-grained chlorite. The brownish, turbid color of the chip whose edge extends from the top to the bottom of the right margin of the photo is typical for this sample of hornfels.

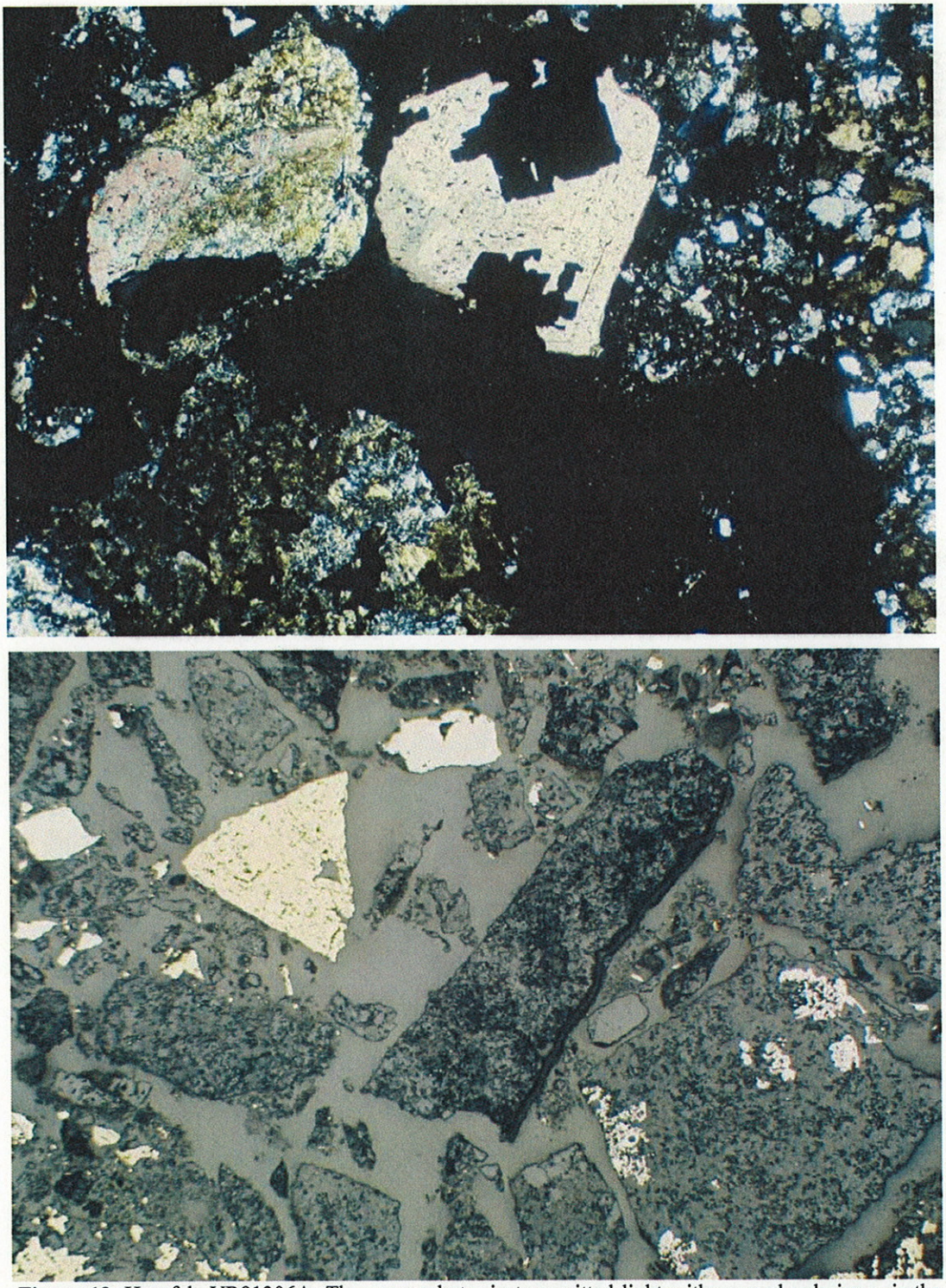


Figure 13. Hornfels VR91306A. The upper photo, in transmitted light with crossed polarizers, is the continuation of Figure 12, showing coarse-grained dolomite above center and, on the left, in association with fine-grained chlorite. The lower photo, in plain reflected light, width of field 2.6 mm, shows to the left of center a large, triangular grain of liberated chalcopyrite with adjacent white grains of liberated pyrite. The chip at the lower right shows the typical fine-grained aggregates of pyrite that occur within the hornfels.

Sample VR71275A

The core, reported to be of pyroxenite (Table 1), is slightly greenish and equigranular, with apparent grain sizes in the 1 5 mm range. One end of the core may have a poorly developed, rough fracture surface, but the other is clearly a random, non-planar break. No carbonates were detected at the core ends. Disseminated sulfides occur throughout the core length.

The chips in the crushed sample are irregular to equant and seem to be uniformly representative of the mass. A random split was taken and was further crushed for the preparation of the optical section. The section contains >100 chips, all of which are <2 mm across. Most are megascopically slightly brownish and translucent, a few are poorly translucent to opaque, and one of the larger chips in the section is of pyrite. Other than that chip, however, the sulfides are sub-millimetric and sparse, and their abundance was estimated to be 0.3%.

Microscopic examination revealed that the poorly translucent chips are of siltstone, which is texturally uniformly massive and varies from pyrrhotite-bearing to sulfide-barren (Fig. 14). The pyrrhotite occurs as anhedral grains or irregular aggregates, 30 to 300 μm across, with one of the larger or two of the smaller occurrences per chip.

The pyroxenite contains major amounts of clinopyroxene and small amounts of orthopyroxene, accompanied by minor amounts of plagioclase. The quantitative mineralogy is given in Table 7. The clinopyroxene is the coarser grained of the two pyroxenes; the largest clinopyroxene is a prismatic grain ~0.8 × 3 mm, whereas the largest orthopyroxene is about half that size. The orthopyroxene has been the more susceptible to alteration, and much of the talc in the sample occurs as fine-grained alteration rims, veinlets, and complete replacements of the orthopyroxene. Plagioclase varies from fresh to partly altered, the latter mainly network veins of a low-birefringence mineral that is probably chlorite. Brown amphibole occurs among the interstices of pyroxene aggregates, and as a replacement of the pyroxene. Accessory mica occurs

Table 7. Quantitative mineralogy of VR71275A

wt%				
	quartz	2.1	talc	43.1
	plagioclase	7.0	chlorite	6.4
	amphibole	7.6	lizardite	1.7
	clinopyroxene	28.1	pyrrhotite	0.3
	enstatite	3.5	pentlandite	0.3

as reddish brown biotite (phlogopite), and only a trace of micaceous alteration ('sericitization') of the plagioclase is present. The mica content is too low for detection in the X-ray study.

The opaque-mineral assemblage is complex. The principal non-sulfide opaque mineral is ilmenite, and only a trace amount of magnetite was observed; abundances of both, however, are too low to be detectable in the X-ray diffractogram. The sulfides consist of pyrite (including the megascopically identified chip), chalcopyrite, pyrrhotite, marcasite, pentlandite, and a trace of what is thought to be cubanite. The marcasite occurs as microcrystalline aggregates that form particles containing numerous oriented voids or inclusions (Fig. 15). Also evident in one aggregate is coarser grained pyrite whose appearance suggests possible co-crystallization with the marcasite. The fine grain size and the pervasive and numerous aligned voids are combined features that are characteristic of marcasite derived by alteration of precursor pyrrhotite. The marcasite is associated with the pyroxenite chips, and none occurs in the siltstone. The sulfide in the siltstone is pyrrhotite, whereas nearly all of the pyrrhotite in the pyroxenites has been converted to marcasite, but with pentlandite unaffected.

The estimated relative abundance of the sulfides is marcasite > chalcopyrite > pentlandite > pyrite > pyrrhotite. The megascopic estimate of 0.3% sulfides is low; the optical examination suggests a higher value, perhaps 0.6%, which is still lower than the bulk-sample chemical value of 0.99 wt% S (Table 1).

Although no carbonate minerals were observed during the optical examination, a subsequent application of alizarin solution to a portion of the unmounted crushed sample revealed the presence of sub-millimetric calcite veinlets in two of the chips. The calcite was identified by its red stain rather than from effervescence. Application of 15% HNO_3 to the sample resulted in immediate and vigorous effervescence from the two veinlets. As well, four other chips were observed to effervesce, but it was uncertain whether the source was calcite or dolomite.

The measured NP of the bulk sample is 24.6 (Table 1). The sample does not contain olivine and has little serpentine (Table 7), thus suggesting that a significant portion of the NP is carbonate-sourced. However, the low C_{total} (Table 1) does not support the suggestion.

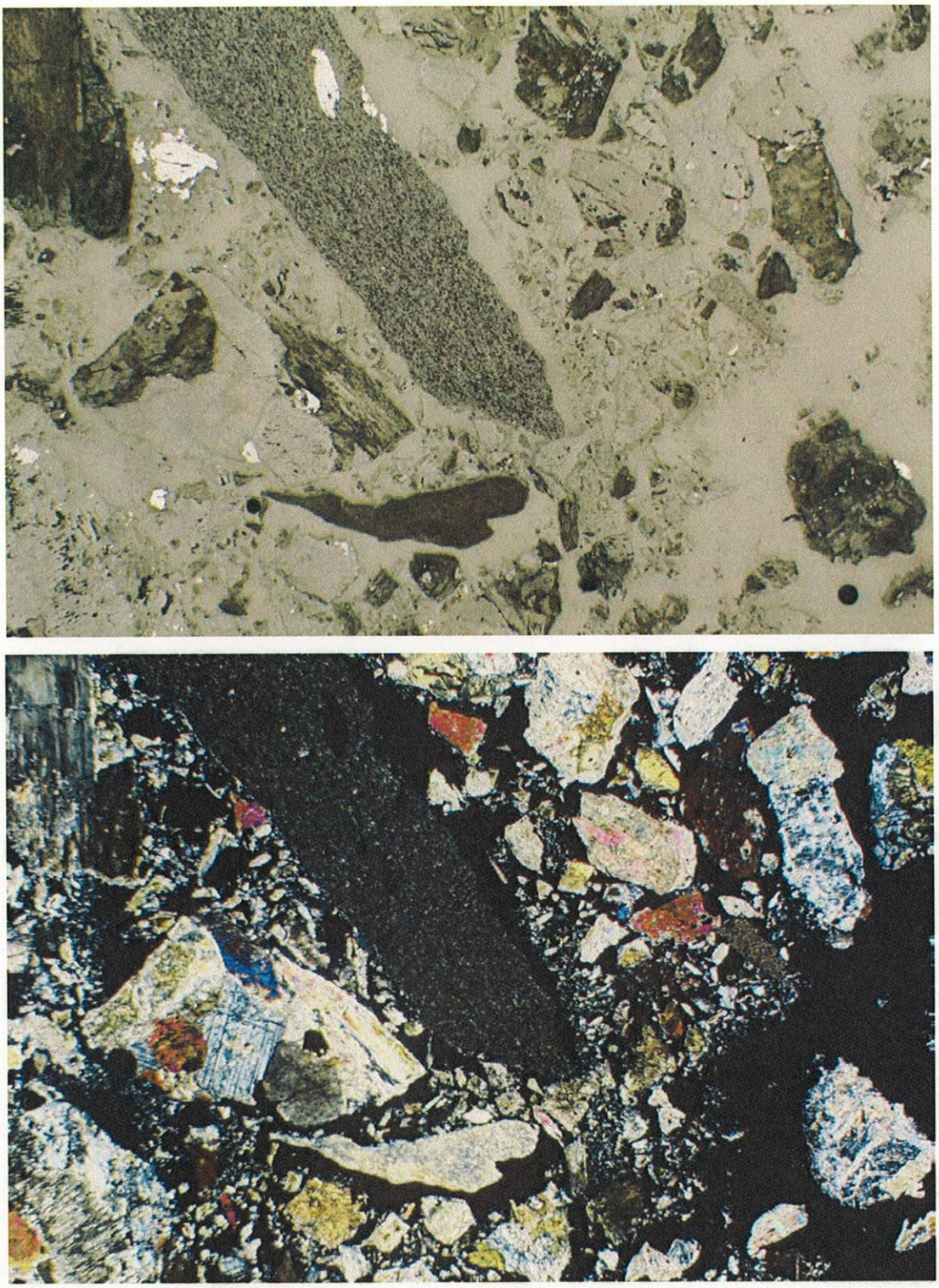


Figure 14. Sample VR71275A in plain reflected light (top) and in same field in transmitted light with crossed polarizers (bottom), width of field 5.1 mm. The elongate, fine-grained chip trending northwest is siltstone with pyrrhotite (white). In the lower photo, the gray twinned grain slightly below mid-height on the left is plagioclase, and the bright variegated particles are talc.

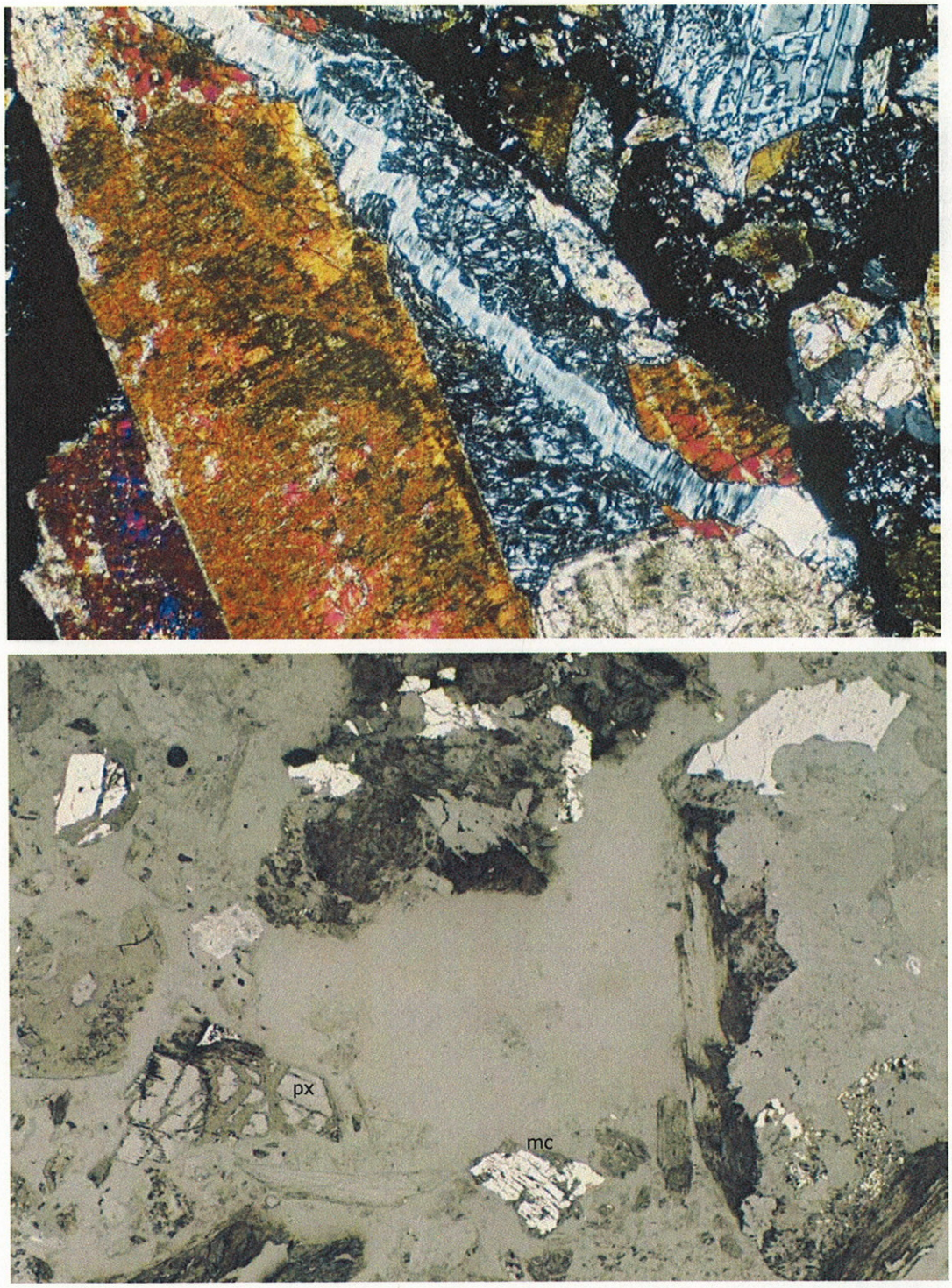


Figure 15. Sample VR71275A. The upper photo, in transmitted light with crossed polarizers, width of field 5.1 mm, shows a large prismatic clinopyroxene grain on the left, and adjacent on the right is chlorite cut by a cross-fiber veinlet, also of chlorite. At the top right is plagioclase veined by chlorite. In the lower photo in plain reflected light, width of field 2.6 mm, the whitish particle at the top right is ilmenite, the whitish particle below center is marcasite (**mc**), and to its left is veined orthopyroxene (**px**).

Sample VR91267A

Crushed sample VR91267A, which is classified as peridotite (Table 1), was noted to be similar in appearance to that of the preceding sample of pyroxenite. However, the core of the peridotite sample is the darker of the two, and even though the size of the coarsest grains in both seems to be alike megascopically, the peridotite has less color contrast among the minerals and therefore gives the impression of being the finer grained. Pyrrhotite ± chalcopyrite occurs as sparingly disseminated grains that are up to 2 × 5 mm, and one segmented particle is ~2½ × 8 mm. A poorly visible, pale greenish, irregular and ramifying veinlet, variable from 1 to 3 mm in width and probably consisting largely of serpentine or chlorite, cuts the core almost perpendicular to the elongation. One portion within the veinlet, about ½ mm wide and 7 mm long, consists solidly of calcite; otherwise, however, calcite is erratic and sparse within the remainder of the veinlet, and only a trace of calcite was detected in the remainder of the host peridotite.

The optical section contains >100 chips, all of which are <2 mm across. Megascopically visible sulfide grains span the size range of the chips. Viewed microscopically in transmitted light, a notable feature is the higher content of plagioclase relative to that in preceding pyroxenite VR71275A. The grain-size difference from that of VR71275 is indistinct except that plagioclase is locally coarser, and one of the observed laths is 1.7 mm long. The rock consists largely of clinopyroxene, plagioclase, and chlorite (Table 8). The presence of 1% olivine in the X-ray quantitative mineralogy is at marginal detection limits because of the complexity of the X-ray diffractogram, and no olivine was observed in the optical section. Orthopyroxene is present in only small amounts because most has been extensively altered (Fig. 16), and the mineral was not detected in the X-ray pattern. Because of its low olivine content, the rock is perhaps more appropriately grouped with pyroxenite rather than with peridotite.

Table 8. Quantitative mineralogy of VR91267A

wt%				
	quartz	1.9	chlorite	26.5
	plagioclase	20.0	talc	6.3
	biotite	6.7	lizardite	3.8
	amphibole	6.5	pyrrhotite	3.8
	clinopyroxene	21.5	ilmenite	2.1
	olivine	1.0		

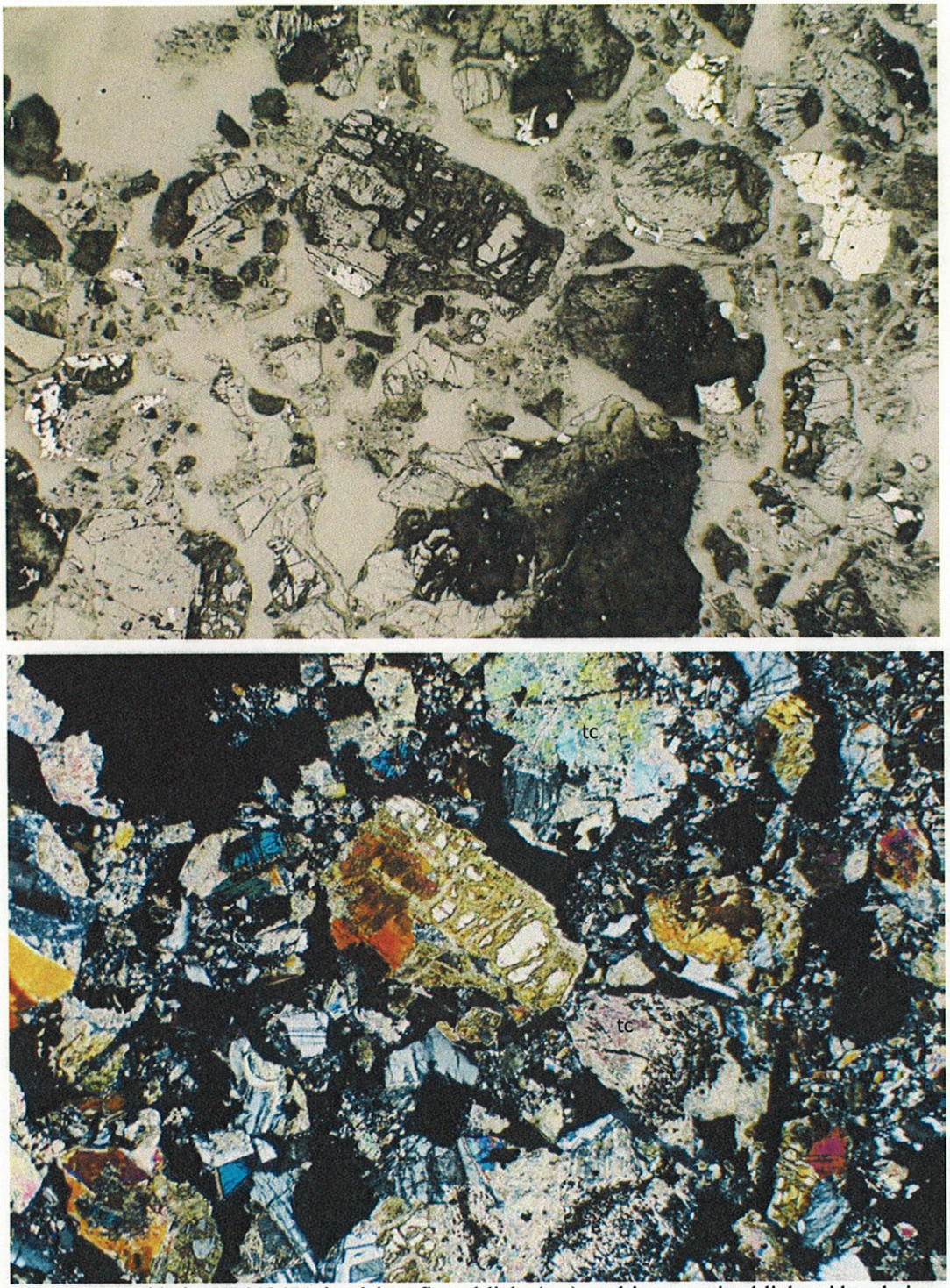


Figure 16. Peridotite VR91267A in plain reflected light (top), and in transmitted light with polarizers crossed, width of field 5.1 mm. Near the center is a veined, largely replaced stubby prism of orthopyroxene; the attached high-reflectance grain (upper photo) is magnetite with laths of ilmenite, and the large whitish grains at the upper right corner and at the extreme left are pyrrhotite. In the lower photo, the brownish mineral associated with the orthopyroxene is amphibole, the gray-to-white grains with lamellar twinning are plagioclase, the solidly bright blue grains are clinopyroxene, and the variegate grains are talc (**tc**).

Only one monomineralic carbonate grain, a liberated cleavage fragment about 230 μm along an edge, was observed in the section. A small chip of chlorite contains a cluster of several grains of carbonate, the largest 150 × 250 μm. Tests with alizarin solution indicated the liberated grain and the cluster to be dolomite, thus contrasting with the presence of veinlet calcite observed in the core.

The sulfides in the section occur both as liberated grains and as intergrowths within the pyroxenite. The largest sulfide grain, almost 1 mm across, consists of chalcopyrite and lesser pyrrhotite, with the two in a simple 'mutual boundary' contact; the pyrrhotite contains traces of replacement marcasite. Other grains vary from pyrrhotite–pentlandite–chalcopyrite intergrowths to liberated monomineralic pyrrhotite and chalcopyrite; pentlandite, however, typically occurs as middlings with pyrrhotite. A few grains contain laths or rods of chalcopyrite in pyrrhotite; the texture is identical to that shown in Figure 8 of Part 1. The sulfide relative proportions in the section are pyrrhotite > chalcopyrite > pentlandite. The sulfides are unevenly distributed, and some fields of view in the section are almost sulfide-barren whereas others have percentage amounts. The average content was estimated to be ≥1%.

The measured NP of the sample is 22.2 (Table 1), which indicates that a significant proportion of the NP must be present as carbonates. Testing of a portion of the unmounted crushed material by the application of alizarin solution did not give an observable reaction. However, upon the addition of 15% HNO_3, three areas gave a slow effervescence, which is typical of the reaction from dolomite rather than calcite. Two of the areas continued to effervesce, without exhaustion, for several minutes, suggesting that the dolomite particles were not minute.

Sample VR71373A

Unlike all preceding cores, which are quarters, sample VR71373A is a half core, ~63 mm in diameter. The sample is of 'mineralized peridotite', and the megascopic appearance is like that of pyroxenite VR712754A. The sulfide content is about 5% and is predominantly pyrrhotite, apparently with pentlandite > chalcopyrite. The bulk of the sulfides occurs as large (2 3 mm) equant to elongate particles evenly distributed throughout the rock. No fractures are evident.

The optical section contains >50 chips, the largest ~2½ × 4 mm. Many of the chips consist solely of sulfides, and megascopically visible sulfide fines bring the total content of these minerals to percentage amounts. Microscopic examination revealed that pyrrhotite > chalcopyrite > pentlandite, but all three are abundant. Marcasite is common but not as widespread; it appears to have formed locally as partial to rarely complete replacements of pyrrhotite (Fig. 17). The partial replacements are invariably concentrated at the margins of the pyrrhotite, and in some cases the marcasite projects into the surrounding silicates as sawtooth-like, extremely fine-grained, fibrous crystals. Trace amounts of pyrite occur as subhedral grains and aggregates within pyrrhotite and within marcasite (Fig. 17). One chip consists largely of two, almost-touching, elongate segments of homogeneous pyrite whose combined large size, 0.26 × 1 mm, is unusual; the pyrite seems to have been part of a veinlet, but the texture is not definitive. Primary magnetite and ilmenite are present, but ilmenite is predominant among the coarser, equant-type grains whereas the content of magnetite is supplemented by thread-like grains that accompany serpentine in altered olivine (Table 9). Textures of the sulfides vary from monomineralic and liberated, to variously intergrown (Fig. 18), depending mainly on the extent to which the particle had been crushed.

The host rock was optically identified as containing major amounts of olivine, plagioclase, and clinopyroxene, among which olivine is the most extensively altered. Plagioclase is almost fresh, but all olivine has been at least partly altered to a mesh texture in which the veinlets are of serpentine and threads of magnetite within the serpentine (Figs. 18, 19). Although a few pseudomorphs after olivine are present, serpentinization seems not to have progressed beyond mesh-texture development; rather, local overprinting by chloritization of the partly serpentinized olivine has produced the pseudomorphs, hence accounting for the lack of a gradation from mesh textures to total serpentinization. Chlorite and talc occur abundantly as late-stage minerals. Brown amphibole and biotite are commonly associated with plagioclase–

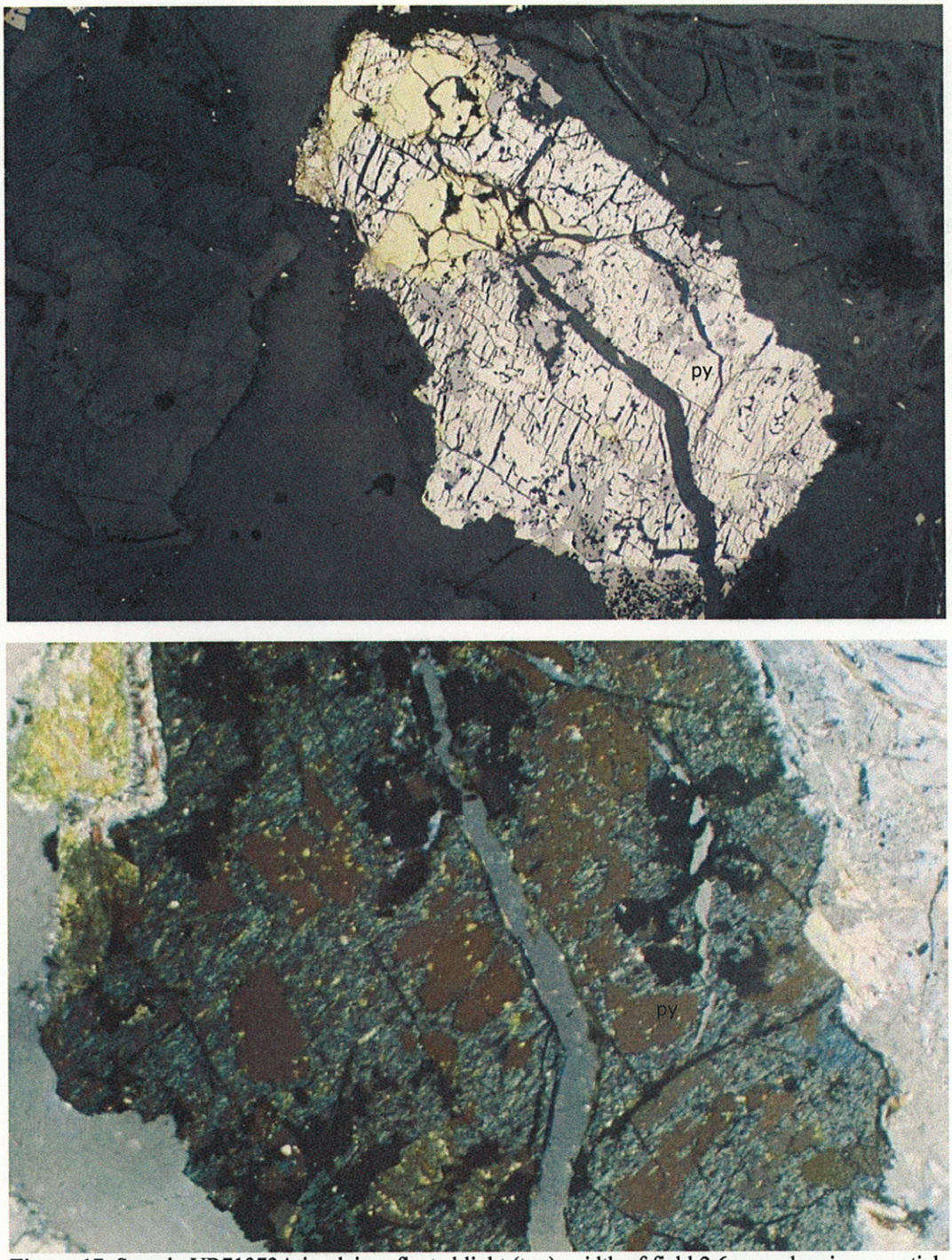


Figure 17. Sample VR71373A in plain reflected light (top), width of field 2.6 mm, showing a particle interpreted to be a pseudomorph after pyrrhotite. The yellow mineral is chalcopyrite, and the main white with parallel cracks is marcasite, within which are smooth white grains of pyrite (**PY**). The gray mineral is magnetite, and the slightly brownish gray grains to the right of chalcopyrite at the top are ilmenite; the black 'veinlets' are epoxy-filled cracks. The lower photo is the same area at higher magnification (width of field 1.25 mm) and slightly rotated clockwise; **PY** is the same grain as labelled in the upper photo. The strongly anisotropic, finely polycrystalline matrix is marcasite, and the black grains are magnetite.

Table 9. Quantitative mineralogy of peridotite sample VR71373A

wt%				
	quartz	1.7	talc	7.6
	olivine	8.8	lizardite	3.3
	clinopyroxene	14.0	magnetite	5.9
	plagioclase	13.8	ilmenite	1.5
	amphibole	6.4	pyrrhotite	5.6
	biotite	4.6	pentlandite	1.6
	chlorite	22.8	dolomite	2.5

clinopyroxene intergrowths (Fig. 19), and orthopyroxene prisms, which have been particularly susceptible to replacement by talc, are insufficiently abundant to have been included in the quantitative mineralogy (Table 9). The X-ray data indicate that the serpentine mineral is lizardite, and no asbestiform serpentine was observed either macroscopically or microscopically.

Only two grains of carbonates were observed in the optical section, and both have a distinct association in that they occur as the infill of chlorite-lined vugs. One of the grains is about 100 μm across, but the other approximates 1 mm. Testing of the carbonates with alizarin solution showed the mineral to be calcite (Fig. 20). The occurrences indicate that the calcite is part of the peridotite assemblage rather than related to later veining.

In subsequent testing of a portion of the crushed sample, no reaction was observed upon the application of alizarin solution. With 15% HNO_3, however, several areas effervesced slowly to rapidly. The results suggested that both dolomite and calcite were present, but the lack of persistence of the effervescence is likely an indication that the grains were small and were rapidly consumed. The 2.5% dolomite reported in the quantitative mineralogy (Table 9) is too high relative to the content of carbonates observed in the optical section, but the detection of dolomite further suggests that two carbonate minerals are present in the bulk sample.

The measured NP value of 32.4 is the highest in the ten-sample suite. A substantial portion of the NP is attributable to the presence of olivine and serpentine; the C_{total} of 0.06 wt% (Table 1) indicates a supplementary contribution of NP by carbonate minerals whose chemically measured magnitude of abundance is in accord with the microscopic and megascopic observations.

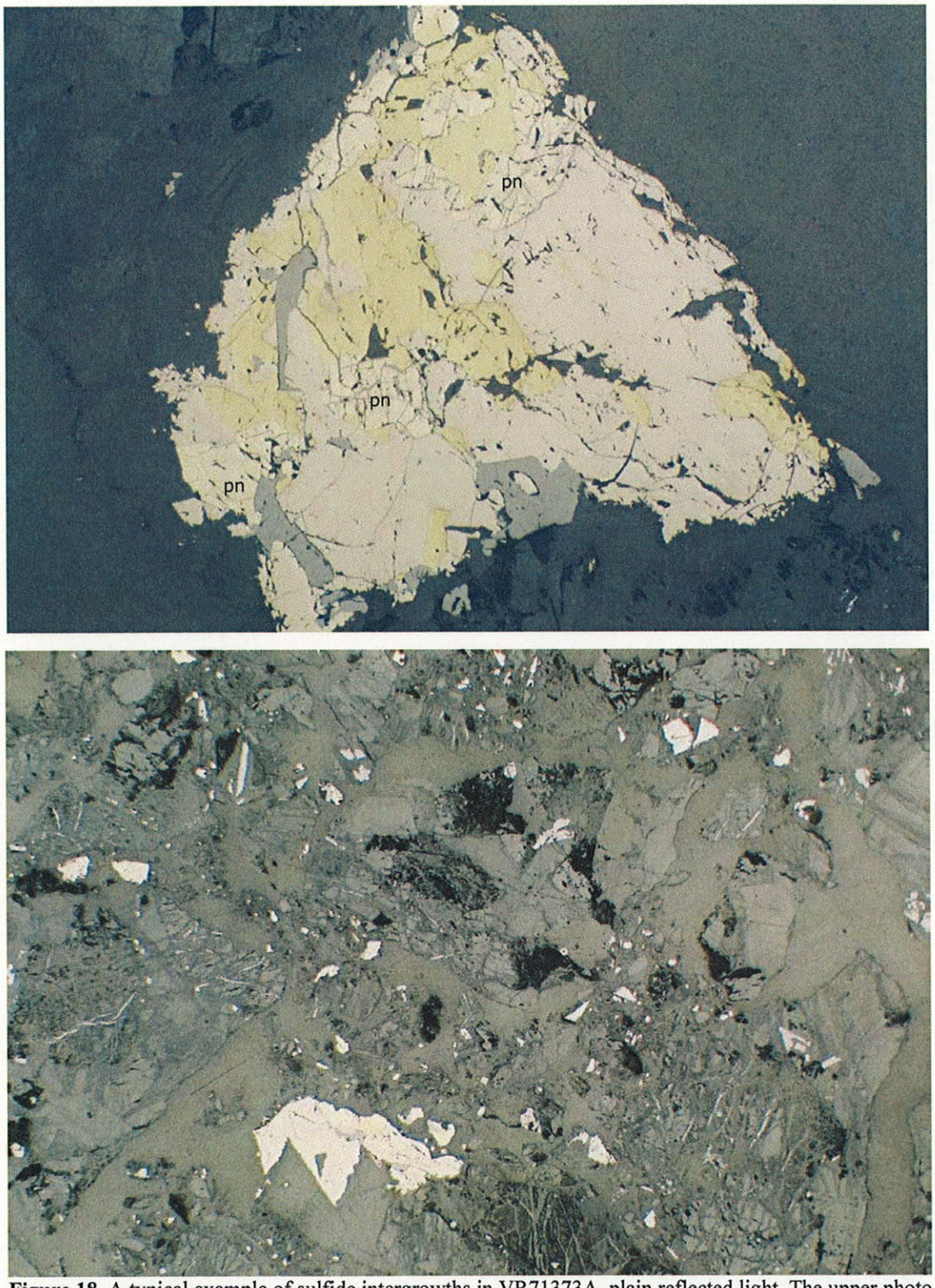


Figure 18. A typical example of sulfide intergrowths in VR71373A, plain reflected light. The upper photo (width of field 2.6 mm) shows yellow chalcopyrite, slightly pinkish pyrrhotite, pentlandite (**pn**), and grayish ilmenite. The lower photo (width of field 5.1 mm) shows mainly whitish pyrrhotite. Olivine is identifiable by the presence of whitish, thread-like grains of magnetite associated with serpentinization. Figure 19 is the same field of view in transmitted light.

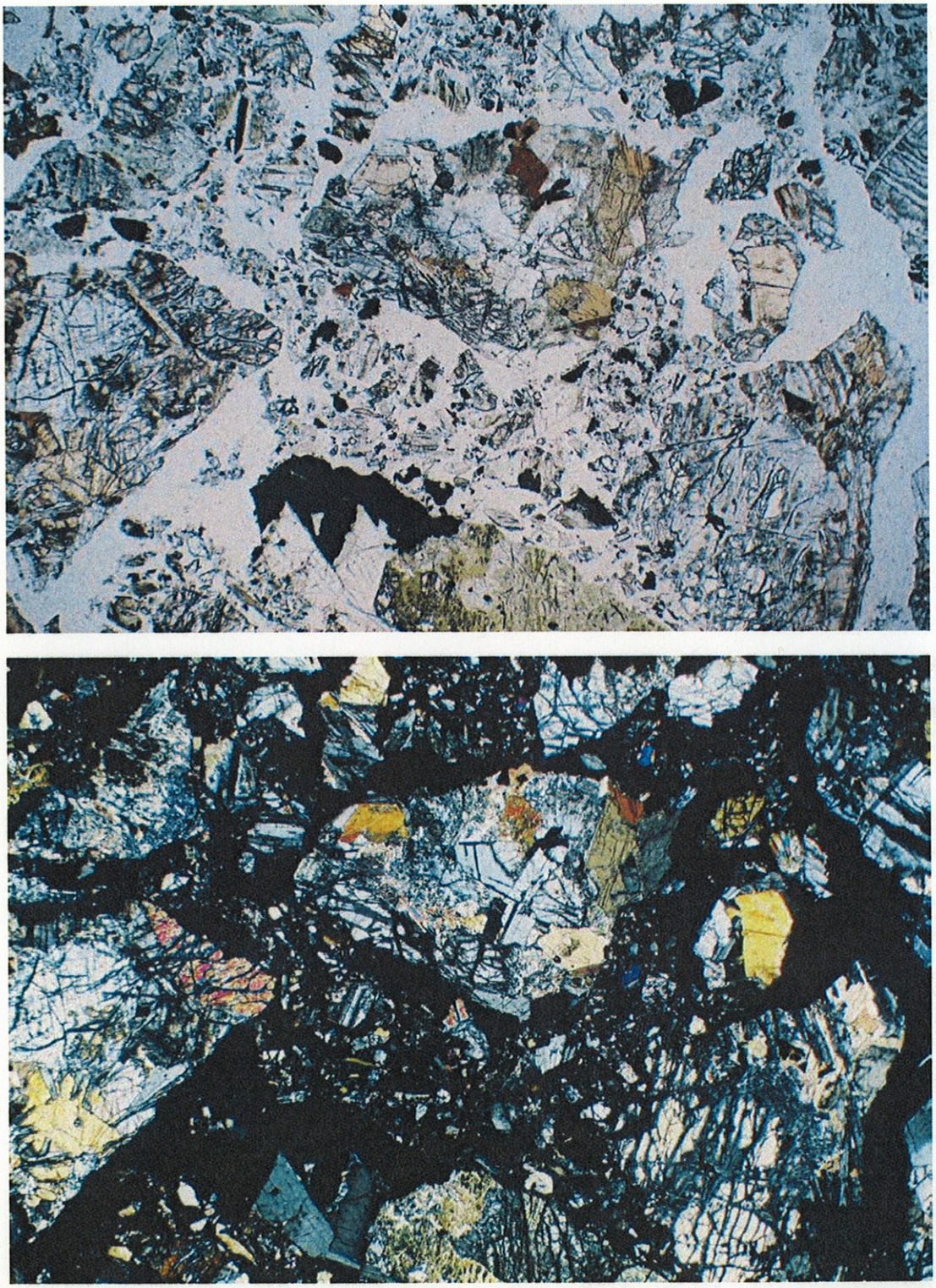


Figure 19. VR71373A in plain transmitted light (top), and with polarizers crossed (bottom), showing the same field of view as in the lower photo of Figure 18. In the upper photo, the brownish grains on the right of the chip slightly above center are amphibole, and to their left the associated gray, twinned grains (lower photo) are plagioclase.

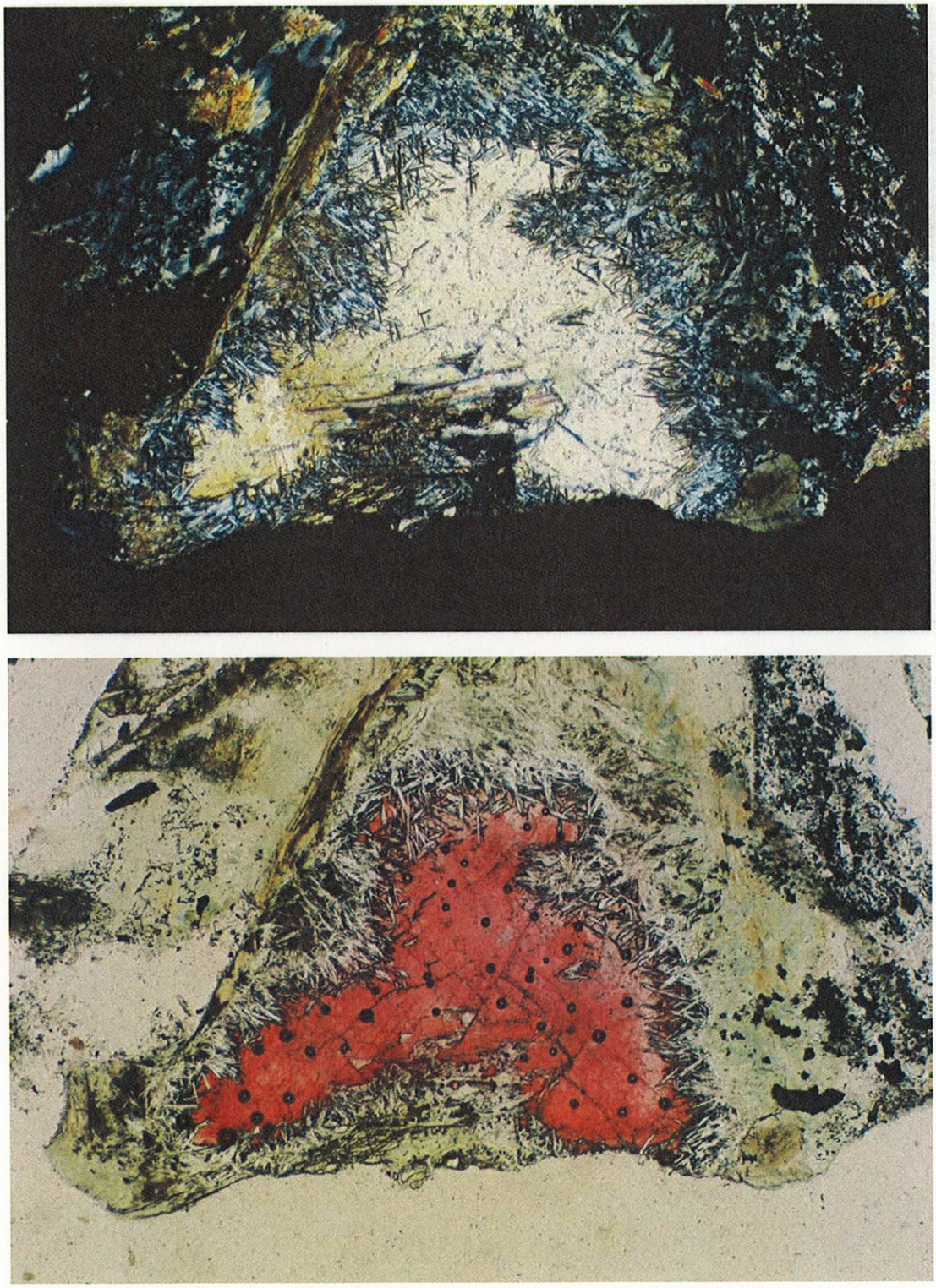


Figure 20. Sample VR71373A in transmitted light, width of field 2.6 mm. Upper photo, with polarizers crossed, shows acicular to lath-like chlorite projecting into a former vug infilled with calcite. The lower photo, in plain light, shows the distinct effect of alizarin solution, which stains the calcite to a vivid red

Sample VR90181A

The sample is a cut half-core of massive sulfide in which at least three sulfide minerals are present and are taken to be pyrrhotite, chalcopyrite, and pentlandite, with pyrrhotite predominant and the other two in percentage amounts. The sulfides have a chaotic, brecciated appearance, with some centimeters-size pyrrhotite-dominant fragments apparently cemented by chalcopyrite–pentlandite; in contrast, other fragments are of mixed sulfides and have at least a partial pyrrhotite-rich rim, thus suggesting that reversals occurred in the order of sulfide crystallization. One end of the core is a random break, but the other end is a rough fracture surface at a steep angle to the core length. Part of the fracture surface is black and possibly chloritic, and part of the same surface is discontinuously calcite-bearing. Otherwise, however, no calcite was detected in the core.

The crushed material, after further reduction of the size of the chips in a random split, was used for the polished thin section. The section contains >50 chips that are 1 2 mm across, plus abundant finer particles. Nearly all are sulfides and associated magnetite; microscopic examination showed that the non-opaque content is negligible (<0.1%). The sulfide assemblage consists of pyrrhotite > chalcopyrite > pentlandite. No marcasite or pyrite was observed. Textures are relatively simple (Figs. 21, 22). Pentlandite occurs mainly as large homogeneous grains, and although flames of pentlandite in pyrrhotite are present, they account for only a small fraction of a percentage of total pentlandite.

The sample was not subjected to quantitative mineralogical analysis because of the low content of non-opaque minerals. However, the few translucent grains that were observed occurred mainly at the edges of sulfide particles and were tentatively identified to be a carbonate mineral. Testing with 15% HNO_3 gave no reaction, thus suggesting that the veinlets consisted of siderite [$FeCO_3$]. Because siderite had not been identified previously in the Eagle assemblages, five areas were examined by SEM–EDS analysis. All proved to be siderite. The spectra for three of the grains, which illustrate the maximum compositional variation obtained, are shown in Figures 22 and 23. Substitution of Fe by Mg, Mn, and Ca is evident but is not appreciable, and the average composition is well toward that of end-member siderite.

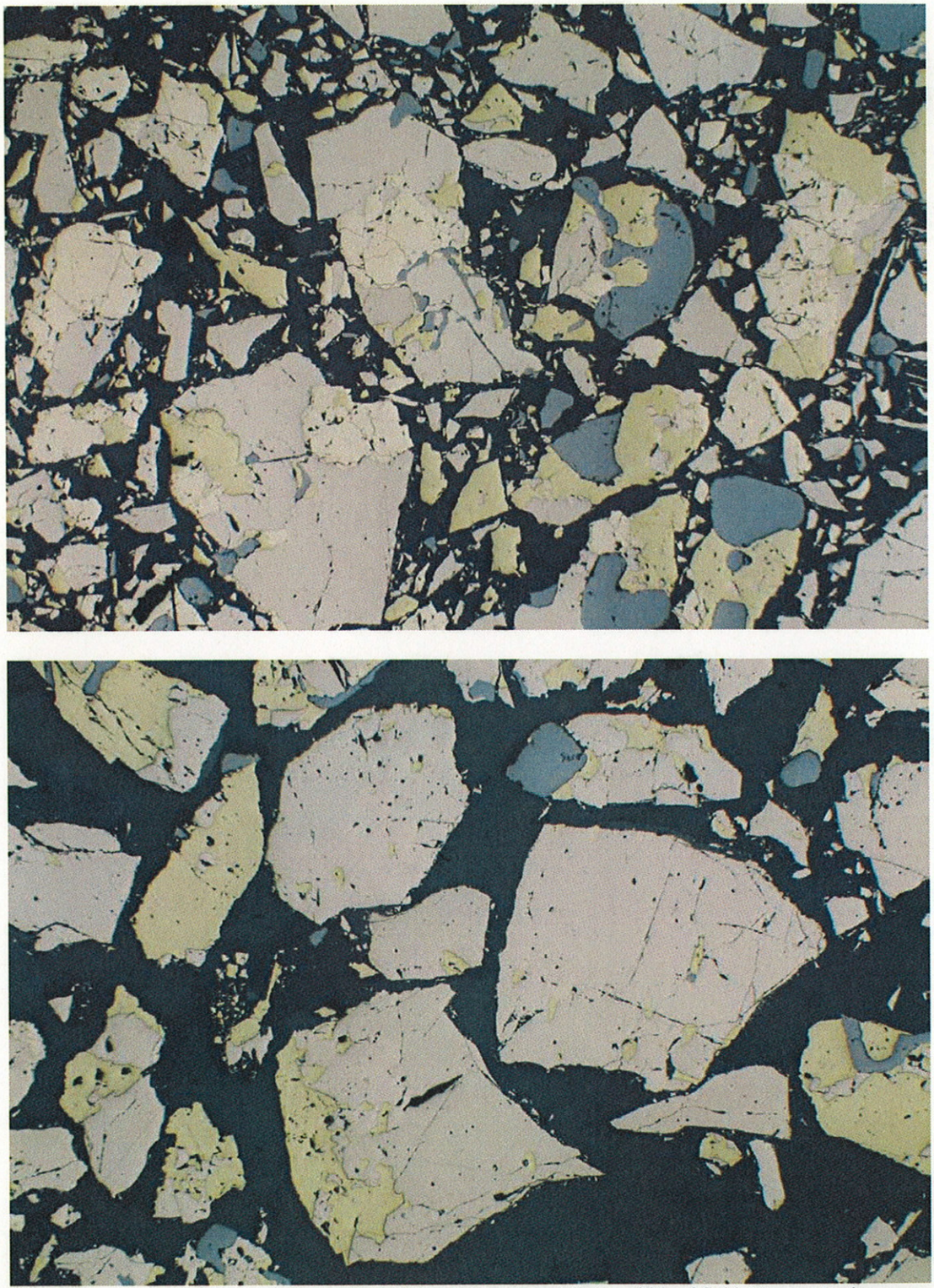
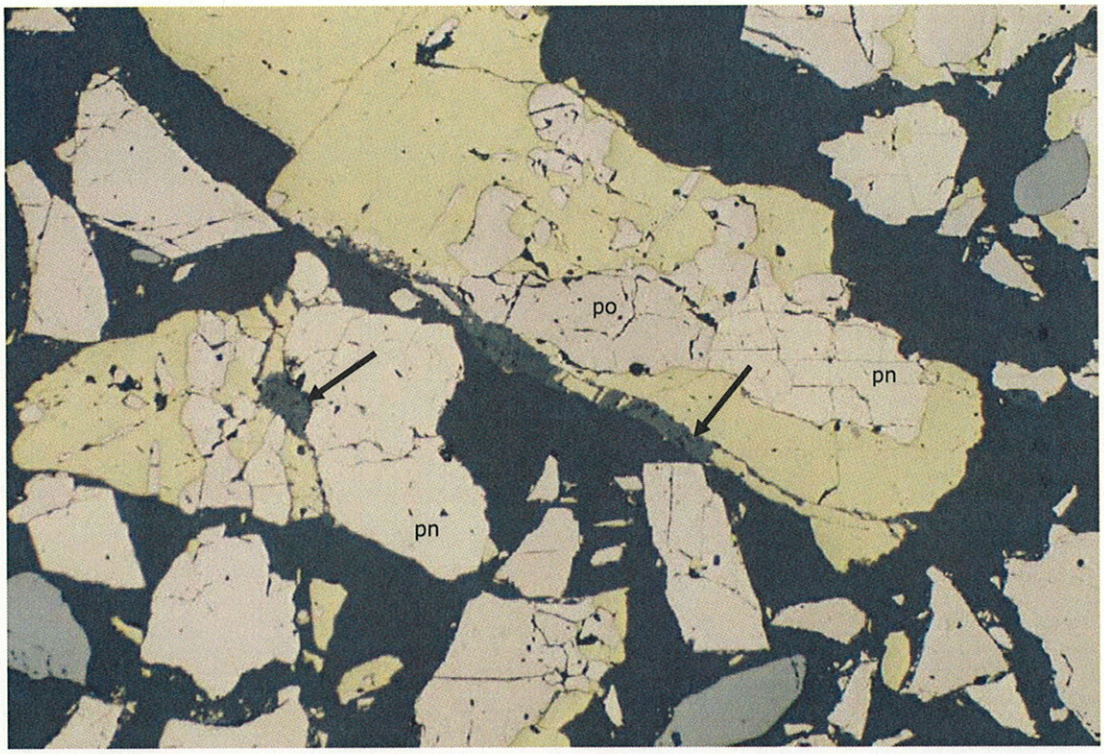


Figure 21. Massive sulfide sample VR90181A in plain reflected light, width of field 5.1 mm. In the upper photo, yellow grains are chalcopyrite, slightly pinkish = pyrrhotite, off-white = pentlandite, gray = magnetite, and no other minerals are present. In the lower photo, the arrows at the bottom right and in the large pyrrhotite grain left of center point to siderite veinlets.



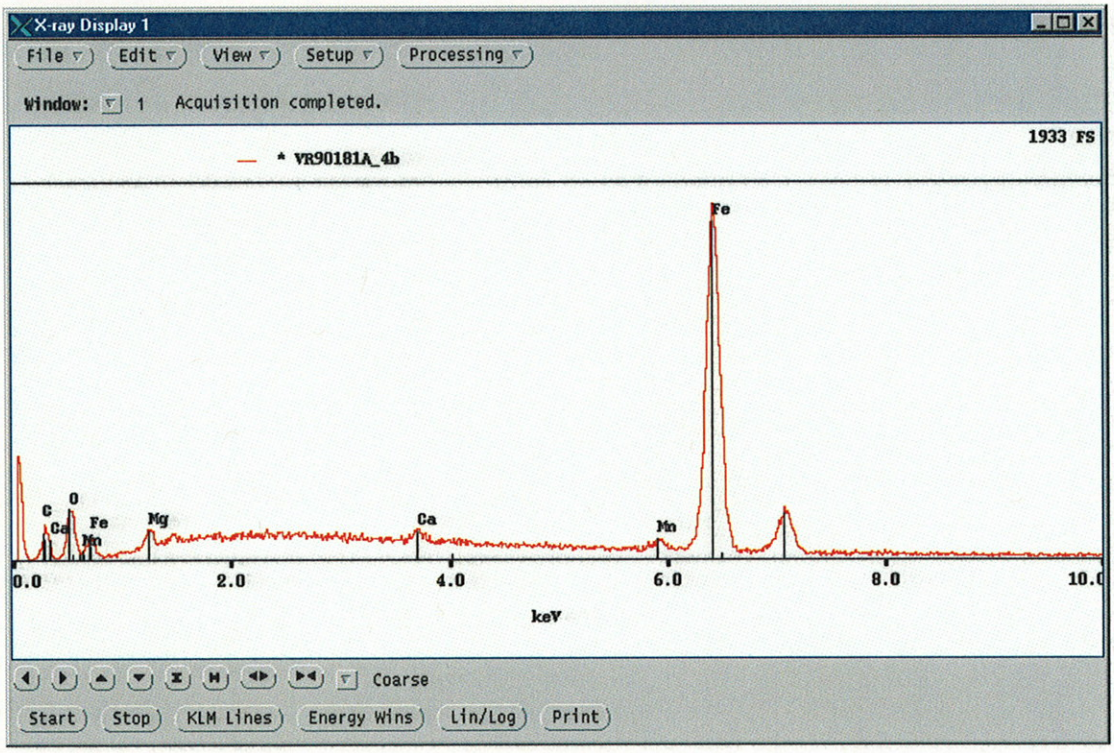


Figure 22. Massive sulfide sample VR90181A in plain reflected light, width of field 2.6 mm; yellow is chalcopyrite, **po** is pyrrhotite, and **pn** is pentlandite. The two arrows point to a grain of siderite and a veinlet of siderite. The EDS spectrum is for the veinlet. The spectrum for the grain is similar to that shown in the lower part of Figure 23.

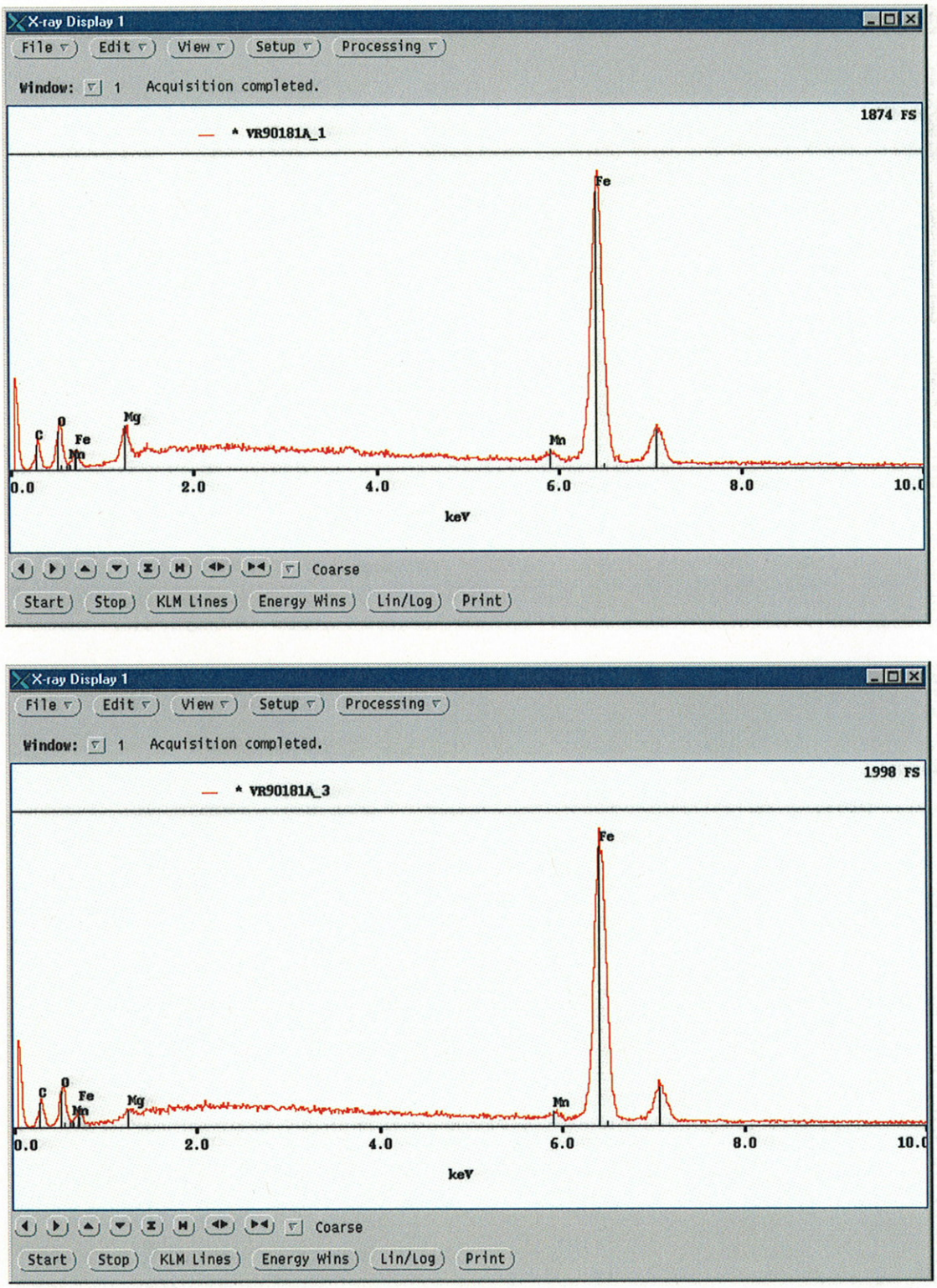


Figure 23. EDS spectra of siderite in VR90181A. The upper spectrum is for the veinlet on the left in the lower photo of Figure 21. The lower spectrum, for an occluded grain in sulfides, shows only traces of Mg and Mn; similar results were obtained for the occluded grain on the left in the photo of Figure 22.

Sample VR90125A

The sample is of semi-massive sulfides, megascopically identified as predominantly of pyrrhotite, with pentlandite and chalcopyrite common but much subordinate in abundance. The cut surface of the half-core shows a fairly uniform distribution of sulfides, whereas at the core exterior there are two slightly finer grained, seemingly mafic-poor areas that are also relatively sulfide-poor. One end of the core is a random break, but the other is a rough, steep-angle fracture along which a small portion is a chloritic or serpentinitic surface. No calcite was detected at the fracture surface or in any part of the core. The crushed sample, after splitting and size reduction, was used for the polished thin section.

The optical section contains >100 chips, the largest ~2 mm across. Microscopic examination showed that, unlike the samples of massive sulfides, silicates predominate and sulfides are subordinate. Pyrrhotite is the most abundant sulfide, but both chalcopyrite and pentlandite are common. A few grains of pyrrhotite contain flames of pentlandite, but quantitatively nearly all pentlandite occurs as anhedral grains, like those of pyrrhotite and chalcopyrite. A few grains of pyrrhotite contain flames and rods of marcasite (Fig. 24), but extensive replacement of pyrrhotite by marcasite of the type illustrated in Figures 15 and 17 is not present, and there is no relationship between flame-like pentlandite and marcasite other than their exclusive occurrence within pyrrhotite. Although several grains of ilmenite were observed, the principal primary oxide is magnetite rather than ilmenite, and one of the magnetite grains is 300 × 550 μm across. Magnetite also occurs as thread-like grains associated with the serpentine alteration of olivine.

The silicate assemblage consists principally of plagioclase, clinopyroxene, olivine, and alteration products (Figs. 25, 26). A few grains of orthopyroxene are present, but are insufficient to have been detected in the quantitative mineralogical analysis. Talc is the most abundant

Table 10. Quantitative mineralogy of semi-massive sulfide sample VR90125A

wt%				
	plagioclase	13.2	talc	20.0
	clinopyroxene	17.6	lizardite	3.1
	olivine	7.4	pyrrhotite	16.2
	amphibole	2.4	pentlandite	4.2
	magnetite	9.7	chalcopyrite	2.7
	biotite	1.5	dolomite	2.0

replacement mineral, and although chlorite is optically evident, the X-ray data indicate that most of the fine-grained alteration products are talc. The seemingly mafic- and sulfide-poor areas noted megascopically are probably of the type illustrated in Figure 25, wherein the assemblage consists chiefly of an intergrowth of clinopyroxene and plagioclase.

A portion of the crushed sample was tested with alizarin solution and then with 15% HNO_3, and with neither was the presence of carbonates detected. Although one carbonate-mineral particle associated with chlorite was observed in the optical section (Fig. 27), all but a minute amount of the bulk-sample NP of 23.9 (Table 1) must be assigned to the silicate assemblage.



Figure 24. Sample VR90125A in plain reflected light, width of field 0.625 mm, showing oriented rods and flames of marcasite (white) within pyrrhotite. The attached sulfide on the left is pentlandite.

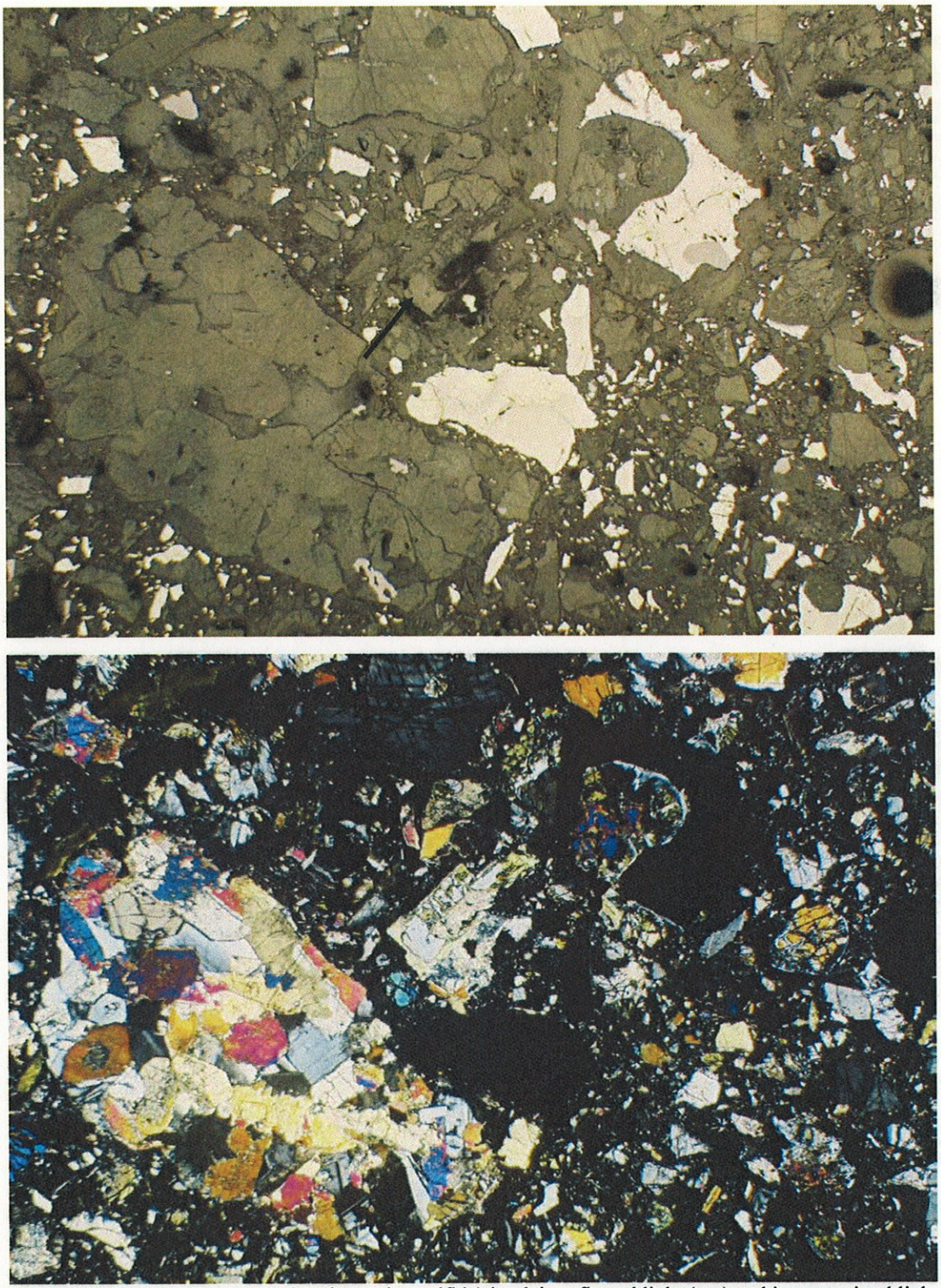


Figure 25. Sample VR90125A (semi-massive sulfide) in plain reflected light (top) and in transmitted light with crossed polarizers (bottom), width of field 5.1 mm. The large sulfide particle slightly below center consists mainly of pyrrhotite and pentlandite, and other whitish grains are mainly pyrrhotite. The left half of the field consists chiefly of a large particle of intergrown clinopyroxene (colored grains, lower photo) and plagioclase (twinned, gray to white). The arrow at the center of the upper photo points to a prismatic grain of orthopyroxene, partly altered to talc.

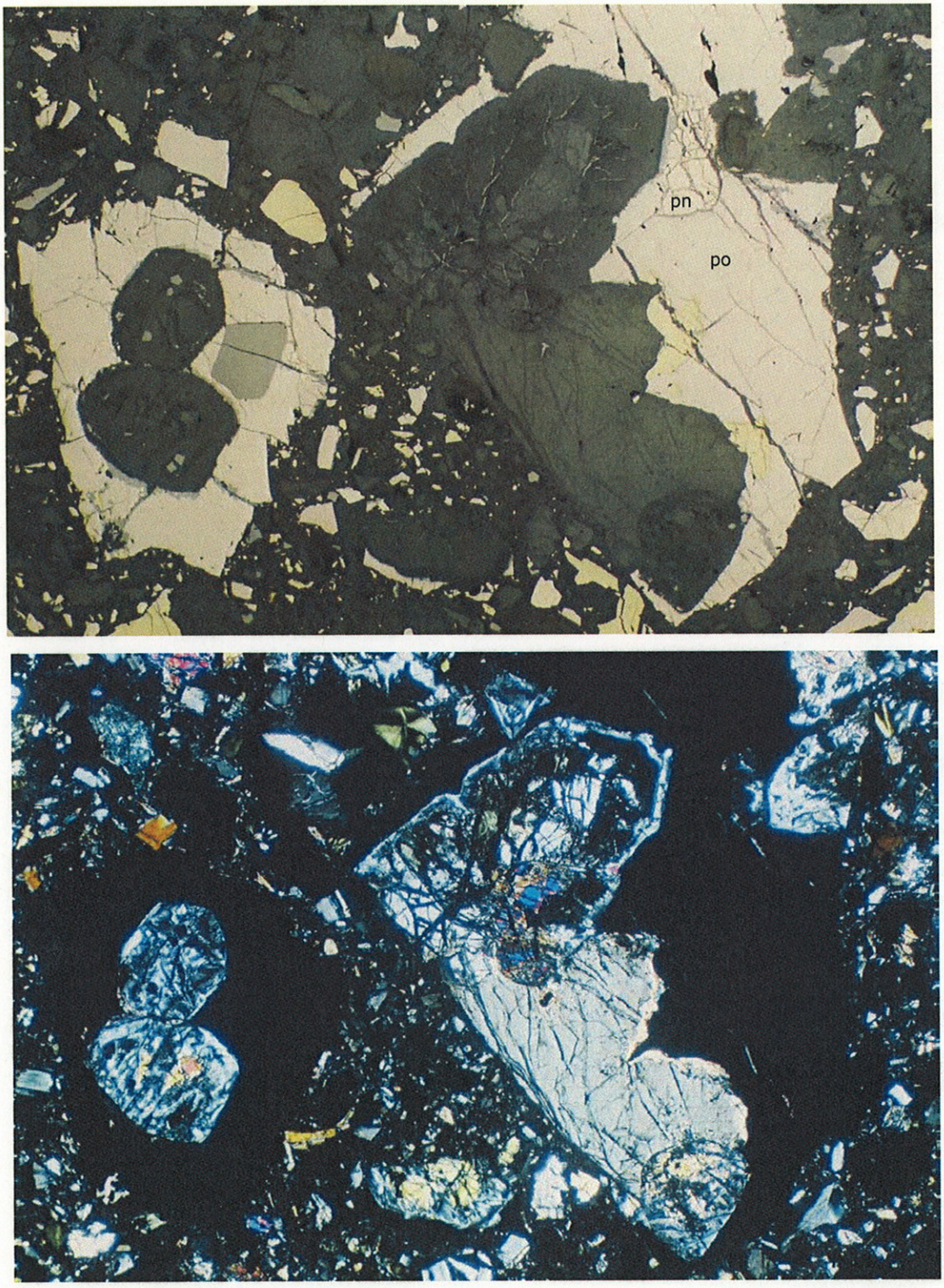


Figure 26. Semi-massive sulfide VR90125A in plain reflected light (top) and in transmitted light with polarizers crossed (bottom), width of field 2.6 mm. The yellow mineral in the upper photo is chalcopyrite, slightly pinkish is pyrrhotite (**po**), and off-white is pentlandite (**pn**). Threads of magnetite to the left of **pn** are in altered olivine, and on the far left are two equant grains of almost completely serpentinized olivine enclosed within pyrrhotite and magnetite.

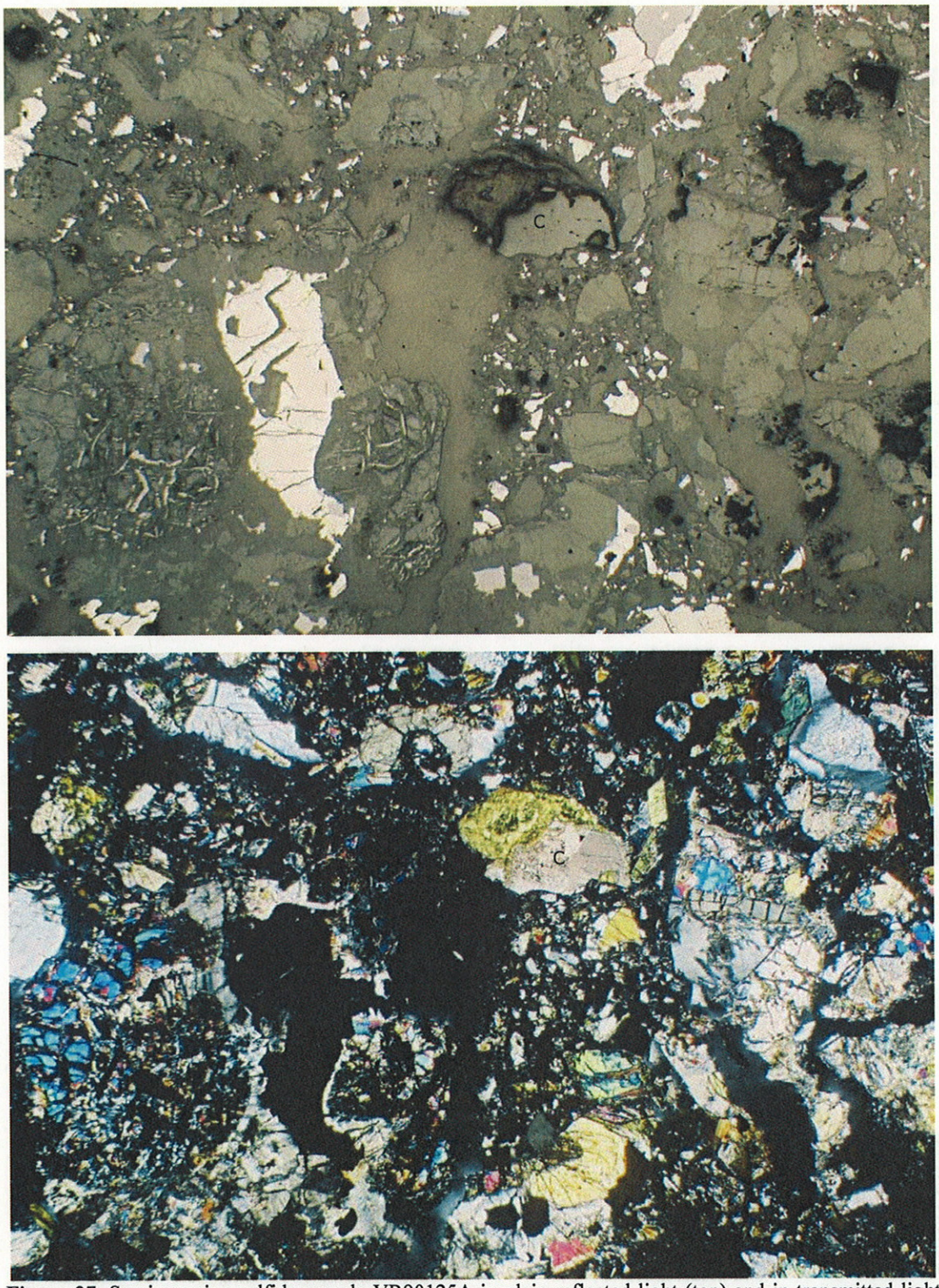


Figure 27. Semi-massive sulfide sample VR90125A in plain reflected light (top) and in transmitted light with crossed polarizers (bottom), width of field 5.1 mm. Most of the white grains in the upper photo are pyrrhotite, and flanking the largest particle (lower left) are threads of magnetite in partly serpentinized olivine. In the lower photo, above and right of center is a yellowish, fine-grained aggregate of chlorite to which is attached a large particle of a carbonate mineral, probably calcite (**C**).

DISCUSSION

The NP of numerous individual minerals has been determined using the Sobek method (Jambor et al. 2001, 2002); the results for several minerals relevant to the study of the Eagle samples are summarized in Table 11. It is evident from the data that few non-carbonate minerals yield high NP values, and that olivine and lizardite would be the principal non-carbonate sources of NP in the Eagle samples. It should also be borne in mind that the NP values in Table 11 are for samples containing 100% of the specified mineral.

The NP values for the Eagle samples have been determined with a modified Sobek method, presumably because it has been contended that the vigorous reaction in the Sobek test yields NP values that are too high in terms of 'accessible' NP. For the two minerals of principal concern, olivine and lizardite, Jambor et al. (2001) obtained Sobek NP values of 23.9 and 16.1, respectively, and 42.0 and 37.3 by the modified method (the olivine, however, had been reacted for 48 h rather than 24h). For the lizardite, a repeat determination about a year later, and by a different laboratory, gave NP values of 16.1 (Sobek) and 25.3 (modified method*). Thus, whereas the Sobek and modified tests generally yield little difference in the NP results for most minerals, the difference is greatest for olivine and lizardite. In assessing NP values and in attempting to achieve a reconciliation between the observed mineralogy and the measured NP values, it is necessary to bear in mind that the static-test results for ultramafic rocks are apparently strongly influenced by the methodology that has been employed to measure the NP.

Table 11. NP values of minerals as determined by the Sobek method

Mineral or Group	NP Range	*n*	Mineral or Group	NP Range	*n*
olivine (forsterite)	23.9 40.2	4	biotite (phlogopite)	2.7 8.8	3
pyroxene	0.5 9.5	9	chlorite (clinochlore)	1.5 12.5	6
amphibole	0.7 8.7	12	talc	1.7	1
K-feldspar	0.5 1.4	4	lizardite	16.1 22.5	2
albite Ab_{80}-Ab_{98}	0.5 0.6	2	magnetite	1.7	1
anorthite An_{50-52}	2.6 5.3	2			
anorthite An_{65-93}	10.7 12.5	3			

Data from Jambor et al. (2000, 2002, 2004); *n* = number of different samples tested.

*The modified method of Lawrence and Wang (1997) wherein the minimum pH at the acidification stage is 2 2.5 rather than 1.5 2.0, thereby decreasing the amount of acid dissolution of the sample. NP is also dependent on particle size, and for forsterite the value increased from 29.4 at a particle size of 250 212 μm, to 89.6 for a particle size of <44 μm (Jambor and Dutrizac 2002).

REFERENCES

Jambor, J.L. and Dutrizac, J.E. (2002) The effect of particle size on the neutralization potential in static-test predictions of acid drainage. *In* Recycling and Waste Treatment in Mineral and Metal Processing: Technical and Economic Aspects (B. Björkman, C. Samuelsson, J.-O. Wickström, eds.), Vol. 2, 651-663. The Minerals, Metals, Materials Soc., Warrendale, PA.

Jambor, J.L., Dutrizac, J.E., Chen, T.T. (2000) Contribution of specific minerals to the neutralization potential in static tests. *In* Proceedings from the Fifth International Conference on Acid Rock Drainage, Vol. 1, 551-565. Society for Mining, Metallurgy, and Exploration, Littleton, CO.

Jambor, J.L., Dutrizac, J.E., Groat, L.A., Raudsepp, M. (2002) Static tests of neutralization potentials of silicate and aluminosilicate minerals. Environmental Geology **43**, 1-17.

Jambor, J.L., Dutrizac, J.E., Riveros, P.A. (2004) Prediction of acid mine drainage: effect of the time gap between crushing and the static test. *In* REWAS 2004, Global Symposium on Recycling, Waste Treatment and Clean Technology. The Minerals, Metals, Materials Soc., Warrendale, PA (in press).

Lawrence, R.W. and Wang, Y. (1997) Determination of neutralization potential in the prediction of acid rock drainage. In Fourth International Conference on Acid Rock Drainage, Vol. 1, 449-464. MEND, Natural Resources Canada, Ottawa.

LRC (2004) Environmental mineralogy of samples from the Eagle deposit, Michigan – part 1. Report prepared by Leslie Research and Consulting for Geochimica, Inc., Ojai, CA.

APPENDIX 1

QUANTITATIVE PHASE ANALYSIS OF FOUR POWDER SAMPLES USING THE RIETVELD METHOD AND X-RAY POWDER DIFFRACTION DATA.

J.L. Jambor, Ph.D.
Leslie Research and Consulting
316Rosehill Wynd
Tsawwassen, B.C. V4M 3L9

Mati Raudsepp, Ph.D.
Elisabetta Pani, Ph.D.
Dept. of Earth & Ocean Sciences
6339 Stores Road
The University of British Columbia
Vancouver, BC V6T 1Z4

March 31, 2004

EXPERIMENTAL METHOD

The four samples "VR71325A", "VR71100A", "VR71499A" and "VR71213 were ground into fine powder to the optimum grain-size range for X-ray analysis (<10μm) by grinding under ethanol in a vibratory McCrone Micronising Mill for 7 minutes. Step-scan X-ray powder-diffraction data were collected over a range 3-70°2θ with CuKα radiation on a standard Siemens (Bruker) D5000 Bragg-Brentano diffractometer equipped with a diffracted-beam graphite monochromator crystal, 2 mm (1°) divergence and antiscatter slits, 0.6 mm receiving slit and incident-beam Soller slit. The long fine-focus Cu X-ray tube was operated at 40 kV and 40 mA, using a take-off angle of 6°.

RESULTS AND DISCUSSION

The X-ray diffractograms were analyzed using the International Centre for Diffraction Database PDF-4 using Search-Match software by Siemens (Bruker). X-ray powder-diffraction data were refined with Rietveld Topas 2.1 (Bruker AXS). The results of quantitative phase analysis by Rietveld refinement are given in Table 1. These amounts represent the relative amounts of crystalline phases normalized to 100%. Rietveld refinement plots for the samples are shown in Figures 1 - 4.

Table 1. Results of quantitative phase analysis (wt.%)

	Ideal Formula	18776 VR91620	18779 VR71109	18782 VR71275	18784 VR71373	18789 VR91625	18790 VR90125	18794 VR90425	18796 VR91267	18797 VR91306
Quartz	SiO_2	47.0	29.7	2.1	1.7	29.4		27.9	1.9	32.5
K-feldspar	$KAlSi_3O_8$		11.6					8.5		9.4
Plagioclase	$NaAlSi_3O_8 - CaAl_2Si_2O_8$	27.5	6.6	7.0	13.8	15.4	13.2	8.8	20.0	18.9
Muscovite	$KAl_2AlSi_3O_{10}(OH)_2$	15.0	39.6			37.5		43.0		13.4
Biotite	$K(Mg,Fe^{2+})_3AlSi_3O_{10}(OH)_2$				4.6		1.5		6.7	
Chlorite	$(Mg,Fe^{2+})_5Al(Si_3Al)O_{10}(OH)_8$	9.6	10.1	6.4	22.8	13.4		9.9	26.5	18.0
Talc	$Mg_3Si_4O_{10}(OH)_2$			43.1	7.6		20.0		6.3	
Hornblende	$Ca_2(Mg,Fe^{2+})_4Al(Si_7Al)O_{22}(OH)_2$			7.6	6.4		2.4		6.5	
Lizardite	$Mg_3Si_2O_5(OH)_4$			1.7	3.3		3.1		3.8	
Calcite	$CaCO_3$					0.6				
Ankerite	$Ca(Fe^{2+},Mg,Mn)(CO_3)_2$				2.5		2.0			1.0
Augite	$(Ca,Na)(Mg,Fe,Al,Ti)(Si,Al)_2O_6$			28.1	14.0		17.6		21.5	
Enstatite	$Mg_2Si_2O_6$			3.5						
Pentlandite	$(Fe,Ni)_9S_8$			0.3	1.6		4.2			
Chalcopyrite	$CuFeS_2$						2.7			4.1
Pyrite	FeS_2	0.5	1.4					1.9		2.0
Pyrrhotite	$Fe_{1-x}S$		1.1	0.3	5.6	3.1	16.2		3.8	0.8
Rutile	TiO_2	0.5				0.6				
Ilmenite	$Fe^{2+}TiO_3$				1.5				2.1	
Forsterite	Mg_2SiO_4				8.8		7.4		1.0	
Magnetite	$Fe^{2+}Fe_2^{3+}O_4$				5.9		9.7			
Total		100.0	100.0	100.0	100.0	100.0	100.0	100.0	100.0	100.0

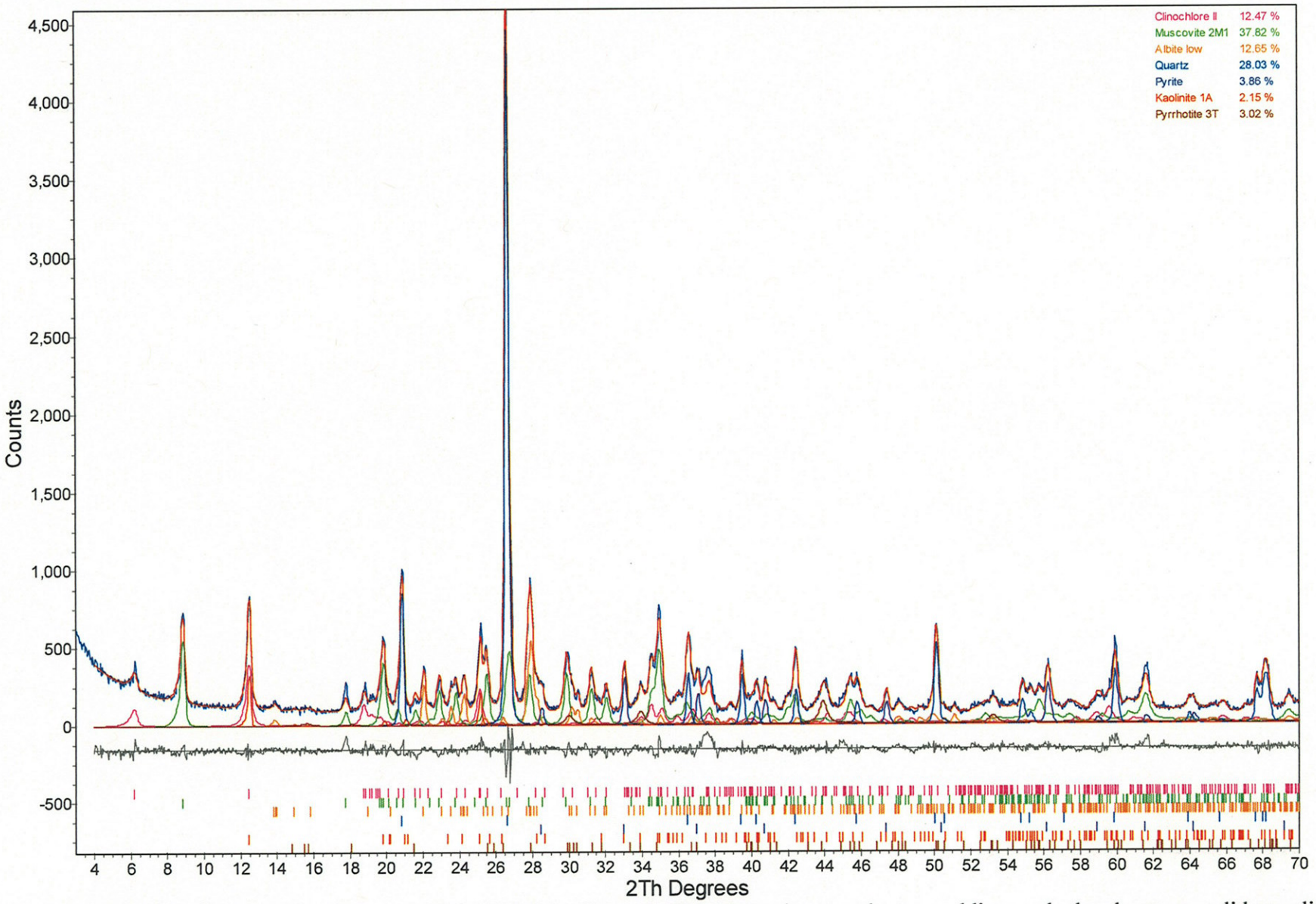


Figure 1. Rietveld refinement plot for sample **VR71100** (blue line - observed intensity at each step; red line - calculated pattern; solid grey line below – difference between observed and calculated intensities; vertical bars, positions of all Bragg reflections). Coloured lines are individual diffraction patterns of all phases.

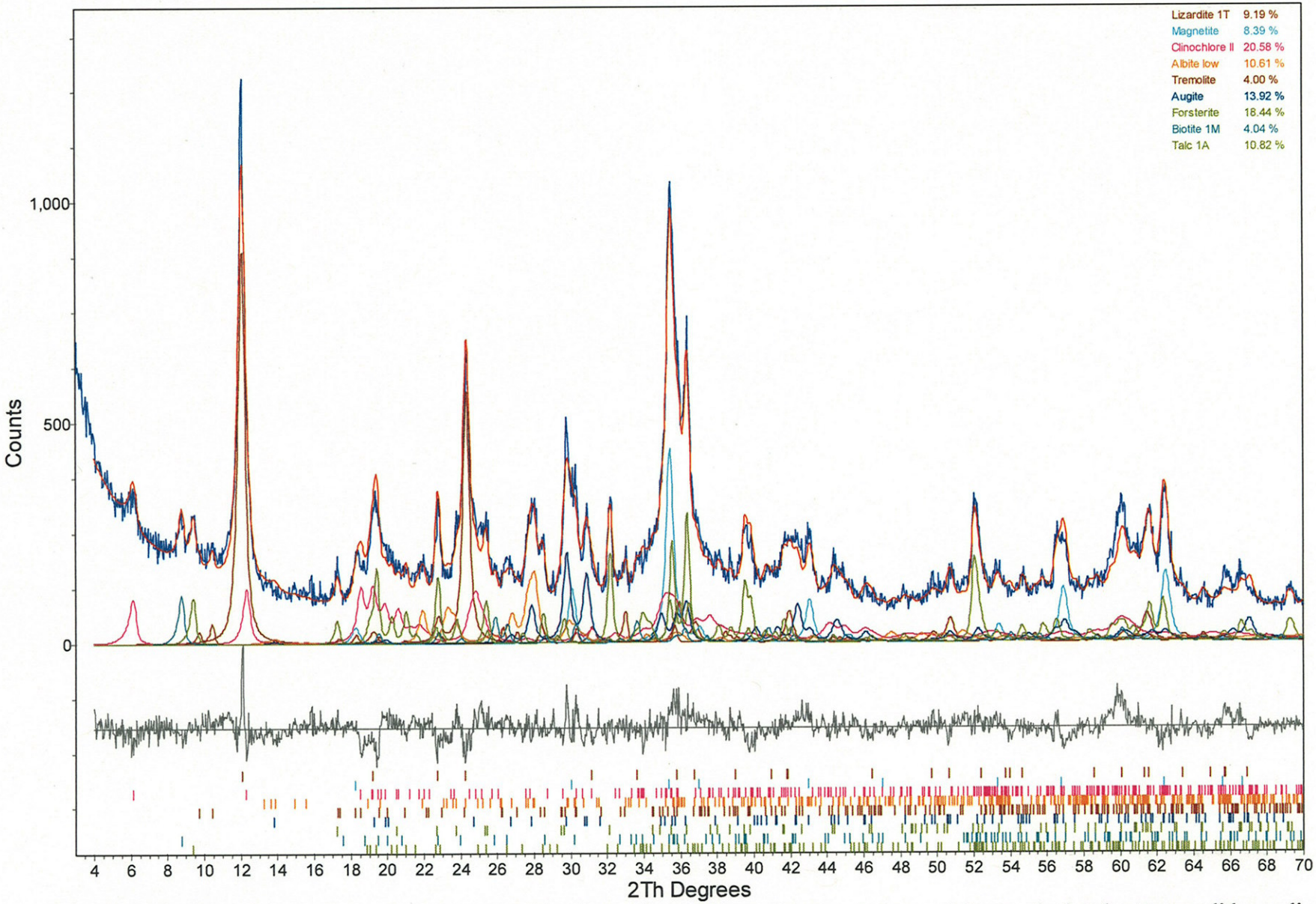


Figure 2. Rietveld refinement plot for sample **VR71213** (blue line - observed intensity at each step; red line - calculated pattern; solid grey line below – difference between observed and calculated intensities; vertical bars, positions of all Bragg reflections). Coloured lines are individual diffraction patterns of all phases.

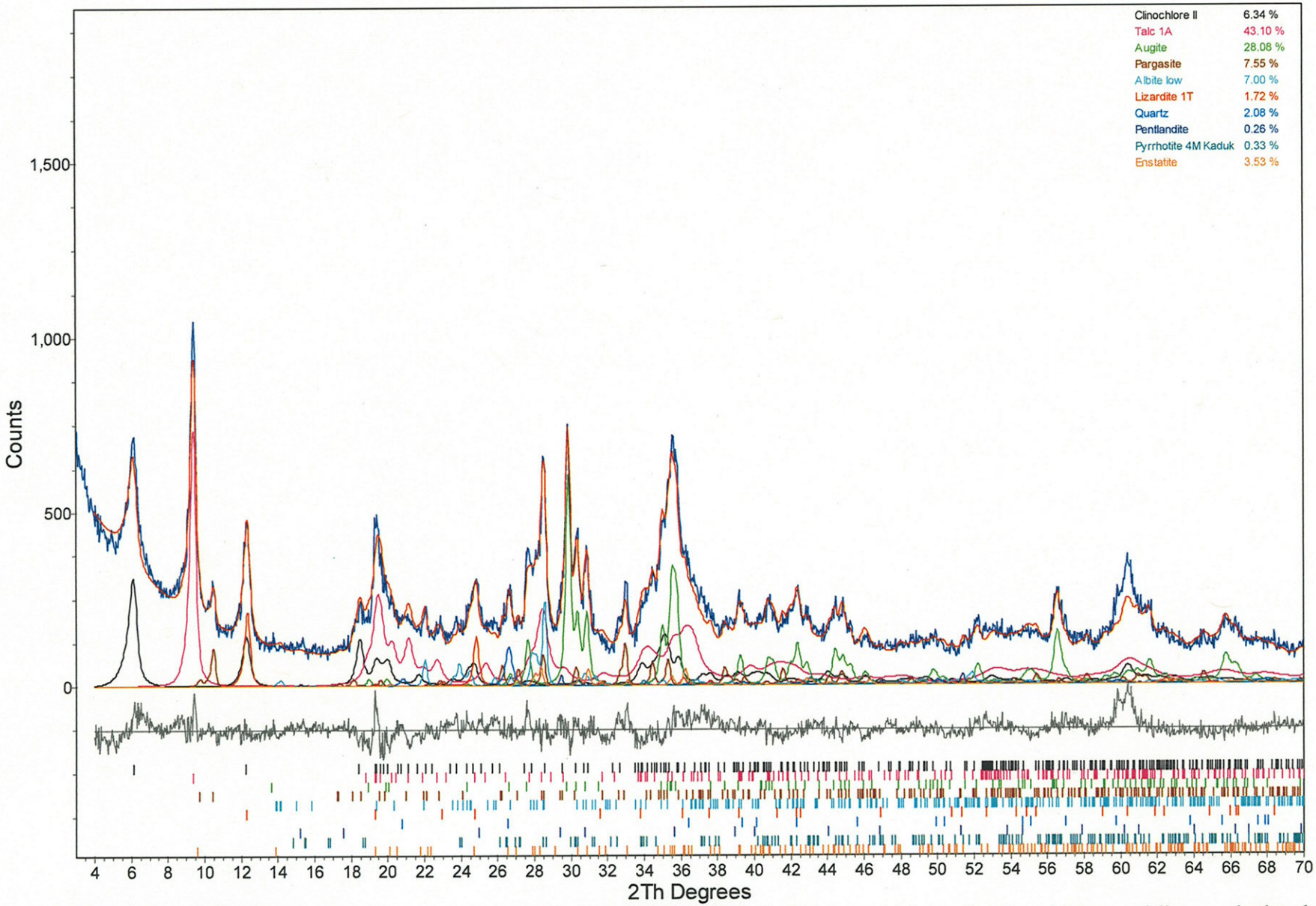


Figure 3. Rietveld refinement plot for sample **CEMI 18782 (VR71275A)** (blue line - observed intensity at each step; red line - calculated pattern; solid grey line below – difference between observed and calculated intensities; vertical bars, positions of all Bragg reflections). Coloured lines are individual diffraction patterns of all phases.

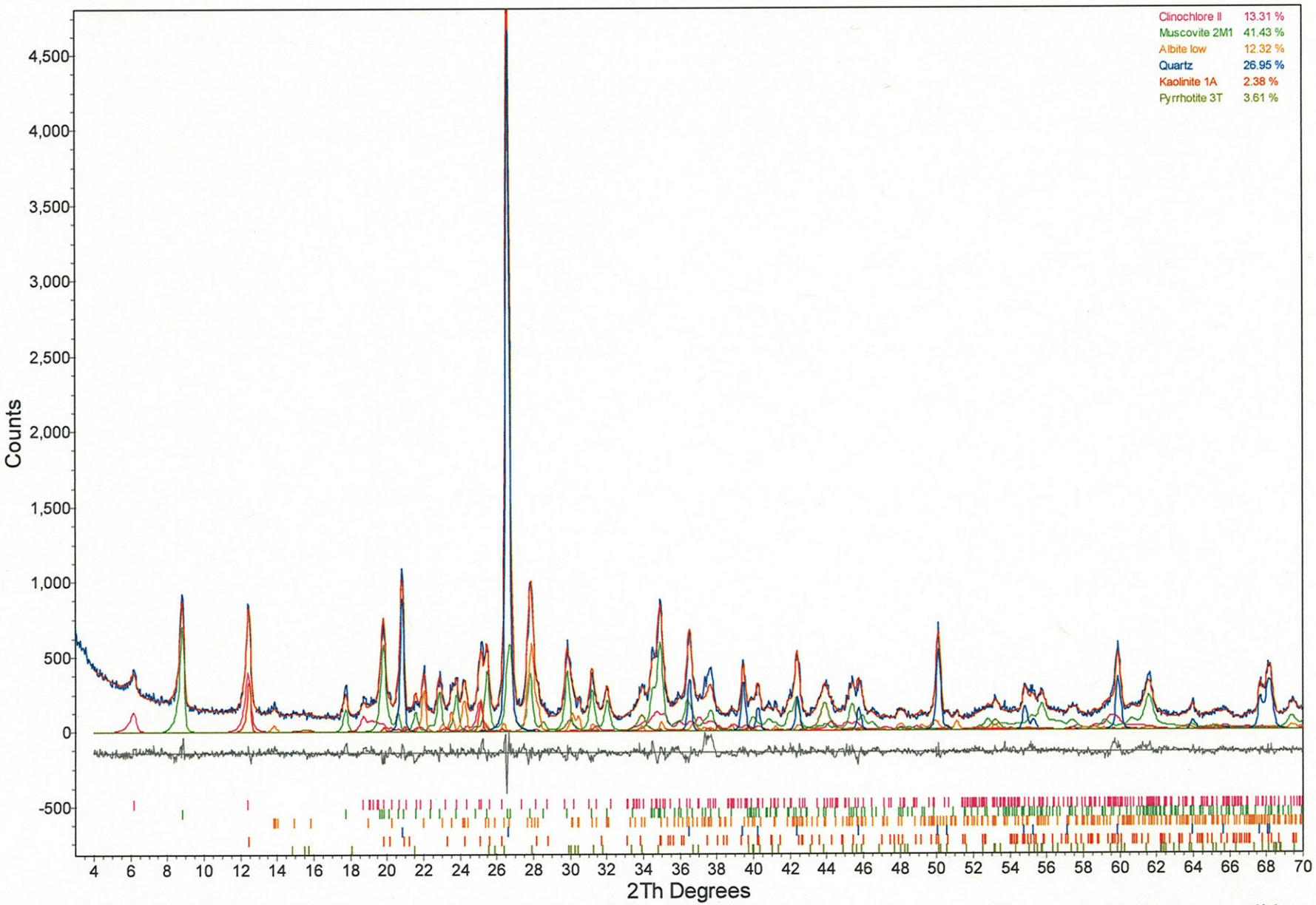


Figure 4. Rietveld refinement plot for sample **VR71499A** (blue line - observed intensity at each step; red line - calculated pattern; solid grey line below – difference between observed and calculated intensities; vertical bars, positions of all Bragg reflections). Coloured lines are individual diffraction patterns of all phases.

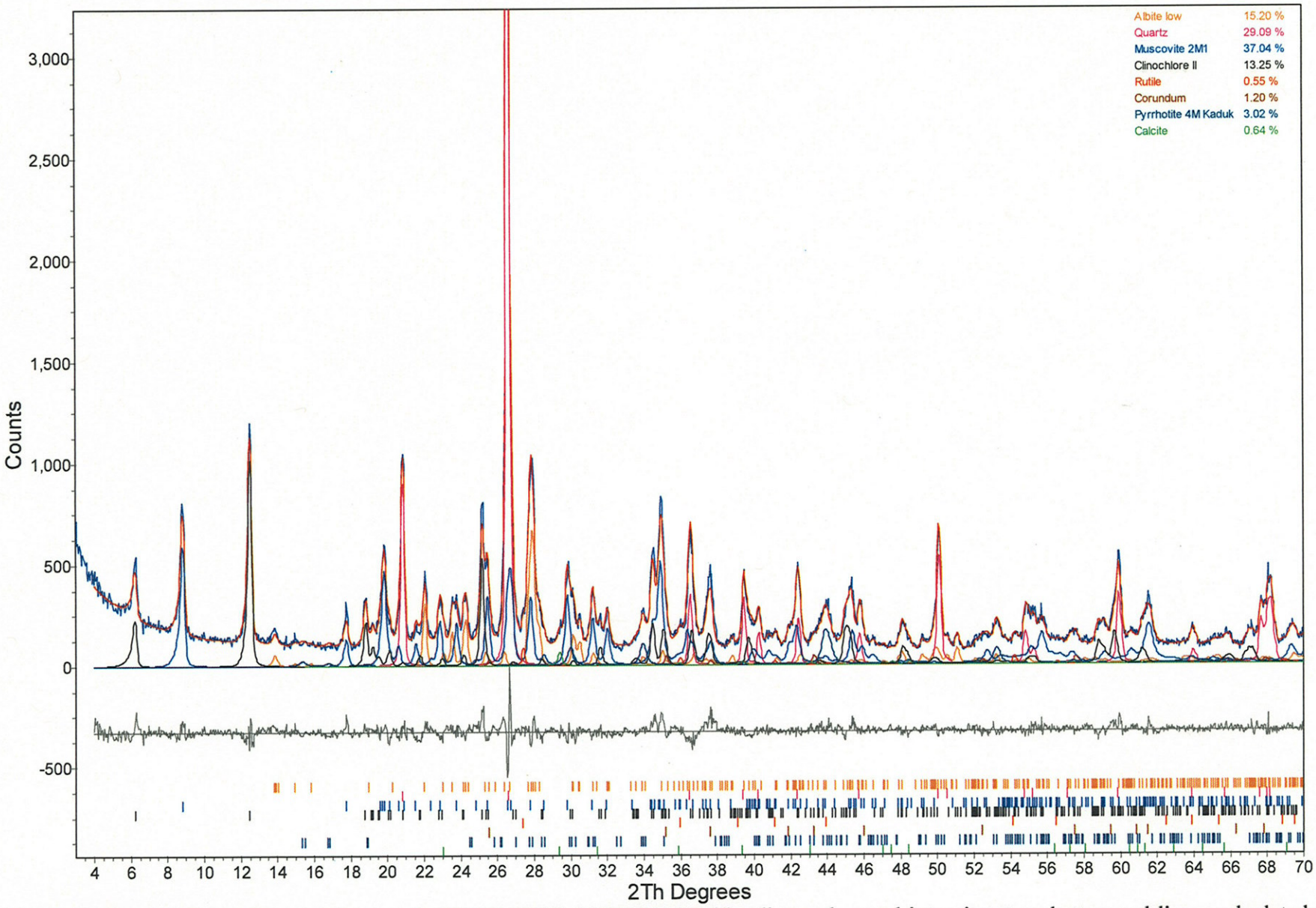


Figure 5. Rietveld refinement plot for sample **CEMI 18789 (VR91625A)** (blue line - observed intensity at each step; red line - calculated pattern; solid grey line below – difference between observed and calculated intensities; vertical bars, positions of all Bragg reflections). Coloured lines are individual diffraction patterns of all phases.

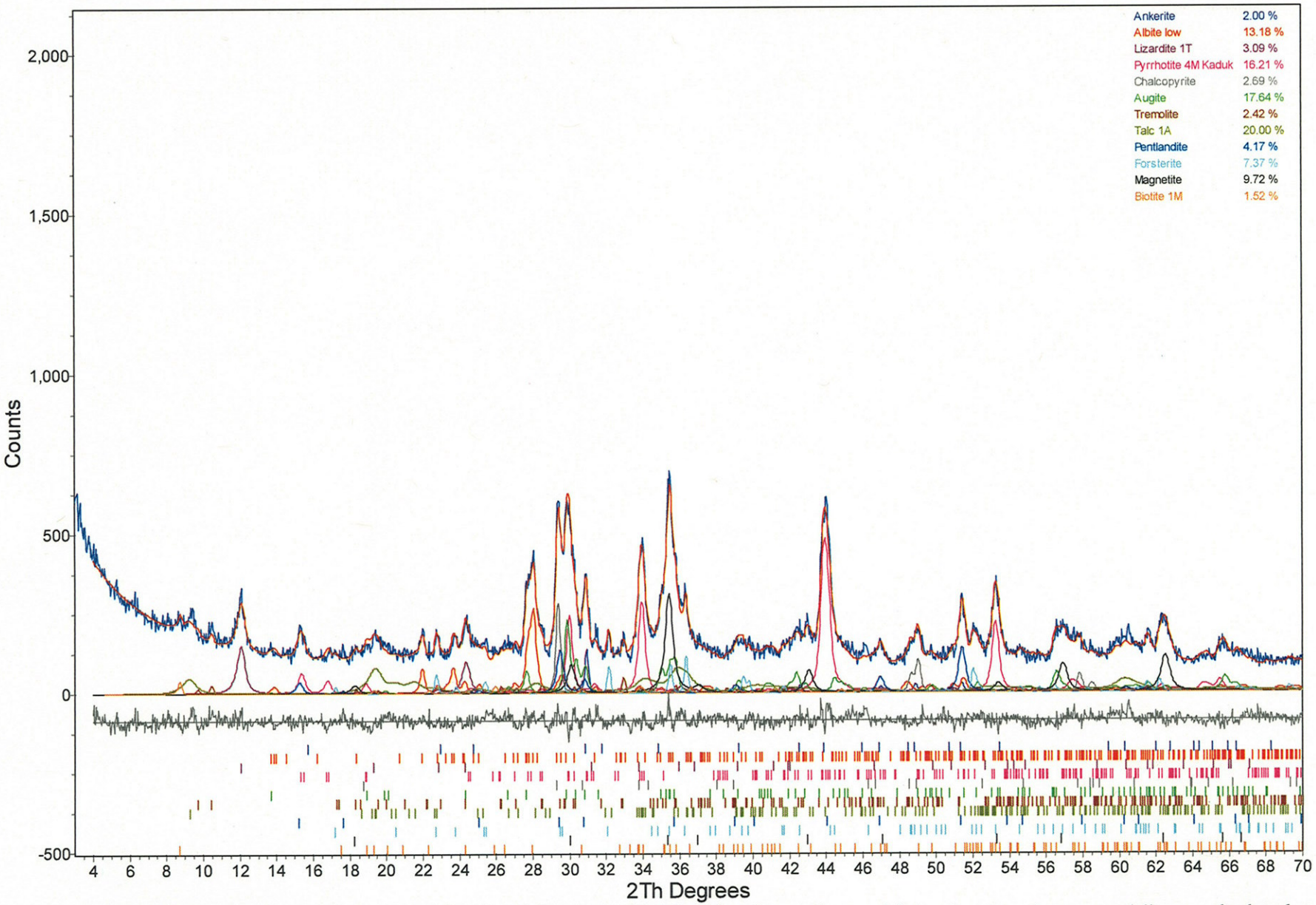


Figure 6. Rietveld refinement plot for sample **CEMI 18790 (VR90125A)** (blue line - observed intensity at each step; red line - calculated pattern; solid grey line below – difference between observed and calculated intensities; vertical bars, positions of all Bragg reflections). Coloured lines are individual diffraction patterns of all phases.

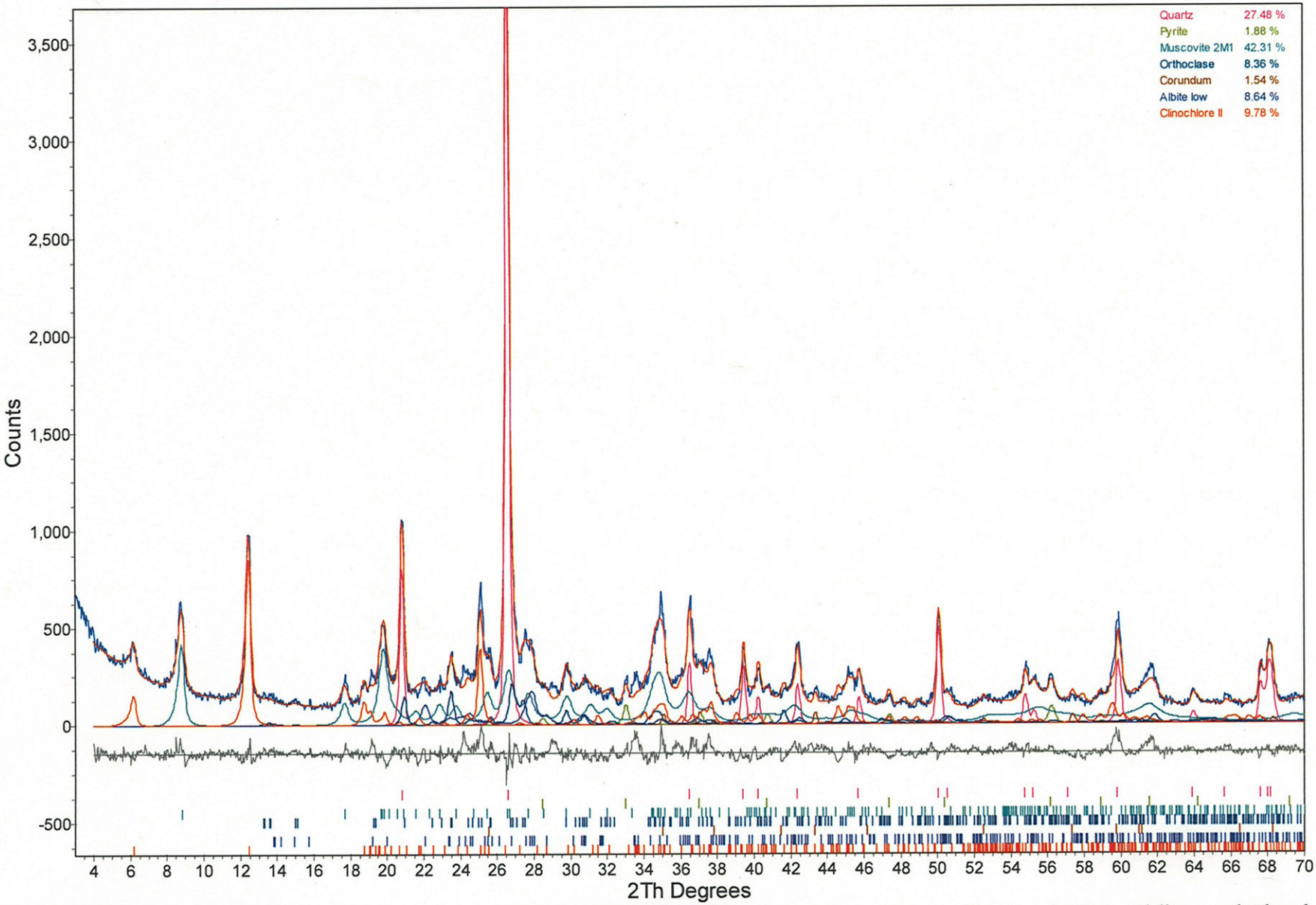


Figure 7. Rietveld refinement plot for sample **CEMI 18794 (VR90425A)** (blue line - observed intensity at each step; red line - calculated pattern; solid grey line below – difference between observed and calculated intensities; vertical bars, positions of all Bragg reflections). Coloured lines are individual diffraction patterns of all phases.

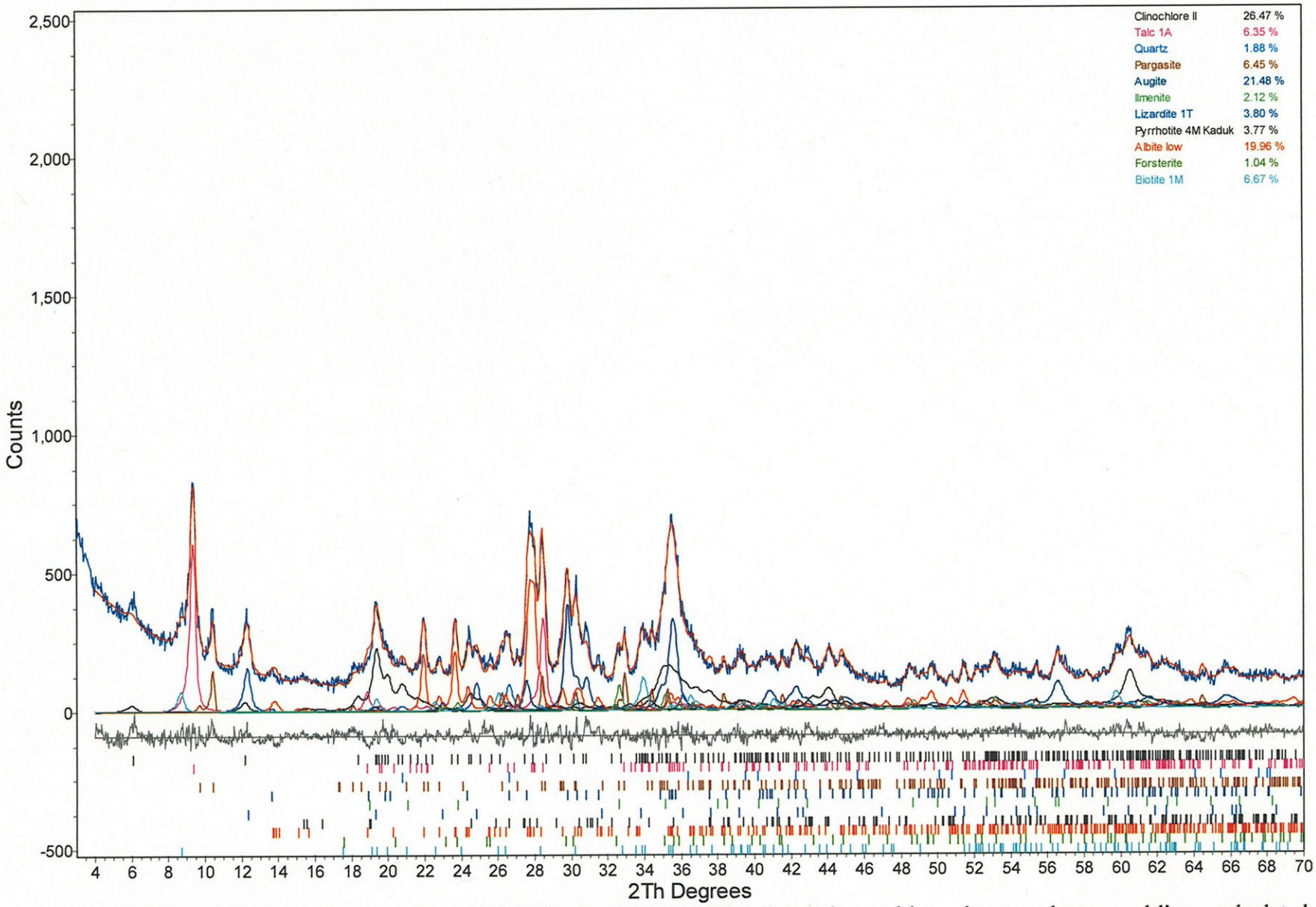


Figure 8. Rietveld refinement plot for sample **CEMI 18796 (VR91267A)** (blue line - observed intensity at each step; red line - calculated pattern; solid grey line below – difference between observed and calculated intensities; vertical bars, positions of all Bragg reflections). Coloured lines are individual diffraction patterns of all phases.

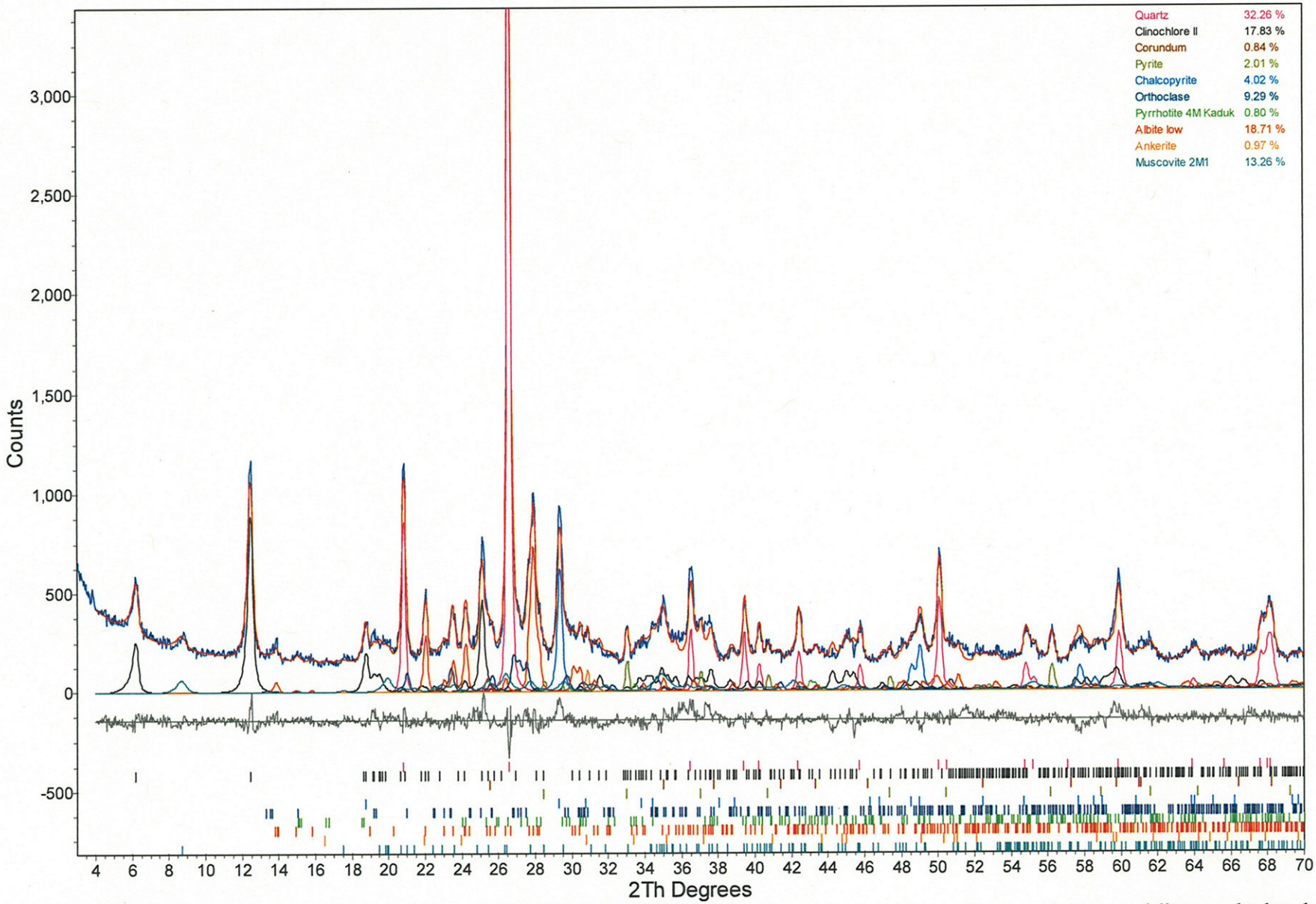


Figure 9. Rietveld refinement plot for sample **CEMI 18797 (VR91306A)** (blue line - observed intensity at each step; red line - calculated pattern; solid grey line below – difference between observed and calculated intensities; vertical bars, positions of all Bragg reflections). Coloured lines are individual diffraction patterns of all phases.

APPENDIX 2

EDS analyses of carbonates and chlorite

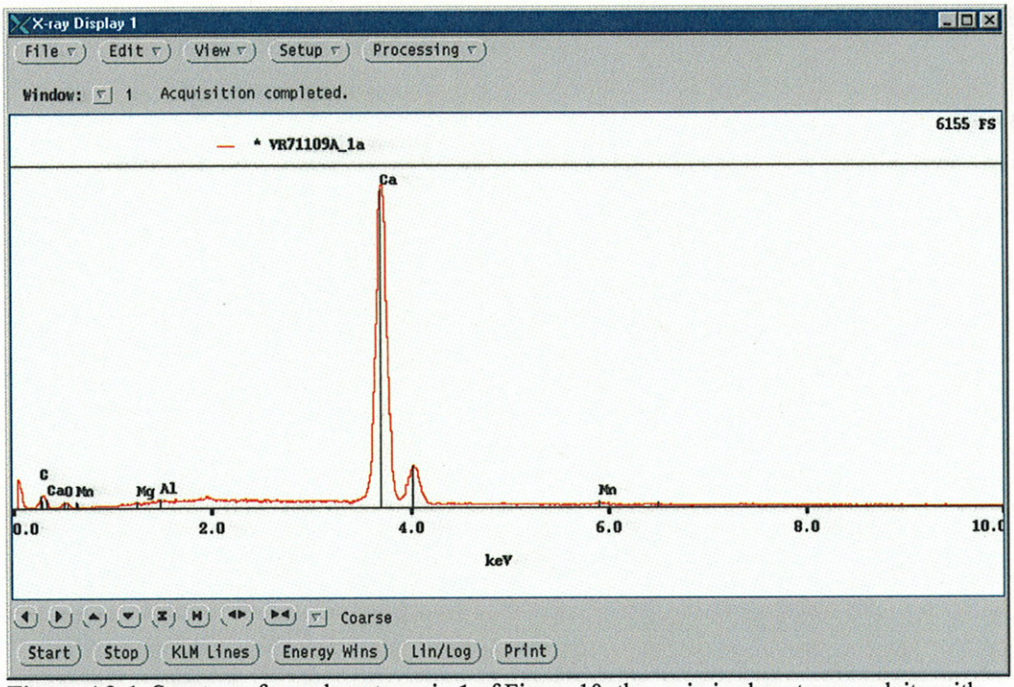


Figure A2-1. Spectrum for carbonate grain **1** of Figure 10; the grain is almost pure calcite with no more than traces of other elements.

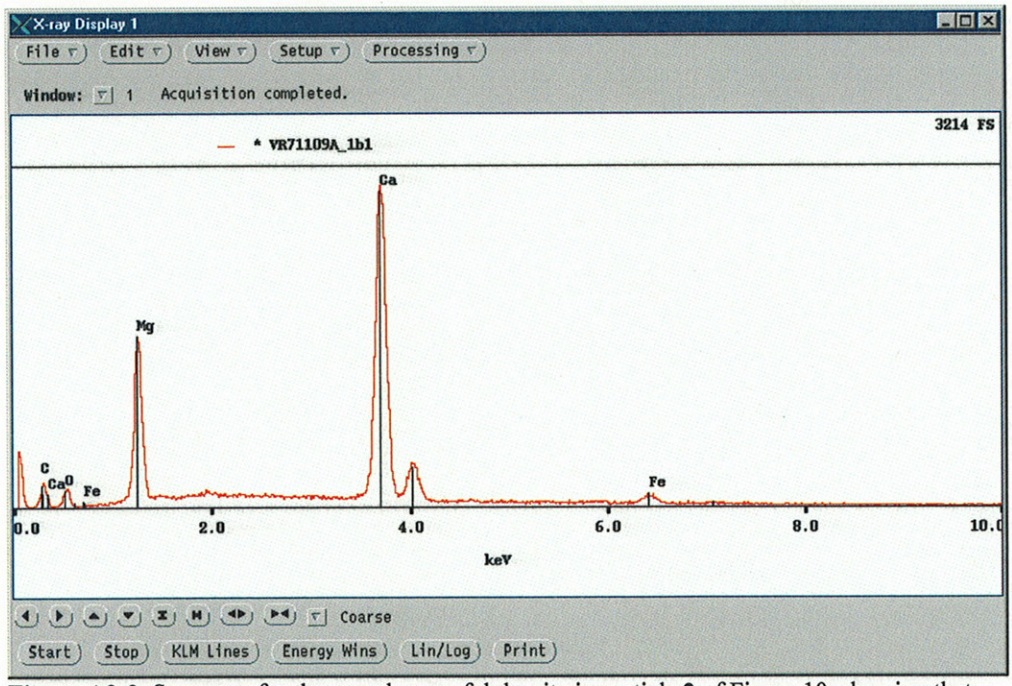


Figure A2-2. Spectrum for the zoned core of dolomite in particle **2** of Figure 10, showing that only a small amount of Fe is present.

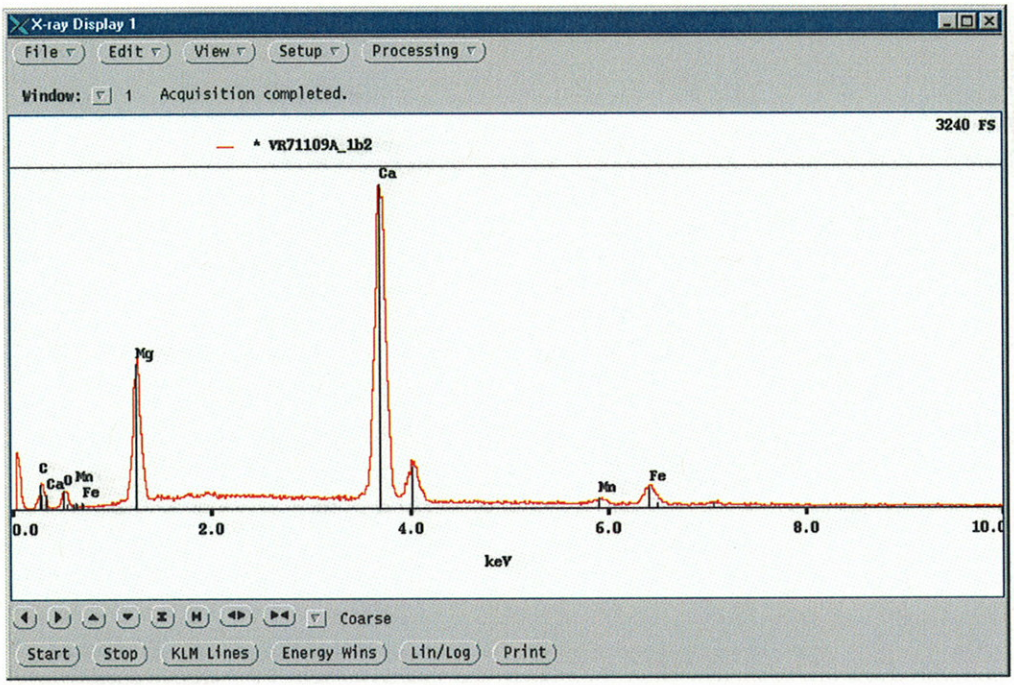


Figure A2-3. Spectrum of the zoned dolomite in particle **3** of Figure 10. The Fe and Mn contents are slightly higher than those in particle **2**.

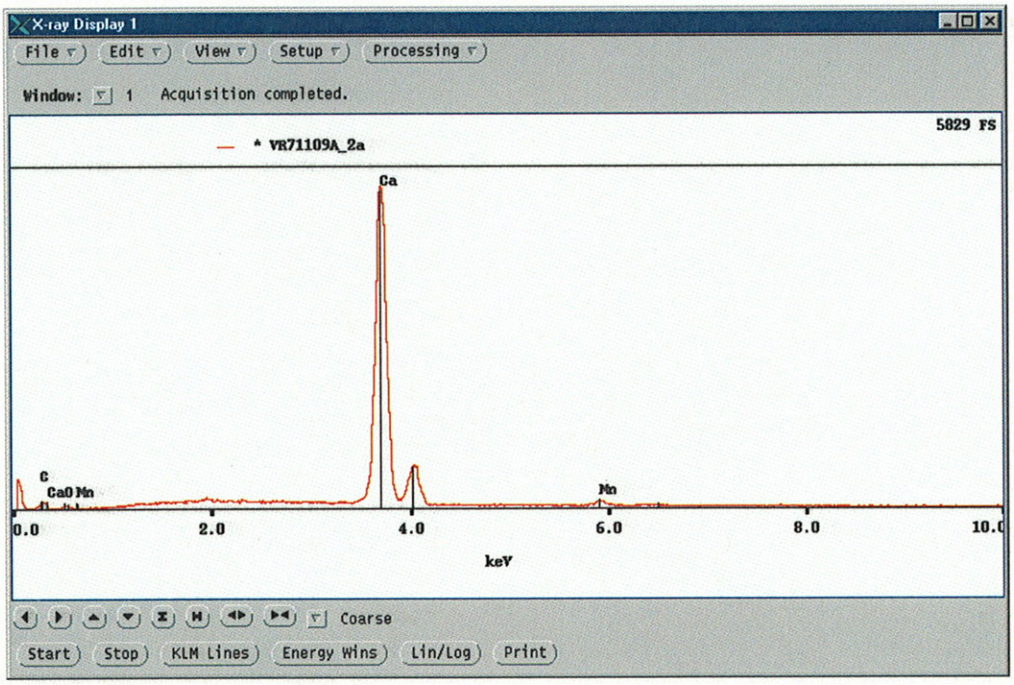


Figure A2-4. Spectrum of grain **1** calcite in VR71109A, Figure 8, lower photo. The calcite is almost of end-member composition, with only a trace of Mn detectable.

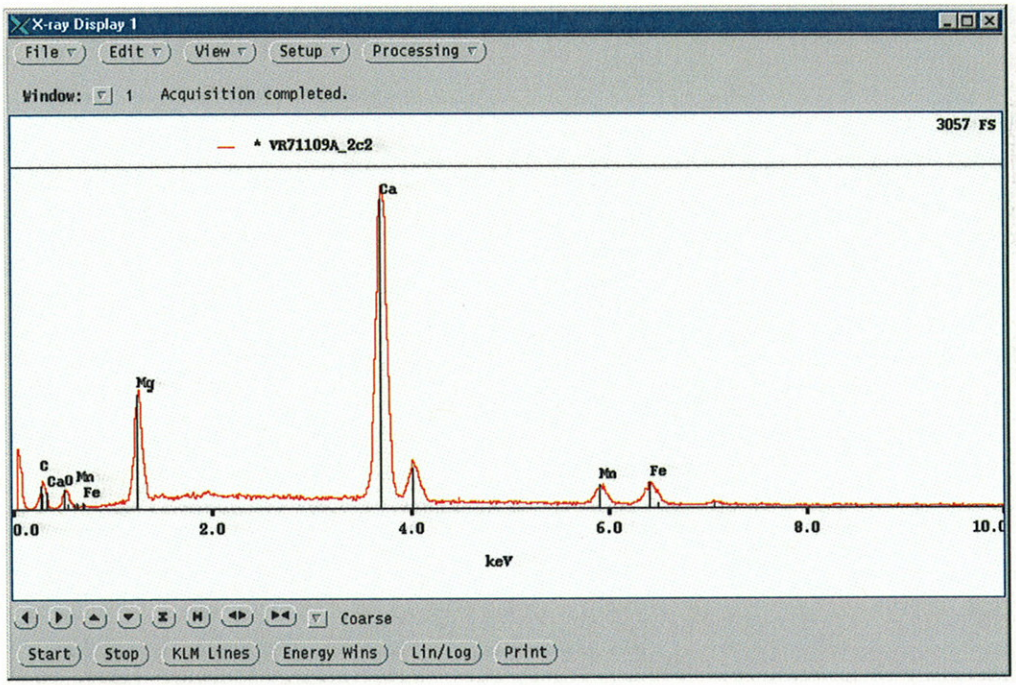


Figure A2-5. Spectrum of dolomite in area **3** of VR71109A. The dolomite is a slightly zoned particle that is surrounded by the main carbonate mass, which is almost pure calcite. The combined Fe + Mn contents are the highest that were obtained for dolomite in the Eagle samples.

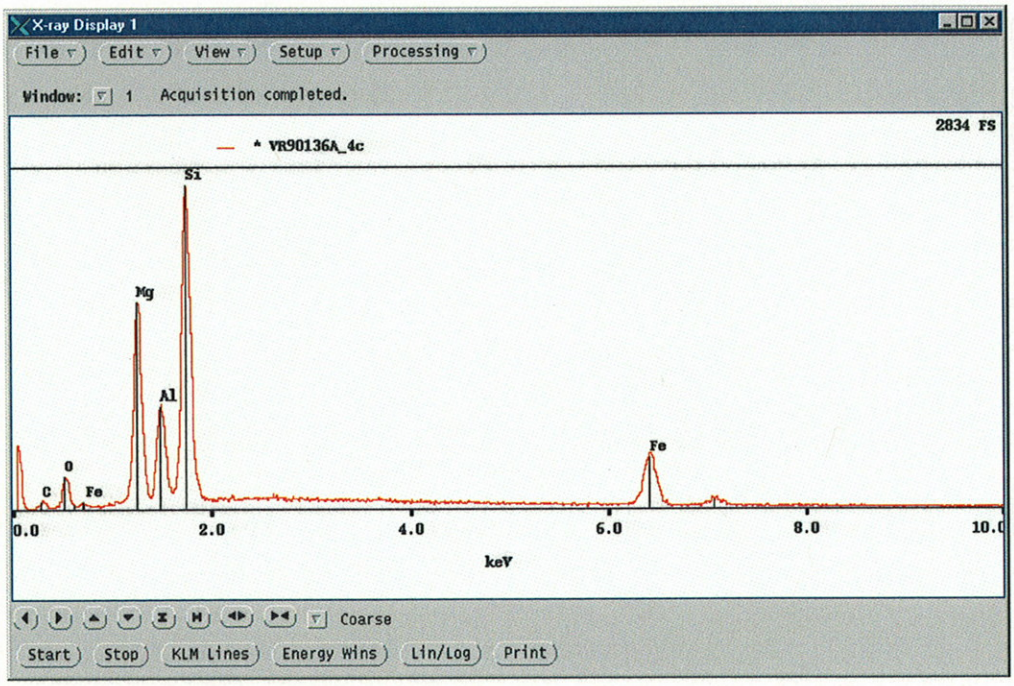


Figure A2-6. Chlorite in VR91306A. The spectrum is for the brownish mass associated with carbonate shown on the left of Figure 12.

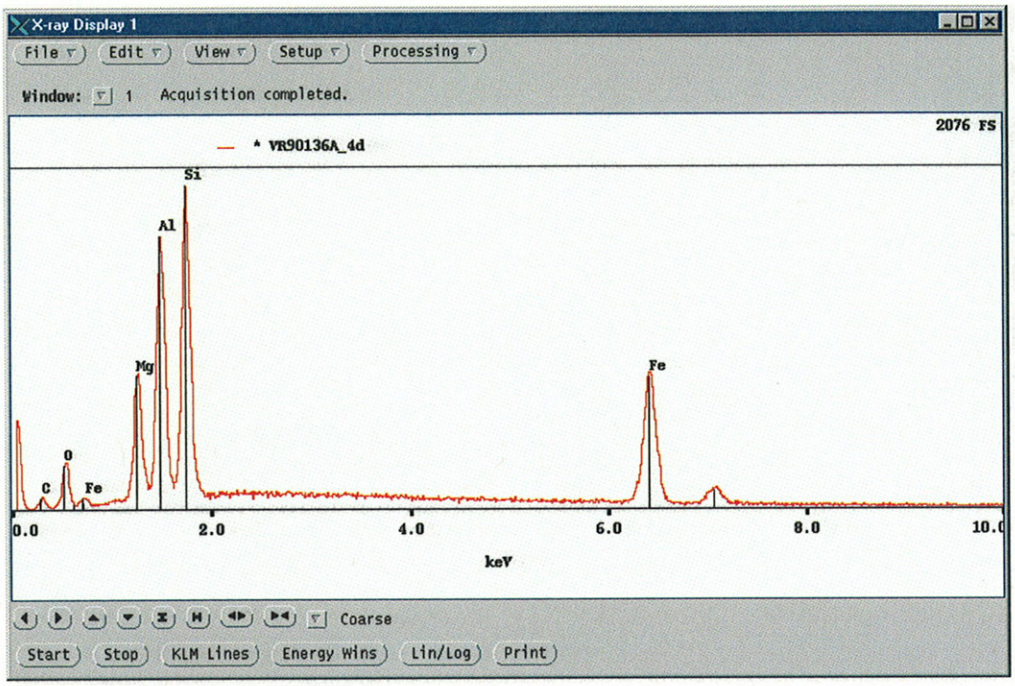
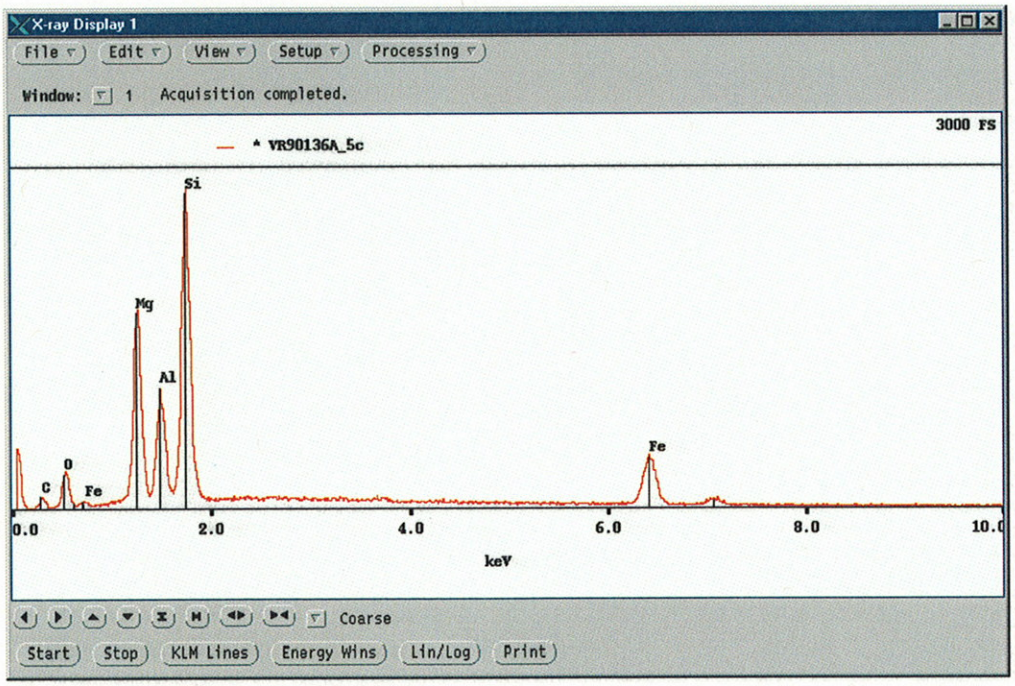


Figure A2-7. Chlorite in VR91306A. The spectrum is for the almost colorless particle shown on the right of Figure 12. The particle is richer in Fe and Al, and has less Mg than the brownish particle at the left of Figure 12.



FigureA2-8. Spectrum of the chlorite veinlet at the far left of Figure 11, sample VR91306A. The composition is close to that of the brownish chlorite aggregate at the left of Figure 12.

ELECTRON-MICROPROBE COMPOSITIONS OF CARBONATES

The carbonate grains illustrated in Figures 8 and 10 were analyzed to obtain a correlation with the EDS spectra. Whereas the correlation proved to be feasible for calcite, which is homogeneous and unzoned, specific correlations were not possible for zoned dolomite because it was not possible to return to exactly the same point at which the EDS analyses were obtained. Nevertheless, the data confirm the spectral indications that Fe and Mn in both calcite and dolomite are typically low; many of the spectra that were obtained, but which are not illustrated, showed Fe and Mn contents to be at the lowest end of the substitutional range. Thus, for calcite the average composition is interpreted to >95 molar % $CaCO_3$, and for dolomite the average is at least 90 molar % $CaMg(CO_3)_2$. No ankerite has been detected.

Microprobe compositions of carbonates in VR71109A

EDS spectra	A2-1		A2-2		A2-3		A2-4					
Mineral	calcite		dolomite		dolomite		calcite		dolomite		calcite	
Grain, Fig.	Gr. 1, Fig. 10		Gr. 2, Fig. 10		Gr. 3, Fig. 10		Gr. 1, Fig. 8		Gr. 2, Fig. 8		Gr. 3, Fig. 8	
Spot	a	b	a	b	a	b	a	b	a	b	a	b
Wt% MgO	0.05	0.05	19.12	19.74	19.29	19.15	0.18	0.11	17.66	18.55	0.14	0.11
CaO	55.74	55.11	30.71	30.30	30.59	30.62	53.59	55.21	30.36	30.30	55.80	54.83
MnO	0.69	1.15	0.32	0.32	0.37	0.33	2.14	2.01	1.18	1.01	0.67	0.69
FeO	0.22	0.21	2.21	2.07	2.27	2.33	0.18	0.06	4.53	3.30	0.25	0.24
$[CO_2]$*	44.36	44.15	46.53	46.80	46.69	46.57	43.69	44.73	46.62	46.68	44.51	43.72
Sum	101.06	100.67	98.89	99.23	99.21	99.00	99.78	102.12	100.35	99.84	101.37	99.59
					formula contents							
Mg	0.00	0.00	0.90	0.92	0.90	0.90	0.01	0.01	0.83	0.87	0.01	0.01
Ca	1.97	1.96	1.04	1.02	1.03	1.03	1.93	1.94	1.02	1.02	1.97	1.97
Mn^{2+}	0.02	0.03	0.01	0.01	0.01	0.01	0.06	0.06	0.03	0.03	0.02	0.02
Fe^{2+}	0.01	0.01	0.05	0.06	0.06	0.06	0.01	0.00	0.12	0.09	0.01	0.01

TECHNICAL MEMORANDUM

DATE: 27 June 2005

TO: **Jon Cherry (KMC-Eagle)**

FROM: Mark J. Logsdon (Geochimica)

SUBJECT: **TOTAL METALS IN SOLIDS FROM ORE**

cc: **A. Duex, A. Ware, F. Fox, R. Sawyer (KMC); S. Donohue (F&VD); G. Smary (WNJ)**

BACKGROUND

The Eagle Ni-Cu deposit, Michigamme County, Michigan, will be developed as an underground mine. The Project anticipates two classes of ore-grade material, Massive Sulfide Unit (MSU) and Semi-Massive Sulfide Unit (SMSU) ores. Both classes of ore represent magmatic segregation of high-density iron, nickel and copper sulfides. The principal ore minerals are pyrrhotite [$Fe_{1-x}S$], pentlandite [$(Fe,Ni)_9S_8$], and chalcopyrite [$CuFeS_2$]. The differences between the classes relate to how much, if any, of the primary silicate minerals (predominantly olivine, pyroxene, and calcium feldspar) were trapped along with the sulfides as the rock crystallized.

Geochimica, Inc. (Aptos, CA) was asked to compile and evaluate existing information on metals in the solid phase of both ores and development rock for the Eagle Project. The analysis of the development rock samples was compiled in Geochimica (2005a). This memorandum is based on eighty-nine (89) ore samples. The samples have been prepared for analysis using the EPA-approved digestion techniques identified in the Sampling and Analysis Plans, and all have been analyzed using an inductively-coupled plasma methodology. Instrumental analysis of the plasmas has been by either ICP-MS or ICP-AES, depending on which analytical method has the lower method detection limit for the specific metal. All data used in this analysis meet the QA/QC requirements for the Eagle Project based laboratory reports and our review of those against the data-quality objectives for the project. Because these are the most sensitive analytical methods used in scientific studies of mine wastes, almost all samples have reported values above the method detection limits. For the few samples that had individual metals less than detection, a value of one-half the limit of detection was used for the ore samples.

ISSUES

What is the best point-estimate of concentration, at the upper 95th percentile of the confidence interval, in Eagle ores for each of the following metals:

Antimony (Sb)

Arsenic (As)
Barium (Ba)
Beryllium (Be)
Cadmium (Cd)
Chromium (Cr)
Cobalt (Co)
Copper (Cu)
Lead (Pb)
Magnesium (Mg)
Manganese (Mn)
Mercury (Hg)
Nickel (Ni)
Selenium (Se)
Silver (Ag)
Tin (Sn)
Zinc (Zn)

TECHNICAL APPROACH

The technical approach to evaluating metals in ore samples is identical to that used for development rock in Geochimica (2005). Within the data set of 89 ore samples, for each of the subject metals we computed (a) standard descriptive statistics and (b) a histogram with cumulative percentages. These exploratory computations form the basis for selection of the most appropriate statistic for point estimation of development rock, given the empirical distribution of the data.

Figure 1 shows the histogram for arsenic concentrations in 89 samples of ore that have been vetted for QA/QC as of this analysis, including both MSU and SMSU samples.

Figure 1 Arsenic (As) Concentrations (ppm) in Eagle Project Ores

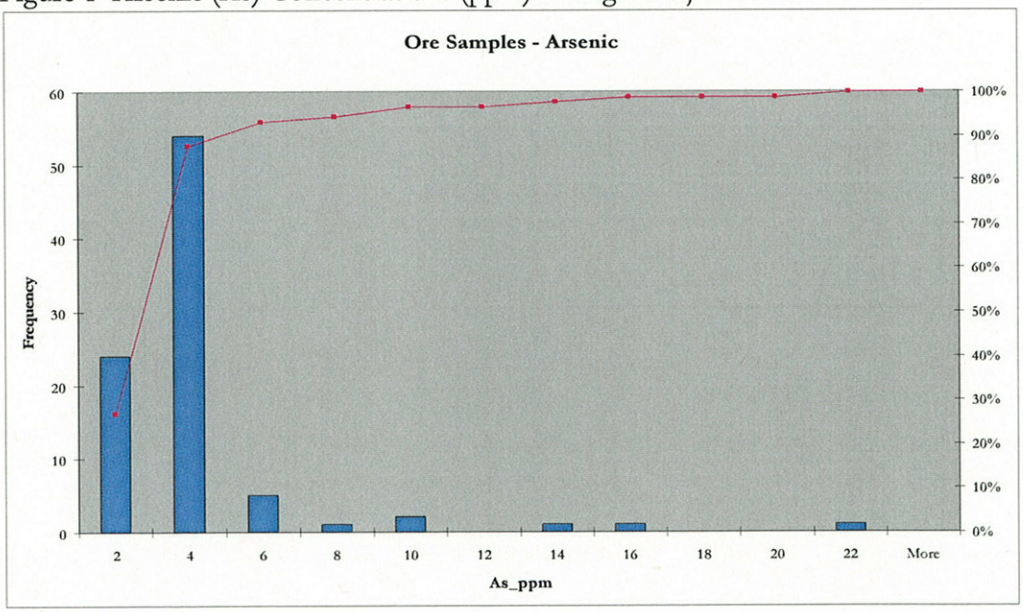
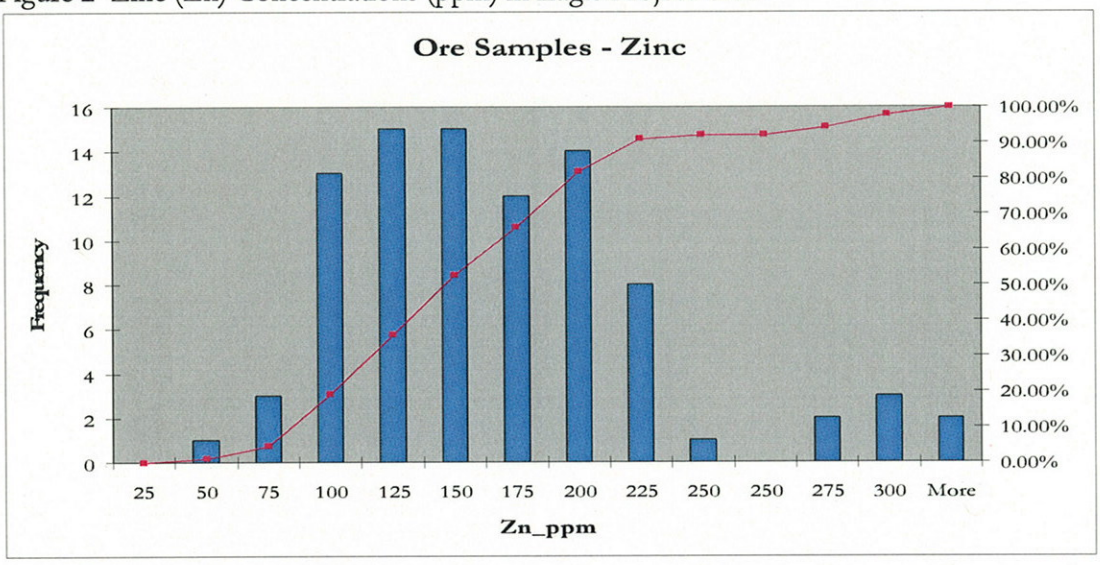


Figure 2 shows the histogram for zinc concentrations in 89 samples of ore that have been vetted for QA/QC as of this analysis, including both MSU and SMSU samples.

Figure 2 Zinc (Zn) Concentrations (ppm) in Eagle Project Ores



As was shown also for metals in development rocks, the empirical distributions of metals in ore samples is very far from normally distributed. The sorts of empirical distributions shown in Figures 1 and 2 mean that the most common measure of descriptive statistics, the sample mean, is not an appropriate point estimator. For strongly skewed or other non-normal data, the best unbiased estimator is the sample median (e.g., Wonnacott and Wonnacott, 1977).

As discussed in Geochimica (2005), for strongly skewed data (such as arsenic in Figure 1) or polymodal data (such as zinc in Figure 2), the only theoretically sound basis for constructing a confidence interval around a point estimator is to use a simulation technique called "resampling". For the ore samples, as for the development rock, we apply the resampling technique called the "bootstrap" (Efron, 1979), in which one begins with the actual sample data, and then constructs a large number of equivalently sized data sets by selecting randomly (with replacement) from the original data, then ordering the outputs of those 're-sampled" data to calculate the confidence interval desired. As for the development rock analysis, we have selected 10,000 as the number of repetitions for resampling. The bootstrap procedure is compiled in a computer code called RESAMPLING STATS and was exercised for this task using version 5.0.2 (Simon, 1999). Sensitivity of the results to choices of resample density and other technical issues of statistics were addressed in Geochimica (2005).

DATA

Attachment 1 provides the compiled data and the histograms for each of the 17 metals in ore samples.

RESULTS

The calculations of the median and the upper 95th percentile of the median are summarized in Table 1. Table 1 converts weight percent (parts per hundred) for the laboratory data report to parts per million for copper, magnesium, and nickel (Cu, Mg, and Ni)[1], for comparability across all metals.

Table 1 Median and Estimated 95th Percentile-of-the-Median Concentrations for 16 Metals in Eagle Projec5 Ores

Metal	Median (ppm)	95th %-ile (ppm)
Antimony (Sb)	0.34	0.40
Arsenic (As)	2.7	2.9
Barium (Ba)	20	20
Beryllium (Be)	0.08	0.10
Cadmium (Cd)	3.27	3.67
Chromium (Cr)	961	1,180
Cobalt (Co)	665	740
Copper (Cu)	25,800	31,110
Lead (Pb)	43.4	48.0
Magnesium (Mg)	88,900	95,600
Manganese (Mn)	947	1,020
Mercury (Hg)	0.03	0.04
Nickel (Ni)	25,900	31,500
Selenium (Se)	41	50
Silver (Ag)	9.66	11.10
Tin (Sn)	3.7	4.2
Zinc (Zn)	144	160

The reported results in Table 1 reflect the significant figures reported for each metal in the laboratory data reports.

DISCUSSION

Table 2 compares the upper 95th percentile estimate with published values for average crustal rocks and average igneous rocks. As for Table 1, results for copper, magnesium, and nickel (Cu, Mg, Ni) are converted to parts per million for this comparison.

[1] For development rock, only Mg was present in sufficient concentration to be reported as percent. However, in the ores, of course, Ni and Cu are principal species, present at percent to tens of percent levels.

Table 2 Comparison of Estimated 95th Percentile Concentrations for 16 Metals in Eagle Ores with Average Crustal and Average Igneous Rocks

Metal	95th %-ile (ppm)	Average Crustal [1] (ppm)	Average Igneous Rocks [2] (ppm)
Antimony (Sb)	0.40	0.2	0.51
Arsenic (As)	2.9	1.8	1.8
Barium (Ba)	20	425	595
Beryllium (Be)	0.10	2.8	3.6
Cadmium (Cd)	3.67	0.2	0.19
Chromium (Cr)	1,180	100	198
Cobalt (Co)	740	25	23
Copper (Cu)	31,110	55	97
Lead (Pb)	48	13	16
Magnesium (Mg)	95,600	20,900	17,600
Manganese (Mn)	1,020	950	937
Mercury (Hg)	0.04	0.08	0.33
Nickel (Ni)	31,500	75	94
Selenium (Se)	50	0.05	0.05
Silver (Ag)	11.10	0.07	0.15
Tin (Sn)	4.2	2	2.5
Zinc (Zn)	160	70	80

(1): Krauskopf and Bird, 1995, Appendix IV,
(2): Hem, 1985, Table 1

The order of the concentrations for the upper 95th percentile of the median is reasonable for the rocks. Magnesium (Mg) is a major element in the rocks (especially in the SMSU samples, which have significant silicate mineral concentrations). The Eagle Project is a prospective nickel – copper (Ni-Cu) ore body, so it is reasonable that the upper control limit for estimates of Ni and Cu should be very high compared to world-wide rock averages. Several of the so-called "siderophile" (those found characteristically with iron) and "chalcophile" elements (those that bond to sulfur in crustal rocks) are often associated with Ni-Cu ores, including cadmium (Cd), cobalt (Co), silver (Ag), and zinc (Zn). Chromium (Cr), a lithophile element, is commonly associated with oxide and alumino-silicate minerals in ultramafic rocks. Selenium (Se) (a congener for sulfur) is commonly found in sulfide minerals.

Barium (Ba) is common in rock-forming minerals and is common in some sulfide ore bodies, but in these samples is actually well below their crustal and igneous-rock averages, as also are beryllium (Be). Mercury (Hg) is low to distinctly low in the ores compared to crustal and igneous values. Antimony (Sb), arsenic (As), lead (Pb), manganese (Mn), tin (Sn), and zinc (Zn) are close to their average crustal and igneous values.

REFERENCES

Efron, B., 1979. Bootstrap Methods: Another Look at the Jacknife. *Annals of Statistics*, vol. 7, p. 1026.

Geochimica, 2005. Total Metals in Solids from Development Rock. Contractor Report, March 17, 2005.

Hem, J.D., 1985. *Study and Interpretation of the Chemcial Characteristics of Natural Water (3rd Ed).* U.S. Geological Survey Water-Supply Paper 2254.

Krauskopf, K.B. and D.K. Bird, 1995. *Introduction to Geochemistry (3rd Ed).* New York: McGraw-Hill Inc.

Simon, J.L., 1999. *RESAMPLING STATS User's Guide (v 5.0.2).* Arlington, VA: Resampling Stats Inc.

Wonnacott, T.H. and R.J. Wonnacott, 1977. *Introductory Statistics for Business and Economics (2nd Edition).* New York: John Wiley & Sons.